Genetic regulation of membrane trafficking, exosome secretion, growth and dense-core granule biogenesis in the *Drosophila* accessory gland



Siamak Redhai
St Hugh's College

University of Oxford

A thesis submitted in fulfilment of the requirements for the degree of Doctor of Philosophy

Supervisor: Professor Clive Wilson
Department of Physiology, Anatomy and Genetics

‘’The fool doth think he is wise, but the wise man knows himself to be a fool’’

– Shakespeare, *As You Like It* (Act V, Scene I)

I. Declaration

The work presented in this thesis was undertaken in Professor Clive Wilson's laboratory at the Department of Physiology, Anatomy and Genetics, University of Oxford, between 2012 and 2016. I, Siamak Redhai, confirm that the work presented in this thesis is my own, except where collaborative studies were presented, which is indicated in the respective sections. This work has not been submitted for any other degree at this university or any other institute of learning.

II. Acknowledgment

I would like to firstly express my greatest gratitude to Clive Wilson who has not only been a wonderful supervisor but also a great mentor for the duration of my DPhil. Your enthusiasm and willingness to always make time to discuss new ideas and results has truly inspired me to continue with a career in academia. My scientific knowledge and skills in *Drosophila* genetics have benefited enormously as a result of your guidance and I leave your lab feeling a great sense of fulfilment with my time as a DPhil student.

Let us not forget the other members of the Wilson Lab who have, in their own unique way, made my time here unforgettable. Carina Gandy, you have been a wonderful gatekeeper of flies and also a great friend. Your patience with me has been incredible, and I would like to thank you from the bottom of my heart. Aaron Leiblich, your willingness to always engage in a conversation, mostly but not always about science, has broadened my horizons. Your openness to sharing results and thoughts on future experiments has shown me the benefits of having this attitude towards research. I would also like to thank Mihindukulasuriya (Sumeth) Perera who has helped me so much throughout my DPhil, not mentioning the countless westerns blots he has done. His approach to science is refreshing and inspiring, and he can teach one or two life lessons to even the most experienced of us. Shih-Jung Fan, your keen eye for detail never ceases to amaze me and, of course, your brilliant suggestions for future experiments are second to none. I would also like to express my thanks to Josephine EEU Hellberg, who has been extremely generous and supportive, and who I have learnt a lot from through our countless philosophical discussions. Also, Mark Wainwright who has helped me understand fly genetics and taught me how to dissect the reproductive gland in females. Thank you to all other members of the Wilson group and Goberdhan group, some of whom have recently embarked on their experience here. Kristie McCormick, thank you for your help with RT-PCR experiments and also for sharing your views on controversial matters. I would also like to thank Daniel Stevens for sharing his knowledge on questions relating to clinical research. Thank you to Benjamin Kroeger for helping with super resolution microscopy, Felix Castellanos for supplying me with flies and Irina Stefana for her critical assessment. I am also grateful to Laura Corrigan, who helped me find my feet when I first arrived in the lab.

The only reason why I am even able to write this acknowledgment section let alone complete my DPhil is down to my mother. She is an incredible woman who has

constantly sacrificed a lot for me. Her undivided love has made me the person I am today and I will always be indebted to her. I would also like to thank my brother who has supported me in whatever I have done, he has a wonderful insight into life and I have learnt a great deal from him.

I am extremely thankful to my partner, Anna. She has had an enormous amount of patience and love for me. Her continuous positivity and willingness to listen to my ideas as well as sharing her own, and to provide constant support has got me through my DPhil.

Last but not least, thank you to all my friends who have supported me and seen me through my educational experiences.

III. Abstract

Many epithelial cell types, particularly those in glands, employ distinct regulated and constitutive secretory pathways to perform their functions. Understanding how membrane trafficking and secretion are coupled to other cellular functions like growth, which is also thought to be linked to secretory and endocytic functions, is fundamental to cell biology and to certain pathologies such as diabetes and cancer. During my DPhil, I have been developing the secondary cells (SCs), which reside in the male *Drosophila* accessory gland, as a new *in vivo* system to dissect out the genetic regulation of membrane trafficking and its link to secretion and cell growth. SCs are epithelial cells located at the distal tip of each accessory gland. They contain a number of large intracellular compartments (>5 μm diameter) allowing membrane trafficking to be easily visualised. This in turn makes scoring specific trafficking phenotypes in normal and genetically manipulated cells very reliable.

Using imaging of both live and fixed cells, I show that SC compartments have specific Rab signatures characteristic of both secretory and endolysosomal compartments. The late endosomal and lysosomal marker, Rab7, is predominantly found on acidic compartments whilst Rab11, a slow recycling endosomal marker, is localised on the membranes of about ten non-acidic compartments containing dense-core granules (DCGs) and the protease angiotensin-converting enzyme (ANCE). I show that Rab GTPases regulate the maturation and number of compartments, the secretion of intraluminal vesicles, called exosomes, and the growth of SCs. Rab11 and Rab7 appear to control the balance between large non-acidic and acidic compartments in SCs, while Rab35, which coats smaller fast-recycling endosomal compartments (~1 μm), also controls the number of these large compartments.

BMP signalling regulates SC growth and membrane trafficking. Using knockdown experiments, I show that all components associated with BMP signalling are involved in this process. Interestingly, I demonstrate that as well as ANCE, Dpp, the fly homologue of mammalian BMP 2 and 4, is localised inside DCGs of SCs. Dpp is the predominant ligand controlling SC growth and exosome secretion via autocrine and paracrine mechanisms. Interestingly, mating elicits the secretion of DCG compartments (DCGs), a process dependent on the Synaptosomal-associated protein 24kDa, SNAP24. BMP pathway activation is also increased in a Dpp-dependent fashion, presumably as a result of Dpp secretion, and it accelerates the rate of DCG biogenesis. I propose a model in which Dpp regulates the replenishment of DCGs in response to release via an autocrine feedback loop.

IV. List of abbreviations

Abbreviations	Description
Abd-B	**Abd**ominal-**B**
Acp	**Ac**cessory gland **p**roteins
AG	**A**ccessory **g**land
ALiX	**A**poptosis **l**inked factor **X** or **AL**G-2 **i**nteracting protein **X**
ANCE	**An**giotensin-**c**onverting **e**nzyme
Arf	**A**DP-**r**ibosylation **f**actor
BMP	**B**one **m**orphogenetic **p**rotein
BMPR1A	**B**one **m**orphogenetic **p**rotein **r**eceptor, type **1A**
CA	**C**onstitutively **a**ctive
CFP	**C**yan **f**luorescent **p**rotein
COPI	**Co**at **p**rotein **I**
COPII	**Co**at **p**rotein **II**
Dad	**D**aughters **a**gainst **D**pp
DCG	**D**ense-**c**ore **g**ranule
DN	**D**ominant **n**egative
Dpp	**D**eca**p**enta**p**legic
Dsx	**D**ouble**s**e**x**
ECM	**E**xtra**c**ellular **m**atrix
ED	**E**jaculatory **d**uct
EE	**E**arly **e**ndosomes
EEA1	**E**arly **E**ndosome **A**ntigen **1**
EGFR	**E**pidermal **g**rowth **f**actor **r**eceptor
ER	**E**ndoplasmic **r**eticulum
ERES	**E**ndoplasmic **r**eticulum **e**xist **s**ite
ESCRT	**E**ndosomal **s**orting **c**omplexes **r**equired for **t**ransport
Esg	**Es**car**g**ot
GAP	**G**TPase-**a**ctivating **p**rotein
Gbb	**G**lass **b**ottom **b**oat
GEF	**G**uanine nucleotide **e**xchange **f**actor
GFP	**G**reen **f**luorescent **p**rotein
GPCR	**G**-**p**rotein-**c**oupled **r**eceptors
GPI	**G**lycosyl-**p**hosphatidyl **i**nositol
GTPase	**G**uanosine **t**ri**p**hosphat**ase**
ILV	**I**ntra-**l**uminal **v**esicle
LAMP	**L**ysosome-**a**ssociated **m**embrane **p**rotein
LDLR	**L**ow-**D**ensity **L**ipoprotein **r**eceptor
LE	**L**ate **e**ndosomes
Mad	**M**others **a**gainst **d**ecapentaplegic
MC	**M**ain **c**ell
Med	**Med**ea
mTOR(C1)	**m**echanistic **t**arget **o**f **r**apamycin (complex 1)
MVB	**M**ulti**v**esicular **b**ody
MVBL	**M**ulti**v**esicular **b**ody/ **L**ysosome
NMJ	**N**euro**m**uscular **j**unction

PI3K	**P**hospho**I**nositide 3-**K**inase
PMR	**P**ost-**m**ating **r**esponse
PtdIns()P	**P**hospho**tid**y**lin**o**s**itol-()phosphate
Pten	**P**hosphatase and **ten**sin homologue
Put	**Put**
REP	**R**ab **e**scort **p**rotein
RNAi	**RNA i**nterference
RTK	**R**eceptor **t**yrosine **k**inase
Sax	**Sax**ophone
SC	**S**econdary **c**ell
Scw	**Sc**re**w**
Snap	**S**oluble **N**SF **a**ttachment **p**rotein
SNARE	**S**oluble **N**SF **a**ttachment protein **re**ceptor
SP	**S**ex **P**eptide
Spi	**Spi**tz
SV	**S**ecretory **v**acuole
t-SNARE	**T**arget-associated SNARE
TfR	**T**rans**f**errin **r**eceptor
TGF-β	**T**ransforming **g**rowth **f**actor-**beta**
TGN	**T**rans-**g**olgi **n**etwork
Tkv	**T**hic**kv**eins
TRAPP	**Tra**nsport **p**rotein **p**article
UAS	**U**pstream-**a**ctivating **s**equence
v-SNARE	**V**esicle-associated SNARE
VAMP	**V**esicle **a**ssociated **m**embrane **p**rotein
VDRC	**V**ienna **D**rosophila **R**NAi **C**entre
Vps	**V**acuolar **p**rotein **s**orting
Wit	**Wi**shful **t**hinking
Wt	**W**ild-**t**ype
YFP	**Y**ellow **f**luorescent **p**rotein

Table of Contents

1. Introduction 20
1.1 General overview of cell secretion 21
1.2 Constitutive and regulated secretion 23
1.2.1 Transport through the Golgi 23
1.3 Dense-core granule biogenesis 24
1.4 Rab GTPases 27
1.4.1 Rab trafficking and activation 27
1.5 The endolysosomal system 30
1.5.1 Maturation of early endosomes 31
1.5.1.2 Trafficking to the lysosomes 33
1.5.2 Lysosome biogenesis 34
1.6 Exosome biogenesis and secretion 34
1.6.1 Exosome content and function 35
1.6.2 Mechanisms of exosome formation and secretion 37
1.6.3 Control of exosome secretion by Rab GTPases 38
1.7 Rab GTPases as markers of intracellular membranes 41
1.7.1 Rab function 41
1.8 Signalling and endolysosomes 43
1.8.1 Receptor signalling and endocytosis 43
1.8.2 Sustained signalling on endosomes 44
1.8.3 Lysosomal signalling 47
1.9 Limitations in studying membrane trafficking and signalling 47
1.9.1 Limitations as a result of endosome size 48
1.9.2 Difficulties in corroborating results 48
1.10 *Drosophila melanogaster* as a model genetic organism 49
1.10.1 The GAL4/UAS system 50
1.10.2 $GAL80^{ts}$ control over the GAL4/UAS system 52
1.11 The *Drosophila* accessory gland 52
1.11.1 The AG function 53
1.11.2 Female post-mating behaviour 55
1.11.3 Ovulin and sex peptide function 55
1.11.4 SCs regulate the female PMR 56
1.12 Aims and objectives 57

2. Materials and methods 59
2.1 Fly lines 60
2.2 Reagents 66
2.3 Fly food 68
2.4 Experimental approach 69
2.4.1 Fly husbandry 69
2.4.2 Using the GAL4/UAS/GAL80^{ts} system 69
2.5 Dissection of the male *Drosophila* AG 70
2.6 Immunostaining protocol for AG dissections 70
2.7 Mounting and DAPI staining 70
2.8 Lysotracker staining 71
2.9 Confocal microscopy imaging 71
2.10 Image analysis 71
2.11 Compartment quantification in SCs 72
2.11.1 Non-acidic SV compartments 72
2.11.2 Acidic compartments 72
2.12 Measurement of GFP inside acidic compartments 72
2.13 Exosome secretion assay 73
2.14 Nuclear size measurements 73
2.15 Generation of mosaic clones 73
2.16 Pulse experiments 74
2.17 Western blot analysis 74
2.18 Mating experiments 75
2.19 Female behavioural assays 76
2.20 Transmission electron microscopy 76
2.21 Statistical analysis 77

3. Characterisation of SC biology (Results I) 78
3.1 Introduction 79
3.1.1 Work completed prior to starting my DPhil 79
3.1.2 Rabs as markers of cellular compartments 80
3.1.3 Aims 81
3.2 Results 82
3.2.1 SCs contain acidic and non-acidic intracellular compartments 82
3.2.2 Age-dependent changes in the intracellular compartments of SC 85
3.2.3 Some CD63-GFP is terminally trafficked to acidic LEL compartments 87
3.2.4 SCs compartments have distinct Rab signatures 91
3.2.5 The secretory apparatus of SCs is marked by Rabs 98
3.2.6 Rab11 co-localises with Rab6 and Rab7 on some compartments in SCs 101
3.2.7 SCs compartments are highly dynamic 103
3.2.8 SCs have dynamic filopodia-like structures 106
3.2.9 Electron microscopic analysis of SCs 108
3.2.10 *Arf79F* regulates aspects of secretory trafficking in SCs 110
3.3 Discussion 112
3.3.2 Compartment maturation and directional membrane trafficking 114
3.3.3 Rab GTPases mark internal compartment identity 115
3.3.4 Membrane trafficking to DCG and LEL compartments is directed from the Golgi 117

4. Rab GTPases, SNARE proteins & V-ATPase regulate membrane trafficking, exosome secretion and cell growth (Results II) 119

4.1 Introduction 120

4.1.1 Rab proteins are regulators of membrane trafficking 120

4.1.2 SNARE proteins: regulators of membrane fusion 121

4.1.3 The V-ATPase complex: A proton pump that controls compartment acidification and membrane fusion 123

4.1.4 Aims 125

4.2 Results 126

4.2.1 Exosome secretion and their role in female physiology 126

4.2.1.1 Regulation of exosome secretion by Rab GTPases 126

4.2.1.2 SNARE proteins control exosome release in SCs 131

4.2.1.3 The V-ATPase complex regulates exosome secretion 132

4.2.1.4 Exosomes have important roles in controlling the female post-mating response 134

4.2.2 Regulation of membrane trafficking by Rab GTPases 136

4.2.2.1 Using dominant negative forms of Rab GTPases to assess their function 136

4.2.2.2 Rab5 is needed for normal formation of MVBLs and SVs 140

4.2.2.3 Rab11 controls the number of SVs and the size of the largest MVBL 142

4.2.2.4 Rab11 prevents trafficking of SV contents into the lysosome-like compartment of SCs 149

4.2.2.5 The putative Rab11 GEF TRAPPII controls similar processes to Rab11 in SCs 151

4.2.2.6 Rab35 is localised in small vesicular structures in SCs 153

4.2.2.7 Rab35 is required for trafficking of SV contents to acidic compartments and formation of the lysosome-like structure 155

4.2.2.8 Rab35 is needed for proper recycling of Rab11-positive membranes from the cell surface 159

4.2.2.9 Rab27 has no obvious effects on intracellular trafficking in SCs 161

4.2.2.10 Rab7 controls biogenesis of MVBLs 163

4.2.2.11 Rab7 and Rab35 are involved in maintaining the size of the SC lysosome-like compartment 167

4.2.3 Functions of SNAREs and the V-ATPase in regulating compartment numbers and membrane fusion in SCs 169

4.2.3.1 Synaptobrevin and Syntaxin-1A appear to control fusion of SVs 169

4.2.3.2 Snap24 regulates numbers of large acidic compartments and SVs, potentially by controlling compartment fusion 171

4.2.3.3 V-ATPases control fusion of intracellular compartments and maturation of endolysosomal compartments in SCs 174
4.2.4 Rab GTPases, SNAREs and V-ATPases control SC growth 178
4.3 Discussion 181
4.3.1 Regulation of exosome biogenesis 181
4.3.2 Biogenesis of SVs and endolysosomal maturation and growth by Rab GTPases 182
4.3.3 Fusion regulation by SNARE protein and the V-ATPase complex 184

5. BMP signalling controls SC growth, exosome secretion and dense-core granule biogenesis (Results III) 185
5.1 Introduction 186
5.1.1 Overview of BMP signalling 186
5.1.2 BMP signalling in flies 187
5.1.3 BMP signalling in controlling secretion 189
5.1.4 Dense-cored granule biogenesis 189
5.1.5 Aims 191
5.2 Results 192
5.2.1 All components of the BMP signalling pathway are involved in SC growth and trafficking 192
5.2.1.1 BMP signalling controls growth 192
5.2.1.2 BMP signalling control SC trafficking, MVBL maturation and exosome secretion 196
5.2.1.3 Dpp is the predominant ligand controlling BMP signalling in SCs .. 200
5.2.1.4 Dpp regulates BMP signalling via an autocrine feedback loop 203
5.2.1.5 Dpp controls SV numbers, MVBL maturation and exosome release 205
5.2.2 Trafficking of BMP signalling components 207
5.2.2.1 SCs endogenously express BMP receptors 207
5.2.2.2 Dpp is trafficked to dense-core granules 209
5.2.2.3 Glycophosphatidylinositol-anchored form of GFP mark DCGs 213
5.2.2.4 Driver specific effects on SC expression 214
5.2.2.5 CD63-GFP expression induces formation of DCGs 218
5.2.3 Mating-dependent DCG release 220
5.2.3.1 BMP signalling controls DCG numbers 220
5.2.3.2 Mating triggers release of DCGs 222
5.2.3.3 Readout for BMP activation 226
5.2.3.4 Mating-dependent DCG secretion is coupled to BMP activation 229
5.2.3.5 BMP signalling control mating-dependent DCG secretion 231
5.2.3.6 SNARE-mediated fusion events control DCG secretion 232
5.2.4 BMP regulation of DCG replenishment 234
5.2.4.1 Mating stimulates the formation of DCGs 234
5.2.4.2 Immature DCGs are not secreted during mating 236
5.2.4.3 DCG replenishment is dependent on BMP signalling 236
5.3 Discussion 240

5.3.2 BMP signalling controls compartment biogenesis, endolysosomal trafficking, exosome secretion and growth in SCs 242
5.3.3 Using different GAL4 drivers to study SC function 244
5.3.4 DCG formation and release is coupled to mating 245
5.3.5 Mating-dependent DCG release is accompanied by autocrine BMP activation 246
5.3.6 BMP receptor localisation 246
5.3.7 Regulation of DCG compartments by BMP signalling 247

6. Summary of results & concluding remarks 249
6.1 Summary of findings 250
6.1.1 Summary of results 250
6.2 Cell biological implications and future studies 252
6.2.1 The importance of visualising intracellular compartments 252
6.2.2 The potential of multiple mTORC1 signalling hub 253
6.2.3 Implications for the exosome field 254
6.2.4 Implications for the field of regulated secretion 255
6.3 Concluding remarks 256

7. References 258

List of Figures

Chapter 1

Figure 1.1 Constitutive and regulated secretion. 24
Figure 1.2 Dense-core granule biogenesis. 28
Figure 1.3 Regulation of Rab GTPases activity. 30
Figure 1.4 The endolysosomal system. 34
Figure 1.5 Exosome secretion and signalling. 39
Figure 1.6 Schematic representation of the V-ATPase complex. 43
Figure 1.7 The GAL4/UAS expression system. 55
Figure 1.8 The *Drosophila* accessory gland 58

Chapter 3

Figure 3.1 SCs contain large intracellular compartments 88
Figure 3.2 Age-dependent changes in SVs and endolysosomal compartments. 90
Figure 3.3 CD63-GFP traffics towards MVBLs. 94
Figure 3.4 Rab GTPases mark distinct intracellular compartments in SCs. 99
Figure 3.5 Rab5 and FYVE-domain containing protein co-localise. 100
Figure 3.6 Secretory vacuoles containing ANCE are marked with Rab11 and sometimes Rab7. 101
Figure 3.7 Secretory apparatus is marked by Rab gene traps. 104
Figure 3.8 Rab GTPases co-localise on the same compartments in SCs. 106
Figure 3.9 Secretory and endolysosomal compartment fuse together. 108
Figure 3.10 Tubules extend from late endosomal compartments. 109
Figure 3.11 SCs have dynamic filopodia-like extensions. 111
Figure 3.12 Electron microscopy of the accessory gland and SCs. 113
Figure 3.13 Arf79F controls trafficking out of the Golgi. 115
Figure 3.14 Schematic representation of SCs compartments. 117

Chapter 4

Figure 4.1 Rab GTPases control secretion of exosomes. 134

Figure 4.2 Exosome secretion is dependent on SNAREs. 135

Figure 4.3 The V-ATPase complex is involved in exosome release 137

Figure 4.4 Male-derived exosomes are important for controlling the female post-mating response. 139

Figure 4.5 Dominant negative and constitutively active Rabs have variable phenotypes 142

Figure 4.6 CD63-GFP can be detected in the largest acidic compartments using antibody staining. 143

Figure 4.7 Rab5 regulates formation of secretory vacuoles and multivesicular bodies/ lysosomes. 145

Figure 4.8 Rab11 knockdown induces a strong reduction in Rab11 protein levels. 148

Figure 4.9 Rab11 knockdown decreases numbers of SVs and increases the size of the largest MVBL in SCs. 150

Figure 4.10 Overexpressing Rab11 increases SV numbers and decreases the maturity of the largest MVBL in SCs. 152

Figure 4.11 Rab11 controls trafficking of SVs towards MVBLs. 154

Figure 4.12 TRAPPII controls similar processes to Rab11. 156

Figure 4.13 Rab35 localises to small cytoplasmic vesicles. 158

Figure 4.14 Rab35 is involved in the formation of SVs and MVBLs. 161

Figure 4.15 Overexpression of Rab35 has no effect on trafficking 162

Figure 4.16 Rab35 is required for normal trafficking of Rab11 164

Figure 4.17 Rab27 is potentially involved in intraluminal vesicle formation. 166

Figure 4.18 Rab7 RNAi induces strong knockdown 168

Figure 4.19 Overexpressing Rab7 does not changes SC trafficking. 168

Figure 4.20 Rab7 is involved in biogenesis of MVBLs. 169

Figure 4.21 Knockdown of Rab7 disrupts Golgi distribution 170

Figure 4.22 Rab7 and Rab35 are involved in maintaining MVBL structure. 172

Figure 4.23 Synaptobrevin and Syntaxin1a control fusion of SVs to MVBLs. 175

Figure 4.24 Snap24 regulates fusion of SVs and MVBLs. 177

Figure 4.25 Snap24 control the number of Rab7 positive compartments 178

Figure 4.26 V-ATPase is normally expressed in SCs. 180

Figure 4.27 Trafficking analysis of V-ATPase knockdown. 181

Figure 4.28 Trafficking quantification for V-ATPase knockdown. 182

Figure 4.29 Rab GTPases control SC growth 184

Figure 4.30 Rab GTPases, Snap24 and the V-ATPase complex control SC growth. 185

Chapter 5

Figure 5.1 BMP signalling in mammals and flies. 193
Figure 5.2 All BMP signalling components regulate SC growth. 199
Figure 5.3 Expression of transgene in SCs requires GAL4 driver. 200
Figure 5.4 RNAi induces strong knockdown. 200
Figure 5.5 Multiple BMP signalling components in SCs regulate numbers of SVs, endolysosomal maturation, largest MVBL size and exosome secretion. 204
Figure 5.6 Dpp regulates SC growth in the AG. 206
Figure 5.7 Autocrine Dpp signalling controls SC growth. 208
Figure 5.8 Dpp regulates SC trafficking. 210
Figure 5.9 SCs endogenously express BMP receptors 212
Figure 5.10 Gbb localises to Rab35 compartments. 214
Figure 5.11 Dpp is localised inside dense-cored granules. 216
Figure 5.12 GPI-GFP marks dense-cored granules 217
Figure 5.13 SC GAL4 drivers drive expression of UAS construct at similar levels. 221
Figure 5.14 CD63-GFP expression induces formation of dense-cored compartments. 223
Figure 5.15 BMP signalling regulates dense-core granule numbers. 225
Figure 5.16 Mating stimulates the release of dense-cored granules. 229
Figure 5.17 pMAD is a reliable readout for BMP activation 232
Figure 5.18 Mating results in BMP activation in SCs. 234
Figure 5.19 BMP signalling is involved in the release of dense-cored compartments. 235
Figure 5.20 Snap24 regulated mating-dependent dense-core granule secretion. . 237
Figure 5.21 Mating accelerates the formation of dense-core granules 239
Figure 5.22 Rapid replenishment of DCGs after mating is BMP-dependent. 243
Figure 5.23 Model to explain autocrine regulation of DCG replenishment by BMP signalling in SCs. 245

List of Tables

Table 1.1 List of the conservation, localisation and function of Rab GTPases between *H.sapiens* and *D.melanogaster*. 29
Table 2.1 GAL4 drive lines 60
Table 2.2 SC Compartment characterisation 61
Table 2.3 Rab lines 62
Table 2.4 Other Rab lines 63
Table 2.5 BMP signalling lines 63
Table 2.6 V-ATPase lines 65
Table 2.7 SNARE lines 65
Table 2.8 Miscellaneous UAS-RNAi lines 66
Table 2.9 Buffers and solutions 66
Table 2.10 Primary antibodies 67
Table 2.11 Secondary antibodies 68
Table 2.12 Recipe of fly food 68

1. Introduction

1.1 General overview of cell secretion

In order to understand whole organism physiology, one must appreciate the cellular constituents that contribute to it. Furthermore, unravelling the sub-cellular machinery that drives aspects of individual cellular behaviour remains critical in understanding how phenotypes and pathologies develop. One biological process that is of high interest to cell biologists is the formation of intracellular compartments and secretion of their contents. This simple, yet elusive process involves the control of membrane biogenesis and trafficking, and has been studied extensively across various model organisms.

There are two major pathways by which proteins made in the endoplasmic reticulum (ER) are secreted. In brief, during the transit along the secretory pathway, proteins and other secreted cargo move from the ER towards the *cis*-Golgi and finally arrive at the *trans*-Golgi via a series of vesicular structures and tubules (Figure 1.1) (Burgess and Kelly, 1987). At this stage, proteins destined for constitutive secretion are sorted in vesicles that subsequently fuse with the plasma membrane, whereas during regulated secretion, cargos are aggregated into dense-core granules and are only released after a specific signal (Burgess and Kelly, 1987). Significant insights into the secretory pathway have been gained by studying how viruses enter and exit cells and with the advent of live microscopy in combination with green fluorescent protein (GFP) (Kaether and Gerdes, 1995), some of the dynamic mechanistic details have started to be uncovered.

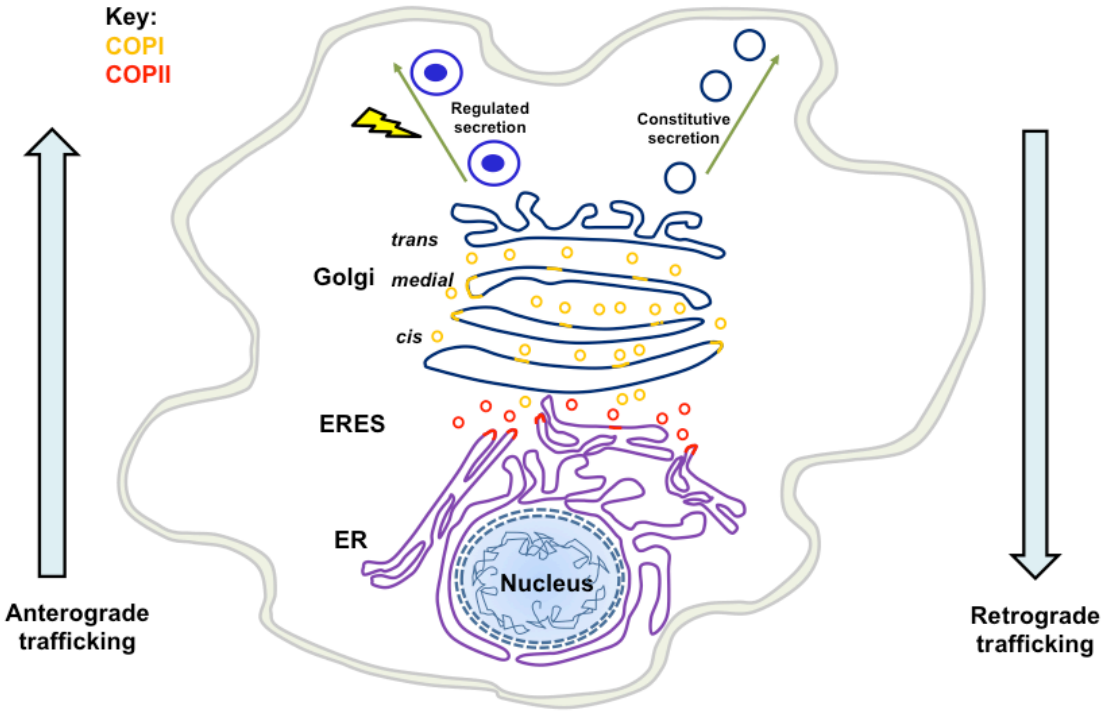


Figure 1.1 Constitutive and regulated secretion.

Molecules destined for secretion are trafficked through the endoplasmic reticulum (ER) and are localised at ER exit sites (ERES). This anterograde movement is regulated by COPII vesicles which facilitate the arrival of cargo at the *cis*-Golgi. Through various pathways, proteins are transported through the different sections of the Golgi until they reach the *trans*-Golgi region. Here, proteins destined for regulated secretion are aggregated to form dense-core vesicles that bud from *trans*-Golgi tubules, where they await a signal to permit their secretion. Retrograde traffic enables the backward movement of molecules towards the ER, a process regulated by COPI. Proteins destined for constitutive secretion are trafficked into vesicles that also bud from the *trans*-Golgi. They are secreted without the need for a specific stimulus.

1.2 Constitutive and regulated secretion

Secretion via the constitutive pathway serves as an integral part of almost all eukaryotic cell functions such as transporting receptors and adhesion molecules to the plasma membrane to permit cell-cell signalling, cell growth and cell differentiation (Farhan and Rabouille, 2011). Generally, this pathway occurs at a constant level and does not need a specific signal to stimulate the release of cargo. However, anterograde (forward) trafficking can be diverted along other pathways and some cargos can be retrieved by retrograde (backward) trafficking prior to secretion, processes that are highly regulated (Figure 1.1). Randy Schekman, Thomas C. Südhof, and James Rothman shared the 2013 Nobel Prize in Physiology or Medicine for uncovering some of the proteins involved in controlling part of this pathway ("for their discoveries of machinery regulating vesicle traffic, a major transport system in our cells" – Nobel prize announcement press release 2013).

1.2.1 Transport through the Golgi

Newly synthesised proteins destined for secretion are transported on the projections that emanate from the ER exit sites (ERES) to the *cis*-Golgi (Figure 1.1). During this process, cargos are concentrated in distinct domains at the ERES projections, which are enveloped by coat protein II (COPII), the main regulator of anterograde trafficking (Stephens, 2003). Subsequently, with the aid of microtubule-driven traffic, COPII-positive vesicles bud off and move towards the *cis*-face of the Golgi, where their contents are transferred into the lumen of cisternae (Yoshihisa et al., 1993, Novick et al., 1981). This is a multistep process, requiring a variety of different proteins that control the motility of vesicles and their tethering, docking and fusion to the Golgi membrane (Brandizzi and Barlowe, 2013). Retrograde traffic, involving COPI-coated vesicles, delivers proteins back to the ER as part of a quality control mechanism to

ensure that ER-resident proteins are in their appropriate location and to prime the next set of vesicles for another round of anterograde transport (Figure 1.1) (Spang, 2013).

The polarized nature of the Golgi complex gives a natural pathway for the movement of secreted molecules. Once at the Golgi, these molecules undergo heavy post-translational modification *en route* to the terminal stacks (Novick et al., 1980) There are several models proposed to describe how secreted proteins are trafficked through the different regions of the Golgi. In the vesicular model, Golgi cisternae are static and cargos are transported between different stacks via small vesicular compartments. In contrast, the cisternal-maturation/ progression model predicts that cargos remain in the lumen of cisternae which mature/progress in a directional manner from *cis* to *trans* (Emr et al., 2009). A somewhat older model that has been recently revived suggests that the progression towards the *trans* stacks is mediated by tubular extensions (Mironov et al., 2005).

Whatever the mechanism of cargo movement may be, proteins are directionally transferred from *cis*- to *trans*-Golgi network (TGN) where they accumulate in distinct regions of tubules that extend from the TGN. In specialised secretory cells, vesicles are seen to bud from specific microdomains of tubules and ultimately fuse with the plasma membrane in a regulated fashion (De Matteis and Luini, 2008). Studies into how proteins aggregate into dense-cored vesicles have revealed that the lipid composition or specific receptors present on their membrane may facilitate the selection of cargo destined for regulated release (Kim et al., 2006).

1.3 Dense-core granule biogenesis

The biogenesis of dense-core granules (DCGs) is important for mass secretion of proteins such as insulin, renin and peptides derived from proopiomelanocortin e.g adrenocorticotropic hormone (Kim et al., 2006). Formation of DCGs at the TGN (Figure

1.2) is a highly regulated event and one of the best candidates implicated in this process are granins (Meldolesi et al., 2004). This family of proteins are involved in the driving force needed to form DCGs at the TGN. Kim et al 2001 illustrated that silencing of Chromogranin A lead to a reduction of DCGs whilst its overexpression induces DCG formation in neuroendocrine cells. The authors concluded that Chromogranin A functions as an on/off switch for DCG biogenesis (Kim et al., 2001). Further studies have established a role for cholesterol in curving membrane and in creating lipid rafts domains that give rise to DCGs (Wang et al., 2000).

DCGs are packaged with a variety of different proteins. Indeed, by segregating proteins into DCGs, it provides them with a unique microenvironment that is necessary for their post-translation modification (Kim et al., 2006). For example, in newly formed DCGs, proinsulin is modified into its mature active form (Hou et al., 2009) . How specific proteins are directed into DCGs remains an actively debated subject. One model proposes that specific sorting receptors residing at the TGN function to capture granule-destined proteins (Figure 1.2) (Dikeakos and Reudelhuber, 2007). Whilst another model suggests that all proteins are directed towards DCGs and during DCG maturation, proteins destined for constitutive secretion are funnelled into low-density vesicles secreted constitutively (Dikeakos and Reudelhuber, 2007). Irrespective of the sorting mechanism, once DCGs are loaded with proteins they await a specific signal to permit their secretion.

Newly formed immature DCGs must undergo a maturation program to convert them into a mature form (Figure 1.2) (Kim et al., 2006). This process involves acidification of their lumen, a process regulated by the V-ATPase proton pump (Taupenot et al., 2005). Not only is the acidification of DCGs important for the association of granins with lipid rafts to initiate the DCG formation but also for processing the proteins residing in the dese-core region (Tanaka et al., 1997). In some cell types, maturation of DCGs

also requires homotypic fusion involving the fusion regulator SNAREs (Urbe et al., 1998). Mature DCGs are stored until a secreting signal stimulates the cell, causing DCGs to fuse to the plasma membrane in a process regulate by SNAREs and Rab GTPases (Figure 1.2) (Hou et al., 2009).

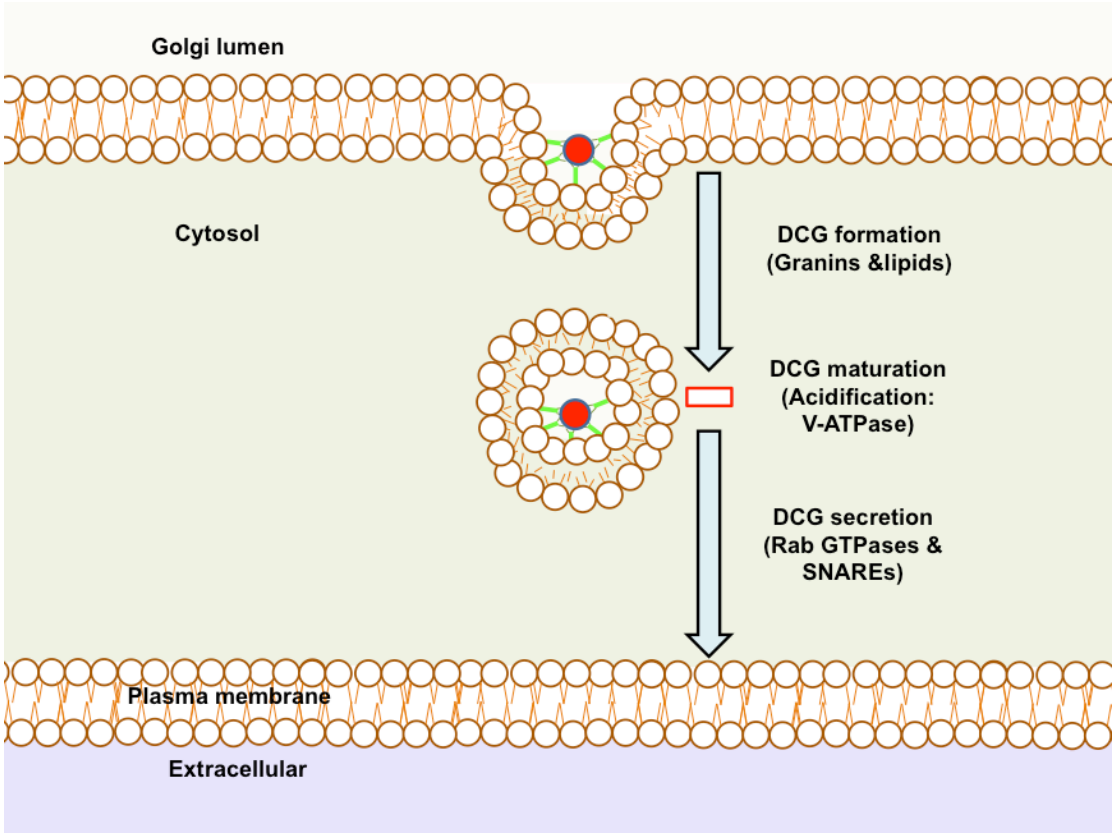


Figure 1.2 Dense-core granule biogenesis.

There are several mechanisms involved in sorting proteins destined for regulated secretion into dense-cored granules (DCGs). One mechanism is by the action of specific 'sorting receptors' (highlighted in green lines) present at the Golgi, which facilitates the inclusion of proteins into dense-cores. Once formed, DCGs undergo a maturation program involving acidification until they are competent for secretion. DCGs are secreted following a specific signal, a process regulated by Rab GTPases and SNARE proteins.

1.4 Rab GTPases

Rab GTPases are found in all eukaryotes and are considered to be the largest class in the small Ras-like GTPase family. Rab GTpases are highly conserved between mammles and flies (Table 1.1). They are also markers of different organelles (Barr, 2013). When active, Rabs bind to a variety of different effector proteins and impinge on almost all membrane trafficking pathways including but not limited to vesicles recognition, vesicle motility, membrane tethering, and membrane fusion (Barr, 2013, Stenmark, 2009). Indeed, in order for these complex processes to be faithfully executed, the identity of organelles must be maintained at all times, a process involving Rab proteins (Grosshans et al., 2006).

1.4.1 Rab trafficking and activation

Upon synthesis, inactive Rab proteins are chaperoned by Rab escort protein (REP) to Rab geranylgeranyltransferase, which ensures Rabs are prenylated to facilitate their delivery onto membranes. GDP dissociation inhibitor (GDI) dissociation factor (GDF) prevents GDP release from Rabs (Matsui et al., 1990) and assists the insertion of Rab proteins onto targeted membrane (Ullrich et al., 1994). Activation of Rabs is achieved once it is bound to GTP, a process that is catalysed by specific Guanine nucleotide exchange factors (GEFs), which exchanges GDP with GTP (Figure 1.3) (Barr and Lambright, 2010). As previously mentioned, active Rabs can interact with a variety of effector proteins to execute changes in the flow of membrane trafficking. Because of their intrinsic GTPase activity, Rab proteins switch themselves off, but this process typically needs to be catalysed by specific GTPase-activating proteins (GAPs) that bind GTP-bound Rabs and promote hydrolysis of GTP to GDP (Figure 1.3) (Barr and Lambright, 2010). A major function of Rab proteins is their ability to regulate endolysosomal maturation.

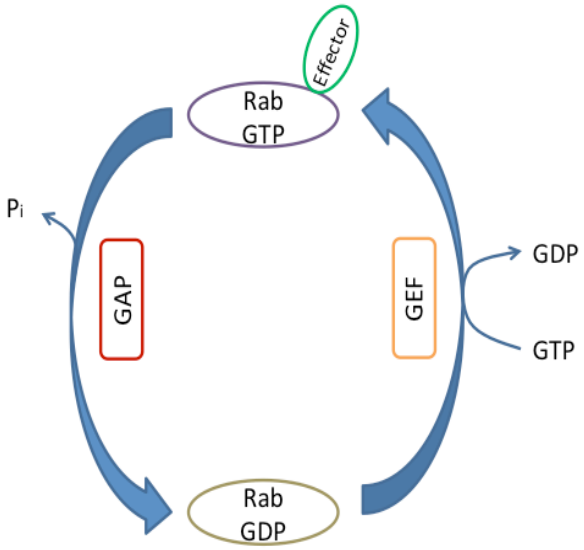


Figure 1.3 Regulation of Rab GTPases activity.

Rab activation is achieved once it is bound to GTP, a process catalysed by Guanine nucleotide exchange factors (GEFs). Upon activation, Rab proteins interact with effector proteins to regulate membrane trafficking. GTPase-activating proteins (GAPs) interact with GTP-bound Rabs to catalyse the hydrolysis of GTP to GDP and bring about the inactivation of Rab proteins.

Table 1.1 List of the conservation, localisation and function of Rab GTPases between *H.sapiens* and *D.melanogaster*.

H. sapiens	*D. melanogaster*	Localisation	Function
Rab1a,b	Rab1	ER/*cis*-Golgi	ER-Golgi transport
Rab2a,b	Rab2	ER/*cis*-Golgi	Retrograde transport golgi-ER.
Rab3a,b,c,d	Rab3	Synaptic vesicles	Neurotransmitter release by exocytosis
Rab4a,b	Rab4	EEs, REs	Invovled in transport and recycling protein from PM
Rab5a,b,c	Rab5	Phagosomes, EEs, CCV, PM	EE fusion
Rab6,b,c	Rab6	Golgi	Intra-Golgi transport and ER-Golgi trafficking
Rab7	Rab7	LE, MVBs, lysosomes	Late endosomes to lysosome conversion
Rab8a,b	Rab8	TGN, PM	Recycling proteins from TGN and PM
Rab9a,b	Rab9	LEs	Retrograde transport from endosome to TGN
Rab10	Rab10	ER	Recycling proteins from TGN and PM
Rab11a,b	Rab11	RE, TGN	Recycling proteins from TGN and PM, MVB secretion
Rab12		REs	Exocytosis
Rab13		REs, TGN, BPM	Recycling proteins from TGN and PM
Rab14	Rab14	ER, TGN, golgi, EEs	Apical membrane trafficking and TGN to PM transport
Rab15		EEs, REs	Sorting proteins to PM from endosomes and RE
Rab17		Melanosomes, REs	Transcytosis
Rab18	Rab18	Lipid droplets	Lipid droplet formation
Rab19	Rab19	Golgi	Unknown
Rab20		Macropnocytic cups, LEs, mitochondria	Recycling at the apical membrane
Rab21	Rab21	EEs	Involved in endocytosis
Rab22a,b,c		EEs	Endosomal transport and trafficking to the PM
Rab23	Rab23	PM, endosomes	Involved in transport to PM and recycling proteins
Rab24		ER	Autophagosome biogenesis
Rab25		RE	RE to PM trafficking
Rab26	Rab26	Melanosomes	Exocytosis

Rab27a,b	Rab27	MVBs, Melanosomes	Exocytosis, MVB secretion
Rab28		Unknown	Unknown
Rab29		*cis*-Golgi, TGN, RE, EE	Ciliogensis
Rab30	Rab30	ER, Golgi	Maintain structural integrity of Golgi
Rab32	Rab32	Mitochondria, melanosomes	Mitochondrial fusion, transport to melanosomes from TGN
Rab33a,b		DCG, Golgi	Autophagasome formation
Rab34		Golgi, macropinosomes	Intra-Golgi transport, lysosome positioning
Rab35	Rab35	Fast RE, PM	Fast recycling to PM, MVB secretion
Rab36		Golgi	Spatial distribution of LE/ Lysosomes
Rab37		Secretory granules	Exocytosis
Rab38		Melanosomes	Involved in TGN to melanosome trafficking
Rab39a,b	Rab39	Golgi	Involved in endocytosis
Rab40a,b,c	Rab40	Golgi, RE	Endosome trafficking and transport
Rab41		Golgi	ER-Golgi trafficking
Rab42		Unknown	Unknown
Rab43		ER, Golgi	ER-Golgi trafficking
Rab44		Unknown	Unknown
Rab45		ER, Golgi	Invovled in P38-mediated apoptosis

1.5 The endolysosomal system

The endolysosomal system consists of a series of compartments that are distinguished by their morphology, membrane composition, luminal acidity and content (Figure 1.4) (Huotari and Helenius, 2011). At the start of this pathway lies the early endosomes (EEs), which receive input from the plasma membrane after endocytosis – a process involving invagination of membrane to form internal vesicles carrying extracellular cargo and plasma membrane constituent's e.g signalling receptors (Doherty and McMahon, 2009). Endocytosis involves multiple routes, comprising both clathrin-dependent and -independent pathways. In most cases, these newly formed vesicles traffic towards and fuse with the EEs to transfer their contents (Doherty and McMahon, 2009).

1.5.1 Maturation of early endosomes

The EE is a dynamic organelle with numerous tubules that extend to different regions of the cell (Figure 1.4). Like the Golgi, EEs are also major sorting hubs. Some proteins can return back to the plasma membrane via recycling endosomes e.g. transferrin receptor (TFR) and Low-Density Lipoprotein Receptor (LDLR) (Grant and Donaldson, 2009), whereas other proteins that regulate membrane fusion such as the *S. cerevisiae* SNARE, Snc1, undergo retrograde traffic from EEs to the TGN where they are repackaged onto new vesicles (Lewis et al., 2000). Alternatively, EEs can undergo a maturation program involving remodelling their surface molecules and changing their luminal acidity through the action of the V-ATPase complex (Huotari and Helenius, 2011, Hurtado-Lorenzo et al., 2006). As such, the pH decreases from roughly 6.5 in EEs to around 4.8 in lysosomes. This drop in acidity triggers the release of ligand-receptor complexes to allow recycling of membrane bound-receptors and ultimately activates pH-sensitive proteases to degrade the luminal material when it is delivered to lysosomes (Ukkonen et al., 1986, Zhao et al., 2014).

As EEs start to mature along the endolysosomal pathway, they begin to accumulate intraluminal vesicles (ILVs) that are formed by the inward budding and scission of the limiting membrane (Thery et al., 2002). During this period, EEs undergo an identity change by exchanging Rab GTPases (Deretic, 2005). The late endosomal multivesicular body (LE)/MVB marker Rab7, through a process known as Rab conversion, rapidly replaces Rab5 on the membrane of EEs (Figure 1.4) (Rink et al., 2005). The molecular switch controlling this transition has been identified as SAND-1/Mon1 in *Caenorhabditis elegans,* which regulates the localisation of Rab5 and Rab7 GEFs (Poteryaev et al., 2010). For simplicity, the transition from EE to LE/MVBs is here referred to as a stepwise event, not involving intermediary compartments as suggested in other models and reviewed by (Huotari and Helenius, 2011) .

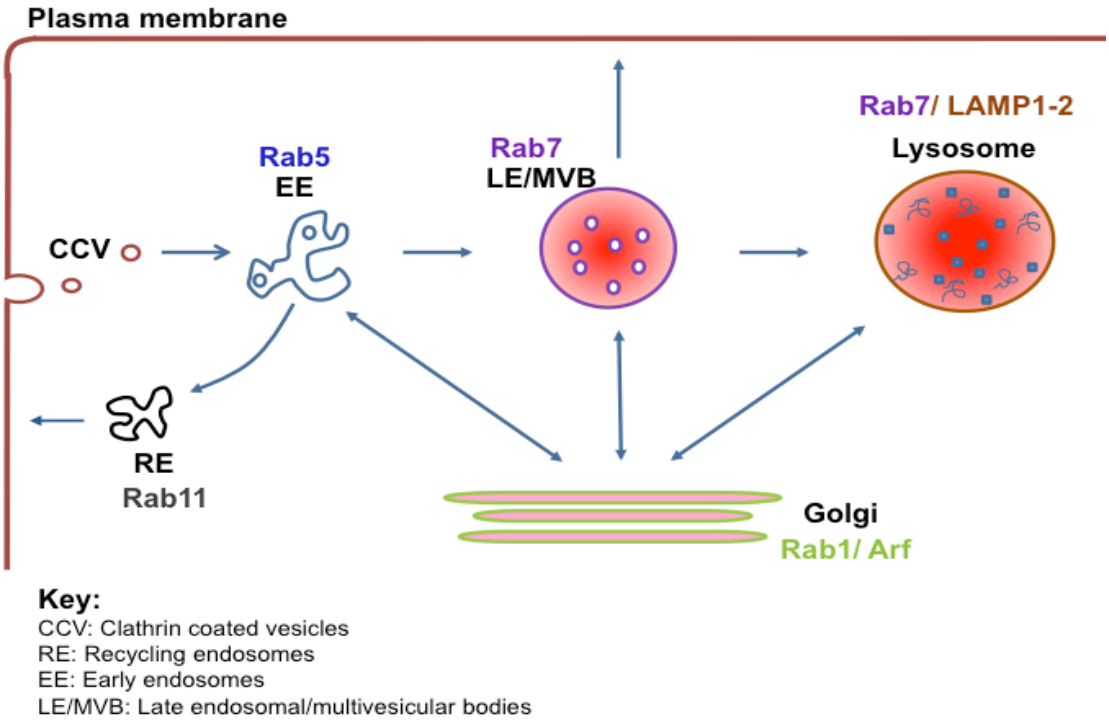


Figure 1.4 The endolysosomal system.

Endocytosis results in the internalization of extracellular molecules and plasma membrane in clathrin coated vesicles (CCV) which traffic towards early endosomes (EE). At this point, proteins can be recycled back to the plasma membrane by recycling endosomes (RE). Early endosomes can mature into late endosomes/ multivesicular bodies (LE/MVB) by undergoing a Rab switch, the process of exchanging Rab5 for Rab7. LE/MVB accumulate many intraluminal vesicles that can be secreted if LE/MVBs fuse with the plasma membrane. Alternatively, LE/MVBs can fuse with lysosomes to initiate the degradation of their luminal content. The Golgi sits at the centre of this pathway giving and receiving materials from EE, LE/MVBs and lysosomes.

1.5.1.2 Trafficking to the lysosomes

The LE/MVB continues to mature and accumulate even more ILVs through the sequential action of endosomal sorting complex required for transport (ESCRT-0, I, II, III) and ALG-2 Interacting protein X (ALiX) which is an ESCRT-III-binding protein and involved in the abscission of ILVs (Babst, 2011). Together, these proteins also control the sorting of ubiquitinated cargo into ILVs (Katzmann et al., 2001). Recently, it has been shown that ILV formation terminates receptor signalling by depriving receptors from contact with the cytosol where downstream signalling targets are located (Zhang et al., 2000, Lloyd et al., 2002). Moreover, particularly since ILVs are thought to be devoid of a protective glycocalyx, they are also suggested to facilitate the degradation of membrane and lipids when LE/MVBs fuse to the lysosomes (Huotari and Helenius, 2011).

There are numerous models proposed to explain how material from the LE/ MVBs reaches the lysosomes (Figure 1.4) (Luzio et al., 2007). In the vesicular model, LE/MVBs contents are transferred to the lysosomes by intermediary vesicles that bud from the late endosomal compartments. In the second model, LE/MVBs transiently ‘’kiss’’ the lysosomal compartment (Storrie and Desjardins, 1996). During this brief period, materials are exchanged and the LE/MVB subsequently retracts, e.g. ‘’runs’’. Alternatively, the late endosomal compartments may fuse with the lysosomes forming a hybrid compartment that effectively behaves as a lysosome (Luzio et al., 2010). None of these models, however, have explicitly been proven, and it is likely that certain cell types adopt different strategies for trafficking material to the lysosomes.

1.5.2 Lysosome biogenesis

The biogenesis of the lysosomes is central to degradation and recycling of incoming material from earlier compartments and the Golgi (Saftig and Klumperman, 2009). Lysosomes, as well as late endosomes, are also major regulators of the overall growth of cells by serving as a nutrient-sensing hub (Settembre et al., 2013, Kim et al., 2008). While its importance is clear, differentiating the LEs/MVBs from lysosomes is a current challenge in the field. Many researchers use the Lysosomal associated membrane proteins 1 and 2 (LAMP1/2) as markers of lysosomes (Fukuda, 1991), yet their presence is also observed on LEs (Falcon-Perez et al., 2005). Moreover, lysosomes also lack a unique Rab signature, since like LE/MVBs, they are also Rab7-positive (Humphries et al., 2011).

The lack of lysosomal specific markers is most likely because the endocytic pathway is a continuum of constantly maturating compartments. As such, the gold standard method to identify these organelles is by their electron dense appearance under an electron micrograph (Jonek et al., 1971). Lysosomes seem to indirectly acquire lysosome-specific hydrolases from the TGN where they are tagged with the targeting signal mannose-6-phosphate (Rohrer and Kornfeld, 2001). As mentioned previously, the drop in pH accompanied by the acquisition of specific hydrolases triggers the degradation of internal material. Interestingly, recent studies have highlighted that in a subset of specialised cells, lysosomes are secreted (Blott and Griffiths, 2002), and serve to facilitate bone resorption (Baron et al., 1985).

1.6 Exosome biogenesis and secretion

There is an alternative route for LE/MVBs to take, which involves travelling towards the plasma membrane and fusing with it to release their ILV content as exosomes into the extracellular milieu (Colombo et al., 2014). Research into the function of exosomes

has had a massive revival over the last decade. From their initial characterisation as ‘’rubbish bags’’ used to jettison unwanted protein, exosomes are now thought to also signal to other cells and reprogramme their behaviour (Colombo et al., 2014). This ability arises because exosomes carry a plethora of signalling proteins, in some instances both ligand and receptor complexes, as well as RNAs and DNAs that are thought to elicit signals when taken up by recipient cells (Figure 1.5)(Tkach and Thery, 2016). What causes LE/MVBs to either fuse with lysosomes or the plasma membrane is not entirely understood. Indeed, by committing to one pathway there is bound to be material that would otherwise be destined for another. It remains to be seen if there are sub-classes of LE/MVBs that potentially fuse selectively either with lysosomes or the plasma membrane.

1.6.1 Exosome content and function

Exosomes further extend the signalling capabilities of cells to more than just cell-cell contact and ligand-receptor interactions. Several recent studies have highlighted the diverse roles of these nanovesicles and are reviewed in (Kourembanas, 2015, Raposo and Stoorvogel, 2013). A landmark paper in the cancer field suggested that exosomes educate distant sites and prime them for incoming metastatic invasion (Costa-Silva et al., 2015). Park *et al* (2011) showed that exosomes, derived from prostate cells, transfer the progesterone receptor and calcium signalling tools to sperm, potentially increasing motility (Park et al., 2011), although this has been disputed. In our lab, we have shown that exosomes from male flies are transferred to females during mating, where they also fuse with sperm and interact with other cells in the female reproductive tract to control her behaviour (Corrigan et al., 2014). Exosomes can therefore act as signalling exchangers between organisms.

Since exosomes are derived from ILVs formed in endolysosomal compartments, they carry different cargos to other secreted vesicles such as microvesicles, which bud from the plasma membrane (Kowal et al., 2016, Thery et al., 2002). These specific exosome markers include proteins enriched in endolysosomal membranes. For example, CD9, CD63, and CD81 are four transmembrane domain-containing tetraspanins typically identified in exosome samples. Whilst the use of tetraspanins as exosome markers is common in the field, they are by no means a gold standard, since they can be found on other compartments and vesicles (Kowal et al., 2016).

When imaged by electron microscopy, exosomes isolated by standard techniques like ultracentrifugation appear cup-shaped and are roughly 40-110 nm in diameter, smaller than most microvesicles secreted from the plasma membrane (110-1000nm) (Lobb et al., 2015). Other techniques used to profile exosomes include Nanoparticle tracking which uses Brownian motion to assign size to vesicles (Mehdiani et al., 2015). A standard practice has been to combine these methods to provide more conclusive evidence that isolates contain exosomes.

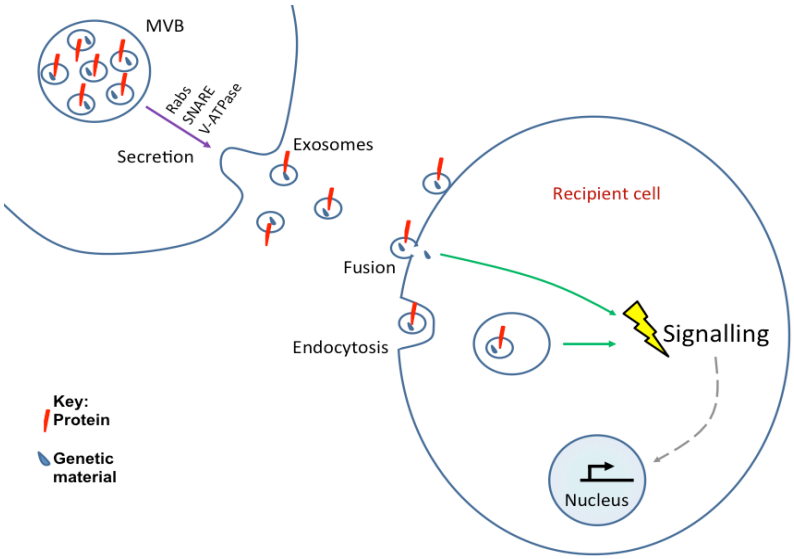


Figure 1.5 Exosome secretion and signalling.

Exosomes formed inside late endosomal multivesicular bodies (MVBs) are secreted once MVBs fuse with the plasma membrane. Exosomes carry genetic material and proteins that are capable of regulating gene expression once internalised by recipient cells.

1.6.2 Mechanisms of exosome formation and secretion

The ESCRT machinery has a central role in the formation of ILVs and the sorting of ubiquitinated cargo into newly formed vesicles. ESCRT-0, I and II have roles in recognising and clustering ubiquitinated proteins prior to their inclusion on ILVs (Bilodeau et al., 2002, Shields et al., 2009), whereas ESCRT-III deforms the limiting membrane and is involved in the final scission events (Wollert et al., 2009). More recently, it was shown that syntenin, a PDZ-domain containing protein, binds to ALiX, which in turn recruits the ESCRT-III complex to begin the formation of ILVs (Baietti et al., 2012). However, an ESCRT-independent mechanism has also been described in oligodendroglial cell lines, which uses sphingomyelinase to produce ceramide lipids to initiate membrane curvatures (Trajkovic et al., 2008).

The trafficking of MVBs towards the cell surface and the final fusion event with the plasma membrane is highly regulated. SNARE proteins are well documented for their involvement in fusing membranes together. Briefly, SNARE proteins on vesicles (v-SNAREs) couple to and form a complex with SNAREs on targeting membranes (t-SNARE) to overcome the repulsive forces between the two membranes and form a fusion pore (Chen and Scheller, 2001). VAMP7 (v-SNARE) has been implicated in MVB exocytosis in the human leukemia K562 cell line (Fader et al., 2009). Recently, Ykt6, a SNARE protein, was shown to control the secretion of Wnt-positive exosomes (Gross et al., 2012). Interestingly, increased intracellular calcium triggers SNARE-mediated fusion events, and its involvement in exosome secretion has been reported (Savina et al., 2003). Aside from its role in acidifying compartments, the V-ATPase proton-pumping complex also appears to be involved in membrane fusion (Merz, 2015). In *C. elegans*, the V_0 multi-subunit complex, which spans the lipid bilayer, has been proposed to regulate MVB secretion (Figure 1.6) (Liegeois et al., 2006). How the

V_0 complex controls this process is not yet known, though it may involve recruiting SNARE proteins.

1.6.3 Control of exosome secretion by Rab GTPases

Rab GTPases are one of the most studied regulators of exosome secretion (Figure 1.5). By overexpressing dominant negative constructs, Savina et al (2002) was the first to show that Rab11 controls TfR-positive exosome secretion in K562 cells (Savina et al., 2002). It was later proposed that Rab11 exerts this action by promoting docking and fusion of MVBs to the plasma membrane in a calcium-dependent manner (Savina et al., 2005). Although a GFP-tagged version of Rab11 localises to the limiting membrane of MVBs in these cells (Savina et al., 2005), in many other systems it primarily decorates recycling endosomes and early sorting endosomes (Lock and Stow, 2005). It remains unclear if the localisation of Rab11 on MVBs could be a result of overexpression of a tagged construct, and the effects on exosomes secretion might be due to altered trafficking upstream or downstream of MVB secretion.

In screening GTPase-activating proteins (GAPs) as potential Rab regulators, Hsu et al (2010) found that three GAPs controlling the fast recycling marker, Rab35, perturbed exosome release from oligodendrocytes. Knockdown and expression of a dominant negative form of Rab35 revealed that it was involved in docking MVBs to the plasma membrane (Hsu et al., 2010). In the same year, Rab27A/B was also shown to play a crucial role in exosome secretion (Ostrowski et al., 2010). The authors showed that Rab27B was needed for the movement of MVBs, whereas Rab27A was involved in the fusion and docking of MVBs to the plasma membrane. Additionally, Rab2B, Rab5A, Rab7 and Rab9A are also implicated in exosome secretion (Colombo et al., 2014).

Although these findings are important, the role of Rab proteins in exosome secretion in other cell types seems to be more controversial. For example, in *Drosophila* S2 cells, Wingless/Evi-positive exosome (Evi is a receptor for Wnt protein) secretion was severely affected when Rab11 was silenced, whereas these effects were not seen when Rab27 and Rab35 were down-regulated (Beckett et al., 2013). Importantly, it remains to be seen if these differences reflect the fact that certain Rabs are involved in cell type-specific exosome secretion or that they control the secretion of different populations of endolysosomal compartments.

When Rab GTPases are active, they bind to a variety of different effector proteins to control membrane trafficking (Barr, 2013). Although no examples are currently identified, some of these effectors may be involved in the movement of LE/ MVBs *en route* to the plasma membrane. Interestingly, Rab27 has been shown to bind to the myosin V motor protein (Jordens et al., 2006), whilst Rab11 binds myosin Vb (Gidon et al., 2012). Though not confirmed yet, the binding of Rabs to motor proteins may trigger the actin-guided movement of LE/MVBs towards the cell surface prior to secretion.

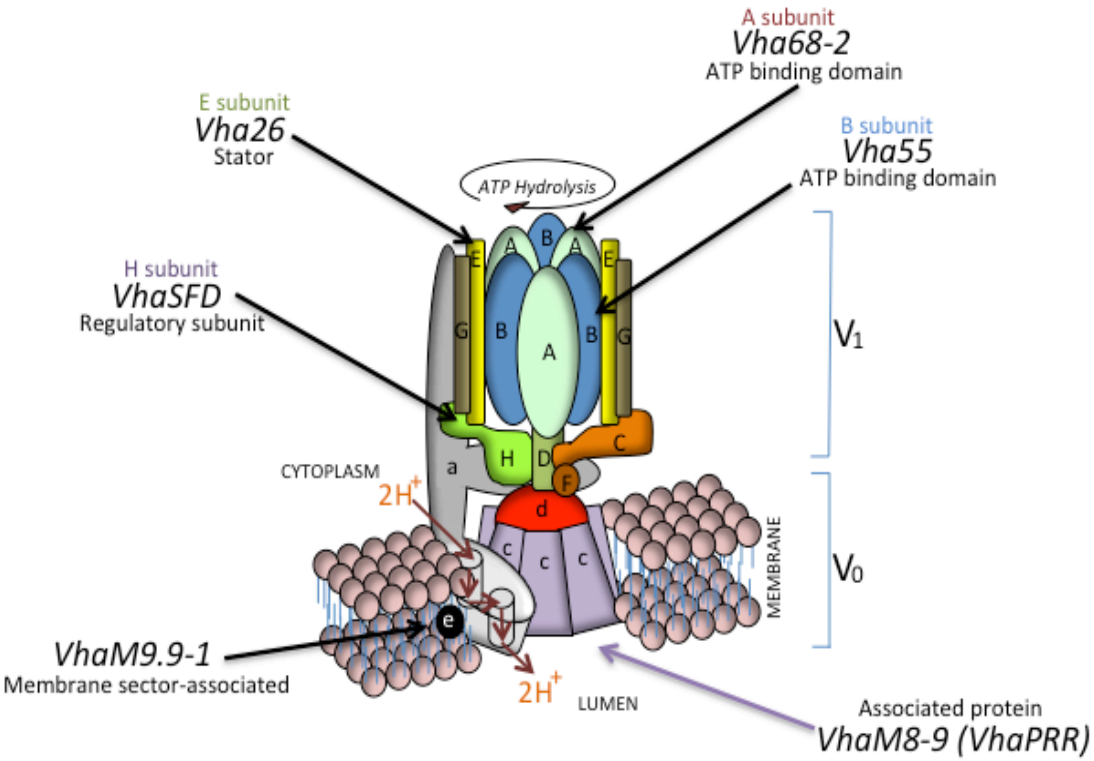


Figure 1.6 Schematic representation of the V-ATPase complex.

The V-ATPase complex is made up of multiple subunits. The membrane spanning V_0 subunits are suggested to be involved in regulating fusion events, whilst the V1 subunit is responsible for driving the molecular motor to hydrolyse ATP. Schematic adapted from Hannah Ledbury (Part II biochemistry student, Oxford).

1.7 Rab GTPases as markers of intracellular membranes

A key feature of Rab GTPases is their distinct localisation on different intracellular organelles. Indeed, tagged versions of Rab proteins are often used to illuminate the organelles they reside on (Hutagalung and Novick, 2011). Rab5 has been shown to be a classical marker of early endosomes, whilst Rab7 defines late endosomes and lysosomes (Barr, 2013). The exchange of Rab5 for Rab7 permits the forward transition of early endosomes to late endosomes, indicating that both these Rabs can be found on the same organelle during the Rab switch (Figure 1.4) (Rink et al., 2005).

Interestingly, by using high-resolution microscopy, it has been observed that different Rab proteins could occupy the same organelle but have distinct sub-domains. The slow recycling endosomes, often occupied by Rab11 and Rab4, are another example of Rabs having distinct domains on the same compartment (Sonnichsen et al., 2000). By tracking the routes that transferrin receptors take after endocytosis, Sheff et al (2002) showed that TfR arrives at Rab5 positive early endosomes and is then recycled back onto the plasma membrane through Rab4/11 recycling endosomes (Sheff et al., 2002). What causes the specific recruitment of Rabs to these domains is not entirely understood, but it is suggested to involve local synthesis of phosphatidylinositol-3-phosphate (PtdIns(3)P).(Jean and Kiger, 2012).

1.7.1 Rab function

The heterogeneity of Rab effectors permits them to carry out a variety of different processes including fusion of compartments. One of the best studied is the Rab5 tethering factors early endosome antigen 1 (EEA1) and rabenosyn 5. Active Rab5 and PtdIns(3)P jointly bind EEA1, which in turn recruits syntaxin6 and controls the homotypic fusion of early endosomes (Simonsen et al., 1999). Overexpressing a GTP-locked form of Rab5 (constitutively active) increases homotypic fusion rates of EEs

and increases their overall size, and as a result constitutive activation of Rab5 is often used as a technique to enlarge and visualise EE (Roberts et al., 1999). The FYVE finger domain of Rabenosyn 5 is required for its localisation to early endosomes, where it indirectly interacts with syntaxin6 and 13 via VPS45 (Nielsen et al., 2000). These effectors therefore serve as a molecular link to harness Rab activity and change membrane trafficking. In contrast, the role of Rab7 in fusion of late endosomes is not very clear, but several studies have implicated its involvement, and for fusion between late endosomes and lysosomes (Vanlandingham and Ceresa, 2009, Bucci et al., 2000).

Rab GTPases are also essential for regulating signalling pathways and consequently the control of cell growth, proliferation and differentiation. The activation of receptors usually results in their endocytosis and arrival at the early endosomes (Goh and Sorkin, 2013). This sorting point dictates whether a receptor is recycled back to the plasma membrane, via slow/ fast recycling endosomes, or is degraded in the lysosomes. Signalling by the epidermal growth factor receptor (EGFR) stimulates early endosome fusion by activating Rab5 and commits the receptor down the endolysosomal route where it is later degraded in lysosomes (Chen and Wang, 2001). The conserved growth-controlling mammalian target of rapamycin (mTOR) pathway is suggested to be partly controlled by Rab GTPases. In a screen of Rab proteins controlling mTOR signalling, Rab1, Rab5, Rab7, Rab11 and Rab23 were all identified as potential regulators (Li et al., 2010). In a recent study, Rab1A overexpression was shown to promotes mTORC1 signalling and increase the progression and invasiveness of colorectal cancer (Thomas et al., 2014). Conversely, knockdown of Rab1A selectively inhibited these traits, suggesting that Rab1A is an mTORC1 activator. Indeed, in many human cancers, Rab expression and function is perturbed leading to poor prognosis (Goldenring, 2013). Therefore, modulating the activity of Rab proteins is currently a target of pharmaceutical drugs.

1.8 Signalling and endolysosomes

In order for cells to receive a signal at the plasma membrane and activate downstream effectors to regulate gene expression, the components of the signalling pathway must be trafficked appropriately. In fact, this traffic-signalling relationship ensures that ligands are properly packaged and secreted, whilst ligand-bound receptors are rapidly endocytosed to modulate signalling (Palfy et al., 2012). At the most basic level, endocytosis simply regulates the number of receptors at the plasma membrane, therefore controlling the level of activation. In recent years, it has become clear that endocytosis can potentiate signalling, debunking traditional views that these two processes are separate events (Villasenor et al., 2016).

1.8.1 Receptor signalling and endocytosis

The receptor tyrosine kinase (RTK) family of signalling proteins provides several good examples of the various links between signalling and endocytic trafficking. Upon activation, RTKs are recruited into clathrin-coated pits by interacting with adaptor proteins (Good et al., 2011). Ligand-induced activation of the EGFR leads to phosphorylation of Src kinase, which in turn phosphorylates clathrin heavy chain and stimulates clathrin-coated pit formation (Wilde et al., 1999). Another example involves G-protein coupled receptors (GPCRs), because their activation leads to the recruitment of β-arrestin which links GPCRs with endocytic components such as clathrin heavy chain, thus facilitating its inclusion into endocytic vesicles (Gurevich et al., 1995). These examples demonstrate that activation of signalling alters the rate of endocytosis, and therefore the number of receptors at the cell surface.

Signalling pathways can also be further regulated upon endocytosis, as first proposed in the late 70s. A well-characterised example is the downregulation of signalling upon EGFR activation, involving sorting of the receptor to ILVs of MVBs, therefore leading

to trafficking to the lysosome where the EGFR is degraded (Futter et al., 1996). The physiological consequence of this event is apparent during *Drosophila* oogenesis, where endocytosis-mediated attenuation of RTK signalling is crucial for proper border cell migration (Jekely et al., 2005).

Endocytosis also has been shown to control the distribution of morphogens, such as Wnt and Dpp, in *Drosophila*. In the anterior-posterior axis of the *Drosophila* wing disc, Dpp is dispersed across a 40 cell-wide domain, and can only generate a long-range concentration gradient upon endocytosis (Teleman and Cohen, 2000). Indeed, in mutant flies defective in endocytosis, Dpp distribution is restricted demonstrating that endocytosis is needed for the graded spread of Dpp (Teleman and Cohen, 2000, Gonzalez-Gaitan and Jackle, 1999). A prevailing model suggests that after internalisation in receiving cells, Dpp is trafficked along the endocytic pathway and secreted again, thereby presenting the ligand to adjacent cells. However, others have shown that Dpp movement is independent of endocytosis (Belenkaya et al., 2004). Indeed, a recent study combined quantitative mathematical modelling with the genetic production of loss and gain of function clones for different BMP receptors to illustrate that Dpp gradient formation occur without receptor-mediated transcytosis (Schwank et al., 2011).

1.8.2 Sustained signalling on endosomes

Conventional signalling is suggested to primarily occur at the cell surface, where ligands bind to and activate membrane-bound receptors, leading to changes in gene expression. More recently, it has become clear that signalling can also be initiated and sustained in endosomes prior to trafficking towards lysosomes. This theory was first postulated after the EGF receptor was found to be active in endosomes following biochemical fractionation (Oksvold et al., 2001, Di Guglielmo et al., 1994). The

difficultly, however, is differentiating this signal from that generated at the plasma membrane. One possible advantage of these so called 'signalling endosomes' is perhaps to transmit information over long distances, especially in neurons where the site of activation at the plasma membrane is far away from the nucleus and passive diffusion would simply be too slow.

The neurotrophin, nerve growth factor (NGF), and its receptor, TrkA, are internalised at the distal end of axons and continue signalling to the soma to inhibit the intrinsic cell death pathway of neuronal cell bodies by promoting expression of genes crucial for survival (Watson et al., 2001). Interestingly, using live microscopy, early endosomes containing activated NGF/TrkA were observed to be transported in a retrograde manner, providing evidence that the microtubule-mediated movement of Rab5-positive endosomes can initiate a signal (Howe et al., 2001). In fact, in animals lacking functional dynamin, a GTPase involved in endocytosis, the movement of endosomes is restricted and signalling is perturbed (Wu et al., 2007). Therefore, the motility of endosomes allows signals to be transported over long distances and bridges the gap between the plasma membrane and the site of gene expression within the cell body.

There are several other properties of endosomes that enable them act as platforms for signalling. By a small volume, endosomes favour ligand-receptor interactions to continue signalling beyond the plasma membrane (Sorkin and von Zastrow, 2009). Moreover, the membranes of endosomes are enriched in lipids such as PtdIns3P that act as scaffolds for the recruitment of FYVE-domain containing proteins, which for example, are critical for transforming growth factor beta (*TGF-β)* signalling (Sorkin and Von Zastrow, 2002). Ligand activation of the *TGF-β* type 2 receptor results in the hetero-tetrameric assembly between two type 2 and two type 1 receptors in mammals (Massague, 2012). This subsequently triggers the phosphorylation of the type 1 receptor by the type 2 receptor serine-threonine kinase and initiates phosphorylation

of receptor-regulated SMADs (R-Smad). R-Smad can form a complex with the common mediator Smad (co-Smad) and translocate to the nucleus to regulate gene expression (Wrighton et al., 2009) both in the presence and absence of *TGFβ* signalling, however, it is thought that the retention of the complex in the nucleus is greater when signalling is running (Lo, RS and Massgue, J, 1999).

Activation of the *TGFβ* receptor complex results in its internalisation and trafficking to the early endosomes where it interacts with SARA – a FYVE domain-containing adaptor (Penheiter et al., 2002). Interestingly, SARA presents R-SMAD to the type 1 receptor where they are phosphorylated on endosomes (Runyan et al., 2009). This has been suggested to potentiate signalling. Similarly, endofin, a member of the FYVE-domain containing family, was shown to potentiate signalling by interacting with *TGFβ* receptor and SMAD4 to promote SMAD2-SMAD4 complex formation.

Gleason et al., 2014 illustrated that the *C.elegans* type 1 BMP receptor is capable of binding to the retromer complex which facilitates its intracellular recycling. Indeed, they showed that in retromer mutant animals, the type 1 receptor are trafficked towards the lysosomes, and this inhibits signalling activation. Interestingly, the recycling of the type 2 receptor was shown to be retromer-independent, but required ARF-6. These data suggest that after internalisation, the two types of BMP receptors are trafficked in distinct recycling pathways to return to the plasma membrane for another round for signalling. What is unclear from this study is whether signalling can still occur inside recycling compartment *en route* to the plasma membrane.

From the 'signalling endosome' hypothesis spawns many questions. 1) Do these compartments differ from sorting endosomes e.g early endosomes? 2) To what level do signals generated in endosomes differ from those at the plasma membrane? 3) Why do we need signalling endosomes and what is their physiological role? What

cannot be denied, however, is that endosomes and signalling cascades are intimately linked.

1.8.3 Lysosomal signalling

There are other components of the endolysosomal system apart from endosomes that promote as well as suppress signalling, namely the lysosome. These compartments are major degrading stations that help destroy damaged or unwanted proteins and regulate key cellular processes like Ca^{2+} signalling, but they also play a fundamental role in nutrient sensing and activating signalling pathways that control growth and cell metabolism (Settembre et al., 2013). Interestingly, the concentration of different amino acids inside the lysosomes dictates the binding of the mTORC1 complex on its surface. From there, mTORC1 regulates global cell growth (Goberdhan et al., 2016). In cases where lysosomes are unable to form normally or the mTORC1 complex fails to be recruited onto these structures (Kim et al., 2008), downstream signalling is perturbed (Betz and Hall, 2013).

1.9 Limitations in studying membrane trafficking and signalling

The wealth of knowledge that we have gained by studying membrane biogenesis and secretion, along with the signalling pathways that control these events, has provided the basis for many targeted therapies. For example, endocytosis is a key step in controlling viral entry into cells and many drugs have been developed to specifically inhibit this route (Mercer et al., 2010, Biswas et al., 2007). Yet, although the basic process of endocytosis is understood, the detailed molecular machinery controlling it and the multiple downstream trafficking decisions remains elusive. This is partly because endocytosis is extremely dynamic, making it difficult to visualise the complex molecular events underpinning it. Indeed, in studying these processes, we are limited

by the temporal and spatial resolution of conventional microscopes. Even electron microscopy, which provides much higher resolution, falls short because of its static nature. However, with the advent of super-resolution microscopy, combining high-resolution 3D-imaging with real-time observations (Galbraith and Galbraith, 2011), some of these challenges may be addressed.

1.9.1 Limitations as a result of endosome size

Endocytic organelles are typically very small, ranging between 200-1000nm, so it is difficult to resolve them as vesicular structures, even when tagged with fluorescent markers. Scientists, however, have developed cunning techniques to make these compartments more accessible to microscopic analysis. The overexpression of a constitutively active form of Rab5 enlarges endosomes, permitting a unique insight into the lumen of these compartments (Roberts et al., 1999). Additionally, the application of drugs such as the ionophores monensin and nigericin to tissue cultures achieves similar results (Savina et al., 2005). Indeed, by using these techniques we have developed an understanding of the maturation of endosomal compartments and the formation of intraluminal vesicles. However, these manipulations, although useful, disrupt the highly interconnected network of compartments trafficking to and from the endolysosomal system and create structures that are clearly abnormal.

1.9.2 Difficulties in corroborating results

There are many publications in the field of endocytosis and the endolysosomal trafficking, but quite frequently they report conflicting results and conclusions. This is partly down to the experimental procedures employed, as well as the fact that manipulations, such as endosomal enlargement, often do not recapitulate real cellular events. Additionally, trafficking events are often specialised in different cell types, so highlighting so-called ‘universal regulators’ of these processes remains a challenge.

Moreover, most studies in this field use an *in vitro* setting. For example, a breakthrough study identifying an ESCRT-independent pathway for exosome biogenesis was reported using Giant unilaminar vesicles (GUVs) (Falguieres et al., 2008, Trajkovic et al., 2008), but this relied heavily on pharmaceutical manipulation. There are many advantages in using *in vitro* experiments to biochemically characterise cell biological structures that are often difficult to study in the same way *in vivo*, for example, purifying endosomes and exosomes. However, the relevance of *in vitro* findings in a physiological context must be carefully considered.

To fully interpret *in vitro* findings, genetically tractable *in vivo* systems must be employed to rapidly test hypotheses. In order for this to be achieved, the *in vivo* system in question needs to be representative of a wide range of cell types, the intracellular compartments should ideally be large enough to visualise without enlarging them artificially, and multiple imaging techniques and assays should be available to trace the membrane trafficking events involved.

1.10 *Drosophila melanogaster* as a model genetic organism

The fruit fly, *Drosophila melanogaster*, has been widely employed in many laboratories across the globe to answer a myriad of biological questions. Its development as a genetic system can be traced back to its founding father, Thomas Hunt Morgan (Muller, 1946). He used flies to refine the chromosomal theory of inheritance and was awarded the 1933 Nobel Prize in Physiology or Medicine (Morgan, 1910, Morgan, 1911a, Morgan, 1911b). Over the past four decades, many brilliant scientists have used genetics approaches in flies and have been rewarded by the identification of a fruitful horde of genes that direct key developmental programs such as organogenesis and

segmental patterning, many of which are conserved across species (Rubin and Lewis, 2000, Bellen et al., 2010).

Indeed, at the turn of the century, Craig Venter and colleagues successfully sequenced the *Drosophila* genome using the ‘’shot-gun’’ approach in preparation for their analysis of the human genome roughly a year later (Adams et al., 2000). It quickly became clear that many human genes implicated in diseases have counterparts in *Drosophila*, further supporting the idea that had emerged over the previous decade that some human disorders could be modelled in the fly (Reiter et al., 2001). In fact, there are now fly models for cardiac diseases, neurodegeneration and various cancers to name but a few (Pandey and Nichols, 2011).

1.10.1 The GAL4/UAS system

The rich genetic heritage of flies has enabled the development of a variety of techniques to manipulate specific genes both in whole animals and in a tissue specific manner. One of the most notable is the GAL4/UAS system (Brand and Perrimon, 1993). This approach allows the expression of genes under the upstream activating sequence (UAS) promoter element specifically in cells expressing the ‘driver’ GAL4 (Figure 1.7). The system involves the yeast transcriptional activator GAL4 binding to one or more UAS elements inserted upstream of the gene or transcript of interest. In the absence of GAL4, the UAS-regulated transgene remains silent. Expression is only achieved in flies that also carry a GAL4 introduced by a genetic cross. The expression of GAL4 can be restricted to specific tissues by placing it under the control of a cell type- or tissue-specific promoter (Duffy, 2002).

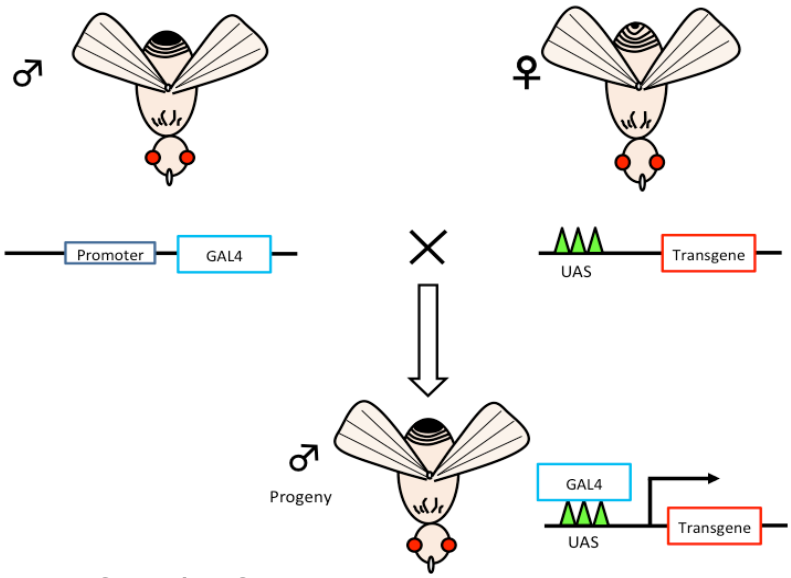


Figure 1.7 The GAL4/UAS expression system.

The binding of GAL to a UAS can initiate expression of specific genes downstream of the UAS element. This system can be further controlled by incorporating a tissue specific promoter to drive GAL4 expression of a UAS-regulated gene. In *Drosophila*, by mating flies carrying tissue specific GAL4 drivers with flies carrying a UAS controlled gene of interest, one can induce tissue-specific gene expression, for example in the eye.

1.10.2 GAL80^{ts} control over the GAL4/UAS system

Using the GAL4/UAS system, the gene of interest is expressed throughout development and adulthood; however, additional regulation can be introduced to restrict gene expression to a certain period in the fly's lifetime. The modification of a temperature-sensitive form of the GAL4 repressor, GAL80, enables temperature-dependent control over genetic expression (Suster et al., 2004). GAL80^{ts} is usually ubiquitously expressed in flies, repressing GAL4 activity and preventing transcription. Exposing flies to a temperature of 28.5°C or higher inactivates GAL80^{ts} and permits GAL4-regulated expression of UAS-coupled genes. This control over gene expression can ensure that developmental processes are unaffected by transgene expression and therefore allows specific temporal and spatial regulation in adults (Duffy, 2002). As a result, this technique is at the heart of many experiments in this thesis.

The genetic techniques mentioned above are very commonly used in fly studies. Geneticists continue to harness the power of *Drosophila* to develop an increasingly greater range of sophisticated techniques to answer fundamental biological questions *in vivo*. In fact, this is why I elected to use the fly to study how cells control the biogenesis of membrane and secretion. Specifically, in this thesis, the *Drosophila* accessory gland was used to model these processes.

1.11 The *Drosophila* accessory gland

The *Drosophila* accessory glands (AGs), along with the testes, seminal vesicles and the ejaculatory duct (ED) form the male reproductive tract (Figure 1.8). Like the mammalian prostate and seminal vesicles, the AG secretes a complex mixture of proteins that contribute to the seminal fluid and is transferred to females during mating (Wilson, 2016). The AG is comprised of a monolayered epithelium surrounded by a striated muscular sheath, which contracts during mating to expel the luminal content

through the ED and into the female (Figure 1.8) (Bairati, 1986). The contents of the AG lumen are derived mainly from the secretory processes of two bi-nucleated epithelial cell types. The main cells (MCs) are the most numerous, with roughly 1000 per gland; they appear hexagonal and flat, and distributed uniformly throughout the epithelium (Bertram et al., 1992). There are roughly 40 secondary cells (SCs) clustered at the distal tip of each gland (Bertram et al., 1992). They are larger and more spherical than MCs (Figure 1.8). This rounded feature elevates them above MCs, causing their apical surfaces to protrude directly into the AG lumen.

1.11.1 The AG function

In *paired* mutants males, the AG fails to develop properly and consequently renders the malel sterile (Xue and Noll, 2000). The ability of male flies to regulate fertility in addition to other physiological responses elicited in the female, is predominantly attributed to the epithelial cells that populate the AG, particularly the MCs. The analysis of MC function was first assessed by Kalb *et al* (1993) who ablated these cells using diphtheria toxin and found that they had a key role in inhibiting the female post mating response (PMR; see Section 1.11.2) (Kalb et al., 1993). Since then, we have learnt that MCs secrete a characteristic cocktail of proteins, including proteases and anti-proteases, that helps protect females from subsequent matings and promotes the male's reproductive success in the 'battle of the sexes' (Wolfner, 2007). Although, much less is known about the role of SCs in reproduction, they have been implicated in controlling some aspects of the PMR. Using P-element mediated enhancer traps, Bertram et al (1992) showed that MCs and SCs have unique gene expression patterns (Bertram et al., 1992). Moreover, a recent study also showed that these two cell types have distinct genetic profiles highlighting their respective role in controlling the female PMR (Sitnik et al., 2016).

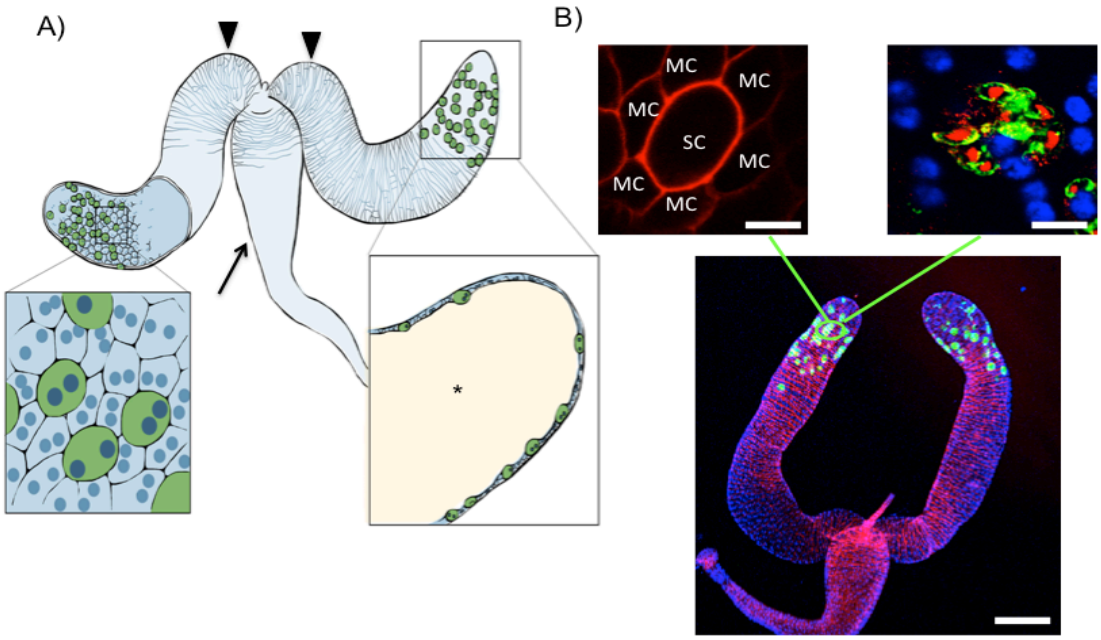


Figure 1.8 The *Drosophila* accessory gland.

The Drosophila accessory gland (AG) is a bi-lobed structure surrounded by a muscular sheath (**A**- arrow head). During mating the AG contracts to expel the content of the lumen (**A**, right insert - *) through the ejaculatory duct (**A**- arrow) and into the female. The AG is composed of two epithelial cell types– Main cells (MCs) and Secondary cells (SCs), which are morphologically distinct (**A** and **B**- left insert). The septate junctions between these two cell types can be marked with Fasciclin3 (Fas3). SCs contain large intracellular compartments that can be marked with tetraspanins such as CD63-GFP (green). SCs are bi-nucleated (**B**- right insert, blue) and some of their compartments contain dense-cores filled with ANCE (**B**-right insert, red). Scale bar for top two right inserts are 10 µm, for bottom panel is 150 µm. Schematic **(A)** was drawn by Jopsephine Hellberg (Wilson Lab, DPAG).

1.11.2 Female post-mating behaviour

Female *Drosophila* display stereotypical changes after mating. The short-term response (within the first 24 hrs) includes stimulation of ovulation, increased food consumption, sperm storage and egg-laying (Ram and Wolfner, 2007). Expression of genes encoding anti-microbial peptides also occurs during this period. The long-term effects involve preventing females from remating and reducing her overall lifespan (Apger-McGlaughon and Wolfner, 2013). These physiological changes in the female after mating are mainly attributed to two accessory gland proteins (Acps) produced by the MCs termed ovulin and sex peptide (SP) (Chapman et al., 2003). The donation of these two proteins along with other Acps ensures that the male continues to influence the reproductive behaviour of females long after mating is completed.

1.11.3 Ovulin and sex peptide function

Females that mate with *ovulin* (*Acp26Aa* – encoding *ovulin*) mutant males show a 44% decrease in ovulation and egg laying, implicating this gene in controlling the early stages of the PMR, usually not exceeding past the first day (Heifetz et al., 2005). Sex Peptide (SP) is another peptide that has been studied in great detail. SP was initially isolated from high performance liquid chromatography (HPLC) fractions of AG and subsequently characterised to inhibit the receptivity of females to remating and to increase long-term egg-laying (Kubli and Bopp, 2012). This MC-derived peptide is released into the AG lumen and binds sperm via its N-terminus in the female uterus only after sperm has been stored (Peng et al., 2005). Indeed, binding of SP to sperm facilitates its gradual release into the females where it controls physiology over periods of up to a week (Peng et al., 2005). Although there are several Acps that have been reported to have related functions, SP remains the master regulator of these processes (Ram and Wolfner, 2007).

In spite of our understanding about the roles of MC-derived Acps in controlling female physiology, we know much less about how the SC contributes towards maintaining the PMR. Indeed, for many years, there was a lack of genetic tools to specifically target SC-specific genes and functions. SCs have unusually large intracellular membrane-bound (roughly 5 μm diameter), initially called 'vacuoles' and contained in them are various filamentous structures surrounding a dense-core granule (Rylett et al., 2007). Prior to my work, the only protein identified in the DCGs was angiotensin-converting enzyme (ANCE), which is secreted into the AG lumen, and suggested to have roles in processing peptides (Figure 1.7) (Rylett et al., 2007).

1.11.4 SCs regulate the female PMR

More recently, SCs or their products have been shown to have roles in the PMR. In fact, in SCs that have reduced numbers of 'vacuoles' as a result of mutations in the Hox gene *Abd-B*, the processing of certain peptides e.g ovulin, is aberrant (Gligorov et al., 2013). What remains unclear is whether these observations are a direct function of SCs or if SCs communicate to MCs and alter their behaviour. Work from our lab also implicates the SCs in controlling the PMR. In virgin males, SCs selectively grow in the epithelium. Interestingly, in multiply-mated males, this growth is accelerated and some SCs delaminate and migrate towards the proximal tip of each gland where they are transferred to females after mating (Leiblich et al., 2012). Recent unpublished work from the Wilson Lab has shown that growth can be uncoupled from migration, suggesting these two effects are independent of each other.

Leiblich et al (2012) showed that BMP signalling is fundamental for the growth and migratory behaviour and demonstrated that inhibiting BMP signalling specifically in SCs disrupted the PMR in females. Subsequent work suggested that SCs produce and secrete exosome-like structures. BMP signalling was also involved in the biogenesis

and secretion of exosomes (Corrigan et al., 2014). Indeed, inhibiting BMP signalling in SCs reduces the secretion of exosome and their subsequent transfer to females. Females that fail to receive male-derived exosomes display an increase in their re-mating frequency whilst other PMR such as egg-laying are left unaffected (Corrigan et al., 2014).

1.12 Aims and objectives

The importance of SCs in controlling the female PMR has recently become clear, although we still lack a detailed understanding of SC secretory mechanism and the signalling pathways that control it. Indeed, even a basic characterisation of the large internal membrane-bound compartments and their internal content is something that was missing when I started my DPhil. Consequently, when I arrived at the Wilson lab, I had the following aims:

1. Characterise the nature of SC compartments.
2. Determine how these compartments are formed and what regulates their numbers.
3. Identify the cargo carried inside SC compartments.
4. Determine what signalling pathways regulate the secretion of these compartments.

The findings presented in this thesis have given multiple new insights into secretory processes and have led to the establishment of various internal and external collaborations. Indeed, this work has contributed greatly to the wider projects of other students in the Wilson lab, and has formed the basis of several successful grant proposals. Additionally, much of this work has contributed to our overall goal to translate our finding into studies that are relevant to various diseases. By the end of this thesis, I hope to have convinced you that the AG provides an unparalleled genetic

in vivo model system in which some fundamental aspects of cell biology can be studied at new levels of detail.

2. Materials and methods

2.1 Fly lines

There are a significant number of *Drosophila* flies used in this thesis, most of which were obtained from public stock centres and some kindly donated by other laboratories. The source of these flies is documented in table 2.1-2.8. Flies from Bloomington stock centre are referred to as BI.

Table 2.1 GAL4 drive lines

Genotype	Source	Description
w; *spi*-GAL4 on II	Kyoto112-114	SC driver
w; *dsx*-GAL4/TM6B	Goodwin (Rideout et al., 2010)	SC and ejaculatory duct driver
w; esg-GAL4 tub-GAL80ts UASGFPnls/ CyO; UAS-flp act>CD2>GAL4/TM6	Edgar (Jiang et al., 2009)	"esgts F/O" SC driver
w, Acp26Aa-GAL4	Goodwin (Chapman et al., 2003)	MC driver
w; spi-GAL4, tubGAL80ts/CyO	Corrigan (Corrigan et al., 2014)	Temperature sensitive SC driver
w; tub-GAL80ts; dsx-GAL4/SM5;TM6	Corrigan (Corrigan et al., 2014)	Temperature sensitive SC driver
w; UAS-CD63-GFP, tubulin-GAL80ts ; dsx-GAL4/SM5.TM6	Corrigan (Corrigan et al., 2014)	SC specific CD63-GFP driver line

Table 2.2 SC Compartment characterisation

All fluorescently labelled Rab proteins are tagged at their N-terminus.

Genotype	Source	Description
w[*];P{w[+mC]=UAS-GFP-myc-2xFYVE} 2, tweek[1]/T(2;3)TSTL, CyO: TM6B, Tb[1]	BI 39695	FYVE domain fused to GFP
w; tub-YFP-Rab5 on III	J-P Vincent (Marois et al., 2006)	Rab5-YFP under tubulin control
w; tub-YFP-Rab7 on III	J-P Vincent (Marois et al., 2006)	Rab7-YFP under tubulin control
w; tub-YFP-Rab11 on III	J-P Vincent (Marois et al., 2006)	Rab11-YFP under tubulin control
w[*]; P{w[+mC]=UASp-GFP.Golgi}14	BI 31422	galactosyltransferase-GFP fusion protein
y[1]w[*]; P{w[+mC]=UASp-YFP.Rab35}15	BI 9821	Expresses Rab35-YFP under UAS
yw; YFP-Rab1 gene trap	Eaton/Karch (Dunst et al., 2015)	Rab1-YFP expressed under endogenous promoter
yw; YFP-Rab5 gene trap	Eaton/Karch (Dunst et al., 2015)	Rab5-YFP expressed under endogenous promoter
yw; YFP-Rab6 gene trap	Eaton/Karch (Dunst et al., 2015)	Rab6-YFP expressed under endogenous promoter
yw; CFP-Rab6 gene trap	Eaton/Karch (Dunst et al., 2015)	Rab6-CFP expressed under endogenous promoter
yw; YFP-Rab7 gene trap	Eaton/Karch (Dunst et al., 2015)	Rab7-YFP expressed under endogenous promoter
yw; YFP-Rab11 gene trap	Eaton/Karch (Dunst et al., 2015)	Rab11-YFP expressed under endogenous promoter
y[1] w[*]; P{w[+mC]=UASp-YFP.Rab5}Pde8[08b] – wtRab5	BI 9775	UAS-regulated Rab5-GFP
y[1] w[*]; P{w[+mC]=UASp-YFP.Rab7}21/SM5	BI 23641	UAS-regulated Rab7-GFP
y[1] w[*]; P{w[+mC]=UASp-YFP.Rab11}sra[32]/TM3, Sb[1] – Rabll-wt	BI 9790	UAS-regulated Rab11-GFP
y[1] w[*]; P{w[+mC]=UASp-YFP.Rab35}15	BI 9821	UAS-regulated Rab35-GFP
yw hsFLP; UAS-HRP-Lamp (III)	Neufeld (Rusten et al., 2006)	UAS-regulated LAMP-HRP

Table 2.3 Rab lines

Genotype	Source	Description
y[1] v[1]; P{y[+t7.7] v[+t1.8]=TRiP.JF03335}attP2 Rab5 (FBgn0014010)	BI 30518	UAS-regulated RNAi against Rab5
y[1] sc[*] v[1]; P{y[+t7.7] v[+t1.8]=TRiP.HMS00145}attP2 Dsor1 (FBgn0010269)	BI 34830	UAS-regulated RNAi against Rab5
CG5915 *Rab7-RNAi*	VDRC 40338	UAS-regulated RNAi against Rab7
y[1] v[1]; P{y[+t7.7] v[+t1.8]=TRiP.JF02377}attP2 Rab7 (FBgn0015795)	BI 27051	UAS-regulated RNAi against Rab7
y[1] v[1]; P{y[+t7.7] v[+t1.8]=TRiP.JF02812}attP2 – Rab11 RNAi	BI 27730	UAS-regulated RNAi against Rab11
CG5771 – *Rab11 RNAi*	VDRC 108382	UAS-regulated RNAi against Rab11
y[1] v[1]; P{y[+t7.7] v[+t1.8]=TRiP.JF02165}attP2 – Rab27	BI 31887	UAS-regulated RNAi against Rab27
y[1] sc[*] v[1]; P{y[+t7.7] v[+t1.8]=TRiP.HMS01523}attP2 – Rab27	BI 35774	UAS-regulated RNAi against Rab27
y[1] v[1]; P{y[+t7.7] v[+t1.8]=TRiP.JF02978}attP2 – Rab35	BI 28342	UAS-regulated RNAi against Rab35
CG9575 – *Rab35 RNAi*	VDRC 101361	UAS-regulated RNAi against Rab35

Table 2.4 Other Rab lines

Genotype	Source	Description
y[1] w[*]; P{w[+mC]=UASp-YFP.Rab5.S43N}01 – Rab5-dn.	BI 9771	UAS-regulated Rab5 DN
y[1] w[*]; P{w[+mC]=UASp-YFP.Rab7.T22N}06	BI 9778	UAS-regulated Rab7 DN
y[1] w[*]; P{w[+mC]=UASp-YFP.Rab11.S25N}35 – Rab11-dn	BI 9792	UAS-regulated Rab11 DN

Table 2.5 BMP signalling lines

Genotype	Source	Description
y[1] v[1]; P{y[+t7.7] v[+t1.8]=TRiP.HMS00011}attP2 – Dpp RNAi	BI 33618	UAS-regulated RNAi against Dpp
y[1] v[1]; P{y[+t7.7] v[+t1.8]=TRiP.JF01090}attP2 – Dpp RNAi	BI 31530	UAS-regulated RNAi against Dpp
y[1] sc[*] v[1]; P{y[+t7.7] v[+t1.8]=TRiP.HMS01243}attP2 – gbb RNAi	BI 34898	UAS-regulated RNAi against Gbb
y[1] v[1]; P{y[+t7.7] v[+t1.8]=TRiP.JF01485} attP2/TM3, Ser[1] - tkvRNAi	BI 31040	UAS-regulated RNAi against Tkv
y[1] v[1]; P{y[+t7.7] v[+t1.8]=TRiP.JF01486}attP2 - tkvRNAi	BI 31041	UAS-regulated RNAi against Tkv
y[1] sc[*] v[1]; P{y[+t7.7] v[+t1.8]=TRiP.HMS02298}attP2 wit (FBgn0024179)	BI 41906	UAS-regulated RNAi against Wit
y[1] v[1]; P{y[+t7.7] v[+t1.8]=TRiP.JF01969}attP2 wit (FBgn0024179)	BI 25949	UAS-regulated RNAi against Wit
w[w1118]; P{GD2546} v46358	VDRC-46358	UAS-regulated RNAi against Sax
y[1] v[1]; P{y[+t7.7] v[+t1.8]=TRiP.JF03431}attP2 - sax	BI 36131	UAS-regulated RNAi against Sax
y[1] v[1]; P{y[+t7.7] v[+t1.8]=TRiP.JF02664}attP2 - put	BI 27514	UAS-regulated RNAi against Punt
y[1] sc[*] v[1]; P{y[+t7.7] v[+t1.8]=TRiP.GL00069}attP2 - put	BI 35195	UAS-regulated RNAi against Punt

y[1] sc[*] v[1]; P{y[+t7.7] v[+t1.8]=TRiP.HMS01944}attP40 - put	BI 39025	UAS-regulated RNAi against Punt
y[1] v[1]; P{y[+t7.7] v[+t1.8]=TRiP.JF01263}attP2 - MadRNAi	BI 31315	UAS-regulated RNAi against Mad
y[1] v[1]; P{y[+t7.7] v[+t1.8]=TRiP.JF01264}attP2 on III	BI 31316	R UAS-regulated RNAi against Mad
y[1] v[1]; P{y[+t7.7] v[+t1.8]=TRiP.JF02218}attP2 - MedRNAi	BI 31928	UAS-regulated RNAi against Med
y[1] sc[*] v[1]; P{y[+t7.7] v[+t1.8]=TRiP.GL01313}attP40 - Med	BI 43961	UAS-regulated RNAi against Med
w; P[w+ UAS-Dad]	Daimark Bennett (Tsuneizumi et al., 1997)	UAS-regulated overexpression of Dad
w;UAS-Dpp-GFP/TM6B GFP Hu (not Tb)	JP Vincent (Teleman and Cohen, 2000)	UAS-regulated overexpression of Dpp-GFP
w;UAS::Dpp-tagRFP1-2/Cyo	Dresden (Michel et al., 2011)	UAS-regulated overexpression of Dpp-RFP
y[1] w[*]; UAS-tkv^{QD}- constit. activ.	Basler (Nellen et al., 1996)	UAS-regulated overexpression of Constitutive active form of Tkv
w[*]; P{w[+mC]=UAS-tkv.Q253D.Nb}3/TM3, Sb[1] Ser[1]	BI 36536	UAS-regulated overexpression of Constitutive active form of Tkv
w[1118]; PBac{544.SVS-1}11 tkv[CPTI002487]	Ky 115-298	YFP gene trap line for Tkv receptor

BMP signalling lines continued.

Table 2.6 V-ATPase lines

Genotype	Source	Description
w[1118]; P{w[+mC]=PTT-GA}VhaSFD[G00259]/CyO	BI 6840	Gene trap for VhaSFD subunit.
CG1088 – *Vha26 RNAi*	VDRC 45377	UAS-regulated RNAi against Vha26
y[1] sc[*] v[1]; P{y[+t7.7] v[+t1.8]=TRiP.HMS01912}attP2/TM3, Sb[1] Vha26 (FBgn0015324)	BI 38996	UAS-regulated RNAi against Vha26
CG17369 – *Vha55 RNAi*	VDRC 46554	UAS-regulated RNAi against Vha55
CG3762 – Vha68-2	VDRC 34390	UAS-regulated RNAi against Vha68-2
y[1] sc[*] v[1]; P{y[+t7.7] v[+t1.8]=TRiP.HMS01056}attP2 Vha68-2 (FBgn0020367)	BI 34582	UAS-regulated RNAi against Vha68-2
CG17332 – *VhaSFD RNAi*	VDRC 19173	UAS-regulated RNAi against VhaSFD
y[1] v[1]; P{y[+t7.7] v[+t1.8]=TRiP.JF02029}attP2 VhaM9.7-1 (FBgn0028664)	BI 26004	UAS-regulated RNAi against VhaM9.7-1

Table 2.7 SNARE lines

Genotype	Source	Description
CG9474 - *Snap24*	VDRC 48034	UAS-regulated RNAi against Snap24
y[1] v[1]; P{y[+t7.7] v[+t1.8]=TRiP.JF03146}attP2 – SNAP24	BI 28719	UAS-regulated RNAi against Snap24
y[1] sc[*] v[1]; P{y[+t7.7] v[+t1.8]=TRiP.HMS01678}attP2/TM3, Sb[1] - Syb	BI 38234	UAS-regulated RNAi against Syb
y[1] sc[*] v[1]; P{y[+t7.7] v[+t1.8]=TRiP.HMS01987}attP40/CyO - Syb	BI 39067	UAS-regulated RNAi against Syb
y[1] v[1]; P{y[+t7.7] v[+t1.8]=TRiP.JF01829}attP2 Syx1A (FBgn0013343)	BI 25811	UAS-regulated RNAi against *Syx1A*

Table 2.8 Miscellaneous UAS-RNAi lines

Genotype	Source	Description
y[1] sc[*] v[1]; P{y[+t7.7] v[+t1.8]=TRiP. GLC01447}attP2– l(3)76BDm – TRAPPII – Rab11 regulation	BI 43258	UAS-regulated RNAi against l(3)76BDM subunit of the TRAPPII complex
CG8385- *Arf79F*	VDRC-103572	UAS-regulated RNAi against Arf79f.
CG6210 - Evi	VDRC-5214	UAS-regulated RNAi against Evi.
UAS-evi-RNAi on III	JP-Vincent (Franch-Marro et al., 2008)	UAS-regulated RNAi against Evi.

2.2 Reagents

Table 2.9 Buffers and solutions

Buffers/ solution	Recipe
Phosphate buffer saline (PBS)	One PSB tablet dissolved in 200ml of ddH_20: Tablet produces solution containing: 0.01M Phosphate buffer 0.0027M KCl 0.137M NaCl pH 7.4
PBST	PSB containing 0.3% Triton X-100
PBSTG 10%	PBST containing 10% Goat serum
PFA 4%	4% Paraformaldehyde in PBS

Table 2.10 Primary antibodies

Antigen	Host species	Source	Reference	Dilution
ANCE	Rabbit	Gift from Prof. E. Isaac, Universityw of Leeds, UK	(Rylett et al., 2007)	1/1000
EEA1	Rabbit	Gift from A. Nakamura, RIKEN Center for Developmental Biology, Kobe, Japan.	(Tanaka and Nakamura, 2008)	1/200
Fasciclin 3 (Fas3)	Mouse	Developmental Studies Hybridoma Bank (DSHB), Iowa, USA.	(Patel et al., 1987)	1/10
Gbb	Mouse	Developmental Studies Hybridoma Bank (DSHB), Iowa, USA.	(Dani et al., 2012)	1/10
GFP	Rabbit	ABCAM #ab6556	(Shakya et al., 2005)	1/2000
GM130	Rabbit	ABCAM #ab30637	(Sinka et al., 2008)	1/400
Phospho-Smad 1/5	Rabbit	Cell signalling – 41D10	(Alarcon et al., 2009, Cao, 2006)	1/400
Rab11	Rabbit	Gift from A. Nakamura, RIKEN Center for Developmental Biology, Kobe, Japan	(Tanaka and Nakamura, 2008)	1/200
Rab7	Rabbit	Gift from A. Nakamura, RIKEN Center for Developmental Biology, Kobe, Japan	(Tanaka and Nakamura, 2008)	1/200
Wishful thinking	Mouse	Developmental Studies Hybridoma Bank (DSHB), Iowa, USA.	(Aberle et al., 2002)	1/10

Table 2.11 Secondary antibodies

Reactivity	Host species	Conjugate	Source	Reference	Dilution
Rabbit	Donkey	Alexa Fluor 647	Life technologies - #A-21245	(Szulwach et al., 2010)	1/400
Rabbit	Donkey	Alexa Fluor 555	Life technologies - #A-31572	(Tian et al., 2012)	1/400
Mouse	Donkey	Alexa Fluor 647	Life technologies - #A-31571	(Knock et al., 2015)	1/400
Mouse	Donkey	Alexa Fluor 555	Life technologies - #A-31570	(Tian et al., 2012)	1/400

2.3 Fly food

All flies were reared on glucose-rich cornmeal/yeast-based recipe that was made in batches according to the recipe provided in Table 2.12. To ensure that fungus did not grow on the fly food, Nipagin was added to every batch. The food was then dispensed into individual vials and stored at 4˚C.

Table 2.12 Recipe of fly food

Total volume: 25 litres

Reagents	Quantity	Source
Agar	241g	Sigma-Aldrich
Glucose	2325g	Sigma-Aldrich
Yeast	787g	Sigma-Aldrich
Cornmeal	1875g	Sigma-Aldrich
Calcium	17g	Sigma-Aldrich
Ethanol (100%)	300ml	Sigma-Aldrich
Potassium sodium tartrate	215g	Sigma-Aldrich
Ethyl-4-hydroxybenzoate (Nipagin)	62.5g	Sigma-Aldrich

2.4 Experimental approach

2.4.1 Fly husbandry

Flies were reared on cornmeal/yeast-based food at a temperature of 18˚C during development, unless otherwise stated. At this temperature GAL4 activity is restricted because the GAL4 repressor, $GAL80^{ts}$, which is present in most of the genotypes employed, is active. Upon eclosion, flies were shifted to 28.5˚C to inactivate the temperature-sensitive $GAL80^{ts}$ and allow GAL4 to induce transgene expression. Other crosses in which the $GAL80^{ts}$ system was not employed were also maintained with a similar temperature switch, so that all experiments were comparable. To make new fly lines containing a combination of transgenic constructs, flies were maintained at 25˚C.

2.4.2 Using the GAL4/UAS/$GAL80^{ts}$ system

As alluded to earlier, the GAL4/UAS system in combination with $GAL80^{ts}$ is an extremely powerful system, which allows cell-specific expression of transgenes in a tightly regulated manner. $GAL80^{ts}$ inhibits the activity of GAL4 at 18˚C but is inactive at 28.5˚C, permitting GAL4-UAS mediated gene expression. In this thesis, this system was combined with various GFP lines (such as CD63-GFP) to allow visualisation of internal SC compartments. Crossing these lines to flies expressing UAS-transgene constructs of interest enables visualisation of the effects of the transgene on SC compartments. Importantly, by switching temperature after eclosion, this system circumvents altering developmental processes, which could be affected if only the GAL4-UAS transgene is used.

To express transgenes specifically in SCs or MCs, GAL4 driver lines expressed only in these cell types were crossed to flies containing selected UAS-transgenes and kept

at 18˚C. Virgin males from this cross, now containing multiple transgenic constructs, were typically sorted and shifted to 28.5˚C to induce SC/MC expression of the transgene. It is important to mention that although the GAL4 lines used in this thesis are expressed in either SCs or MCs in the AG, they may also be expressed in other organs of the fly.

2.5 Dissection of the male *Drosophila* AG

Adult flies were anaesthetised by placing them on a CO_2 pad. Using forceps, their heads and wings were removed. The remaining abdomen and thorax were placed in 4% paraformaldehyde (diluted in PBS) on a Sylgard gel- covered petri dish. The AGs were dissected by gently pulling on the external genitalia and separating them from other tissue such as the testes. Once the AG and ejaculatory duct were isolated, they were allowed to fix for approximately 20 minutes.

2.6 Immunostaining protocol for AG dissections

After dissecting and fixing the AGs, they were washed with PBS for 30 minutes on a shaking platform. The AGs were then blocked using PBST (containing PBS, 0.3% Triton X-100 and 10% goat serum) for 30 minutes. The primary antibody (diluted in PBST) was applied after the AG was blocked and incubated overnight at 4˚C. The AG was then washed 6 times in PBST with 10 minutes incubation periods. After this, the secondary antibody solution (in PBSTG) was applied to the AGs and incubated for 2 hours on a shaking platform in the dark. The glands were washed 5 times for 10 min each with PBST, and then a final wash with PBS was undertaken for 10 minutes.

2.7 Mounting and DAPI staining

The stained glands in PBS were pipetted onto a glass slide and the excess fluid was removed using a tissue, avoiding contact with the AGs. The AGs were then immersed

in a single drop of Vectashield containing DAPI (Vector Laboratories), which is a marker for nuclei. A cover slip was placed on top of the glands and sealed using nail varnish.

2.8 Lysotracker staining

The AG glands of flies were dissected in cold PBS, using forceps that had been washed with 70% ethanol, and incubated for 5 minutes in cold Lysotracker Red diluted in PBS (1/1000). The glands were then washed in cold PBS for 5 minutes. Two cover slips were positioned parallel to each other on a microscope slide and sealed using PBS. The glands were sandwiched in between the cover slips and another cover slip was placed on top of the glands to form a chamber.

2.9 Confocal microscopy imaging

All samples were imaged using a scanning confocal microscope (LSM 510 Axioplan 2, Carl Zeiss). For low magnification images, the Zeiss Plan-Apochromat 10x/0.45 objective was used, while higher magnification images were taken using the Zeiss Plan-Apochromat 63x/1.4Oil DIC objective.

2.10 Image analysis

The analyses of confocal images were primarily made using the LSM Image Browser (Zeiss) software. This was used to measure the largest acidic compartment and analyse z-stack images. For calculating the GFP in the largest acidic compartment, the z-plane in which the largest MVBL was at its greatest diameter was selected and a binary calculation was used to measure the proportion of the area covered by fluorescent GFP using ImageJ. To analyse the number of exosomes in the AG lumen, ImageJ was used to first remove background noise using the 'noise>despeckle' function, and then converted to a binary image. The number of particles was assessed

using the particle analysis function with the following parameters - size: 0-infinity; circularity: 0.00-1.00. The average number of particles for all stacks was then quantified and compared to controls. The processing of images was made using Adobe Photoshop CS5.

2.11 Compartment quantification in SCs

There are a number of different large membrane-bound compartments in SCs and we have broadly categorised them into non-acidic compartments (SVs or DCG compartments) and acidic LELs. The compartments within each SC were counted by scanning through the entire cell. Three SCs were analysed per gland and the mean compartment number calculated. Counts were made for at least 10 different glands.

2.11.1 Non-acidic SV compartments

Non-acidic SVs were classified as CD63-positive, non-acidic compartments with a diameter of >1 μm. DCG compartments were defined as non-acidic compartments with a compact dense core marked by GFP-GPI or ANCE-cross-reactivity, and >1 μm in diameter.

2.11.2 Acidic compartments

LELs were CD63-GFP-positive (on limiting membrane), LysoTracker Red-positive and > 2 μm in diameter.

2.12 Measurement of GFP inside acidic compartments

The z-plane in which the largest LEL was at its greatest diameter was selected and a binary calculation was used to measure the proportion of the area covered by fluorescent GFP using ImageJ, ensuring that none of the signal was saturated.

Importantly, the same confocal settings are used for each experiment. This measurement was used to assess the maturity of the largest LEL compartment.

2.13 Exosome secretion assay

Male flies were introduced to three 4-8-day-old virgin w^{1118} females for 24 hours at 28.5°C to allow them to mate expel as much of the AG luminal content as possible. The next day, females were removed and males were incubated at 28.5°C overnight to allow them to replenish the luminal content of their AGs. The next day, males were dissected and immunostained as previously described (Section 2.6). To examine the release of exosomes, three Z-stack images (with 5 µm interval) from the central region of the gland lumen were taken (at a distance from any SCs), and the number of CD63-GFP-positive compartments was quantified using ImageJ software.

2.14 Nuclear size measurements

The two nuclei of an individual SC and of three surrounding MCs were imaged and their areas calculated using Axiovision software (Zeiss) by outlining the nuclei and measuring the number of pixels within. Three SC/MC clusters were imaged per gland. The relative SC:MC nuclear size was calculated and the ratios averaged across a minimum of 6 glands. Because cell growth and nuclear growth are typically closely linked in SCs, this method was used as a proxy for measuring cell growth.

2.15 Generation of mosaic clones

To generate mosaic clones of SCs in the AG, the *esg*-GAL4 line was used. The expression of *esg* naturally decreases with time and at around five days after eclosion SCs cease to express *esg*. Moreover, in this transgenic line, a ubiquitously expressed temperature-sensitive mutant of the GAL4 inhibitor, GAL80, prevents *esg*-GAL4-dependent expression until the temperature is shifted to 28.5°C. This induces a flip-

out event in SCs to allow GAL4 expression to be driven under actin in newly eclosed virgin males, driving RNAi and nuclear GFP expression specifically in SCs. However, if flies are shifted between 3-5 days after eclosion, only some SCs will be expressing *esg,* thus inducing a flip-out event only in some SCs and leaving the others as 'wild-type'. Nuclear GFP is also seen in flies carrying the following construct *w; esg-GAL4 tub-GAL80^{ts} UAS-FLP; UAS-GFP$_{nls}$ actin>FRT>CD2>FRT>GAL4*.

2.16 Pulse experiments

Flies were incubated at 25°C for 6 days, after which, they were shifted to 28.5°C to induce transgene expression for a limited time of 16 h or 24 h. For pulse experiments that involved mating, 6-day-old males were mated once and then shifted to 28.5°C. Alternatively, males were mated after the induction of gene expression to assay the formation and secretion of new DCGs.

2.17 Western blot analysis

Male AGs expressing SC-specific GFP-GPI from eclosion onwards and *w^{1118}* controls were dissected in ice-cold PBS. To generate female samples, each male expressing GFP-GPI was mated to a single *w^{1118}* female. The whole reproductive tract (with ovaries removed) was subsequently dissected from these females and from controls in ice-cold PBS.

The AG and female reproductive tract lysates were then prepared as previously described in Corrigan et al. (2014). Dissected samples were pooled and homogenised using a motorised pellet pestle (Sigma-Aldrich) in 100µl of lysis buffer (Radioimmunoprecipitation assay buffer; Sigma-Aldrich) supplemented with anti-protease and anti-phosphatase cocktails (Sigma-Aldrich). The lysate was then centrifuged (13000 g; 5 min) and protein content in the supernatant quantified using a

bicinchoninic acid assay kit (Thermo Fisher Scientific).

Blots were prepared as previously described (Corrigan et al., 2014; Rylett et al., 2007). Samples containing homogenised protein (2.5 µg) were added to 5 µl 4x sampling buffer (0.2M Tris-HCl pH 6.8, 12% SDS, 40% Glycerol, 20% β-mercaptoethanol, 0.008% bromophenol blue) and heated for 5 min at 95°C. Protein samples were separated for 30 minutes using 10% mini-Protean TGX precast gels. Separated samples were transferred to a PVDF membrane (Millipore Immobilon-P #IPVH00010) for 1 hour at 100V. The membrane was then blocked with 5% skimmed milk in Tris-buffered saline with Tween-20-(TSBT) for 1 hour and then incubated with either anti-ANCE antibody at 1:1000 (Rylett at al. 2007), anti-GFP at 1:500 (Rabbit, ABCAM ab6556) or anti-actin at 1:10000 antibody (Millipore, Rabbit Cat #04-1040) in TSBT overnight at 4°C on a shaking platform. The membrane was washed 3 times with TBST for 5 minute intervals. The membrane was then incubated with horseradish peroxidase-conjugated anti-rabbit secondary antibody in TSBT with 5% milk (1:20000, Promega #W4018), and then washed 3 times for 5 min. Antibody binding was detected using Clarity™ Chemiluminescent Substrate (Bio-Rad) and a ChemiDoc™ Touch Imaging System (Bio-Rad). Band intensities were measured using the Image Lab™ software (Bio-Rad).

2.18 Mating experiments

To analyse the effects of mating on BMP signalling activity in SCs, control male flies were mated to a single female at either 3 days or 6 days post-eclosion. Immediately after mating, the male flies were separated and the AGs were dissected in fix and stained as described in Section 2.6. In experiments where a GFP-GPI expression pulse was employed, matings were set up at different times, as described in the relevant sections of the Results chapters.

2.19 Female behavioural assays

Males, carrying various genotypes and control w^{1118}, were placed with five 3-8-day-old virgin w^{1118} females for 24 hours at 28.5°C. Females were separated into individual vials and the multiply-mated male was then introduced to three new 3-8 days old virgin w^{1118} females and mating was observed over a 3 hour period at 22°C. The males were discarded and females were separated into individual vials and followed for 70 hours. Egg counts were taken at designated time points and females were tipped into new tubes after each egg count. To test the female's propensity to remating, each female was placed in a new vial with 2 dominantly marked white rough-eyed males for 3 hours. Remating was recorded if at least two of the females had mated with the male during the initial multiple pre-mating and some of the progeny after the second set of crossed had white rough-eyes.

2.20 Transmission electron microscopy

For EM analysis (in collaboration with John Morris – DPAG, Oxford), w^{1118} male flies were dissected and the AG was fixed overnight with 2.5% gluteraldehyde and 4% formaldehyde in PBS. The glands were washed with PBS and then fixed with 1% osmium tetroxide for 20 min. The glands were washed 3 times with distilled water and dehyrated, first using 70%, then 80%, 90% and finally 100% ethanol for 5 min each. The AGs were then incubated in ethanol and Spurr's epoxy resin (1:1) and embedded in 100% Spurr's epoxy resin between two sheets of polythene with polymerization taking place overnight at 60°C. Using a Reichert Ultratome, ultrathin sections were made and mounted on formvar-coated slot grids. The sections were then stained with 2% uranyl acetate and lead citrate. Images were taken using a JEOL 1010 electron microscope (80kV).

2.21 Statistical analysis

For all compartment counts, measurements of intracellular compartments and nuclear size quantifications, three SCs per gland were analysed from a minimum of 10 animals (6 for nuclear size), typically involving 2-3 independent experiments. For analysis of pMad antibody staining patterns, all SCs in each AG were counted. All data were analysed using GraphPad Prism. The Shapiro-Wilk test was used to test for normality. Since not all data in each experiment were normally distributed, a Mann-Whitney *U* test or Kruskal-Wallis test was typically employed. The two-tailed unpaired Student's t test was employed for single pair comparisons, while data involving multiple comparisons were analysed by one-way ANOVA, when the measurements were normally distributed.

3. Characterisation of SC biology

(Results I)

3.1 Introduction

The male's ability to influence his mate through the accessory gland is mainly attributed to the function and products of MCs (Chapman et al., 2003). However, the role of SCs in the PMR has recently been proposed and the large compartments in these cells were implicated in this process. In *Abd-B* mutant males, the compartments of SCs fail to develop properly and the glycosylation of a key PMR regulatory protein, Ovulin, is reduced (Gligorov et al., 2013). This suggests that SC vacuoles or the proteins that reside in them may be responsible for processing these peptides.

When viewed under an electron microscope, most SC compartments have a large central dense-core granule (DCG), which is surrounded by an uncharacterised network of tubular filaments (Figure 3.12). The only protein that has been described to reside in this dense-core region is Angiotensin-converting enzyme I (ANCE; (Rylett et al., 2007)). This enzyme has been postulated to process peptides that are ultimately transferred to females and is therefore proposed to have roles in controlling the male's fertility (Hurst et al., 2003).

3.1.1 Work completed prior to starting my DPhil

What was missing from the literature when I started my DPhil was the lack of genetic tools to firstly manipulate SCs specifically and also mark their intracellular compartments. The Wilson Lab made great progress in developing GAL4-driver lines that were specifically expressed in SCs and paved the way for genetic analysis of SC cell biology and its effects on female behaviour (Leiblich et al., 2012). Subsequent to this, the attention of the Lab turned to marking intracellular compartments and understanding the secretory behaviours of SCs. One of the key tools employed was a transgenic fly carrying the human tetraspanin CD63-GFP under UAS control (Figure

1.7). It marks exosomes both in mammals and flies, and it was found to also label all the large intracellular compartments of SCs (Corrigan et al., 2014).

One of my hypotheses was that some of these large compartments might have unique identities and they might interact with each other in a dynamic manner. However, there was no way of distinguishing the various SC compartments from each other, and therefore it became crucial to identify their Rab signatures.

3.1.2 Rabs as markers of cellular compartments

As mentioned earlier in Section 1.6, Rab proteins are markers of different intracellular membranes and tagged versions of these proteins are often used to visualise different organelles. The large intracellular compartments of SCs give us a unique view into the dynamics of membrane trafficking. Therefore, characterising the Rab proteins that mark the intracellular compartments of SCs is important in order to track different processes along the secretory and endocytic pathway. Initially, I decided to study the localisation of highly conserved Rab proteins Rab1, 5, 6, 7 and 11, since they are known to mark specific compartments of the secretory and endolysosomal system (Pfeffer, 2001).

3.1.3 Aims

The main aim of this part of my study was to characterise SCs and their intracellular compartments. To do this, I focused on using:

1. CD63-GFP to visualise intracellular dynamics,
2. Tagged Rab GTPases and *Rab* knockdown to characterise intracellular compartments,
3. Genetic manipulation of regulators of Golgi trafficking, to determine how these different compartments were formed and their potential function.

Aspects of this study contributed to a paper published in Corrigan, L., et al (2014).

3.2 Results

3.2.1 SCs contain acidic and non-acidic intracellular compartments

Endolysosomal compartments are often acidic and can be identified using pH-sensitive dyes (Yapici et al., 2015). To characterise these compartments in SCs, the pH-sensitive dye, Lysotracker Red, was applied to AGs dissected from W^{1118} control flies. Interestingly, in these glands, wild-type SCs often contained two or three large acidic compartments measuring between 5-10 µm in diameter depending on the age of the fly (Figure 3.1A). We hypothesised that these were presumably late endosomal and lysosomal compartments, an idea that was supported by later studies of specific Rab proteins (Section 3.2.4). The large size contrasts with the size of the endolysosomal compartments found in mammalian cells, which are usually considerably less than 2 µm in diameter. Indeed, aside from coelomocytes in *C. elegans*, there is no other *in vivo* genetic system where cells exhibit large acidic compartments without the need for genetic or pharmaceutical manipulations (Fares and Greenwald, 2001). Therefore, SCs provide a powerful model to study endolysosomal trafficking *in vivo*.

In an effort to visualise the intracellular compartments of SCs, a previous DPhil student employed a transgenic fly carrying the human tetraspanin CD63-GFP under UAS control Corrigan, L., et al (2014). Tetraspanins like CD63 are processed through the Golgi pathway and then presented onto membranes including the secretory, endocytic and plasma membranes (Pols and Klumperman, 2009). CD63-GFP is usually endocytosed via the clathrin-dependent pathway and is processed via the endolysosomal route (Pols and Klumperman, 2009). In SCs expressing CD63-GFP, under *dsx*-GAL4 control, an SC-specific GAL4 driver in the AG, live imaging demonstrated this fusion protein could mark all large intracellular compartments, both

acidic and non-acidic (Figure 3.1B). The non-acidic compartments often varied in size but the largest one rarely exceeded 5 μm in diameter. We hypothesised that since SCs contain non-acidic compartments, these may represent a population of secretory compartments containing stored secretory proteins that would otherwise be degraded in the acidic environment of the large endolysosomes.

ANCE is a secretory protein that has previously been demonstrated to localise in the non-acidic dense-cored secretory compartments of SCs (Rylett et al., 2007) . Staining AGs with an antibody raised against ANCE confirmed that it is localised in compartments whose size was consistent with the size of non-acidic compartments (Figure 3.1C). In 6-day-old males, ANCE staining was rarely observed in other large compartments, which represented an acidic endolysosomes (Figure 3.2A).

In conclusion, SCs have large acidic compartments, which I later show are late endosomes and lysosomes (LELs), and dense-core granule-containing secretory compartments that can be labelled with anti-ANCE antibody. Importantly, all the intracellular compartments of SCs can be marked by CD63-GFP and visualised in both live and fixed conditions.

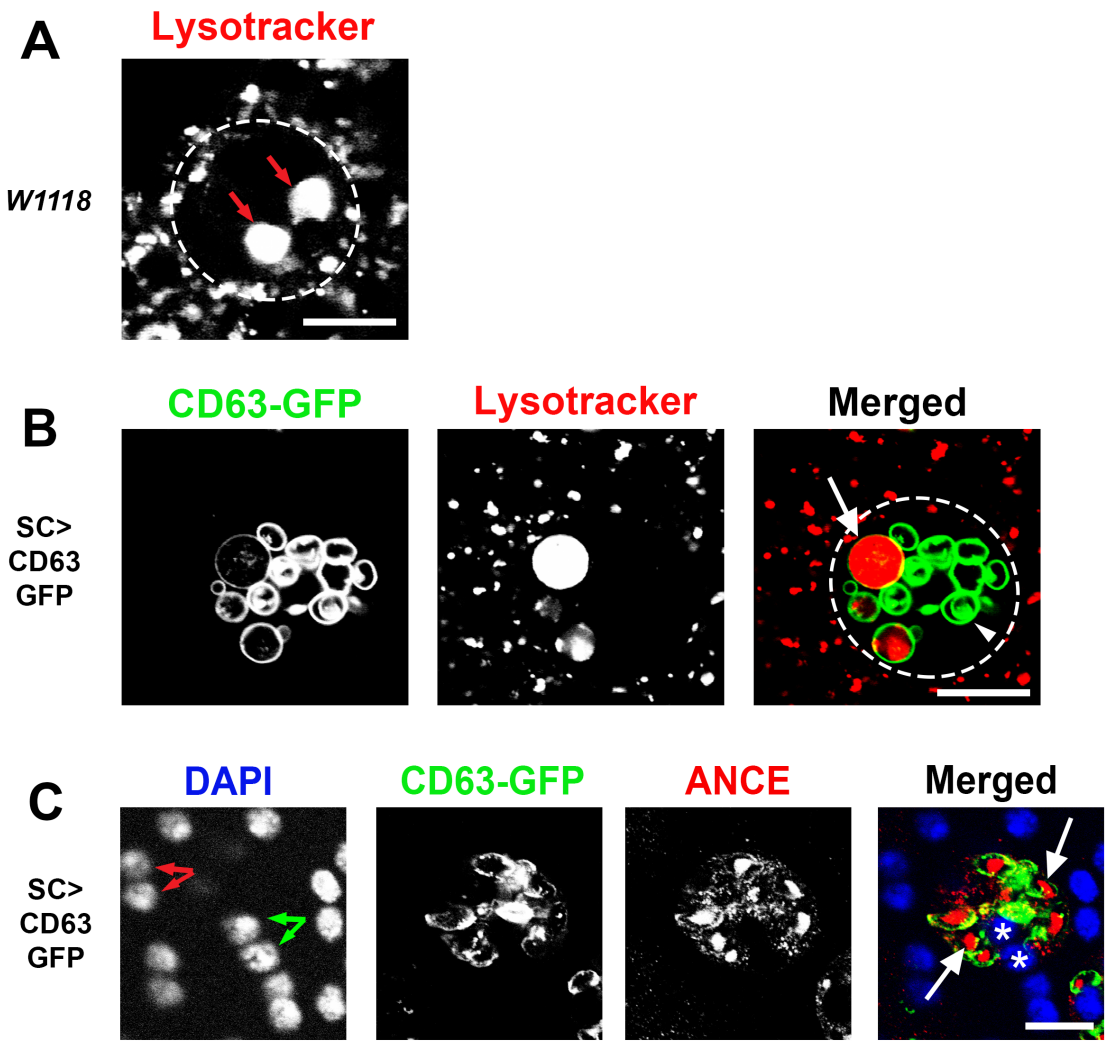


Figure 3.1 SCs contain large intracellular compartments.

A) SCs from 3-day-old *W*^{1118} flies stained with the acidic sensitive dye Lysotracker. Notice the large intracellular acidic compartments (arrows). All intracellular compartments of SCs can be visualised by expressing CD63-GFP **(B)**. SCs from 3-day-old expressing CD63-GFP and stained with Lysotracker illustrates that they have both acidic (arrow) and non-acidic compartments (arrowhead). The AG was imaged live using confocal microscopy with images representing a single z-plane, so do not show all SVs. **C)** Image of fixed SC expressing CD63-GFP, stained with anti-ANCE antibody (red) and DAPI (blue). SCs are bi-nucleated (Green arrows) and surrounded by MCs, which are also bi-nucleated (Red arrows). ANCE localises to the dense-core regions of CD63-GFP positive secretory vacuoles (arrow-merged panel). Scale bar is 10 µm.

3.2.2 Age-dependent changes in the intracellular compartments of SC

Prior findings from the Wilson lab indicated that adult SCs display some age-dependent changes such as growth (Leiblich et al., 2012). To understand how SC compartments mature and to assess the changes in their numbers, AGs were dissected in flies aged between 1-8 days and imaged under live conditions.

I observed that the number of non-acidic compartments significantly increased as males age, e.g. 11.5 +/- 0.13 at day 1 vs. 26.1 +/- 0.9 at day 8 (Figure 3.2A, B). This increase was more pronounced between 1-5 days, after which there was a general plateau in non-acidic compartment numbers (Figure 3.2B), indicating that the majority of these compartments are usually formed by 5 days. There was also a significant increase in the number of large acidic compartments, albeit to a lesser extent than non-acidic compartments e.g. 1.5 +/- 0.2 at day 1 vs. 3.14 +/- 0.3 at day 8 (Figure 3.2B).

Interestingly, the acidic compartments at day 1 appeared to be far smaller than those observed at day 8 (Figure 3.2A). I hypothesised that small acidic compartments may fuse with each other to form a larger, more mature acidic LEL compartment. To address this, we scanned through SCs, found the z-plane at which the largest MVBLs was at its greatest, and measured the diameter of this acidic compartment. We found that the size of this compartment significantly increases from day 1 to day 8 (Figure 3.2C), indicating that the growth of this compartment may be a result of smaller acidic and possibly non-acidic compartments fusing with it (see Figure 3.9). Surprisingly, the size of the largest non-acidic compartment did not change significantly over time and rarely exceeded 5 μm in diameter (Figure 3.2C).In conclusion, the number of large CD63-positive non-acidic compartments (which I call secretory vacuoles [SVs])

increases with time in adult SCs, but their general size does not appear to change. By contrast, the increase in LEL number is less pronounced, but the size of the largest LEL compartment significantly increases as adult flies age.

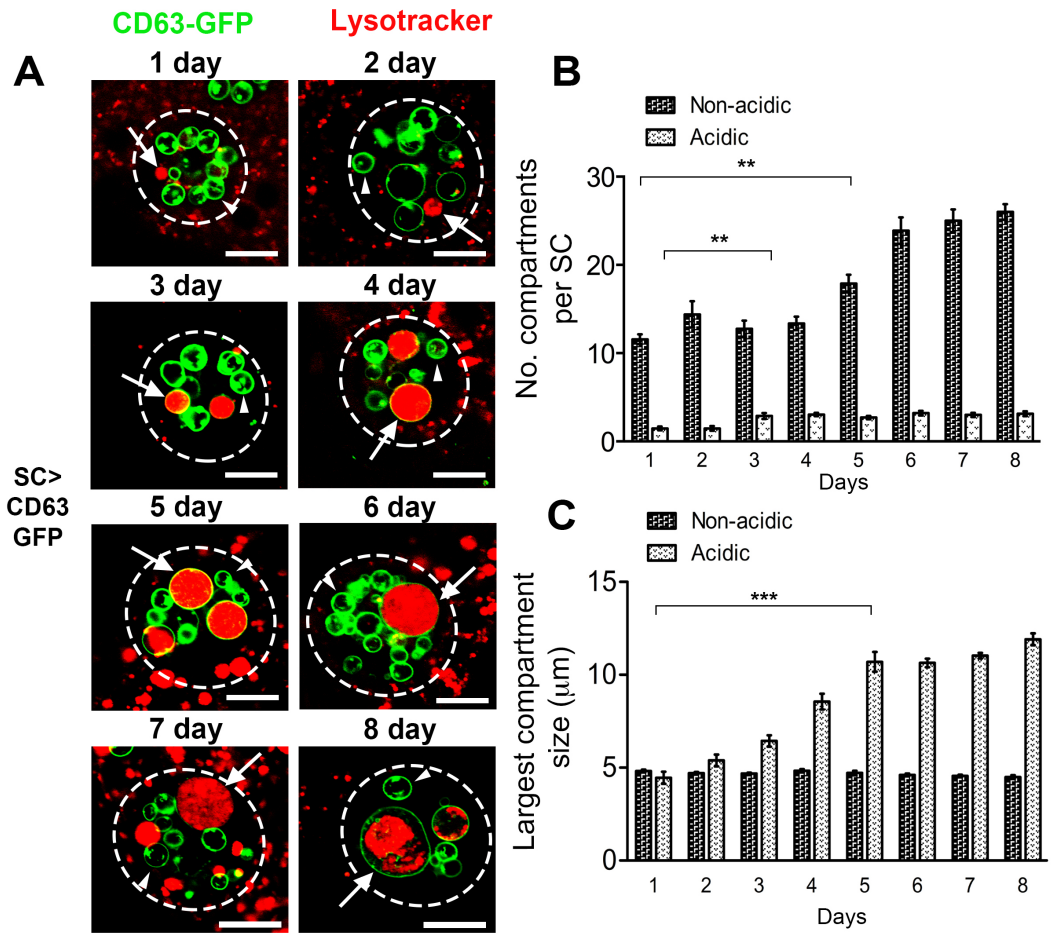


Figure 3.2 Age-dependent changes in SVs and endolysosomal compartments.

SCs expressing CD63-GFP (green) and stained with Lysotracker (red) were imaged live over an 8 day period. We rarely saw any mature large acidic MVBLs at 0-1 days **(A)**, but there were numerous small acidic compartments observed during this time period. We saw a gradual increase in the number of SVs (arrowheads) and LELs (arrow) over the time-course **(B).** Also, the size of the largest MVBL (arrow) increases over time **(C)**. Images represent a single z-plane of the largest LEL. Dashed line indicates the SC perimeter. **P<0.01, ***<0.001, Mann-Whitney *U* test, n=10. Scale bar is 10 μm.

3.2.3 Some CD63-GFP is terminally trafficked to acidic LEL compartments

While I was studying SC compartment biology, Corrigan et al (2014) demonstrated, using short pulse-chase analysis, that CD63-GFP is initially trafficked to two non-acidic compartments and then subsequently to LELs in SCs. This is in support of our hypothesis that this fusion protein is initially trafficked through the Golgi and onto secretory compartments before reaching acidic LELs, potentially via the plasma membrane.

In an effort to further characterise how CD63-GFP is trafficked, once all SC compartments have been labelled, a series of longer pulse-chase experiments were performed. CD63-GFP expression was induced for 4 days in adults, during which all SC compartments were labelled, and then chased for 0-4 days afterwards (Figure 3.3A). In SCs expressing CD63-GFP for 4 days, there were roughly 13.4 +/- 0.8 SVs labelled (Figure 3.3B). This decreased to 9.9 +/- 0.5 SVs after a 1-day chase and to 4.7 +/- 0.2 after a 2-day chase (Figure 3.3B). After a chase period of 4 days, there was hardly any CD63-GFP lining the non-acidic compartments, but the acidic compartments were still labelled (Figure 3.3A). Interestingly, the number of acidic compartments labelled with CD63-GFP also decreased with increasing length of the chase period, albeit to a lesser extent, e.g. 3.5 +/- 0.2 after a 1 day chase compared to 1.8 +/- 0.2 after a 4 day chase (Figure 3.3B).

To ensure that the non-acidic compartments were still present after a 4day chase, SCs were stained with the dense-core marker ANCE. In these cells, ANCE was still present inside the DCG compartments that lacked a CD63-GFP-positive limiting membrane (Figure 3.3C). Interestingly, there was one compartment labelled with CD63-GFP that

did not contain ANCE and presumably represented the LELs that we observed after a 4-day chase (Figure 3.3A).

These data suggest that after CD63-GFP expression has been induced in a pulse for 4 days, there is a gradual decrease in the number of CD63-GFP-labelled SVs as the chase period increases. Since some LELs are still labelled with CD63-GFP, even after a 4-day chase, the traffic of some CD63-GFP seems to be directed towards these compartments, further supporting our classification of these compartments as LELs that receive material from the secretory compartments. This is in line with our previous observation that CD63-GFP traffics first to SVs and later to LELs (Corrigan et al., 2014). Importantly, Corrigan et al. (2014) also showed that CD63-GFP was secreted from SCs into the lumen of the AG on exosomes, so only a fraction of the synthesised protein is ultimately sent to the degradative lysosomal system in SCs.

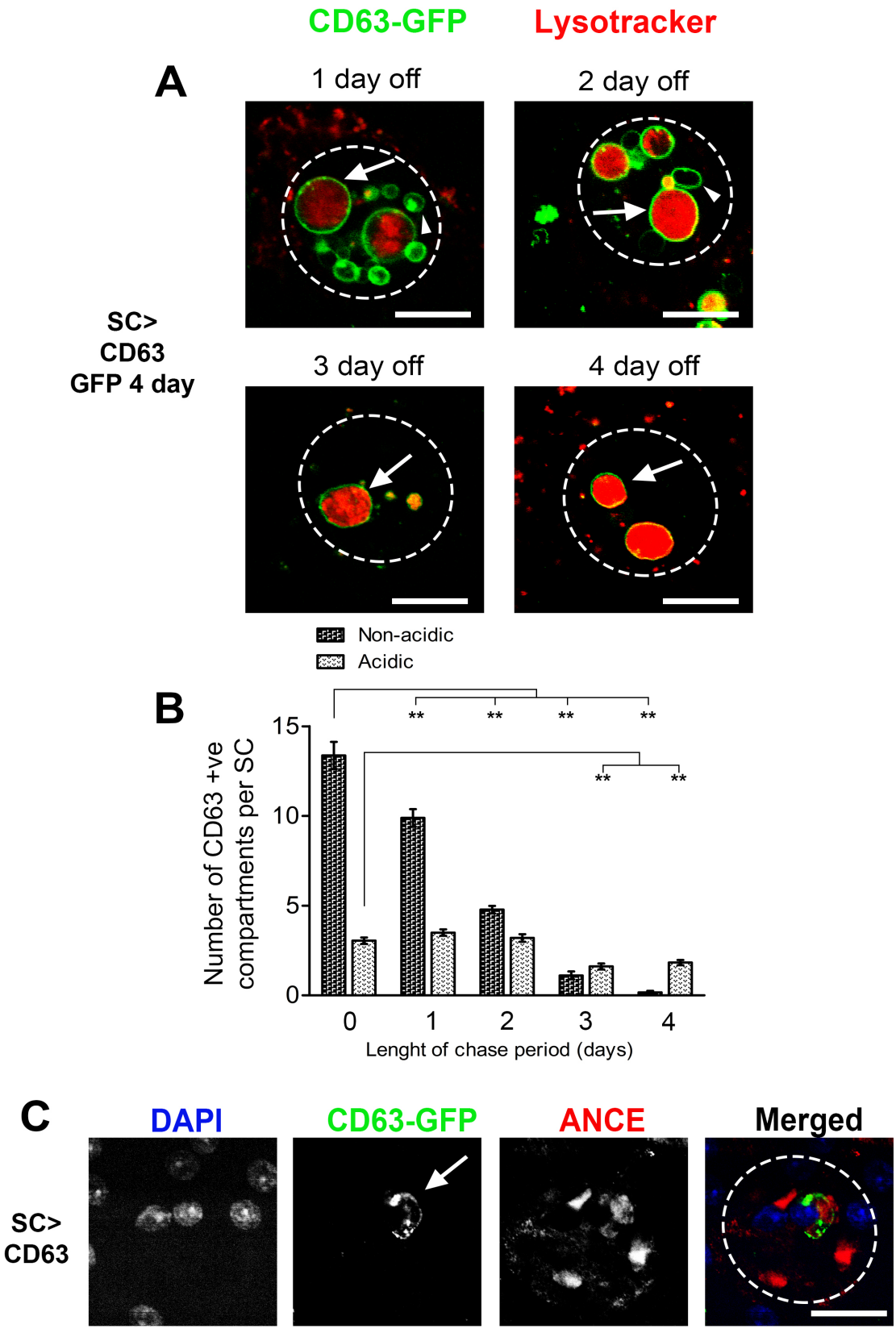

CD63-GFP
Lysotracker
A
1 day off
2 day off
SC>
CD63
GFP 4 day
3 day off
4 day off
Non-acidic
Acidic
B
Number of CD63 +ve compartments per SC
15
10
5
0
**
**
**
**
**
**
0
1
2
3
4
Lenght of chase period (days)
C
DAPI
CD63-GFP
ANCE
Merged
SC>
CD63

Figure 3.3 CD63-GFP traffics towards MVBLs.

SCs expressing CD63-GFP for 4 days and then chased for 0-4 days afterwards **(A)**. Notice that after a 1-day chase period, CD63-GFP lines both acidic (arrow) and non-acidic (arrowhead) compartments, but after 4 days chase, it only lines acidic compartments. **B)** Quantification of the number of compartments, showing that the labelled CD63-GFP SVs gradually decrease in number with increasing chase periods, whilst the acidic compartment is still present. **C)** Fixed SCs expressing CD63-GFP for 4 days and chased for 4 days, stained with DAPI (blue) and ANCE (red). Notice that the only CD63-GFP compartment, representing the remaining acidic compartment, does not encircle the ANCE positive core. **P<0.01, Kruskal-Wallis test, n=10. Scale bar is 10 μm.

3.2.4 SCs compartments have distinct Rab signatures

To classify SCs compartments at a molecular level, we used Rab-YFP constructs driven ubiquitously in flies at moderate levels under the tubulin protein (Marois et al., 2006). As previously mentioned, Rab proteins are widely used as markers of intracellular membranes and organelles. Rab5 is classically considered to be an early endosome marker and its expression in SCs marked a population of small non-acidic puncta, and a few small acidic structures (Figure 3.4A). FYVE-domain containing proteins are typically found on early endosomes (EEs) (Lawe et al., 2000).

To confirm that Rab5 marks EEs, I expressed a GFP-tagged FYVE zinc finger domain and stained these cells with an antibody raised against Rab5. Indeed, in these SCs, FYVE-GFP and anti-Rab5 completely co-localised on the same compartment (Figure 3.5). I therefore refer to these as Rab5 positive early endosomes. The number of non-acidic early endosomes did not change significantly in SCs of flies aged between 1-8 days (Figure 3.4D), suggesting that there is a consistent population of early endosomes in SCs. It is proposed that EEs contribute to, as well as mature, into late endosomal MVBs. Since EEs were sometimes acidic or found to be in close vicinity to acidic compartments, we hypothesise that this may represent a stage in this maturation role.

Expression of the recycling endosome and vesicle trafficking marker, Rab11, exclusively marked most of the non-acidic large compartments in SCs (Figure 3.4B). Interestingly, Rab11-YFP did not line any acidic compartments, but its expression under tubulin control seemed to reduce the number of MVBLs, suggesting that low-level expression of this construct alters the balance of secretory and LEL compartments in these cells. There was a significant increase in the number of Rab11-positive compartments in flies aged from 1 to 4 days, but no further increase between

4 to 8 days (Figure 3.4E). When these SCs where fixed and stained for ANCE, Rab11 marked all ANCE-positive compartments (Figure 3.6B, D), making this a reliable marker for DCG compartments. However, the number of Rab11-positive, non-acidic compartments appeared lower than the number of CD63-GFP-positive SVs in SCs, suggesting that some non-acidic compartments may not carry DCGs. This issue is considered again in Section 5.2.2.5 below. Overall, my data suggest that Rab11 may be involved in the trafficking of DCG compartments, as previously reported in other systems.

I had postulated that the large acidic compartments in SCs were likely to be LELs and receive some of their contents from SV and other compartments. To confirm that SCs possess LEL compartments, I expressed Rab7-YFP in SCs. It marked all large acidic compartments, numbering roughly 3 in living cells (Figure 3.4,C, F), and one central non-acidic compartment in 4-day-old flies (Figure 3.4C). There were also several smaller Rab7 positive puncta some, but not all of which, were acidic (Figure 3.4C).

To further verify the late endosomal and lysosomal origin of the acidic compartments in SCs, I used other markers such as LAMP1-GFP, which have been overexpressed in other *Drosophila* cell types to label LELs (Pulipparacharuvil et al., 2005). However, its overexpression under UAS control significantly altered endolysosomal trafficking and made it difficult to interpret. Interestingly, when Rab7-YFP expressing-SCs were fixed and stained with ANCE, Rab7 was seldom seen on ANCE-positive compartments (Figure 3.6A, C). However, although infrequent, Rab7 did occasionally line compartments that are presumably also Rab11-positive (Figure 3.6A), suggesting that some of the large SC compartments may have mixed identity (see Section 3.2.6).
In conclusion, in SCs, Rab5 marks a set of small compartments that appear to be early endosomes, while Rab7 marks all large acidic compartments and usually one non-acidic compartment that may be ANCE-positive. Conversely, Rab11 marks non-acidic

compartments containing ANCE and is rarely seen on acidic compartments. I conclude that these Rab proteins are reliable markers of secretory and LEL compartments in SCs.

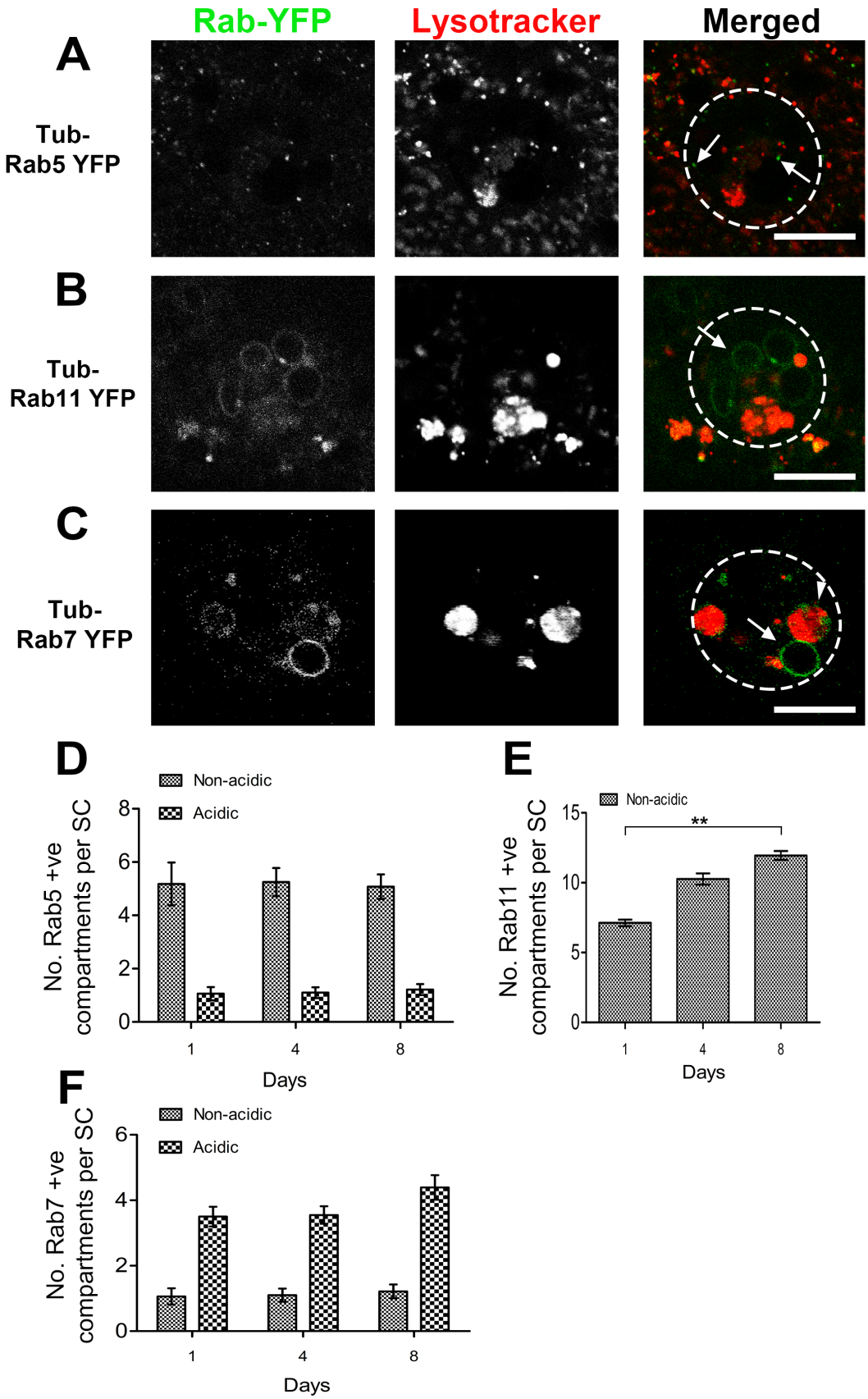

Rab-YFP
Lysotracker
Merged
A
Tub-
Rab5 YFP
B
Tub-
Rab11 YFP
C
Tub-
Rab7 YFP
D
Non-acidic
Acidic
No. Rab5 +ve compartments per SC
Days
E
Non-acidic
**
No. Rab11 +ve compartments per SC
Days
F
Non-acidic
Acidic
No. Rab7 +ve compartments per SC
Days

Figure 3.4 Rab GTPases mark distinct intracellular compartments in SCs.

A) Live imaging of 4-day-old SCs expressing Rab5-YFP under tubulin control. Rab5-YFP is localised to small puncta within SCs (arrows). The number of Rab5 positive puncta does not significantly change from between 1 to 8 days. Rab11-YFP marks a set of non-acidic compartments **(B)** whose numbers increase from 1 to 8 days **(E)**. Rab7-YFP predominantly localises to acidic late endosomal compartments (**C**, arrowhead) but sometimes to one non-acidic compartment (**C**, arrow). The number of Rab7 labelled acidic compartments does not significantly change **(F)**. **P<0.01, Mann-Whitney *U* test, n=10. Scale bar is 10 μm.

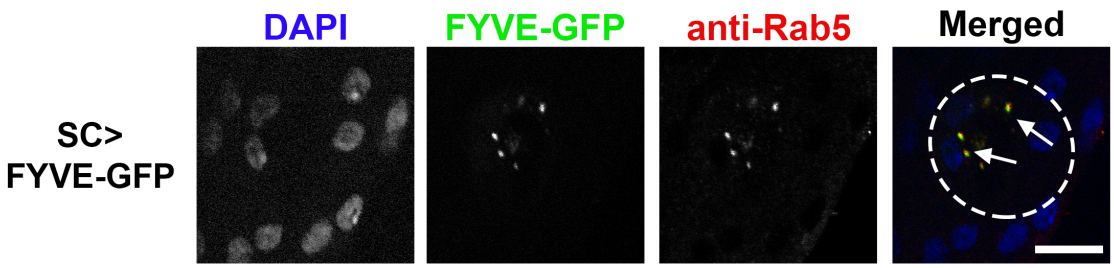


Figure 3.5 Rab5 and FYVE-domain containing protein co-localise.

3-day-old SCs expressing a FYVE-domain zinc finger protein tagged with GFP and stained with an antibody raised against Rab5, showing that they co-localise on the same compartment (arrow). Scale bar is 10 μm.

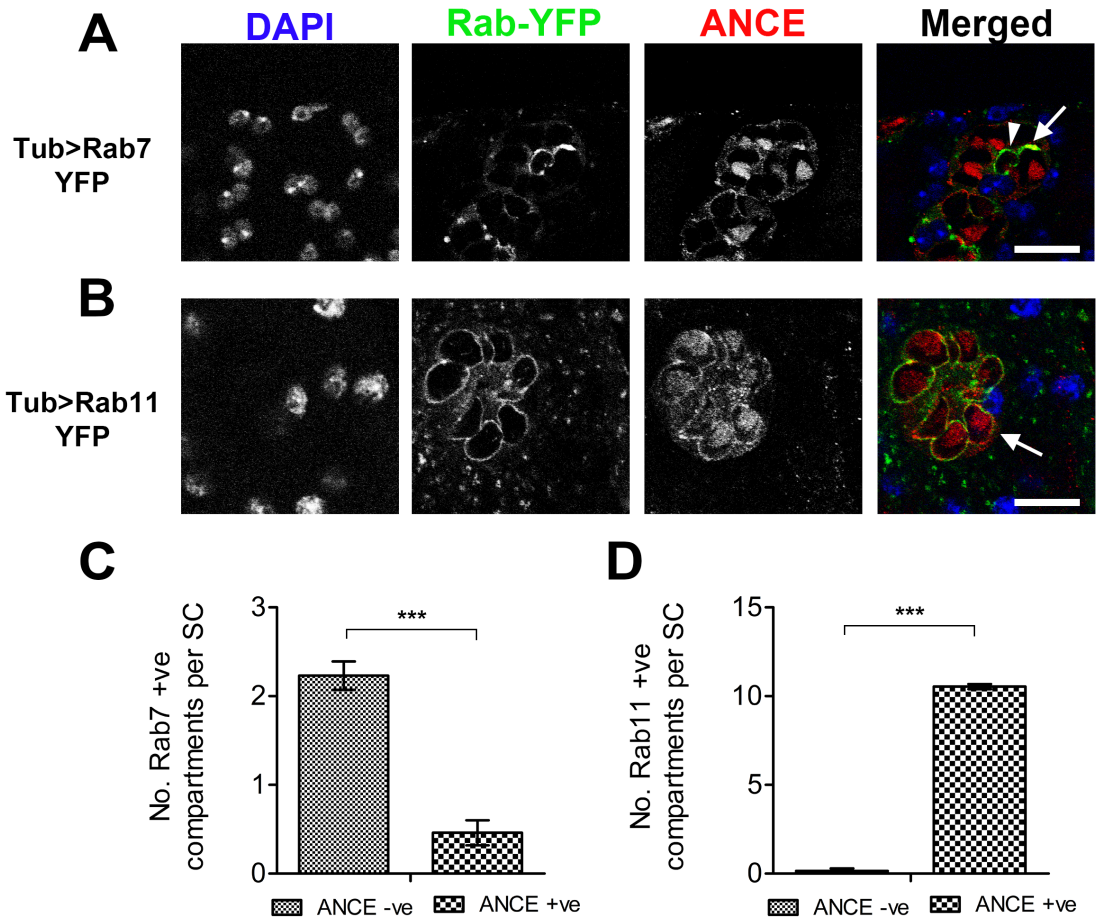


Figure 3.6 Secretory vacuoles containing ANCE are marked with Rab11 and sometimes Rab7.

A) 3-day-old fixed SCs expressing Rab7-YFP and stained with DAPI (blue) and ANCE (red). Rab7 mostly localises to ANCE-negative compartments (arrowhead), but at times can be seen on the limiting membrane of an ANCE compartment (arrow). Quantification for these observations is shown in **(C)**. **B)** Rab11-YFP is seen predominately on ANCE- positive secretory vacuoles (arrow), indicating this Rab as a good marker of dense-core granule-containing secretory vacuoles **(D)**. ***P<0.01, Mann-Whitney *U* test, n=10. Scale bar is 10 μm.

3.2.5 The secretory apparatus of SCs is marked by Rabs

Our observations that Rab11 marks DCG compartments directed us to characterise other components of the secretory pathway such as the Golgi and ER. To highlight these organelles we used Rab GTPases that were previously reported to mark these compartments (Pfeffer and Aivazian, 2004). Rab1 is localised to the ER and the pre-Golgi compartments. In an effort to reduce disruption to these delicate structures by overexpression, we used a Rab1-YFP gene trap line, which expresses this protein at endogenous levels, and that became available during the course of my studies. Expression of Rab1-YFP highlighted a network of interconnected stacks that were usually situated in the centre of SCs and reminiscent of the Golgi apparatus (Figure 3.7A).

To confirm Golgi identity, I used a fly line expressing galactosyltransferase-GFP fusion protein, which localises to Golgi structures in other tissue (Frescas et al., 2006). SCs expressing this construct showed a distinctive central staining pattern (Figure 3.7C) similar to Rab1-YFP. Moreover, I used an antibody raised against the *cis*-Golgi-localised protein GM130 and stained SCs. Interestingly, the staining pattern observed in SCs (Figure 3.7D) was very similar to that of Rab1-YFP, and Golgi-GFP and confirmed our observation that these structures are the centrally distributed Golgi apparatus.

Rab6 is another GTPase that marks the Golgi and controls retrograde transport from the Golgi to the ER (Valente et al., 2010). In addition, Rab6 is also involved in the secretory pathway by decorating vesicles exiting from the Golgi (Martinez et al., 1994). To test whether some of the large SVs might be derived from the Golgi, the Rab6-YFP gene trap was expressed in SCs. Interestingly, Rab6 highlighted a population of large non-acidic SVs (Figure 3.7B) of a similar size to those marked by Rab11, suggesting

that these two Rabs may either mark two classes of SV or in some cases label a mixed compartment in SCs.

In conclusion, SCs have an elaborate network of Golgi stacks that are marked by Rab1, whilst a subset of large secretory compartments is marked by Rab6, further supporting our hypothesis that SVs are derived from the Golgi.

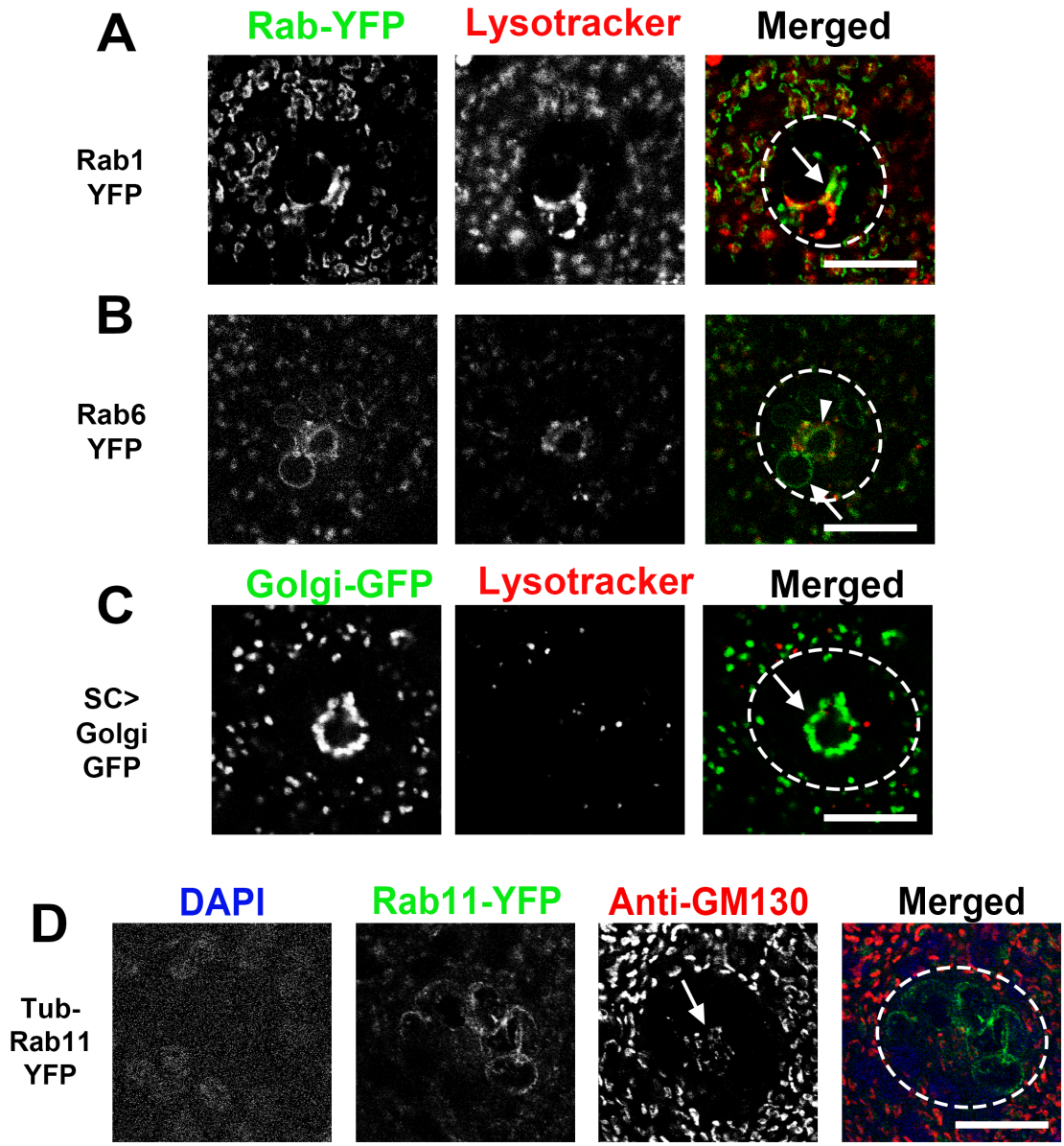


Figure 3.7 Secretory apparatus is marked by Rab gene traps.

Expression of the Rab1-YFP under its endogenous promoter, labels a distinct interconnected network of membrane (**A,** arrow), reminiscent of Golgi-like structures. **B)** Rab6-YFP labelled a set of non-acidic compartments (arrow), some of which were centrally distributed (arrowhead). **C)** SCs expressing Golgi-GFP show a distinct central pattern of labelled membrane. **D)** Fixed SCs expressing Rab11-YFP and stained with GM130, a *cis*-Golgi marker. Antibody staining was centrally distributed confirming that this region is the location of the Golgi. All images were taken from 3-day-old flies. Scale bar is 10 μm.

3.2.6 Rab11 co-localises with Rab6 and Rab7 on some compartments in SCs

Because Rab6 was seen on non-acidic compartments that resembled those marked by Rab11 we hypothesised that both Rab6 and Rab11 might co-localise here. To address this, flies expressing both Rab6-CFP and Rab11-YFP were imaged using real-time microscopy. Interestingly, we observed both Rab6 and Rab11 on at least one SV (Figure 3.8A), suggesting that they co-operate together on this compartment to regulate membrane trafficking. Indeed, we hypothesis that immature DCGs labelled with Rab6 initially form at the Golgi and later mature into Rab11, potentially through a Rab switch.

Since Rab7 also lined one non-acidic, ANCE-positive compartment, we hypothesised that Rab7 and Rab11 might also sometimes co-localise. Indeed, antibody staining of Rab7 in SCs expressing Rab11-YFP showed co-localisation in a specific compartment (Figure 3.8B). We speculate that since this non-acidic compartment possesses both the Rab11 and Rab7 markers, it may form a part of a sorting hub where membrane subdomains and proteins are committed either to an endolysosomal or secretory route. We do not at present know whether Rab7, Rab11 and Rab6 all co-localise on the same compartment, which might represent a sorting hub for membrane trafficking to direct compartments either to a secretory or endosomal fate.

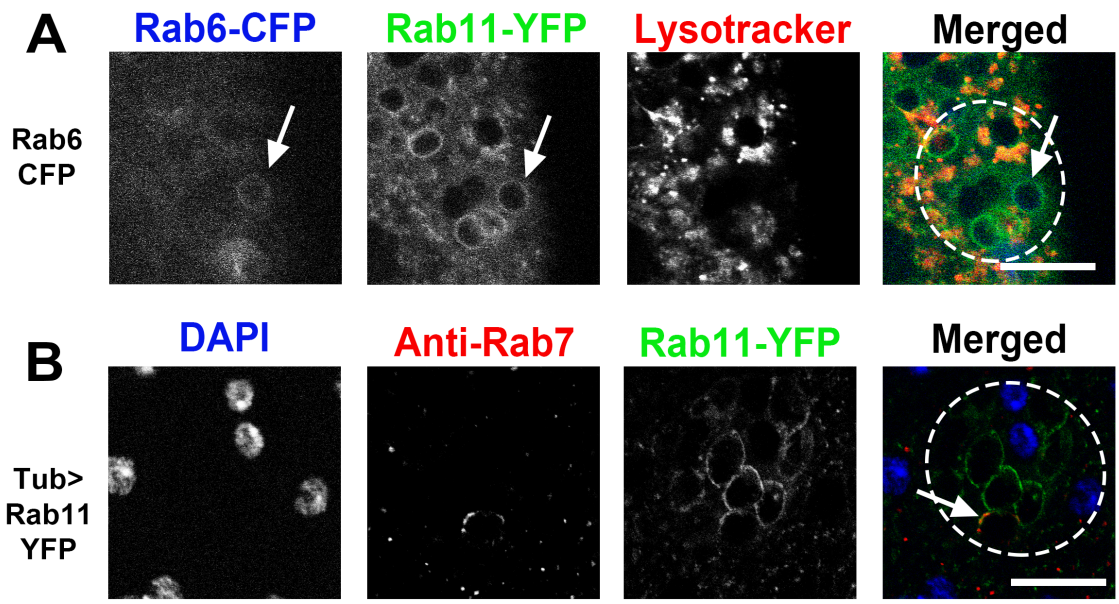


Figure 3.8 Rab GTPases co-localise on the same compartments in SCs.

A) 3-day-old live SCs expressing both Rab6-CFP and Rab11-YFP under their endogenous promoter and stained with Lysotracker. Rab11 was seen to co-localise with one Rab6 compartment (arrow). **B)** SCs expressing Rab11-YFP under tubulin control and stained with an antibody raised against Rab7. Rab11 and Rab7 were seen on the same compartment in SCs (arrow), potentially highlighting this compartment as a sorting station for directing compartments to either a secretory or endolysosomal fate. Scale bar is 10 μm.

3.2.7 SCs compartments are highly dynamic

To test if materials are exchanged between non-acidic SVs and LELs, real-time live imaging of SCs expressing CD63-GFP was performed. Interestingly, over the period of time we imaged these cells (up to 1 minute), we occasionally observed a CD63-GFP positive SV fusing with an LEL (Figure 3.9A), although surprisingly, the luminal content of this hybrid compartment did not freely mix during this time period. This suggests that one mode of delivery of material from SVs to LELs involves compartment fusion.

Since these compartments are able to fuse with each other, we hypothesised that there may be other forms of interactions that might be visualised with a more specific marker. Using real-time confocal microscopy, we observed a range of tubules emanating from the limiting membrane of Rab7-positive late endosomal compartments that seemed to interact with SVs (Figure 3.10). Although others have reported tubule formation in flies, these structures did not contain Rab7 (Burgess et al., 2012). Endosomal tubules have also been observed in mammalian systems, and they have previously been proposed to regulate sorting and recycling of proteins (Grant and Donaldson, 2009).

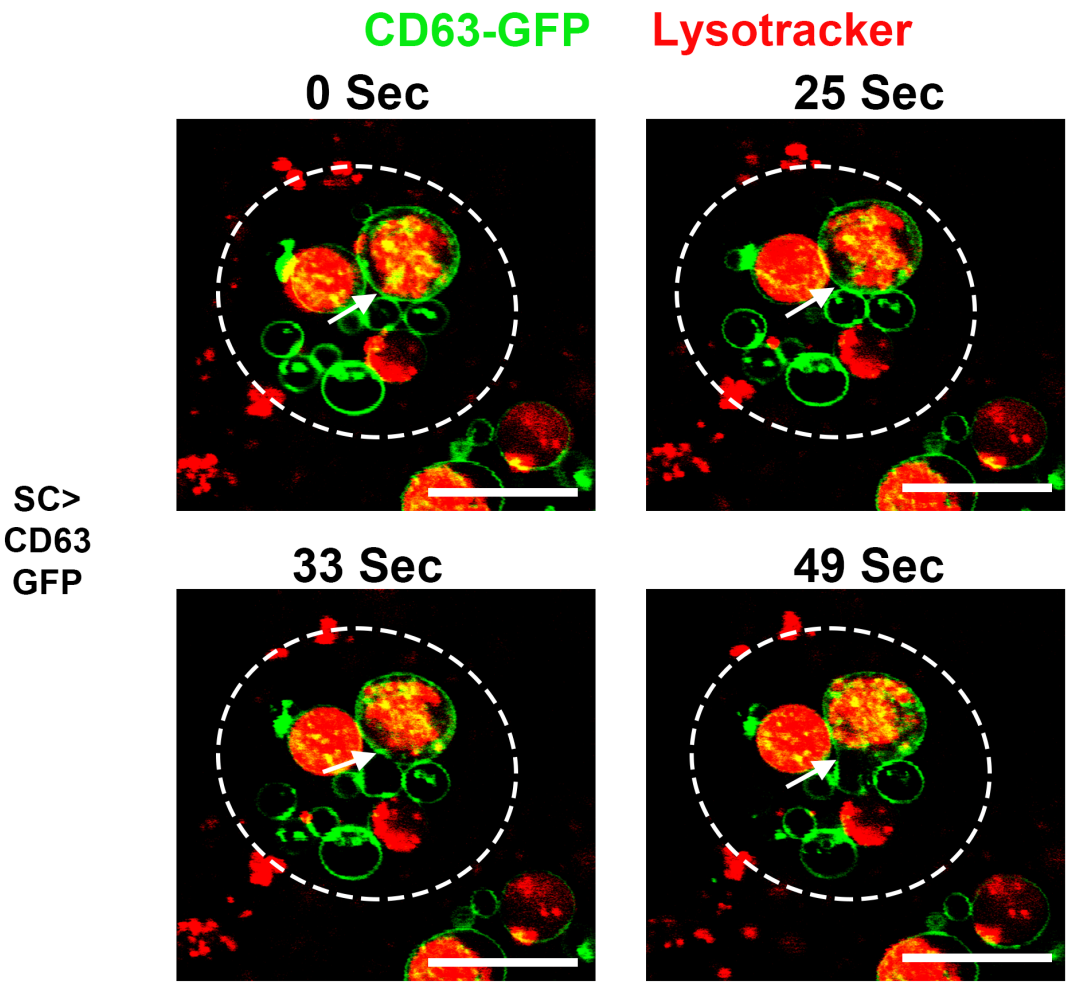


Figure 3.9 Secretory and endolysosomal compartment fuse together.

Live imaging of SCs expressing CD63-GFP for 3 days and stained with Lysotracker imaged over 1 minute time-course. During this period, a non-acidic secretory vacuole was seen to fuse with large acidic compartments (arrow), although the internal content is not seen to freely mix in this time-period. This provides a mechanism for exchanging material between these two types of compartments. Scale bar is 10 μm.

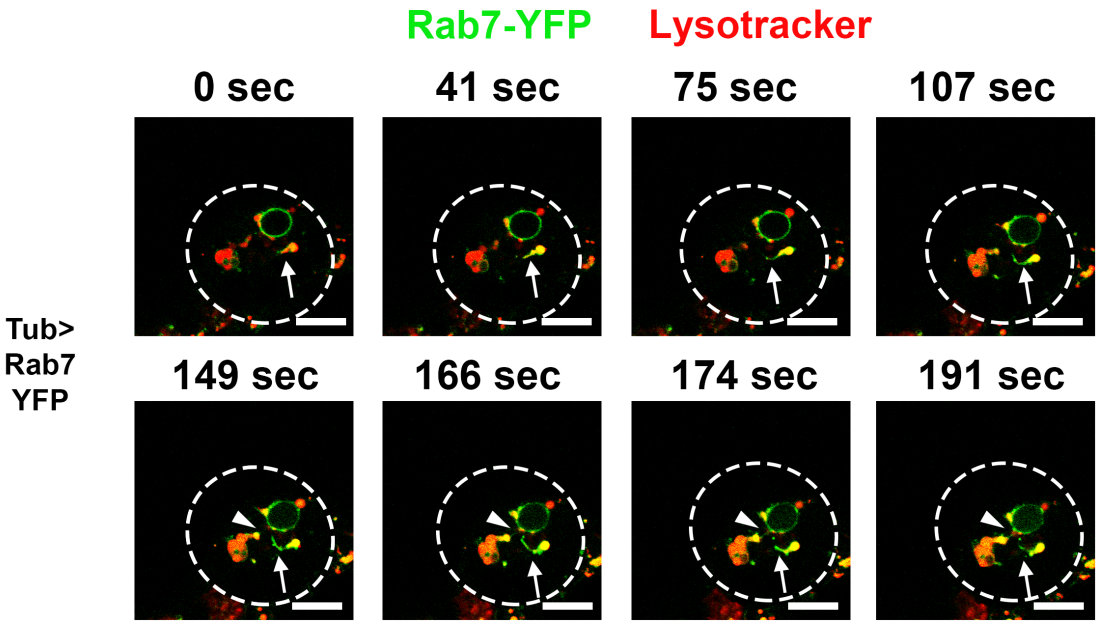


Figure 3.10 Tubules extend from late endosomal compartments.

Real-time confocal imaging was conducted on 3-day-old SCs expressing Rab7-YFP. Rab7-positive tubules emanate from a late endosomal compartment (arrow) and extend towards a non-acidic compartment surrounded by small acidic compartments and then retract, as another tubule extends from the acidic compartment on the left (arrowhead). Scale bar 5 μm for all panels.

3.2.8 SCs have dynamic filopodia-like structures

Previously, Leiblich et al (2012) showed that SCs are able to delaminate and migrate to the proximal tip of SCs in multiply-mated males. In order for this event to occur, SCs must have a mechanism to sense the environment and tether to the surrounding extracellular matrix (ECM). In other cell types, migration is coupled with extending filopodia-like structures, which sense and adhere to the surrounding ECM (Jacquemet et al., 2015).

To assess if SCs possess filopodia or filopodia-like structures, a transverse optical section of the apical region of SCs was imaged using live microscopy. Interestingly, I observed a dynamic network of filopodia-like structures protruding into the lumen and retracting back onto the plasma membrane (Figure 3.11). These structures seemed to emerge from all over the apical membrane. They may be a sensing mechanism for SCs to assess the content of the lumen, and adjust secretion and migration accordingly. Alternatively, or in addition, filopodia have been implicated in extracellular vesicle and exosome secretion in mammalian cells and nematodes.

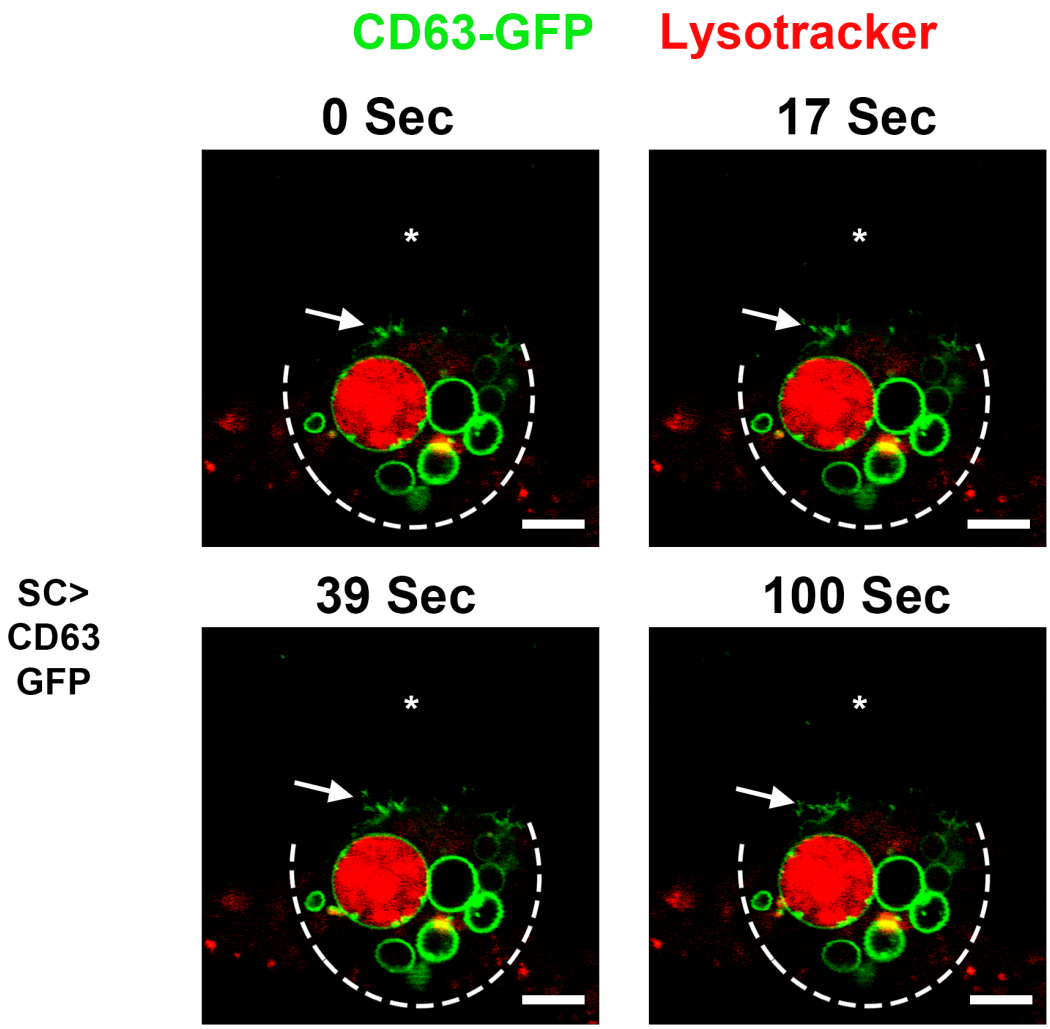


Figure 3.11 SCs have dynamic filopodia-like extensions.

Live imaging of SCs expressing CD63-GFP highlighting the apical section of the cells and the AG lumen (*). Over the time-course, CD63-GFP positive extensions (arrow) were seen protruding into the lumen (*). Images were taken from 3-day-old flies. Scale bar 5 μm for all panels.

3.2.9 Electron microscopic analysis of SCs

SCs possess many unique features such as having a large endolysosomal and secretory system and a distinct network of interconnected Golgi cisternae to support secretion. To analyse these features at high resolution, the ultrastructure of SCs was imaged using electron microscopy of AGs from 3-day-old w^{1118} flies. As previously reported, I observed that SCs contained a number of visible DCG compartments with DCGs surrounded by a network of fibrillar material, which remains entirely uncharacterised (Figure 3.12B) (Rylett et al., 2007). There were also a few large compartments that were void of dense-cores but instead contained smaller vesicles that might be equivalent to the fluorescent puncta seen in acidic compartments using live confocal imaging (Figure 3.12C).

Additionally, we also observed a rich network of Golgi-like structures in SCs (Figure 3.12B), confirming immunostaining images (Figure 3.7). Looking into the AG lumen, we observed very small vesicle-like structures ranging between 20-60 nm that were reminiscent of exosomes, which typically range between 40-110nm in diameter (Figure 3.12A).

Our ultrastructural analysis of SCs confirmed the presence of DCG compartments and other compartments, which do not contain DCGs. Moreover, it also highlighted an elaborate network of Golgi-like structures and small exosome-sized vesicles in the AG lumen.

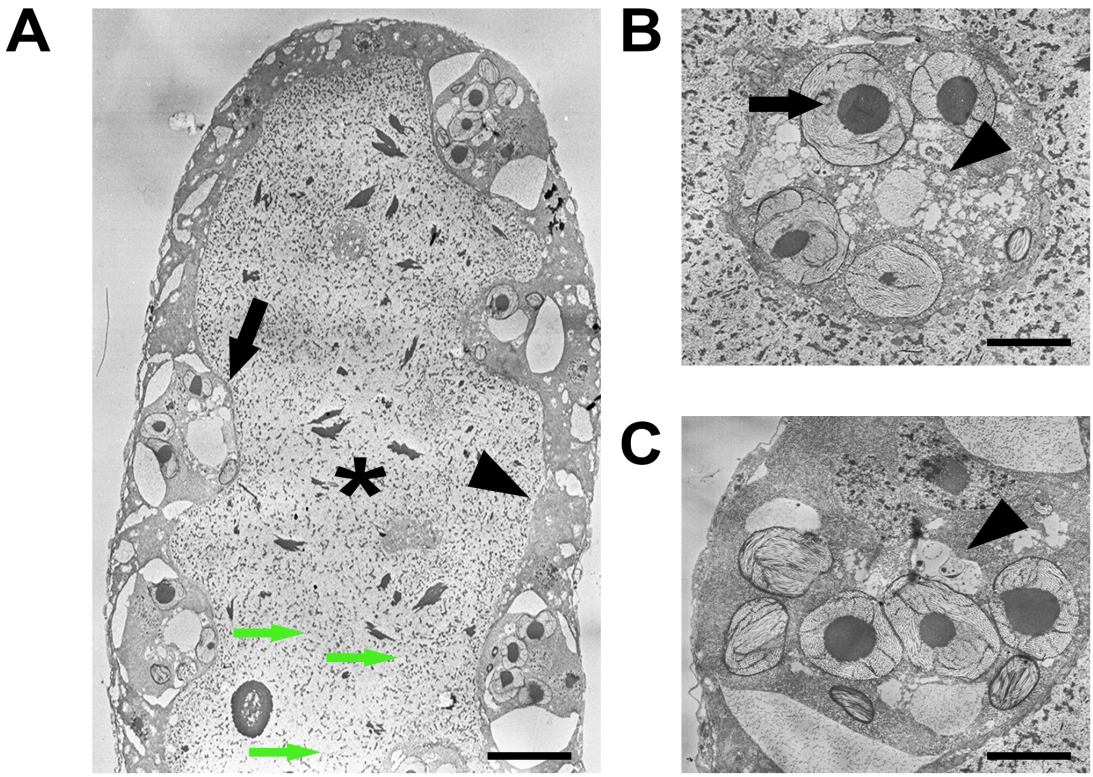


Figure 3.12 Electron microscopy of the accessory gland and SCs.

Electron micrographs were taken from 3-day-old virgin w^{1118} male accessory glands. **A)** Large SCs (arrow) are dispersed amongst smaller MCs (arrowhead) and protrude into the accessory gland lumen (*), where many membrane structures are found including those that have similar profiles to exosomes (40-110 nm – green arrow). **B)** SCs have numerous large electron-dense compartments (arrow) resembling those seen under live microscopy that contain ANCE. **C)** Some compartments appear less-electron dense (arrowhead) and by a process of elimination, may represent the acidic compartments seen under live conditions. EM work was performed in collaboration with Laura Corrigan and Prof. J Morris (DPAG). Scale bar for A) 50 µm, B) and C) 5 µm.

3.2.10 *Arf79F* regulates aspects of secretory trafficking in SCs

The elaborate network of the Golgi stacks that I observed in SCs, along with our previous observation that CD63-GFP appeared to traffic to SVs via the Golgi, prompted us to investigate the regulatory proteins that have roles in trafficking membrane and proteins through this organelle. Arf proteins are a family of GTPases classified into three classes; class I (ARF1, ARF2 and ARF3), class II (ARF4 and ARF5) and class III (ARF6) (D'Souza-Schorey and Chavrier, 2006). ARF family proteins are proposed to directly recruit COPII to the ER and COPI to the Golgi and *trans*-Golgi (D'Souza-Schorey and Chavrier, 2006). Some family members are therefore major regulators of Golgi trafficking.

Arf1 has been extensively studied in various systems. It is predominantly localised to the Golgi, and upon activation recruits its effector, COPI, to the Golgi membrane to initiate the formation of coated transport vesicles and control retrograde trafficking back to the ER (Donaldson and Jackson, 2011). In flies, Arf79F, is homologous to Arf1, and has previously been implicated in the control of retrograde trafficking, lamellipodia formation and the functional connections between the ER and lipid droplet formation (D'Souza-Schorey and Chavrier, 2006).

To understand the role of *Arf79F* in SCs, I silenced *Arf79F* by RNAi expression specifically in SCs**.** Interestingly, this prevented the trafficking of CD63-GFP to the limiting membranes of large compartments (Figure 3.13A). Instead, CD63-GFP accumulated in the central region of SCs where the Golgi is usually situated, suggesting that CD63-GFP might be trapped inside this organelle (Figure 3.13A). There were also small clusters of CD63-GFP-positive acidic compartments around the centre of the SCs, but no large LELs were visible (Figure 3.13A). My observations indicate that *Arf79F* is involved in the trafficking of CD63-GFP, potentially from the

Golgi, to non-acidic vacuoles as well as being required to form the large LELs normally seen in control flies.

To understand if *Arf79F* is required for trafficking secretory products such as ANCE to DCG compartments, I stained SCs expressing RNAi targeting *Arf79F* with ANCE. In these cells, ANCE was not present inside the cores as usually observed in the wild-type condition, but was found concentrated with CD63-GFP in the Golgi region, suggesting that both CD63-GFP and ANCE require *Arf79F* for appropriate despatch from the Golgi (Figure 3.13B). In conclusion, my data suggest that *Arf79F* is involved in trafficking both CD63-GFP and ANCE through the Golgi to DCG compartments and other SVs. It is also required to form large LELs, consistent with the idea that it might control all membrane flux from the Golgi.

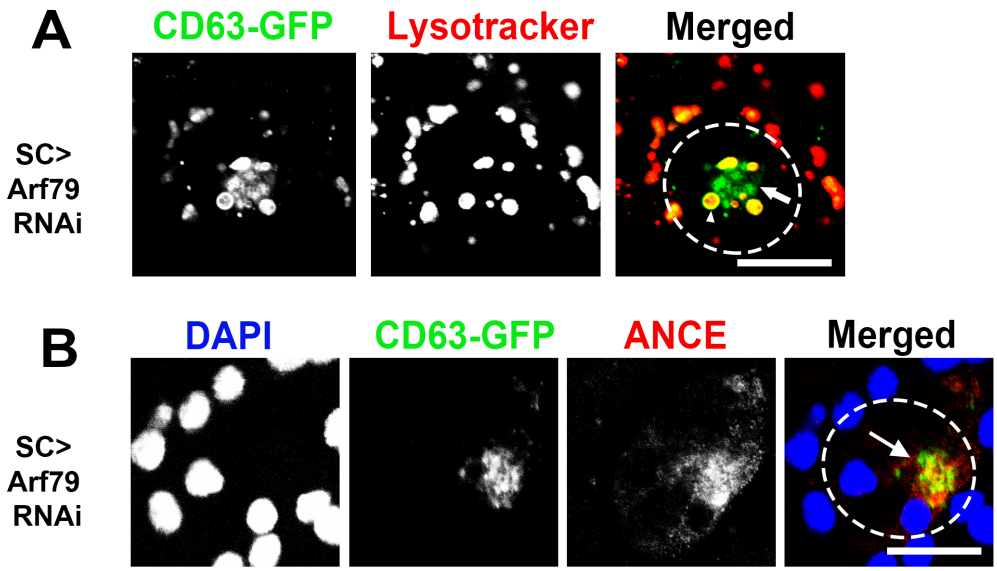


Figure 3.13 Arf79F controls trafficking out of the Golgi.

A) SCs expressing CD63-GFP and *Arf79F* RNAi were imaged live after 6 days. In these cells, CD63 aggregated (arrow) in the central region of SCs and did not line any large non-acidic compartments, although it did seem to smaller acidic structures (arrowhead). **B)** Staining these SCs with ANCE revealed that this secretory protein does not traffic into secretory vacuoles but instead also aggregates with CD63-GFP in the central region (arrow) of the cells were the Golgi is found. Scale bar is 10 μm.

3.3 Discussion

SCs are unique cells situated at the distal tips of the male *Drosophila* AGs. Although some studies have looked into the role that they play in controlling the female post-mating response, the literature regarding the cell biology of SCs remained limited, prior to my studies and those of other members of the group. In this chapter, I have used various intracellular secretory and membrane markers to characterise the internal architecture of SCs. SCs are bi-nucleated with large internal compartments, many of which contain the secretory protein ANCE (Figure 3.14). Using the fusion protein CD63-GFP, we were able to see that SCs have very large LELs (5-10 μm diameter) and non-acidic secretory compartments (2-4 μm diameter) (Figure 3.14). This is in contrast to other *Drosophila* or even mammalian epithelial cell types, which usually have much smaller intracellular compartments (Garcia-del Portillo et al., 1997). This makes SCs an ideal model to study fundamental processes in membrane trafficking associated with secretory cell function at a resolution that has not previously been possible.

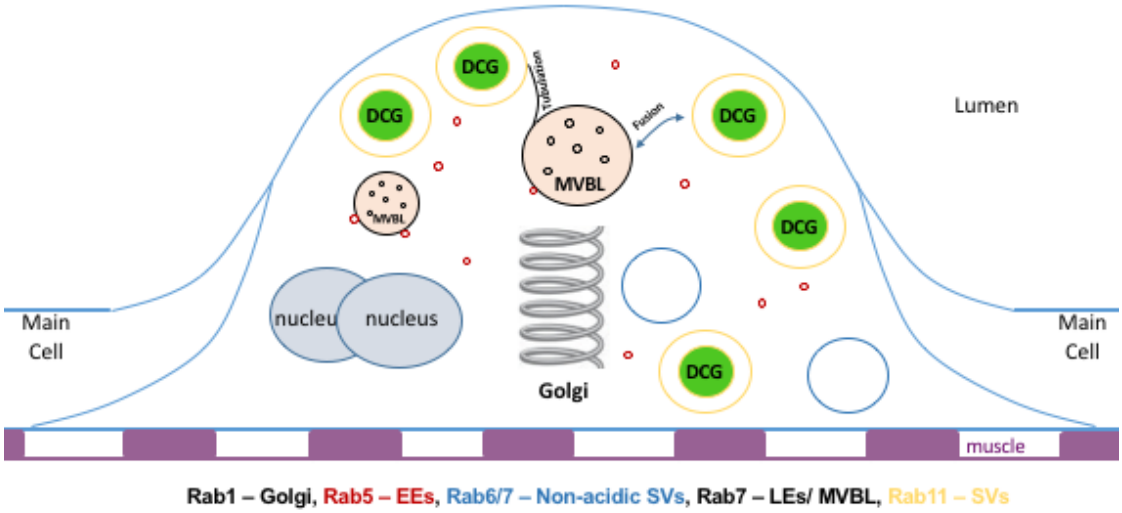


Figure 3.14 Schematic representation of SCs compartments.

SCs have a variety of different compartments that are visualised by expressing different tagged Rab proteins. Rab11 marks a population of dense-cored granules numbering roughly 10 and containing the secretory protein ANCE (Yellow membrane, green core). The endolysosomal compartments can be visualised by using the acidic sensitive dye Lysotracker (Beige). These compartments are predominantly marked by Rab7 (Black membrane), although this Rab is also seen on a few non-acidic compartments that are also marked by Rab6 (non-acidic and DCG negative; Blue membrane). Acidic and non-acidic compartments are able to interact with each other by tubular extensions or fusion. Early endosomes are distinguished by their Rab5 signature (Red membrane), some of which are close to large acidic compartments, presumably because they are undergoing maturation. The Golgi network can be marked by Rab1.

3.3.2 Compartment maturation and directional membrane trafficking

CD63-GFP is a human tetraspanin marker of intracellular compartments, particularly LELs, and of exosomes. In this chapter, I used this construct to understand how SC compartments mature over time, and the directionality of membrane trafficking. I observed that CD63-GFP is present on the limiting membrane of both acidic and non-acidic compartments. Interestingly, it was also found inside both of these compartments as intracellular puncta ranging between 40-200nm, which may represent a population of intraluminal vesicles as seen in other systems. In the next chapter (chapter 4), I show that there are in fact much more CD63-GFP in acidic compartments but its fluorescence has been supressed because of the acidic environment.

Using the acid-sensitive dye Lysotracker Red combined with live imaging, we observed that the acidic compartments increase in size in adults. EM and real-time imaging data support the idea that these large compartments are probably lysosomes that grow during ageing both via fusion to other compartments and presumably by receiving membrane from endocytic events.

In wild-type SCs, the largest MVBL was slightly smaller than in cells expressing CD63-GFP, indicating that overexpression of this fusion protein may be driving membrane and protein trafficking into these compartments. In line with this idea, we followed the transit of CD63-GFP in a series of pulse-chase experiments and observed that this marker transits from SVs to the large LELs where fluorescence is gradually lost. Some CD63-GFP-positive ILVs are seen in these LELs, though it appears that most of the intraluminal fluorescence is quenched. Importantly, Corrigan et al. (2014) demonstrated that CD63-GFP is also secreted in puncta into the AG lumen and

showed that this secretion was regulated by many of the genes involved in mammalian exosome secretion. At the time, we believed that these exosomes were probably derived from the LELs, which contained large numbers of ILVs. However, as I discuss at the end of Chapter 5, we now think that many of them may be formed in DCG compartments, defining a second route of CD63-GFP and membrane trafficking in SCs.

Overall, I conclude that the largest acidic LEL is probably a lysosome that receives a high level of membrane input from the secretory system and plasma membrane. EM analysis suggests that this material is degraded, but not at a sufficiently high rate to prevent the structure from growing over time. Since no tools were available to us to definitely distinguish between lysosomes and mature late endosomes, I refer to these structures as LELs in my thesis.

3.3.3 Rab GTPases mark internal compartment identity

To classify the intracellular compartments in SCs, a variety of different fluorescently tagged Rab proteins were studied in SCs. I identified that Rab5 marks a population of small early endosomes and a few small acidic structures, while Rab7 lines the limiting membrane of large LELs, several small acidic compartments and one large non-acidic compartment (Figure 3.14). This is in line with other studies that have used Rab5 and Rab7 to mark early endosomes and late endosomes and lysosomes respectively. Interestingly, the recycling endosome marker, Rab11, seemed to mark all dense-cored compartments containing the secretory protein ANCE. This suggests that these compartments may ultimately fuse to the plasma membrane to release their contents, although I also obtained evidence that they occasionally fuse to LELs.

Interestingly, homologues of Rab11 have been suggested to control the secretion of mammalian DCGs such as β-cell insulin granules (Sugawara et al., 2009). Under live

conditions, Rab11 was not seen at the surface of acidic compartments, but seemed to alter the size of large LELs, suggesting that increased levels of Rab11 produced by the Rab11-YFP transgene may restrict trafficking into the large LEL structures.

In mammalian systems, Rabs are sometimes seen to be present on the same compartments, but in different sub-domains. In SCs, we observed Rab7 and Rab11 on the same compartment indicating that this compartment may be a decision point in either committing membrane in the compartment to a secretory or LEL fate. Interestingly, co-labelling SCs with fluorescently tagged Rab11 and Rab6 highlighted one compartment that contained both of these Rabs, suggesting that they may work together to control trafficking into DCG and other secretory compartments. The architecture of the Golgi was visualised by using a tagged form of the Golgi-specific Rab1. A recent study highlighted that Rab1 localised to the Golgi is able to activate mTORC1 signalling and this connection between Rab1 and mTORC1 is now being investigated in SCs (Thomas et al., 2014).

Live confocal imaging revealed that non-acidic and acidic compartments are competent to fuse with each other and also interact via Rab7-positive tubules. This provides two different avenues for these compartments to exchange material, subsequent to their formation. In the *Drosophila* salivary gland, PI4KII-GFP tubules are seen to connect the Golgi to the late endosomal compartments (Burgess et al., 2012), while in SCs, Corrigan et al. (2014) have shown that a GFP-tagged form of the lipid kinase, phosphatidylinositol-4-kinase II (PI4KII) connects LEL compartments. These types of interactions may provide a platform for removing specific molecules from DCGs and facilitate their maturation.

My work suggests that SCs are ideally suited to studying the mechanisms by which DCG and LEL compartments are formed and mature. These issues will be considered

again in the following two chapters. However, some aspects like the role of tubulation in compartment maturation remain unexplored, even though it seems likely they provide an important mechanism by which large intracellular compartments select the proteins and lipids that they will ultimately traffic.

3.3.4 Membrane trafficking to DCG and LEL compartments is directed from the Golgi

My pulse-chase experiments suggested that proteins like CD63-GFP that are ultimately destined for secretion or trafficking to the LELs reach their final destination by passing through a Rab6-positive central compartment that acts as a sorting hub. Recent real-time imaging of SCs in the lab has demonstrated that this is indeed the case.

In other cells, Rab6 plays a critical role in trafficking through and out of the Golgi apparatus (White et al., 1999). To verify that like other cell types, SCs also direct membrane trafficking through the Golgi, we expressed RNAi targeting *Arf79F*, the *Arf1* homologue, and showed that knockdown prevented trafficking of CD63-GFP out of the Golgi into SVs. Interestingly, the only acidic compartments identified in these cells were small and filled with CD63-GFP, indicating that Golgi trafficking is also required for the formation of large LELs and for LEL maturation. Mammalian Arf1 is implicated in assembling clathrin coats on the Golgi and small vesicles as well as regulating Golgi trafficking by recruiting COPI vesicles (D'Souza-Schorey and Chavrier, 2006). Although Arf1 is also supposed to regulate retrograde trafficking back to the ER, we hypothesise that a disruption to retrograde trafficking may also affect anterograde trafficking out of the Golgi, since proteins cannot be recycled appropriately as reported in other systems.

A working model that is currently under investigation in the Wilson Lab is that immature DCGs that bud from are initially Rab6 positive and acquire Rab11 as their undergo maturation (see Figure 5.23). This is really exciting as it may identify a secretory Rab switch, which is normally seen during endolysosomal maturation.

In conclusion, I have demonstrated that SCs possess many features found in other secretory cell types, both in flies and mammals. For example, a series of Rabs mark secretory and endosomal compartments in a predictable way and trafficking through the Golgi apparatus is essential for proper formation of these compartments. The unusually large intracellular compartments in SCs make them ideal to study the regulation of membrane trafficking *in vivo*. This has allowed me to investigate the direction of membrane protein trafficking by pulse-chase experiments in this chapter and to define fusion and tubulation events that permit communication between compartments of different identity. In the next chapters, I will use the powerful genetics available in *Drosophila* to dissect out the regulation of membrane trafficking and compartment specification in more detail, and then study how the regulated secretion of these cells is controlled to ensure that compartment biogenesis meets demand.

4. Rab GTPases, SNARE proteins & V-ATPase regulate membrane trafficking, exosome secretion and cell growth (Results II)

4.1 Introduction

Building upon my previous findings presented in Chapter 3, where I identified a number of different compartment subtypes in SCs that are marked by distinct Rab GTPases, I set out to investigate how these Rab proteins control compartment identity in these cells. Several other molecules, including the SNAREs and the Vacuolar-type H^+-ATPase (V-ATPase) have been implicated in the release, fusion and maturation of secretory and endolysosomal compartments in other systems, and some of these were also tested to determine whether the biology of these unusual cells mirrored observation in other *Drosophila* or mammalian cells.

4.1.1 Rab proteins are regulators of membrane trafficking

As previously outlined, Rab GTPases are localised to distinct sub-cellular compartments and, in doing so, provide intracellular compartments with a unique identity or 'Rab signature'. This, in turn, ensures that the flux and traffic of membrane through both the secretory and endolysosomal systems occurs in a faithful manner (Barr, 2013). Rab activation is brought about by their interaction with GEFs, whilst their inactivation is regulated by GAPs (see Section 1.4). Upon activation, Rab GTPases carry out their function by recruiting specific effector proteins. Indeed, in light of this, Rabs can be seen as intermediates between a signal that brings about their activation and an output of functional membrane changes.

In a pioneering genetic study in yeast, it was observed that *Rab8* is involved in vesicular transport from the Golgi to the cell surface plasma membrane (Huber et al., 1993). Subsequent studies uncovered that there are in fact a large family of Rabs controlling specific trafficking events. More recently, Rab5 was shown to control endolysosomal maturation by recruiting SNAREs to permit fusion between the early endosomes and late endosomes (Huotari and Helenius, 2011). Similarly, Rab7 has

been implicated in regulating fusion of LE/MVB and lysosomes, whilst Rab11 and Rab27 have been suggested to control the final fusion of MVBs to the plasma membrane, thus releasing exosomes (Colombo et al., 2014). Whilst Rab11 is classically thought to be a slow recycling endosomal marker, Rab35 has been shown to control fast endosomal recycling at the cell surface, cytokinesis and also exosome secretion (Stenmark, 2009). Interestingly, a recent study showed that Rab35 controls AKT phosphorylation and PI3K signalling, linking Rabs to signalling pathway activation (Wheeler et al., 2015).

In a series of other studies, *Rab1* was shown to control ER to Golgi trafficking and its overexpression was observed to correlate with colorectal cancer, possibly by activating mTORC1 signalling (Thomas et al., 2014). Interestingly, in a seminal study, mouse *Rab1* was able to rescue a yeast mutant lacking its orthologue Ypt1, highlighting the conserved nature of this protein (Plutner et al., 1991). What is clear from all these and other studies is that Rab GTPases not only control membrane identity and trafficking, but also have many additional diverse biological roles. These roles typically involve membrane association and are mediated by various effectors (Stenmark, 2009). However, defining these roles, particularly in complex organisms is challenging, because disruption of membrane trafficking is likely to have multiple knock on effects in cell trafficking and signalling that then indirectly produce further phenotypes. The establishment of the secondary cell system provide new opportunities to assay membrane trafficking defects and therefore characterise the functions of Rabs in a highly secretory cell.

4.1.2 SNARE proteins: regulators of membrane fusion

The first set of SNARE proteins was identified in 1980, by screening temperature-sensitive mutants defective in trafficking in yeast. Subsequent to this, the mammalian

homologues of some of the yeast SNAREs were identified, and other constituents of the SNARE complex, such as VAMP and syntaxin were also discovered and hypothesised to interact with *N*-ethylmaleimide-sensitive factor (NSF) and alpha soluble NSF attachment protein (α-SNAP) (Chen and Scheller, 2001). In the decade following 1980, α-SNAP and NSF (Woodman, 1997). Shortly following this, VAMP, SNAP-25 and syntaxin were identified as membrane receptors for NSF and α-SNAP. Biologists then termed VAMP/synaptobrevin as v-SNAREs, and syntaxin and SNAP-25 as t-SNAREs (see Section 1.6.2). In 1998, the first crystal structure of the SNARE complex was revealed, and further experiments illustrated that SNAREs are able to induce fusion of artificial membranes (Sutton et al., 1998, Jahn and Scheller, 2006).

As mentioned in Section 1.7, some Rab effectors are in fact SNARE proteins. Genetic studies in yeast first linked Rab proteins to SNAREs, when it was shown that *Rab1* mutants could be rescued by overexpressing certain components of the SNAREs (Cai et al., 2007). Indeed, it is clear now that Rab1 is required for SNARE complex formation. Moreover, SNARE proteins have been observed to reside on early endosomes from where they are suggested to control both homotypic fusion and fusion to late endosomes, but they do not determine the specificity of fusion (Cai et al., 2007). Well-documented functions of SNAREs are their roles in controlling neurotransmitter release at synaptic terminals (Kavalali, 2015).

Interestingly, in *Drosophila* salivary glands, type ll phosphatidylinositol 4-kinase (PI4Kll) is suggested to be involved in the correct sorting of the SNARE, SNAP24, and to regulate glue granule secretion by controlling granule fusion to the plasma membrane (Burgess et al., 2012). Given the diverse roles of SNAREs, including endosome fusion, exosome secretion (see Section 1.6.2), and granule exocytosis, it is important that once a SNARE complex is formed, it is efficiently recycled and primed

for another potentially different fusion event. Understanding how SNAREs function in an *in vivo* setting is also of great importance given their diverse roles. This is partly why I decided to also investigate the roles of SNARE proteins in SCs, and also to attempt to better understand their relationships to Rab proteins.

4.1.3 The V-ATPase complex: A proton pump that controls compartment acidification and membrane fusion

The V-ATPase is a proton-pumping, multisubunit complex comprising of two major domains – the V_0 domain and the V_1 domain. The V_0 domain spans the membrane and is responsible for proton pumping, whilst the V_1 domain protrudes into the cytosol and hydrolyses ATP to drive protons across the membrane (Figure 1.6). The mature complex is built by the reversible association of both domains and is dependent on assembly factors present in the ER, but also on the presence of tissue-specific subunits (Forgac, 2007). Interestingly, targeting the V-ATPase to different intracellular membranes is dependent on specific combinations of subunit isoforms, and therefore, provides a mechanism both for forming the mature complex and localising it within the cell (Forgac, 2007).

The V-ATPase complex is best known for its role in acidifying intracellular compartments, a process that is crucial for the endolysosomal system and for the secretory pathway (Nishi and Forgac, 2002). In addition to facilitating degradation of unwanted cellular material in lysosomal compartments, compartment acidification is also important for dissociating ligand-receptor complexes in EEs/LEs, and for forming dense-core granule compartments in the secretory pathway. As previously mentioned, the maturation of EEs to LEs/MVBs and finally lysosomes are accompanied by increasing acidity at each step. How this process is regulated is currently poorly

understood, but one possibility is that the V-ATPase complex increases proton pumping based on the Rab identity of the compartment it resides in.

Recent studies suggest that the V-ATPase complex is also involved in regulating membrane fusion, partly by controlling the acidification of compartments, but also more directly, by assembling the structural components needed to form the fusion pore (Nishi and Forgac, 2002). Mutants for the V_0 subunit show increased lysosomal vacuole numbers, which is indicative of defective fusion in yeast. Loss of function of the Vha-100 V_0 subunit in *Drosophila* neurons, results in more vesicles at synaptic terminals (Hiesinger et al., 2005).

Trying to tease apart how the V-ATPase controls fusion processes through mechanisms other than disruption of acidification is challenging. By using pharmacological disruptions of the V-ATPase, Poea-Guyon *et al.* (2013) proposed that synaptic vesicle exocytosis is not only dependent on the complex's acidification functions, but also involves V_0–V_1 association, which senses compartment acidification and drives consequent fusion (Poea-Guyon et al., 2013). More recently, however, Sreelatha *et al*. (2015) provided compelling evidence using the V-ATPase binding protein, VopQ, that fusion is not dependent on compartment acidification *in vitro* (Sreelatha et al., 2015). These results have led to a model whereby the V-ATPase mediates fusion downstream of SNARE function (Scott et al., 2011). However, it remains unclear how this complex functions *in vivo*.

4.1.4 Aims

In this chapter, I focus on the regulation of membrane trafficking in the endolysosomal system and secretory pathway of SCs with the following aims:

1. To understand specific membrane trafficking steps involved in endolysosomal and secretory compartment maturation using genetic modulation of Rab GTPase.
2. To determine the role of membrane fusion in the endolysosomal and secretory pathways.
3. To identify the roles of the V-ATPase in acidification and biogenesis of SC compartments.

4.2 Results

4.2.1 Exosome secretion and their role in female physiology

4.2.1.1 Regulation of exosome secretion by Rab GTPases

During the early stages of my DPhil, L. Corrigan, showed that CD63-GFP positive puncta were present in the AG lumen when expressed in SCs. She demonstrated that the secretion of CD63-GFP is dependent on the ESRCT, Hrs, and ALiX. To provide further evidence that these puncta represent exosomes, I silenced various Rabs implicated in exosome secretion. *Rab5, Rab7, Rab11, Rab27* and *Rab35* have all been previously reported to have roles in controlling exosome secretion in mammalian systems (Colombo et al., 2014).

To understand if any of these Rabs are also involved in exosome release in SCs, we expressed either RNAi targeting specific Rabs, or overexpressed wild-type (wt) Rabs or overexpressed dominant negative (DN) or constitutively activated (CA) forms of Rabs. To assay exosome secretion, I used a simple method published by Corrigan et al. (2014) to count the number of CD63-GFP-positive puncta in the lumen of the AG (Figure 4.1C), once it had been emptied following multiple matings (see Section 2.13). To induce gene expression, the GAL4/UAS/GAL80^{ts} was used to drive both CD63-GFP and Rab expression specifically in SCs when flies had been temperature shifted shortly after eclosion.

Silencing of *Rab5*, *Rab7*, *Rab11*, *Rab27* and *Rab35* all resulted in reduced exosome secretion by SCs, whilst overexpression of wt-Rab11 also decreased the number of CD63-GFP puncta in the lumen relative to control flies expressing only CD63-GFP (Figure 4.1A, B). Interestingly, exosome secretion was potentially dependent on the

GTP-bound form of Rab7 and Rab11, since expression of DN forms of these Rabs, which also resulted in fewer exosome numbers (Figure 4.1A, B). To rule out non-specific effects of RNAi, we silenced *Evenness interrupted* (*Evi*), which encodes a protein involved in lipid-associated Wnt release, but not required for CD63-positive exosome secretion (Budnik et al., 2016), and counted exosome numbers in the AG. We did not observe a decrease with this treatment, indicating that our exosome phenotypes are not merely a product of overexpressing RNAi constructs in SCs (Figure 4.1A).

Rabs impinge on many aspects of intracellular trafficking. Therefore, to understand the specificity of Rab function in relation to exosome secretion, I focused on Rab11, which marks most of the large non-acidic compartments in SCs. I either expressed an RNAi targeting *Rab11* or overexpressed this Rab and measured the amount of ANCE in the lumen by counting antibody puncta staining. Interestingly, we did not observe an obvious change in the amount of secreted ANCE in the AG (Figure 4.1C), suggesting that modulating Rab11 function does not affect ANCE secretion in SCs. However, this method is not very accurate and to confirm this result, in collaboration with Laura Corrigan (a former DPhil student) and Sumeth Perera (DPhil student in the Goberdhan lab), we performed western blots for ANCE in both virgin males and mated females (see Section 2.17). In males expressing Rab11DN, there was no noticeable change in the level of ANCE in AGs (Figure 4.1D). Interestingly, when females were mated to wild-type males, a specific signal corresponding to ANCE could be detected in reproductive tract lystaes, indicating that AG content is transferred. In males expressing Rab11 DN, although the amount of ANCE transferred to females was not drastically reduced, the transfer of CD63-GFP was completely blocked (Figure 4.1E), suggesting that Rab11 is not involved in ANCE secretion.

In conclusion, I have shown that CD63-GFP puncta are representative of exosomes and that Rab5, Rab7, Rab11, Rab27 and Rab35 are all involved in exosome secretion from SCs. This suggests that the role of these Rabs in controlling exosome secretion is conserved between flies and mammals. Classically, exosomes are thought to be formed inside the MVBL, and our results indicate that Rab7, a marker for this compartment, is involved in exosome secretion. Surprisingly, Rab11, which lines SVs, is also involved in this process, potentially by interacting with Rab7-positive MVBLs.

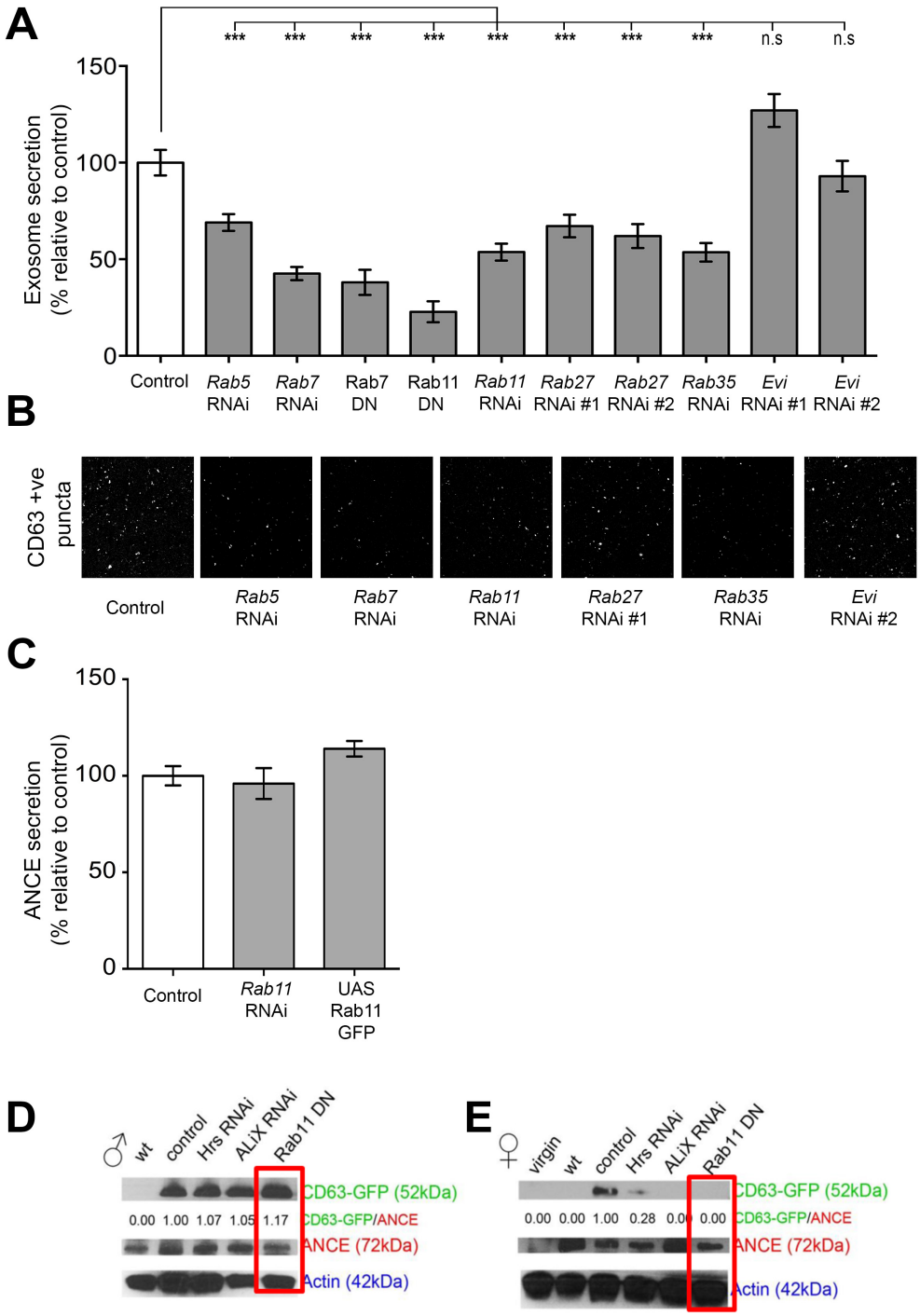

A
***
***
***
***
***
***
***
***
n.s
n.s
Exosome secretion (% relative to control)
150
100
50
0
Control
Rab5 RNAi
Rab7 RNAi
Rab7 DN
Rab11 DN
Rab11 RNAi
Rab27 RNAi #1
Rab27 RNAi #2
Rab35 RNAi
Evi RNAi #1
Evi RNAi #2
B
CD63 +ve puncta
Control
Rab5 RNAi
Rab7 RNAi
Rab11 RNAi
Rab27 RNAi #1
Rab35 RNAi
Evi RNAi #2
C
ANCE secretion (% relative to control)
150
100
50
0
Control
Rab11 RNAi
UAS Rab11 GFP
D
♂
wt
control
Hrs RNAi
ALIX RNAi
Rab11 DN
CD63-GFP (52kDa)
0.00 1.00 1.07 1.05 1.17
CD63-GFP/ANCE
ANCE (72kDa)
Actin (42kDa)
E
♀
virgin
wt
control
Hrs RNAi
ALIX RNAi
Rab11 DN
CD63-GFP (52kDa)
0.00 0.00 1.00 0.28 0.00 0.00
CD63-GFP/ANCE
ANCE (72kDa)
Actin (42kDa)

Figure 4.1 Rab GTPases control secretion of exosomes.

A) The number of CD63-GFP puncta were counted in the AG lumen after flies multiply mated control males either expressed no additional transgene or they expressed various constructs to regulate the activity of Rab GTPases (see Materials and Methods 2.13). The secretion of CD63-GFP puncta was dependent on Rab5, 7, 11, 27 and 35, but not Evi, which regulates the secretion of a different population of exosomes. **B)** Images showing the differences in CD63-GFP puncta in the lumen of the AG after expression of transgenes. **C)** The intensity of ANCE in the AG lumen was measured, showing no difference in secretion when Rab11 was knocked down or overexpressed. **D)** Western blot analysis of the AG from male flies expressing Rab11DN shows no differences in the level of CD63-GFP protein. Similar results were obtained for ALiX and Hrs. **E)** The transfer of CD63-GFP, but not ANCE, to females was reduced when SCs expressed Rab11DN. Western analysis was performed in collaboration with Laura Corrigan and Sumeth Perera. ***P<0.001, Kruskal-Wallis test, n=10.

4.2.1.2 SNARE proteins control exosome release in SCs

The classical route that MVBLs take to release their intraluminal vesicles (ILVs) as exosomes involves fusion with the plasma membrane. Therefore SNARE proteins are likely to be important in this process. Indeed, SNAREs have been implicated in regulating the release of exosomes in other systems; for example, VAMP7 was identified to control the fusion of MVBs to the plasma membrane in K562 cells, a myeloid leukemia cell lines (Fader et al., 2009). More recently, both *Syntaxin1A* and *Ykt6* in *Drosophila melanogaster* have been shown to be required for exosome secretion (Mittelbrunn et al., 2015). To test what the roles of SNARE proteins are in SC exosome secretion, I targeted SNAREs that we thought would be good candidates to be involved in this process and silenced them by expressing RNAi specifically in SCs.

Knockdown of the SNAREs *Snap24*, *Synaptobrevin* and *Syntaxin-1A* resulted in fewer CD63-GFP-positive exosomes in the AG lumen (Figure 4.2), suggesting that this set of SNARE proteins is likely involved in regulating the fusion processes necessary for exosome secretion.

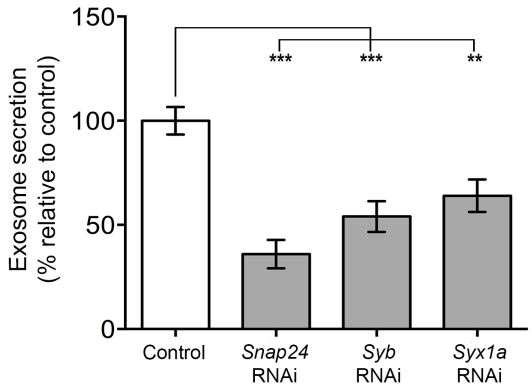


Figure 4.2 Exosome secretion is dependent on SNAREs.

The number of CD63-GFP puncta was significantly reduced when *Snap24*, *Syb* and *Syx1a* were silenced using RNAi. ***P<0.001, Kruskal-Wallis test, n=10.

4.2.1.3 The V-ATPase complex regulates exosome secretion

The role of the V-ATPase in exosome secretion remains poorly researched, partly because untangling its involvement in exosome secretion from other functions is challenging. Despite this hurdle, Liègeosis et al 2006 used genetic approaches in *C.elegans* to illustrate that the V_0 subunit, Vha-5, is involved in apical secretion of hedgehog-positive exosomes independent of proton-pumping (Liegeois et al., 2006). Interestingly, in *Drosophila* S2 cells, silencing of the V_0 subunits, Vha68.2, Vha26, Vha55, and the V_1 subunit, VhaSFD (Figure 1.6), resulted in fewer Evi-positive exosomes being released (Koles et al., 2012).

During my DPhil I supervised the final year projects of two undergraduate students, Hannah Ledbury and Danielle Ellenby, who primarily focused on understanding the role of the V-ATPase complex in SCs. Although I performed all their imaging, they made genetic combinations to investigate the function of the different subunits of the V-ATPase complex and performed statistical tests to analyse the significance of their results.

To investiagate if the V-ATPase regulates the secretion of exosomes in SCs, we performed an RNAi screen targeting major subunits of this complex. Silencing of *Vha68-2*, *Vha26*, *Vha55* and *VhaM9.7-1* reduced the number of CD63-positive exosomes in the AG lumen, while knockdown of the VhaSFD subunit had no significant effect (Figure 4.3). This suggests that the V-ATPase subunit does play a role in exosome secretion. The lack of effect for *VhaSFD*, might either be explained by insufficient knockdown, or this subunit may be dispensable, or its function compensated for by other substitute subunits of the V-ATPase complex. Importantly, our results confirm previous findings observed in *Drosophila* S2 cells, highlighting that the V-ATPase also regulates exosome secretion *in vivo*, though it is unclear how direct this control might be.

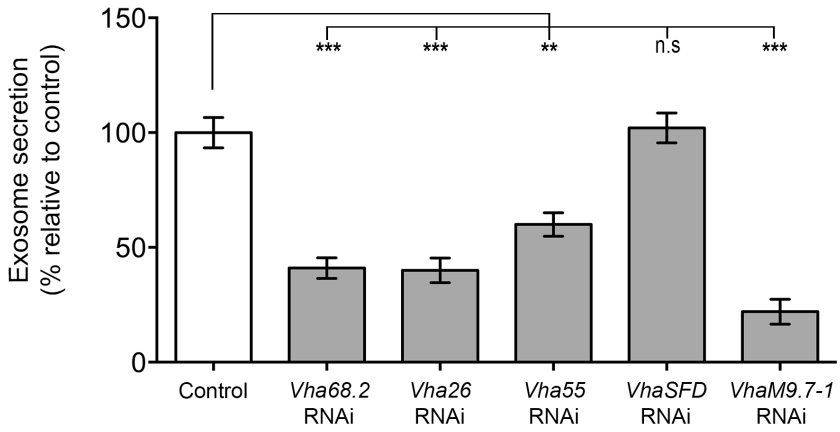


Figure 4.3 The V-ATPase complex is involved in exosome release.

Silencing of the V-ATPase subunits *Vha68.2*, *Vha26*, *Vha55* and *VhaM9.7-1* reduced the number of CD63-GFP positive exosomes in the AG lumen, whilst knockdown of VhaSFD did not significantly change this. **P<0.01, ***<0.001, Kruskal-Wallis test, n=10.

4.2.1.4 Exosomes have important roles in controlling the female post-mating response

Mating in *Drosophila* elicits many stereotyped responses in females, including sperm storage, increased egg laying and food intake, and rejection of subsequent males (see section 1.11). The Wilson lab has previously shown that SC-derived exosomes are transferred to females after mating, where they fuse with sperm and the epithelial cells lining the female reproductive tract (Corrigan et al,. 2014).

To investigate the physiological roles of exosomes in reproduction, I expressed Rab11DN in SCs to decrease exosome secretion into the AG lumen, and thus their transfer to females. Reducing exosome transfer to females did not affect egg laying (Figure 4.4A) or fecundity (Figure 4.4C) but instead caused females to re-mate more often than exosome receiving control flies (Figure 4.4B). I observed that the duration of mating in males expressing Rab11DN was shorter than in controls (Figure 4.4D) and perhaps the results regarding the PMR were because females were not receiving other proteins transferred in the latter part mating. However, another DPhil student obtained similar results when different components of the ESCRT complex, involved in exosome biogenesis, were silenced without affecting the duration of mating.

This suggests that male-derived exosomes specifically regulate the female post-mating behaviour and highlights their role in inter-organismal communication. Indeed, we hypothesise that this is one strategy that males employ to ensure that females produce their offspring.

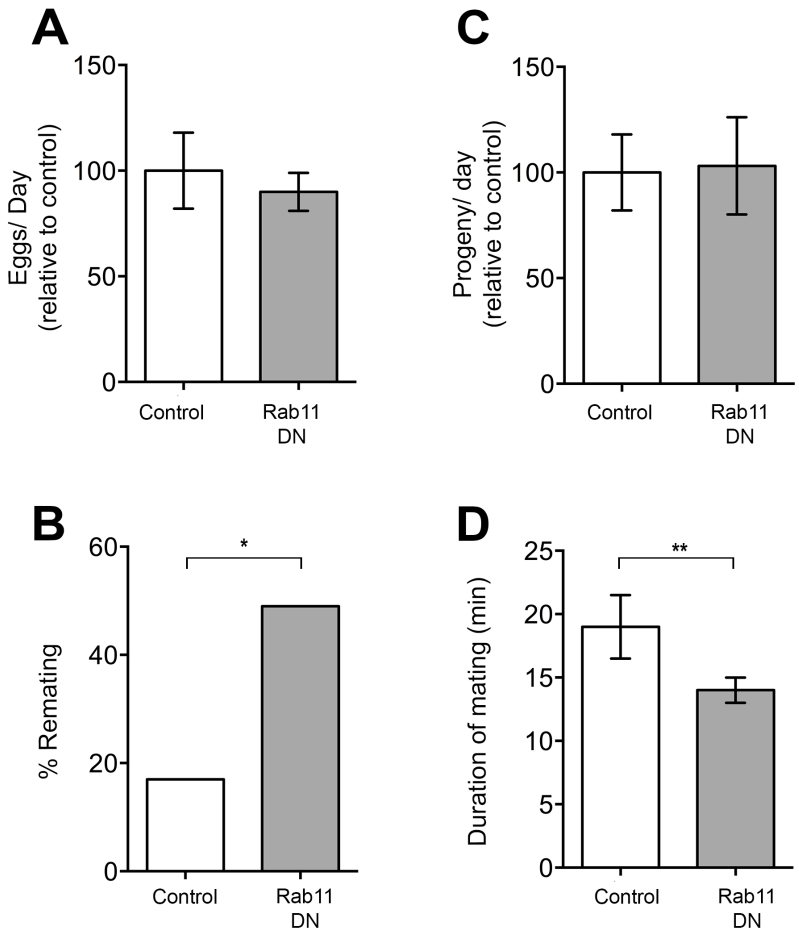


Figure 4.4 Male-derived exosomes are important for controlling the female post-mating response.

A) Reducing the transfer of male-derived exosomes to females by expressing Rab11DN in SCs, does not change the number of eggs laid by her, or the progeny that subsequently develops **(C)**. **(B)** Females display a higher propensity to re-mate to other males if exosomes were not transferred **(D).** The duration of mating is reduced when males express Rab11DN in SCs. *P<0.05, Mann-Whitney *U* test, n=30.

4.2.2 Regulation of membrane trafficking by Rab GTPases

In the previous section, I showed that exosome secretion in SCs is regulated by Rabs, SNAREs and the V-ATPase complex. To what degree and how these proteins regulate intracellular trafficking in SCs will be the focus of this section. In order to dissect the roles of Rabs, I imaged SCs under live and fixed conditions when the activity of specific Rab GTPases was perturbed. I measured various aspects of trafficking such as compartment numbers, compartment size and the maturation of endolysosomal compartments.

4.2.2.1 Using dominant negative forms of Rab GTPases to assess their function

To understand the precise trafficking steps that Rab proteins regulate prior to exosome secretion, I overexpressed the widely used dominant negative (DN) and constitutively active (CA) Rab mutants in SCs using the GAL4/UAS system. Flies overexpressing a dominant negative Rab contain a T/S → N substitution that perturbs GTP binding, whilst in constitutively active mutants a Q → L change results in defective GTPase activity (Hutagalung and Novick, 2011). Expression of Rab5DN often resulted in fewer non-acidic compartments and MVBLs containing significant amount of fluorescent luminal CD63-GFP (Figure 4.5A, B), but these phenotypes were often variable. In Chapter 3, I showed, using pulse-chase analysis, that the largest acidic compartment is most likely a lysosomal-like compartment. Since in control SCs fluorescent CD63-GFP was largely absent in the lumen of the MVB/lysosome-like compartment, I postulated that expressing Rab5DN causes reduced lysosomal maturation, which results in pH-sensitive GFP fluorescing in the higher pH environment, as previously reported in other systems (Couturier et al., 2014). Staining 6-day-old control SCs with an anti-GFP antibody revealed that the largest compartment, which represents a MVBL at this stage, was full of cross-reacting GFP (Figure 4.6), which does not

fluoresce. Therefore, the absence of fluorescent GFP in the MVBLs is a good indicator of compartment maturity.

SCs expressing Rab7DN generally displayed fewer non-acidic compartments and many immature MVBLs filled with CD63-GFP (Figure 4.5C). Indeed, in these SCs the MVBLs were also often smaller indicating that the age-dependent increase in MVBL size is blocked when Rab7 function is aberrant. However, like Rab5DN, the phenotypes using this construct were inconsistent. When I expressed Rab11DN, I also often saw variable phenotypes (Figure 4.5D), making scoring of specific trafficking events difficult. Similar inconsistent results were observed when a CA version of Rab11 was expressed (Figure 4.5E), often producing phenotypes that resembled each other.

In light of these inconsistencies, I decided not to continue using these methods to elucidate the roles of Rab27 and Rab35. As discussed in Section 4.3, DN and CA constructs have been reported to produce different and sometimes opposite effects on Rab activity in other systems (Barr, 2013) and the inconsistent results I observed suggested that the effects might be highly sensitive to expression levels. I therefore opted to use RNAi and overexpression of wild-type forms of Rabs to further dissect the function of these proteins in SCs.

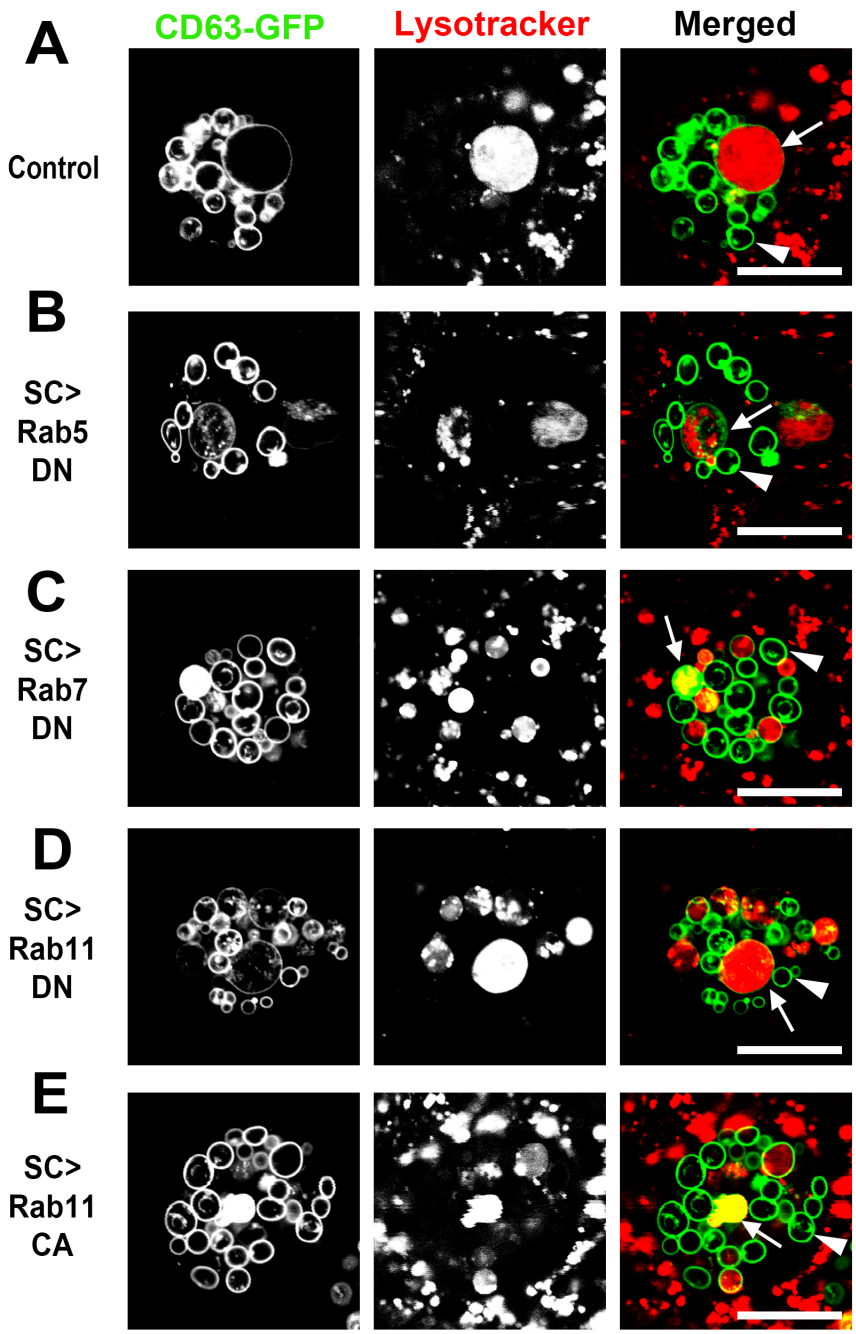


Figure 4.5 Dominant negative and constitutively active Rabs have variable phenotypes.

SCs from 8-day-old males expressing CD63-GFP with no transgene **(A)**, Rab5DN **(B)**, Rab7DN **(C)**, Rab11DN **(D)**, and Rab11CA **(E)**. In control SCs, CD63-GFP fluorescence is absent in the lumen of the largest acidic compartment (arrow). Notice that expression of Rab11DN and CA both give increased number of non-acidic compartments (arrowheads). Images represent single z planes, so do not show all compartments within SCs. Scale bar is 10 μm.

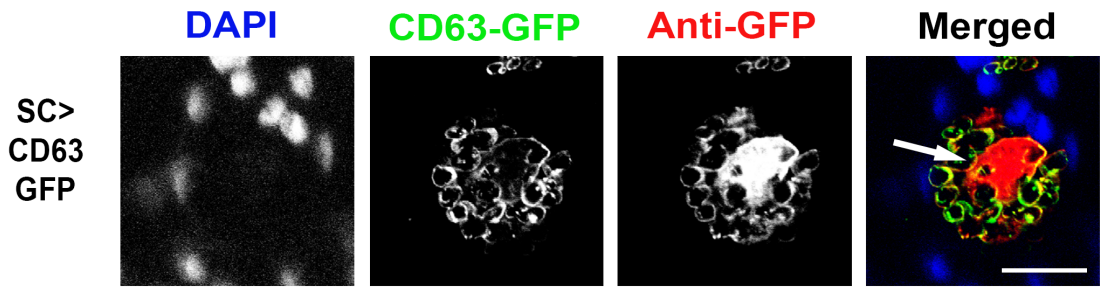


Figure 4.6 CD63-GFP can be detected in the largest acidic compartments using antibody staining.

SC from dissected AG of 6-day-old male expressing CD63-GFP throughout adulthood and stained with an anti-GFP antibody and DAPI. Note the absence in the largest compartment of fluorescent GFP signal, which is still detected with the antibody (arrow) and based on live staining is likely to be the largest acidic compartment. Scale bar is 10 μm.

4.2.2.2 Rab5 is needed for normal formation of MVBLs and SVs

Rab5 is an integral component of the endocytic maturation pathway and is involved in recruiting Rab7 to EEs to permit the formation of LE/MVBs (Haas et al., 2005, Huotari and Helenius, 2011). SCs expressing an RNAi targeting the *Rab5* transcript had a large number of non-acidic SVs that were usually smaller than those observed in control SCs (Figure 4.7A, B, D, E). Interestingly, the acidic MVBLs were also smaller and more numerous (Figure 4.7F, H), supporting the hypothesis that Rab5 may contribute towards the fusion of endosomal compartments to form a mature LE/MVBL in these cells. Because the phenotypes in these cells were much more consistent, counting the numbers of SVs and MVBLs in a full Z-stack of each SC allowed me to demonstrate significant differences in numbers of both compartments compared to controls (Figure 4.7D, F).

In SCs overexpressing wild-type Rab5, the size of the largest acidic compartment was not significantly different from controls (Figure 4.7C, H), but the luminal GFP inside this compartment was considerably higher (Figure 4.7G), indicating that the maturation of this compartment had been suppressed. Interestingly, overexpressing Rab5 also reduced the number of non-acidic SVs (Figure 4.7D), suggesting that Rab5 in SCs is involved in SV formation as well, perhaps because it has an important role in endocytosing membranes that will ultimately contribute to Rab11 compartments. An in-depth analysis of *Rab5* function was not conducted because my research interest at the time lay further down the endolysosomal and secretory pathways. In the future, it would be interesting to understand how the small Rab5 compartments influence trafficking in the larger Rab11 SVs particularly.

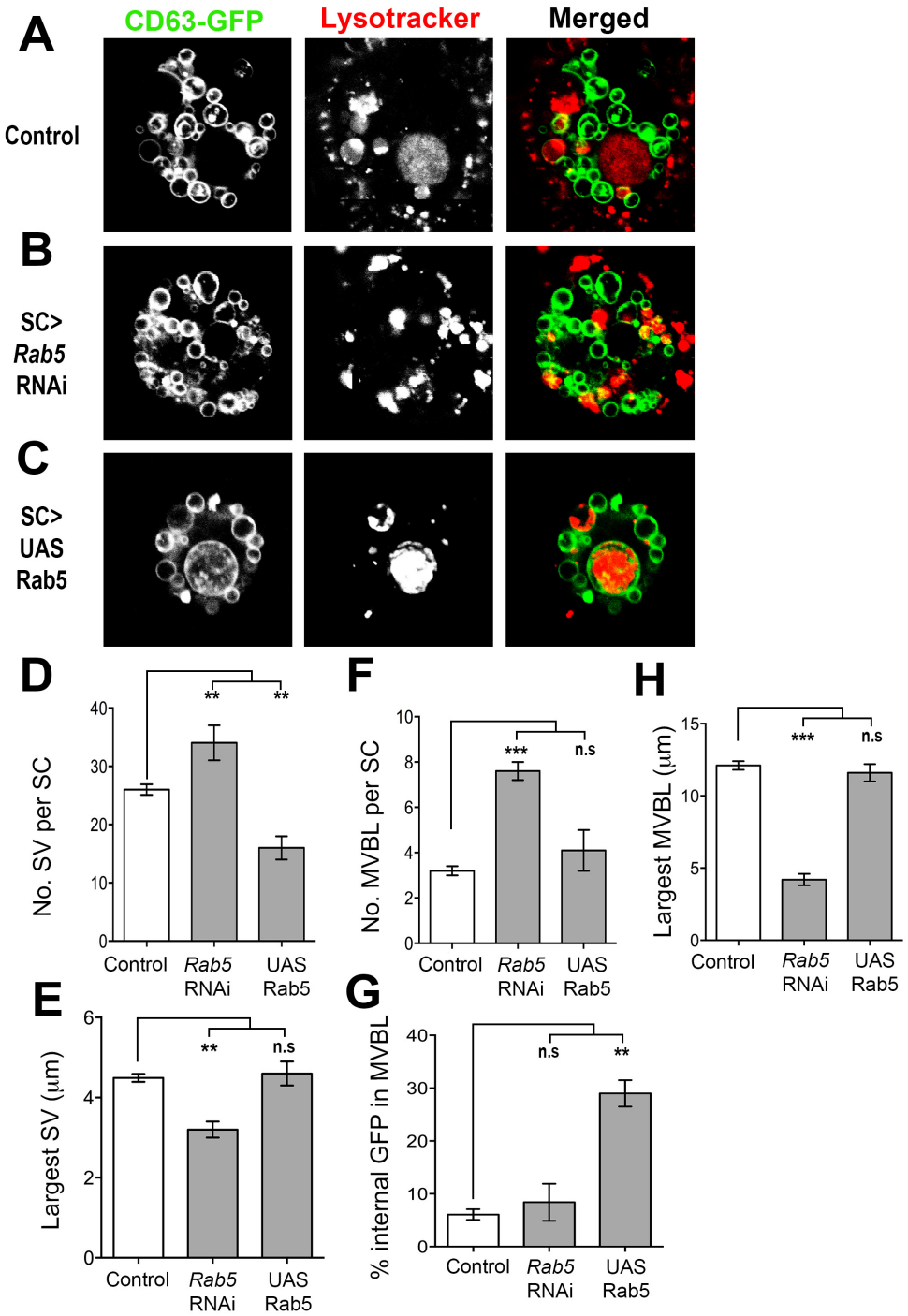


Figure 4.7 Rab5 regulates formation of secretory vacuoles and multivesicular bodies/ lysosomes.

8-day-old SCs expressing either no transgene **(A)**, *Rab5* RNAi **(B)** or overexpressing Rab5-GFP **(C)**. The number of secretory vacuoles (SVs – arrowhead, **D**) and the number of multivesicular bodies/ lysosomes (MVBL – arrow, **F**) were quantified for each treatment. The size of the largest SV and MVBL are shown in **E** and **H**, respectively. The percentage of GFP covering the area of the largest MVBL is given in **G**. **P<0.01, ***<0.001, Kruskal-Wallis test, n=10. Scale bar is 10 µm.

4.2.2.3 Rab11 controls the number of SVs and the size of the largest MVBL

In my first result chapter (Chapter 3), I provide some evidence that Rab11-positive, non-acidic SVs are ultimately derived from membranes trafficking through the Golgi, while their DCG content gives them a secretory function. Indeed, blocking the Golgi pathway by perturbing Arf79F prevents the formation of SVs. To understand how Rab11 controls trafficking of SVs in SCs, I knocked down its transcript with two independent RNAi and measured trafficking events at 1 day, 4 days and 8 days post RNAi expression. Studying the function of Rab GTPases at a single time-point may not give enough detail about processes potentially affected upstream/downstream and that ultimately contribute to the end phenotype. Therefore, I chose the time-points above to allow me to assess how membrane trafficking is changed both early and later on after gene expression.

To confirm that one of these RNAi (BI 22730) was specific, I used the esgF/O^{ts} driver line to produce mosaic clones of SCs, a tool previously employed in this system. In this transgenic line, a ubiquitously expressed temperature-sensitive mutant of the GAL4 inhibitor, GAL80, prohibits *esg*-GAL4-dependent expression until the temperature is shifted to 28.5°C. If newly eclosed virgin males are temperature shifted, all SCs express GAL4 and this leads to a FLP-recombinase induced excision of a DNA sequence blocking the expression of GAL4 under the ubiquitous actin promoter. In this scenario, RNAi and nuclear GFP expression, which 'leaks' into the cytoplasm, is turned on specifically in SCs within the AG at approximately the same level as the *dsx*-GAL4 driver (see section 5.2.2.4). However, if the temperature shift is induced in 3-5-day-old males, some SCs have switched off *esg* and so only some SCs express UAS-regulated transgenes.

Staining esgF/O^{ts} >Rab11 RNAi AGs containing SC expression mosaics with an antibody against Rab11, highlighted that only SCs not expressing the RNAi (GFP-negative) had the distinctive Rab11 staining pattern around the limiting membranes of SVs, whilst in RNAi-expressing cells (GFP-positive), the antibody staining was not present (Figure 4.8). This suggests that this RNAi produces a robust knockdown of endogenous Rab11 expression.

At 1 day post-silencing, the number of SVs and MVBLs was unchanged, perhaps because there was not enough time to reduce Rab11 levels (Figure 4.9A, B, C, E). However, after 4 days post-RNAi expression, there was a significant reduction in the number of SVs and a noticeable decrease in MVBL numbers (Figure 4.9A, B, C, E). Interestingly, the largest lysosome-like compartment was larger than control SCs imaged at 4 days (Figure 4.9F). At 8 days, SCs expressing *Rab11* RNAi had 3 +/- 0.28 SVs compared to 26.1 +/- 0.9 in control SCs (Figure 4.9C). The number of MVBLs was also reduced and the size of the lysosome was significantly larger than controls and filled with fluorescent CD63-GFP (Figure 4.9E, F, G). Importantly, the size of the SVs did not change, suggesting that the size changes are specific to the acidic lysosome (Figure 4.9D).

Given that there was a reduction in SV number with concomitant increase in the size of the lysosome, we hypothesised that knockdown of *Rab11* increases trafficking of SVs or their precursors to the lysosome. Importantly, this mechanism would provide the lysosome with more content, which it appears, is not properly degraded, increasing lysosome size.

To gain further understanding into Rab11 function, we overexpressed wild-type Rab11 tagged with GFP. In comparison to expressing RNAi against *Rab11*, which showed no obvious phenotype after 1 day, overexpressing Rab11-GFP caused a significant

increase in SV numbers within that time (Figure 4.10B, C), suggesting that increasing Rab11 protein very rapidly disrupts SV trafficking. However, the number and size of MVBLs did not change significantly at this time-point.

After 4 days of overexpressing Rab11, the number of SVs had reached 40 +/- 0.79 compared to roughly 13 +/- 0.65 observed in controls, with no apparent change in the number or size of acidic compartments, but MVBLs did contain significant levels of luminal GFP (Figure 4.10B, D, G). Interestingly, after 8 days the number of non-acidic SVs did not further increase (Figure 4.10C), and no changes in the number or size of acidic compartments were observed (Figure 4.10D), although the lysosome-like compartment was filled with luminal GFP (Figure 4.10E), suggesting that lysosomal degradation was not taking place normally at this time point. In this experiment, it was not possible to determine whether the luminal GFP was a result of CD63-GFP or Rab11-GFP since both are expressed simultaneously.

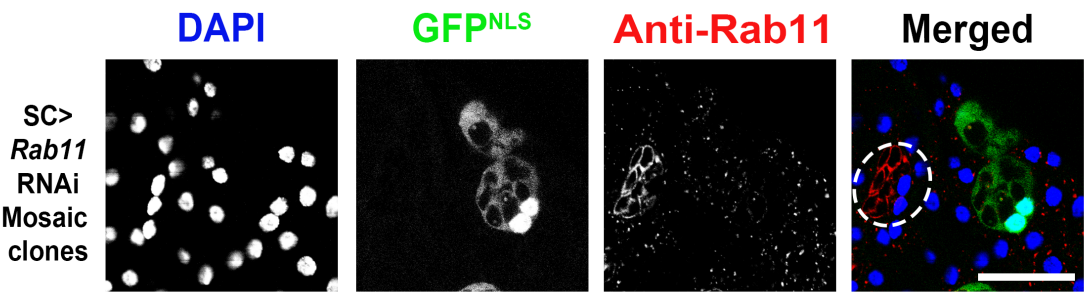


Figure 4.8 *Rab11* knockdown induces a strong reduction in Rab11 protein levels.

Mosaic expression of *Rab11*-RNAi in a subset of SCs reduces the distinctive staining pattern of Rab11 (on – green SCs) seen in non-GFP-expressing SCs (off; white dashed circle). *w; esg-GAL4 tub-GAL80^{ts} UAS-FLP; UAS-GFP$_{nls}$ actin>FRT>CD2>FRT>GAL4* was used to generate mosaic clones of SCs expressing Rab11-RNAi (BI 27730). Scale bar is 20 µm.

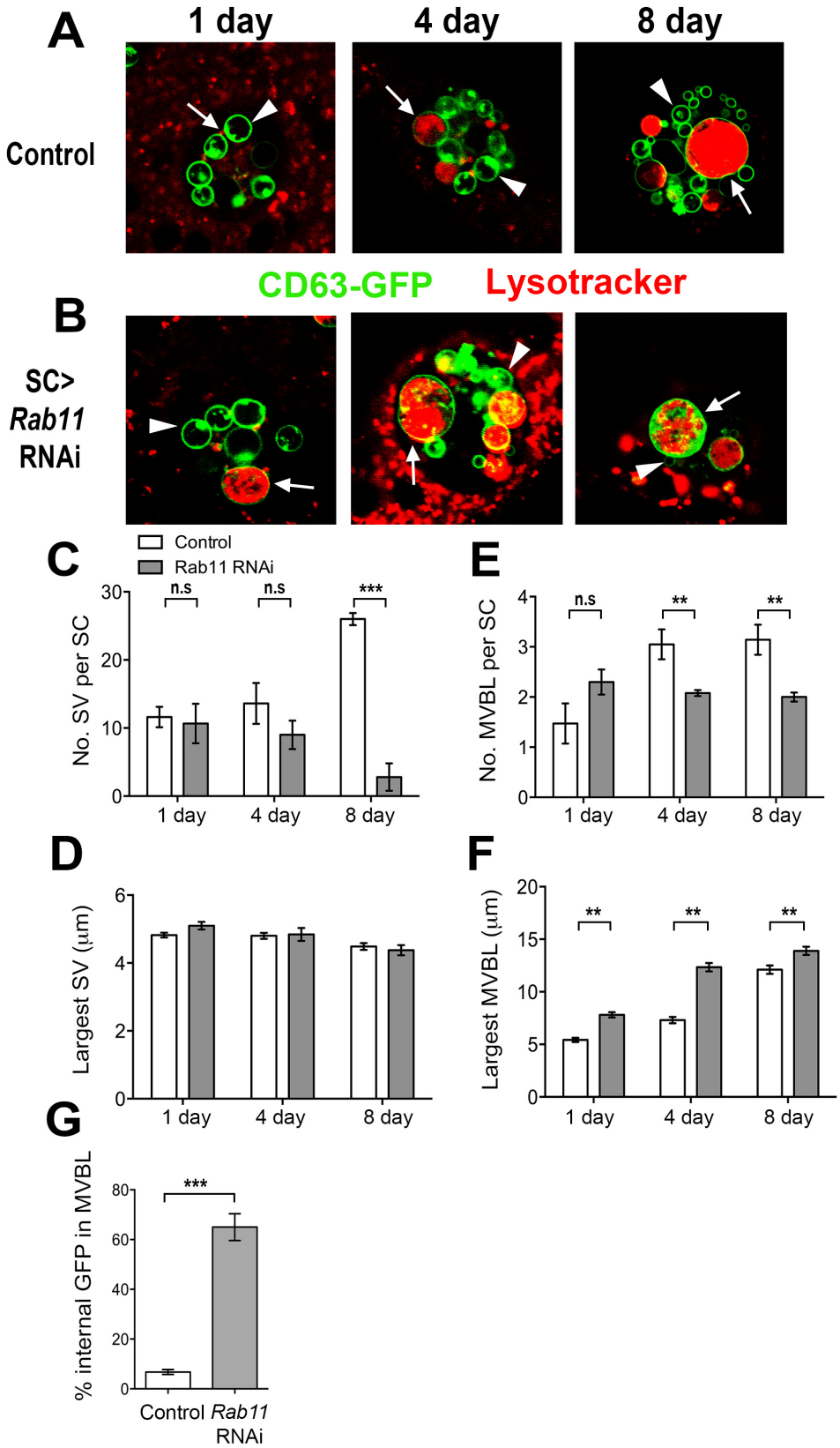

A
1 day
4 day
8 day
Control
CD63-GFP
Lysotracker
B
SC>
Rab11
RNAi
C
Control
Rab11 RNAi
No. SV per SC
n.s
n.s
***
1 day
4 day
8 day
E
No. MVBL per SC
n.s
**
**
D
Largest SV (μm)
F
Largest MVBL (μm)
G
% internal GFP in MVBL
***
Control
Rab11
RNAi

Figure 4.9 *Rab11* knockdown decreases numbers of SVs and increases the size of the largest MVBL in SCs.

SCs expressing CD63-GFP alone **(A)** or in combination with *Rab11* RNAi **(B)** were imaged live at 1, 4 and 8 days after eclosion. Images show a single z-plane containing the largest MVBL at its greatest diameter (arrow) and does not show the total number SVs (arrowhead) in SCs. The number of SVs is significantly reduced in SCs expressing *Rab11* RNAi at 8 days **(C)**, whilst their size is unaffected **(D)**. *Rab11* RNAi increased the size **(F)**, but not the number **(E)** of MVBLs at 8 days, whilst also increasing the luminal fluorescent CD63-GFP in the acidic compartment relative to the total area **(G)**. **P<0.01, ***<0.001, Mann-Whitney *U* test, n=10. Scale bar is 10 μm.

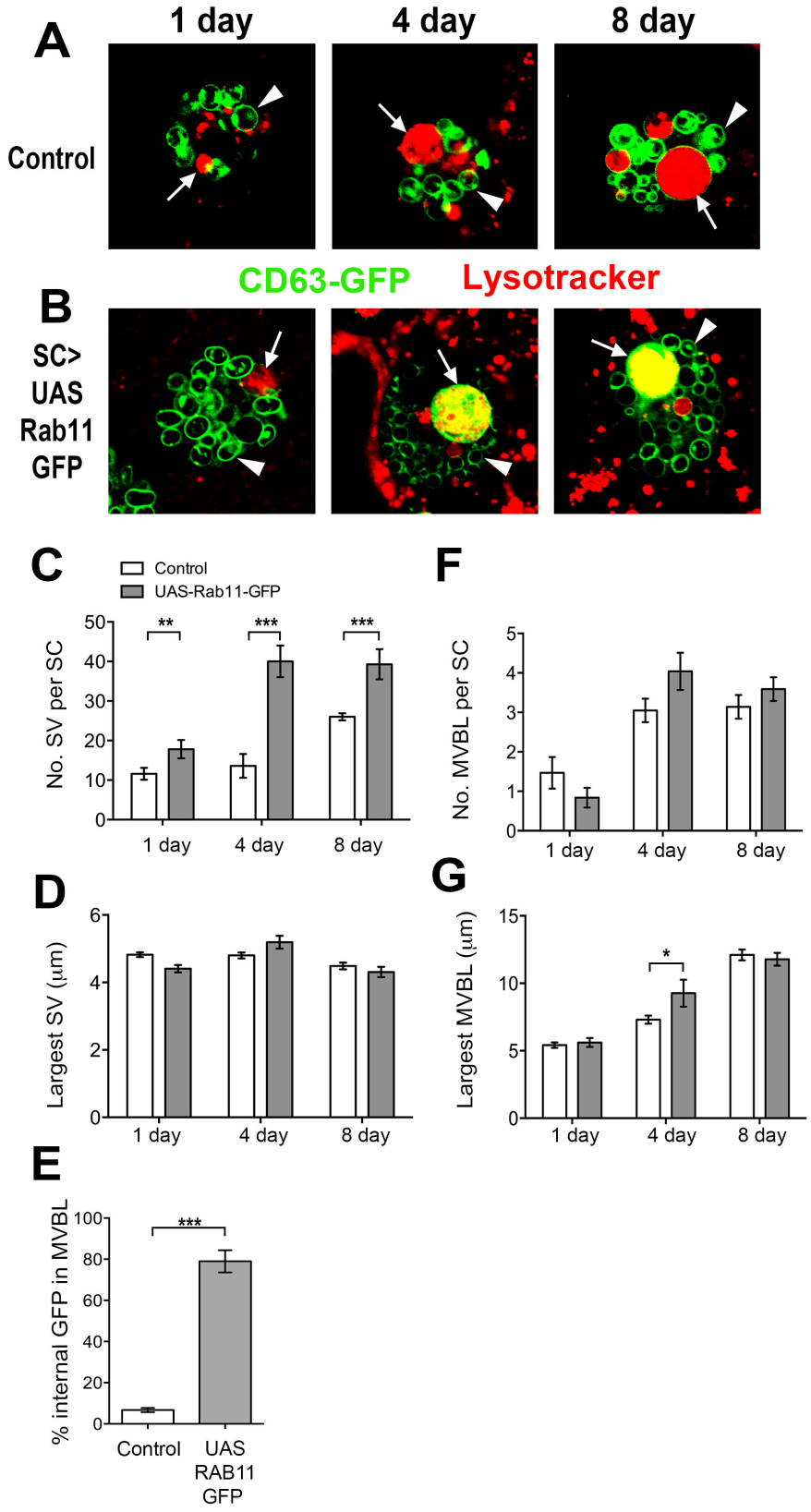

A
1 day
4 day
8 day
Control
B
CD63-GFP
Lysotracker
SC>
UAS
Rab11
GFP
C
Control
UAS-Rab11-GFP
No. SV per SC
**
***
***
1 day
4 day
8 day
F
No. MVBL per SC
D
Largest SV (μm)
G
Largest MVBL (μm)
*
E
% internal GFP in MVBL
***
Control
UAS
RAB11
GFP

Figure 4.10 Overexpressing Rab11 increases SV numbers and decreases the maturity of the largest MVBL in SCs.

SCs expressing CD63-GFP alone **(A)** or with *UAS-Rab11-GFP* **(B)** were imaged live at 1, 4 and 8 days after eclosion. Overexpressing Rab11-GFP for 1 day significantly increases the number of SVs (**B**, arrowhead and **C**), whilst having no effect on the number of MVBLs **(F)**, the size of SVs **(D)** or the formation of the largest MVBL after 8 days **(G)**. SCs expressing Rab11-GFP had a significant amount of fluorescent GFP in the lumen of the largest MVBL (**B**, arrows and **G**). Images show a single z plane. **P<0.01, ***<0.001, Mann-Whitney *U* test, n=10. Scale bar is 10 μm.

4.2.2.4 Rab11 prevents trafficking of SV contents into the lysosome-like compartment of SCs

To confirm that Rab11 controls trafficking of SVs to the lysosome-like structure, SCs expressing *Rab11* RNAi after 8 days were stained with the dense-core granule marker ANCE. In control SCs, ANCE was found inside CD63-positive SVs, and rarely in the large lysosome (Figure 4.11A). Staining SCs expressing *Rab11* RNAi with ANCE revealed that there was a specific signal in the largest SC compartment filled with GFP, representing the lysosome (Figure 4.11B). This suggests that in the absence of Rab11, a greater proportion of the molecules that normally reside in SVs, like ANCE, traffic to the SC lysosome, perhaps via direct fusion of non-acidic compartments to the lysosome. These molecules are not properly degraded, either because the lysosome does not mature normally or because it is overloaded with waste material, thus leading to an increase in size.

In SCs overexpressing Rab11-GFP, there was a significant increase in the number of ANCE-positive SVs, indicating that Rab11 drives the formation of these compartments (Figure 4.11C). Moreover, in these cells, ANCE was also found in the lumen of the largest compartment, which contained fluorescent GFP (Figure 4.11C). One possible explanation is that overexpressing Rab11 increases the rate of SV compartment formation, so that more DCG compartments form. However, either the rate at which the contents of these compartments are trafficked to the lysosome is increased or the degradative capacity of the lysosome is reduced, so that SV contents accumulate in this compartment.

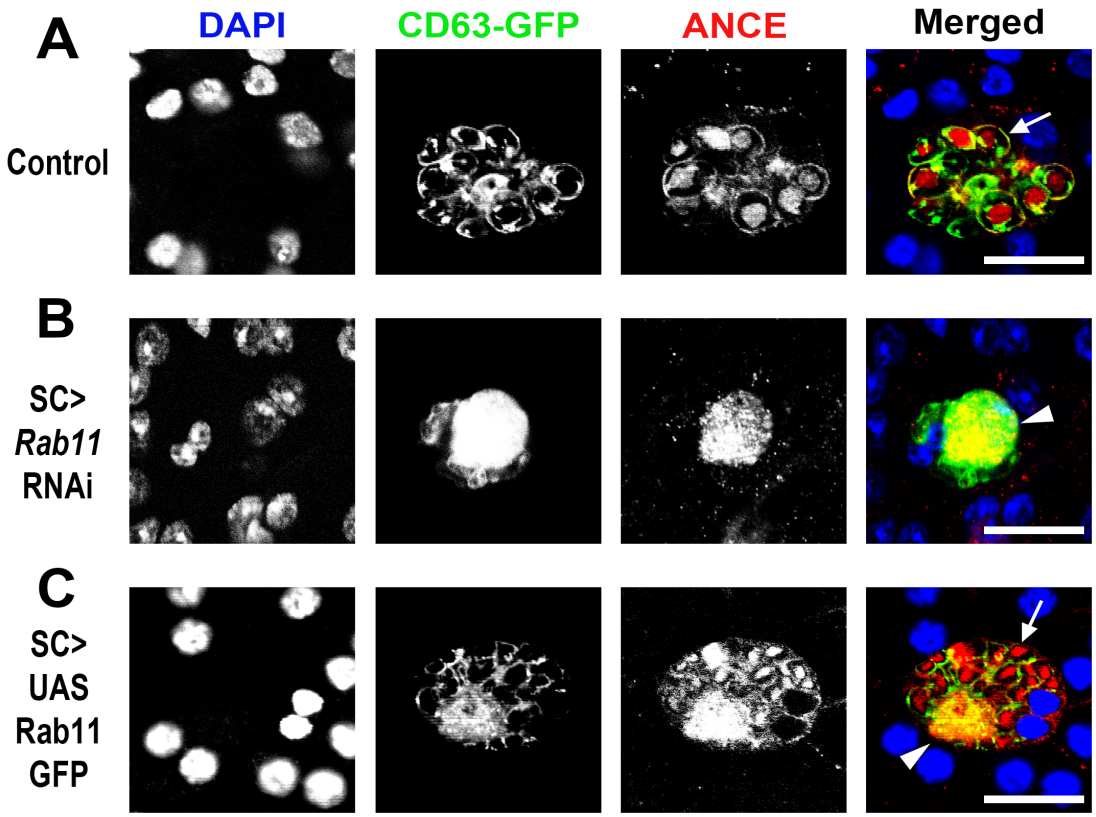


Figure 4.11 Rab11 controls trafficking of SVs towards MVBLs.

Fixed 8-day-old SCs expressing CD63-GFP only **A)**, with *Rab11* RNAi **(B)** or overexpressing Rab11-GFP **(C)** and stained with ANCE. Note that in controls, ANCE is localised inside dense-cored compartments (**A**, arrow) and rarely seen in other compartments. In Rab11 knockdown SCs, ANCE is only seen in one large compartment filled with CD63-GFP (**B**, arrow), resembling the large acidic structure seen by live imaging. **C)** Overexpressing Rab11-GFP increases the number of ANCE positive compartments (arrow), but is also found in a large CD63-GFP positive structure (arrowhead). Scale bar is 10 μm.

4.2.2.5 The putative Rab11 GEF TRAPPII controls similar processes to Rab11 in SCs

The activation of Rab proteins is regulated by GEFs, which catalyse the exchange of GDP for GTP. Studies from yeast suggest that the oligomeric complex transport protein particle II (TRAPPII) may function as a GEF for Rab11 (Ypt31) (Levine et al., 2013, Pinar et al., 2015). If this is the case, loss of function of *Drosophila TRAPPII* should produce a similar SC phenotype to *Rab11* knockdown. Indeed in SCs expressing an RNAi targeting *TRAPPII* (BI 43258) transcripts, there was a significant decrease in the number of SVs and the lysosome-like compartment was enlarged and filled with luminal fluorescent CD63-GFP (Figure 4.12B, C, F, G), essentially phenocopying the effects of *Rab11* loss. Although further biochemical experiments need to be performed to confirm this, it is therefore likely that TRAPPII is involved in activating Rab11 to control SV trafficking in SCs.

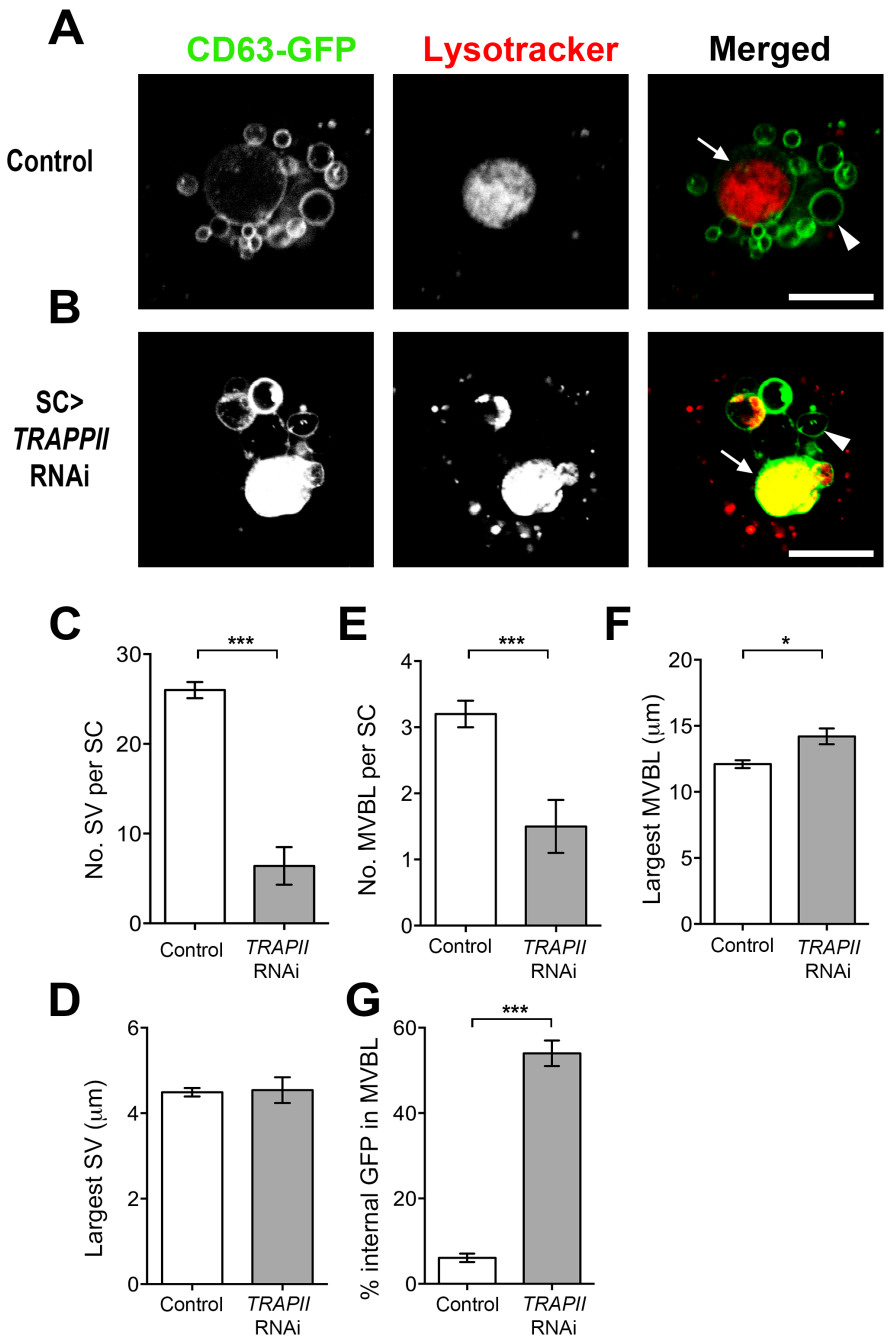


Figure 4.12 TRAPPII controls similar processes to Rab11.

SCs Expressing an RNAi against *TRAPPII* **(B)** for 8 days reduced the number of non-acidic compartments (arrowhead, **B**) compared to controls **(A)**. In these SCs, the size of the largest MVBL (arrow) was increased **(F)**, whilst no such changes were seen to affect SVs **(D)**. The number of MVBLs was also lower in *TRAPPII* RNAi expressing SCs **(E)**. *P<0.05, ***<0.001, Mann-Whitney *U* test, n=10. Scale bar is 10 µm.

4.2.2.6 Rab35 is localised in small vesicular structures in SCs

Rab35 is another putative recycling endosomal Rab implicated in exosome secretion (Hsu et al., 2010). To visualise where Rab35 is localised and gain a better understanding of how it co-operates with other Rab proteins, I overexpressed a GFP-tagged version of this protein in SCs and imaged them live. By conventional confocal microscopy, Rab35-GFP was seen to cluster in small areas in the SCs completely separate from the larger SVs and MVBLs (Figure 4.13A). To confirm that Rab35 is not present on SVs, I stained Rab35-GFP-expressing SCs with an antibody against Rab11. This revealed that Rab11 and Rab35 do not co-localise on SVs or in the small Rab35-positive compartments (Figure 4.13B), suggesting that Rab35 may have a different trafficking role to Rab11.

Since I could not distinguish if Rab35 staining was in fact localised to small compartments using confocal microscopy, I opted to use super-resolution 3D-SIM microscopy, which has a 2-3 fold higher resolving power. Using this method in collaboration with Ben Kroeger, Rab35-GFP was found to be on small vesicular structures, usually less than 1 μm in diameter, and absent from acidic compartments (Figure 4.13C).

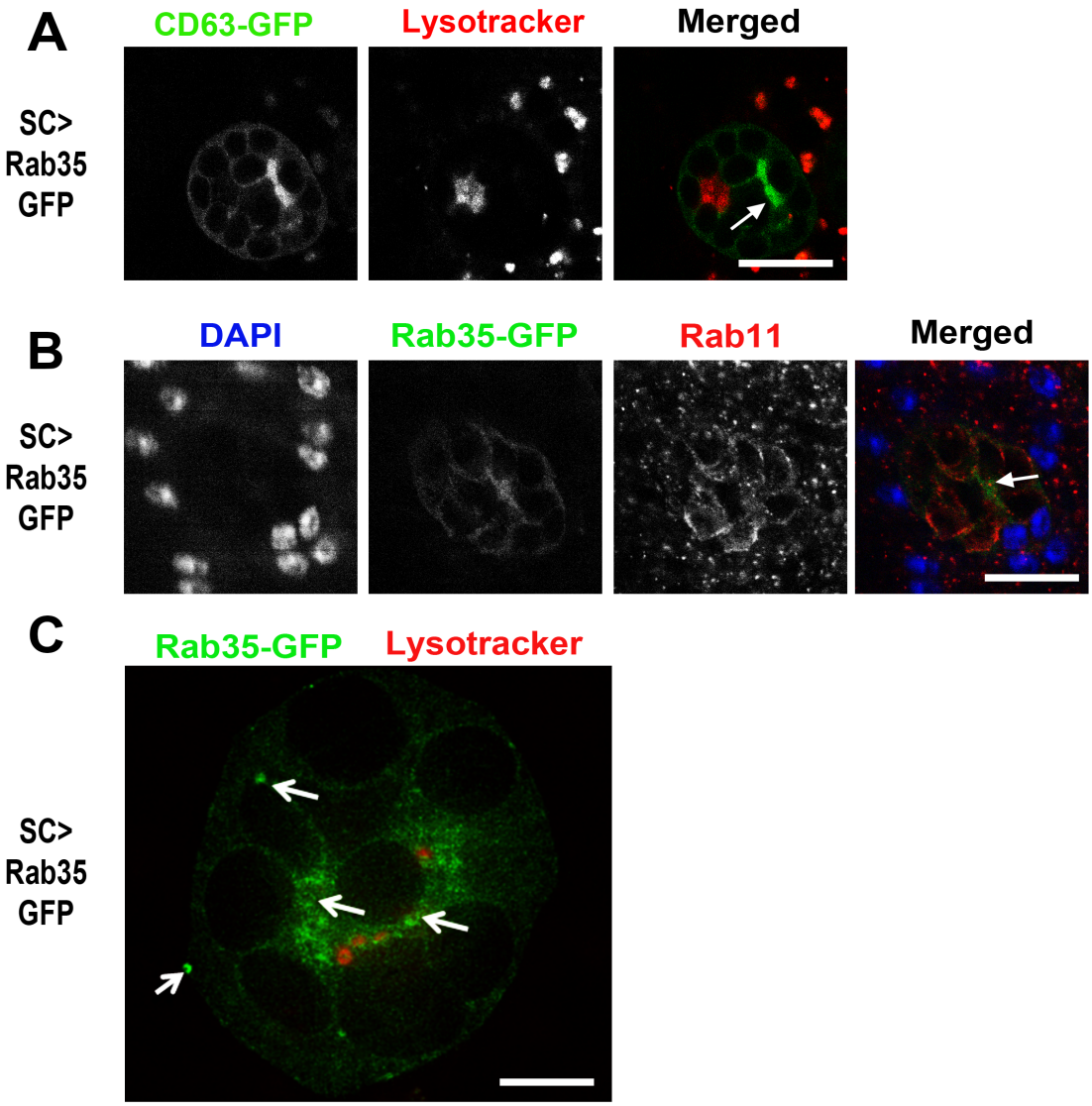


Figure 4.13 Rab35 localises to small cytoplasmic vesicles.

3-day-old live SCs expressing Rab35-GFP stained with Lysotracker **(A)**. Rab35 (**B**, arrow) is seen in a central region distinct from Rab11 positive compartments **(B)**. Super-resolution 3D-SIM microscopy imaging of 3-day-old SCs expressing Rab35-GFP under live conditions and stained with Lysotracker **(C)**. Rab35 is seen on small vesicular structures usually less than 1 µm in diameter (arrow). Scale bar is 10 µm for A and B and 5 µm for C.

4.2.2.7 Rab35 is required for trafficking of SV contents to acidic compartments and formation of the lysosome-like structure

The role of Rab35 in endocytic trafficking is not clearly understood. However, It has been shown to regulate fast recycling of proteins to the cell surface, exosome secretion, cytokinesis, and more recently, PtdIns (4,5)P_2 homeostasis (Klinkert and Echard, 2016). To assess the function of Rab35 in SCs, we used RNAi to silence its transcripts at different time-points. These experiments were performed with two independent RNAi to rule out off-target effects.

SCs expressing a *Rab35* RNAi for 1 day showed no changes in the number of SVs, but had more MVBLs then control SCs (Figure 4.14B, E). By 4 days, the number of SVs doubled to roughly 26 +/- 0.55, whilst the acidic compartments became more numerous and smaller in size whilst containing more GFP fluorescence (Figure 4.14C, E, F), suggesting that they might not be able to fuse with each other to form a larger lysosome as seen in age-matched control flies. Interestingly, at 8 days post-RNAi expression the number of SVs had increased further to roughly 52 +/- 2.16 and their size also decreased (Figure 4.14C, D), indicating that Rab35 is needed for the normal biogenesis of these compartments. Similarly, the number of acidic compartments also increased and their size was smaller.

Overexpressing Rab35-GFP in SCs did not have a significant effect on any aspect of trafficking at the time-points mentioned above (Figure 4.15). Since Rab activity is only on when it is bound to GTP, there is no guarantee that overexpressing wild-type Rab35 would increase Rab35 activity, potentially explaining why we do not see a phenotype. Alternatively, Rab35 may only be needed to negatively regulate the accumulation of SVs and promote formation of the large lysosome-like compartment, in some respects, functioning antagonistically to Rab11. Compared to SV-localised Rab11, Rab35

associates with a completely different set of intracellular compartments, suggesting that its effects on SVs may be indirect, possibly by modulating fusion between the large compartments in SCs.

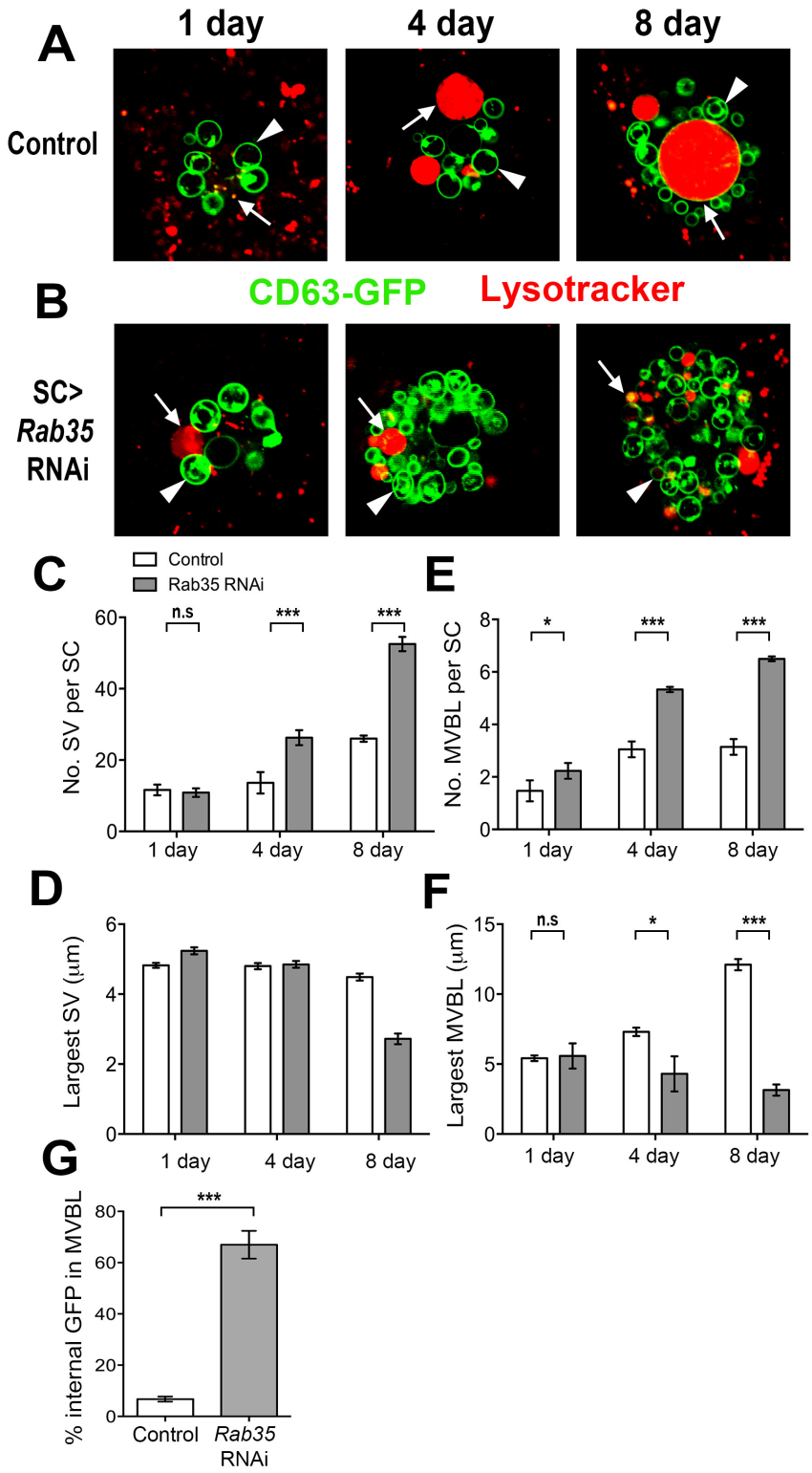


Figure 4.14 Rab35 is involved in the formation of SVs and MVBLs.

SCs imaged live at 1, 4 or 8 days post ecolsion and expressing either no transgene **(A)** or *Rab35* RNAi **(B)**. Knockdown of *Rab35* after 8 days increases the number of SVs (arrowheads, **C**) and MVBLs **(E)**, prevented the formation of a large mature MVBL **(F)** and reduced the size of SVs **(D)**. There was a significant increase in luminal CD63-GFP in MVBLs (G), a phenotype that was rarely observed in age-matched control SCs (A, arrow). *P<0.05, ***<0.001, Mann-Whitney *U* test, n=10. Scale bar is 10 μm.

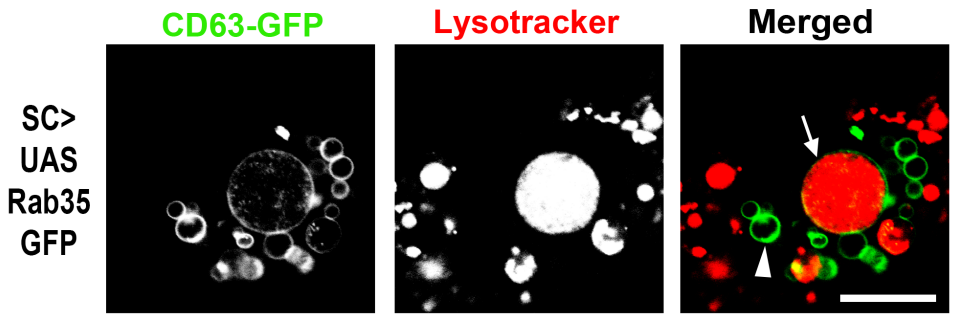


Figure 4.15 Overexpression of Rab35 has no effect on trafficking.

SCs overexpressing Rab35-GFP exhibit no obvious changes in any aspect of membrane trafficking. Scale bar 10μm.

4.2.2.8 Rab35 is needed for proper recycling of Rab11-positive membranes from the cell surface

To further define how Rab35 is involved in controlling SV numbers, SCs expressing *Rab35* RNAi were stained with an anti-Rab11 antibody. Rab11 normally lines SVs of SC (Figure 4.16A) but when *Rab35* was silenced, roughly 50% of SCs did not contain a Rab11 signal inside SCs (Figure 4.16B, C). In these cells Rab11 seemed to accumulate at the exterior of SCs. This suggests that in the absence of Rab35, Rab11 recycling from membranes close to or at the cell surface is aberrant. Indeed, since Rab11 does not line the SVs in some of *Rab35*-RNAi expressing SCs, this may partly explain why SVs build up because their identity is lost and trafficking is disrupted. However, it is important to note that not all SCs displayed the Rab11 mislocalisation phenotype and those that did not, still contained an excess of SVs and small MVBL compartments, suggesting that other mechanisms must be involved.

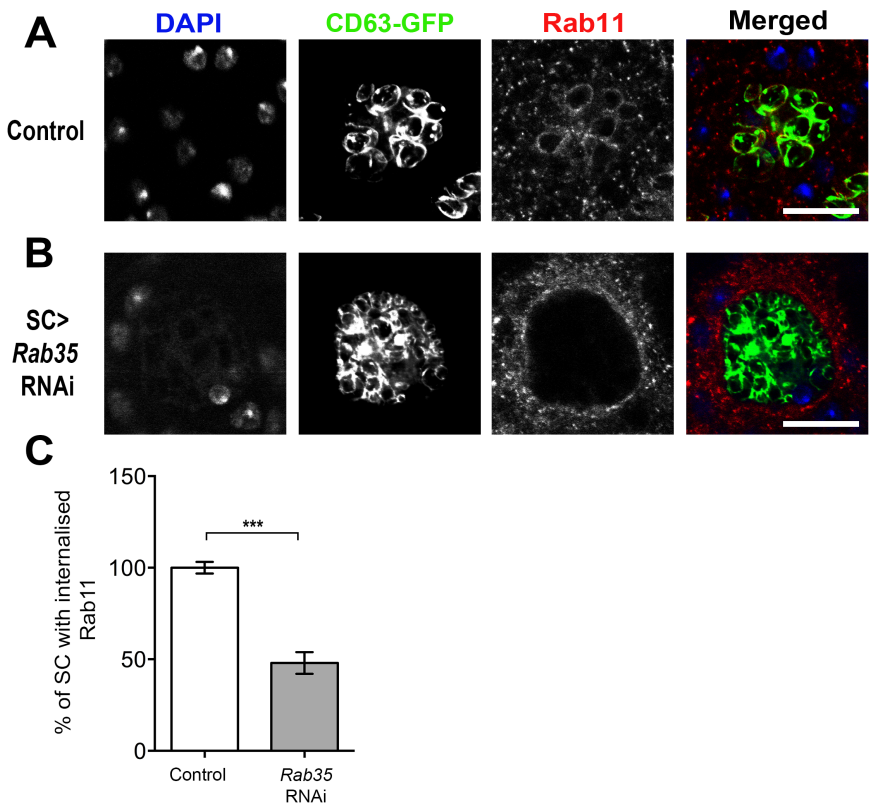


Figure 4.16 Rab35 is required for normal trafficking of Rab11.

Fixed SCs from 8-day-old flies expressing no additional transgene **(A)** or *Rab35* RNAi **(B)** and stained with DAPI (blue) and anti-Rab11 (red). Notice the distinctive pattern of Rab11 in control samples and its complete intracellular absence when some SCs express *Rab35* RNAi. C) Quantification of the proportion of SCs containing intracellular Rab11 staining. ***<0.001, Student *t-test*, n=10. Scale bar is 10 µm.

4.2.2.9 Rab27 has no obvious effects on intracellular trafficking in SCs

Rab27 regulates exosome secretion in HeLa cells by controlling the distribution and docking of MVBs to the plasma membrane (Ostrowski et al., 2010). I have previously shown that *Rab27* silencing reduces the number of SC-specific CD63-GFP-positive puncta secreted into the AG lumen. To understand what trafficking steps Rab27 regulates, I expressed two independent RNAi targeting *Rab27* in adult SCs.

Surprisingly, in SCs expressing *Rab27* RNAi, there was no significant change in the number or size of SVs and MVBLs. However, frequently there was the presence of a large tubular structure in the MVBL that was seldom seen in control flies (Figure 4.17A, B, C). Although preliminary, this result suggests that Rab27 may be involved in the final scission step of exosome biogenesis, but it would require a major high-resolution analysis to follow this phenotype up further.

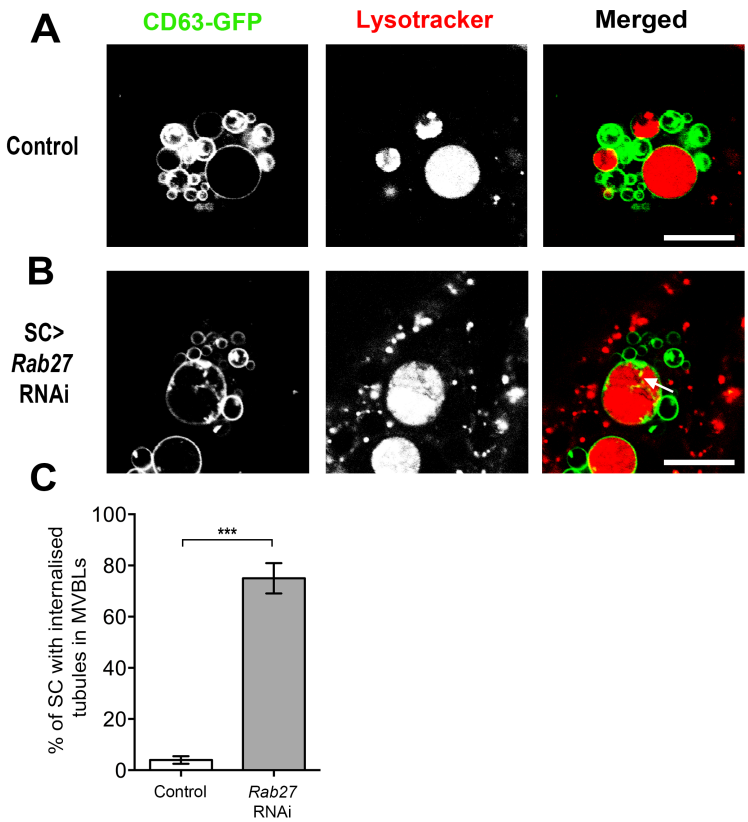


Figure 4.17 Rab27 is potentially involved in intraluminal vesicle formation.

8-day-old SCs imaged live with Lysotracker expressing no additional transgene **(A)** or *Rab27* RNAi **(B)**. Notice in *Rab27* RNAi expressing SC the presence of tubular structures (**B**, arrow) extending form the limiting membrane of MVBLs and into the lumen, a phenotype rarely seen in control samples **(C)**. ***<0.001, Student *t-test*, n=10. Scale bar is 10 μm.

4.2.2.10 Rab7 controls biogenesis of MVBLs

Rab7 sits at an important point in the endolysosomal pathway. It is reported to control the maturation of MVBLs and trafficking towards lysosomal compartments (Huotari and Helenius, 2011). What are the roles of *Rab7* in SCs? To address this, I expressed two independent RNAi targeting *Rab7* and overexpressed Rab7-GFP in adult SCs. Mosaic clones were produced, as previously mentioned, with *Rab7* RNAi (BI 27051) to show that this specifically targets endogenous Rab7 (Figure 4.18).

SCs overexpressing wild-type Rab7 did not display significant changes in any aspects of membrane trafficking (Figure 4.19). By contrast, loss of *Rab7*, induced by RNAi expression for 4 days, caused a massive build-up of small SVs and prevented the formation of large acidic compartments (Figure 4.20B, C, E, F). By 8 days, the number of small SVs had increased further, making SCs appear noticeably larger (Figure 4.20.B, C). Interestingly, at this time-point, there were virtually no MVBLs (Figure 4.20E), suggesting that Rab7, as in other cells, regulates the formation of acidic compartments in SCs.

A straightforward model to explain these results is that loss of *Rab7* prevents the formation of MVBLs and the lysosome-like structure, which partly functions to degrade SVs that are not secreted. Since SVs cannot be degraded, the number of these compartments increases in SCs expressing *Rab7* RNAi. However, SVs were also observed to be smaller in size, suggesting that Rab7 affects their biogenesis in events that I have shown occur around the Golgi. Indeed, Rab7 has been suggested to control trafficking from the Golgi in other systems. For example, loss of function of one Rab7 isoform, Rab7b, causes a re-distribution of the *trans*-Golgi in HeLa cells (Progida et al., 2010).

To test if *Rab7* is involved in controlling the arrangement of the Golgi, SCs expressing *Rab7* RNAi were stained with the *cis*-Golgi marker, GM130. As mentioned previously, GM130 is found centrally distributed in control SCs (Figure 4.21A). Silencing *Rab7* dispersed GM130 staining throughout SCs (Figure 4.21B), indicating that the architecture of the Golgi had been re-arranged, perhaps altering the way in which SVs are made. In conclusion, *Rab7* controls normal MVBL and lysosome formation, but also may regulate SV biogenesis by controlling the Golgi architecture.

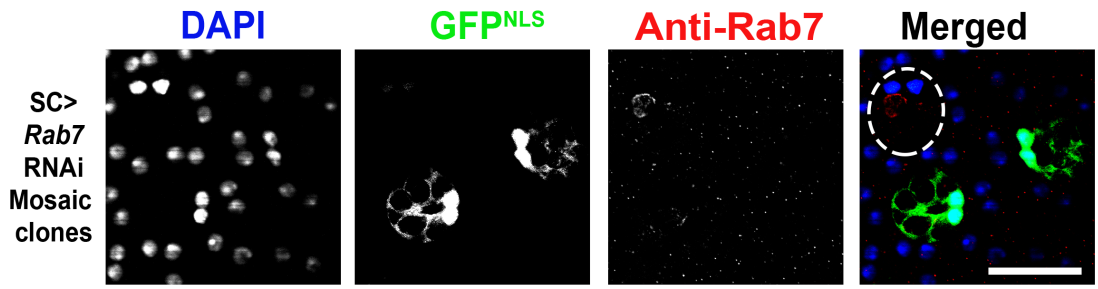


Figure 4.18 Rab7 RNAi induces strong knockdown.

Mosaic expression of *Rab7*-RNAi in a subset of SCs has a stronger effect at reducing the distinctive staining pattern of Rab7 (on – green SCs) than non-expressing SCs (off; white dashed circle). *w; esg-GAL4 tub-GAL80^{ts} UAS-FLP; UAS-GFP$_{nls}$ actin>FRT>CD2>FRT>GAL4* was used to generate mosaic clones of SCs expressing Rab7-RNAi (BI 27051). Scale bar is 20 μm.

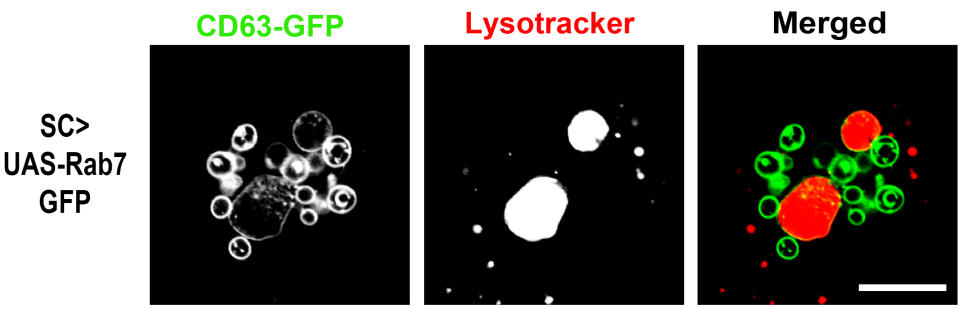


Figure 4.19 Overexpressing Rab7 does not changes SC trafficking.

SCs overexpressing Rab7-GFP for 8 days imaged live using confocal microscopy. Not that there is no GFP in MVBL or an increase in the number of non-acidic SVs. Scale bar is 10 μm.

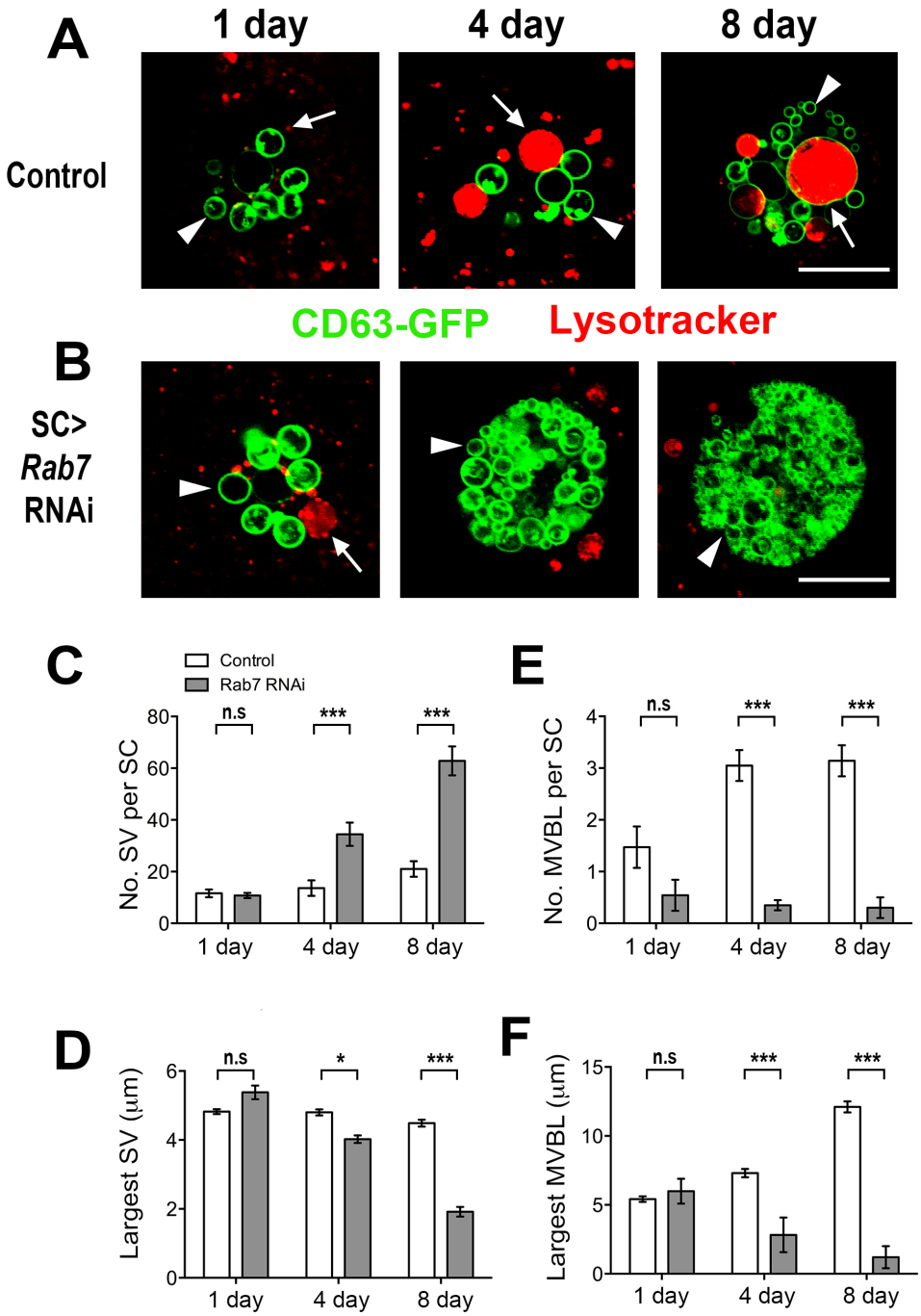


Figure 4.20 Rab7 is involved in biogenesis of MVBLs.

SCs imaged at 1, 4 or 8 day after eclosion expressing CD63-GFP with no other transgene **(A)** or *Rab7* RNAi **(B)**. Knockdown of *Rab7* increases the number of SVs **(C)** whilst reducing their size **(D)**. In these cells, the number **(E)** and size **(F)** of largest MVBL is massively reduced. These SCs appear visibly bigger than age-matched controls **(A)** as a result of being packed with small SVs (**B**, arrowhead). *P<0.05, ***<0.001, Mann-Whitney *U* test, n=10. Scale bar is 10 µm.

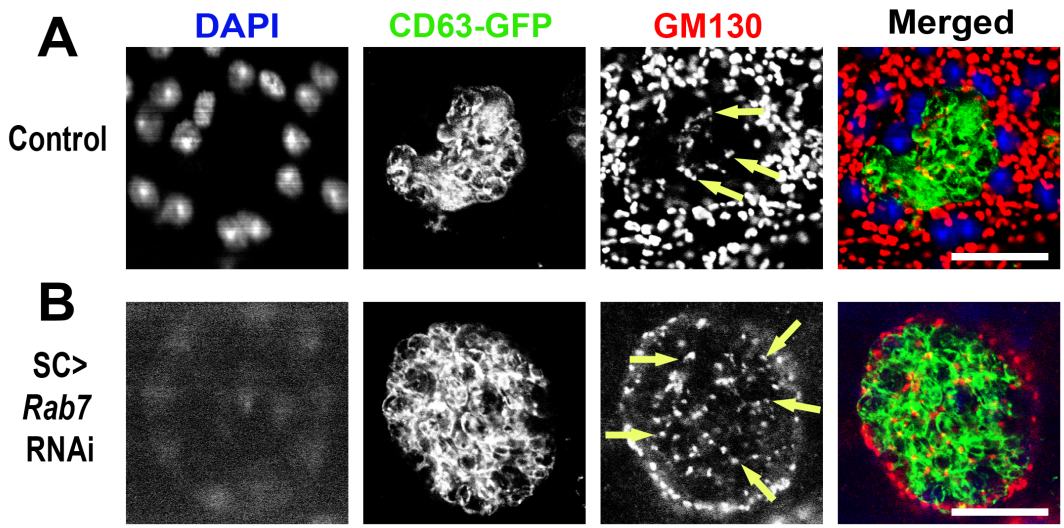


Figure 4.21 Knockdown of Rab7 disrupts Golgi distribution.

Fixed 8-day-old SCs expressing only CD63-GFP **(A)** or *Rab7* RNAi **(B)** and stained with the cis-Golgi marker GM130 (red). DAPI (blue) marks nuclei. Silencing *Rab7* results in the dispersion of Golgi (arrow), which normally appears centrally distributed in control SCs (**A**, arrow). Scale bar is 10 μm.

4.2.2.11 Rab7 and Rab35 are involved in maintaining the size of the SC lysosome-like compartment

I have already shown that Rab7 is needed for the biogenesis of the endolysosomal system in SCs, whilst Rab35 also plays a role in forming large MVBLs. Since the large SC lysosome forms during the knockdown period when these experiments are undertaken, I wanted to test what the roles of *Rab7* and *Rab35* are in maintaining the acidic compartments once they have formed. In order to assess this, I induced the expression of transgenes four days after eclosion, by which time large acidic compartments and the lysosome-like structure had already been established (Figure 4.22A, B).

Control SCs were shifted to 28.5°C 4 days after eclosion to express CD63-GFP for a further 6 days, by which time CD63-GFP clearly lined all compartments including the lysosome-like structure (Figure 4.22A). Interestingly, using this method, but also expressing *Rab35* RNAi simultaneously, I saw that the acidic compartments disassemble into smaller structures (Figure 4.22C). Similarly, when *Rab7* RNAi was expressed after MVBL formation, the effects on the acidic compartments were even stronger, causing them to break up into many smaller compartments (Figure 4.22B). These results support a model whereby both *Rab7* and *Rab35* are not only needed for the formation of mature MVBLs, but also for their maintenance once they have formed. For Rab35, this is particularly surprising, since this Rab does not appear to be associated with the large MVBLs, but it is required to retain them in SCs.

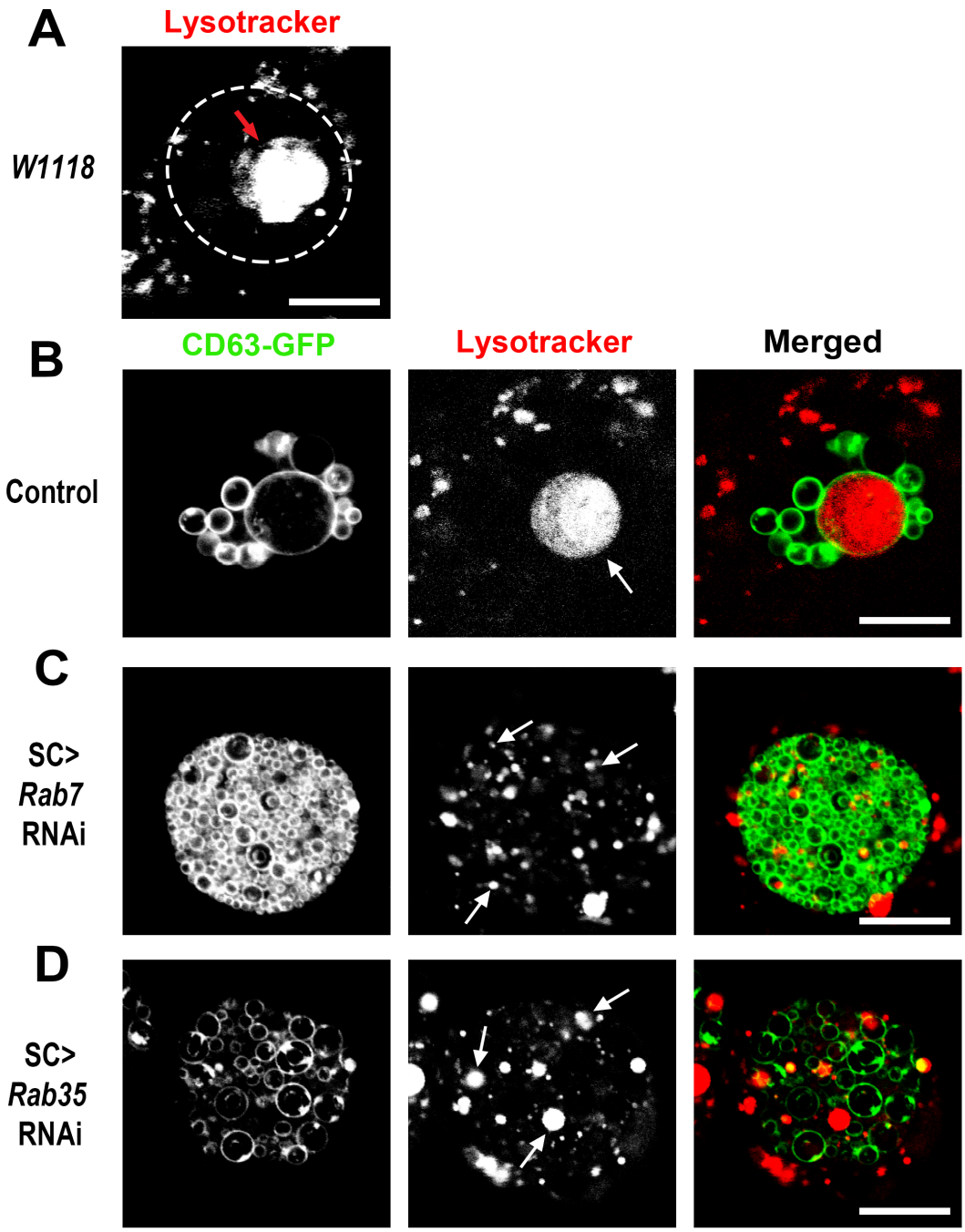


Figure 4.22 Rab7 and Rab35 are involved in maintaining MVBL structure.

A) 4-day-old SCs from *W*^{1118} flies stained with Lysotracker. Note the large MVBL (red arrow). Flies were temperature shifted after 4 days for a further 6 days to induce CD63-GFP expression only **(B)**, with *Rab7* RNAi **(C)** or with *Rab35* RNAi **(D)**. The large acidic MVBL which is normally formed by 4 days (**A, B** arrow) does not appear to be maintained in SCs expressing *Rab7* RNAi **(C)** or *Rab35* **(D)**. *W*^{1118} expressing no transgene (A), or *w; UAS-CD63-GFP tub-GAL80*^{ts}*; dsx-GAL4* expressing no additional transgene (B), *Rab7* RNAi (Bl 27051) *or Rab35* RNAi (Bl 28342). Scale bar is 10 μm.

4.2.3 Functions of SNAREs and the V-ATPase in regulating compartment numbers and membrane fusion in SCs

As mentioned previously, SNARE proteins are major regulators of membrane fusion. Some of the phenotypes observed previously when Rab function is perturbed can be attributed to defective fusion events, e.g. the absence of a large lysosome-like compartment or the accumulation of many SVs. To assess the function of SNARE proteins in SCs, I imaged AGs from males expressing RNAi targeting transcripts encoding the v-SNARE Synaptobrevin (Syb) or the t-SNAREs Snap24 or Syntaxin-1A (Syx1A) for 8 days in adult SCs.

4.2.3.1 Synaptobrevin and Syntaxin-1A appear to control fusion of SVs

To understand the role of Synaptobrevin and Syntaxin-1A, they were both knocked down for 8 days in adult SCs from eclosion onwards. In both cases, SCs were able to form a large lysosome-like compartment, however, it was filled with luminal fluorescent CD63-GFP (Figure 4.23B, C, F, G), suggesting that it had not matured properly or had failed to degrade the increased levels of waste delivered to it. However, the size of this compartment was not increased (Figure 4.23H), suggesting that it was not accumulating an excess of waste material.

Interestingly, the numbers of SVs were increased when these two SNAREs were silenced (Figure 4.23D), indicating that they may both function to control SV fusion to the plasma membrane or other compartments like the MVBLs and lysosome. From these results, I propose that Synaptobrevin and Syntaxin-1A may act as matching v- and t-SNARE in at least one membrane fusion event in SCs, most likely plasma membrane fusion, since perturbing their functions produces similar phenotypes.

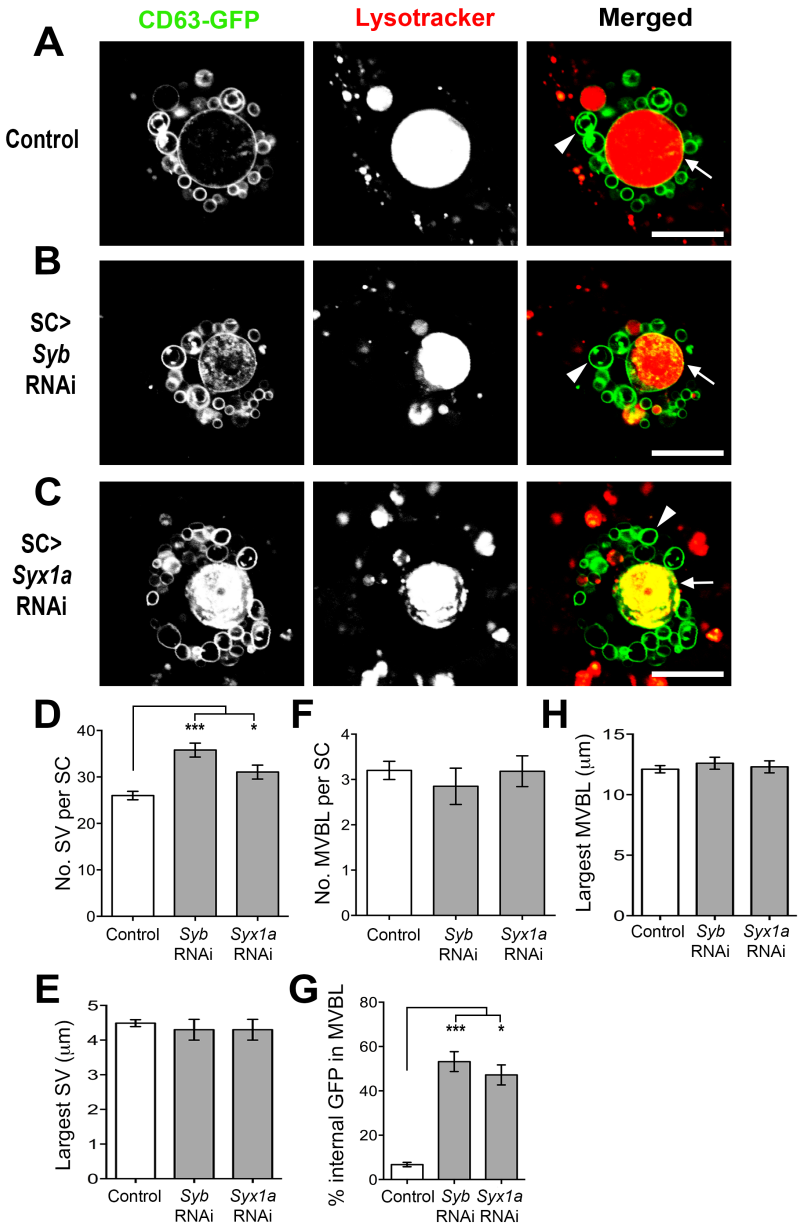


Figure 4.23 Synaptobrevin and Syntaxin1a control fusion of SVs to MVBLs.

Live confocal imaging of 8-day-old SCs expressing CD63-GFP **(A)**, with *Syb* RNAi **(B)** or *Syx1A* **(C)**. Knockdown of *Syb* or *Syx1A* increases the number of SVs **(D)** without causing changes to MVBL numbers **(F)**. In these SCs, the largest MVBL **(H)** or SV **(E)** does not change, but there is significant accumulation of CD63-GFP in the lumen of MVBLs **(G)**. *P<0.05, ***<0.001, Mann-Whitney *U* test, n=10. Scale bar is 10 µm.

4.2.3.2 Snap24 regulates numbers of large acidic compartments and SVs, potentially by controlling compartment fusion

In SCs expressing an RNAi targeting *Snap24*, the number of SVs greatly increased to levels higher than with knockdown of *Syntaxin-1A* (Figure 4.24B, C). Interestingly, unlike the other SNARE knockdowns, silencing of *Snap24* also increased the number of acidic compartments, which were filled with GFP (Figure 4.24E, G), suggesting that *Snap24* regulates fusion and maturation of these compartments. Indeed, the large lysosome-like compartment did not form in these cells (Figure 4.24F). The particularly large number of SVs observed in this background may be a consequence of not forming a lysosome to degrade SVs, in addition to blocking fusion to the plasma membrane.

To further understand the role of *Snap24*, I stained SCs expressing *SNAP24*-RNAi with a Rab7 antibody. In controls, Rab7 is normally found on roughly 3 compartments (Figure 4.25A), however, when *Snap24* was silenced, the number of Rab7 compartments increased to roughly 7 (Figure 4.25B, C), consistent with the idea that this gene does not affect the formation of Rab7-positive compartments, but might regulate their fusion and maturation, as well as affecting fusion of non-acidic SVs.

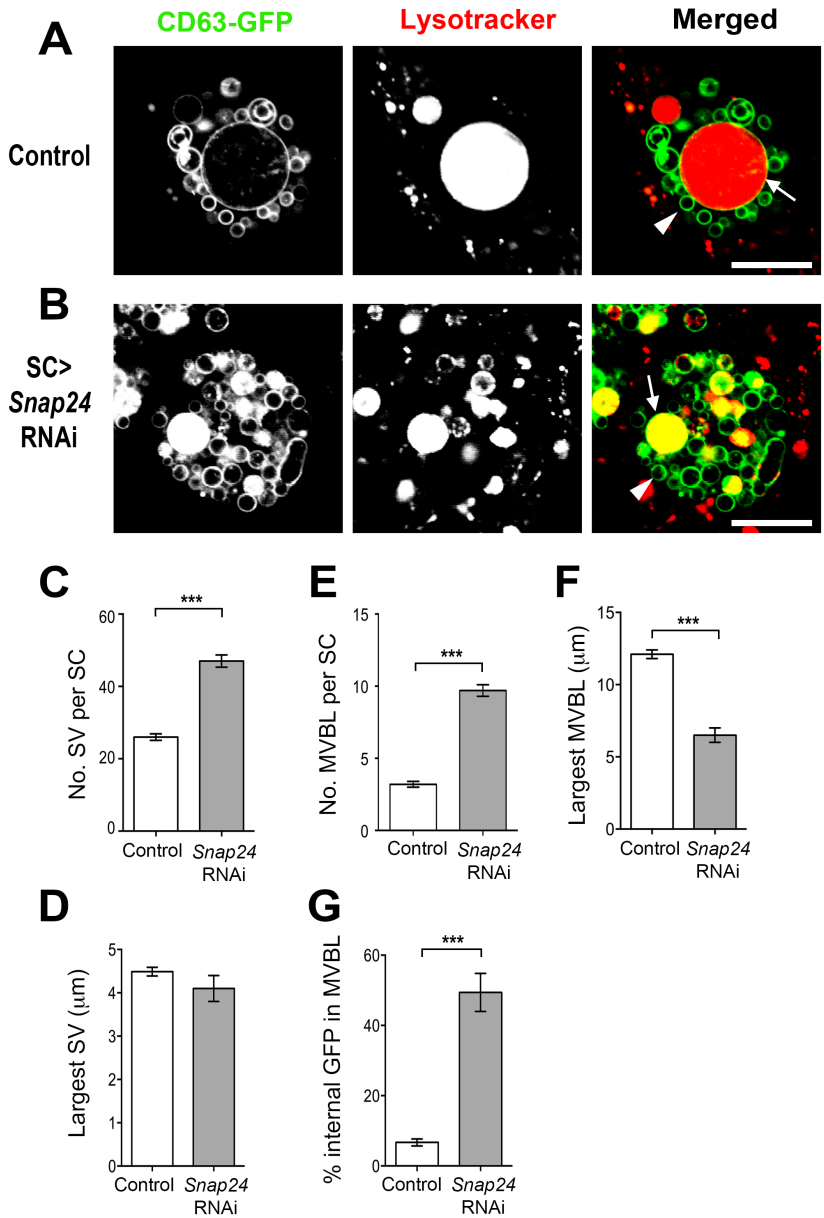


Figure 4.24 Snap24 regulates fusion of SVs and MVBLs.

Live confocal imaging of 8-day-old SCs expressing CD63-GFP **(A)**, or with *Snap24* RNAi **(B)**. Notice the number of SVs **(C)** and MVBL **(E)** increases. The diameter of the largest MVBL is reduced **(F)** but no such changes are seen for SV **(D)**. There is significant GFP fluorescence in MVBLs **(G)**. *** P<0.001, Mann-Whitney *U* test, n=10. Scale bar is 10 µm.

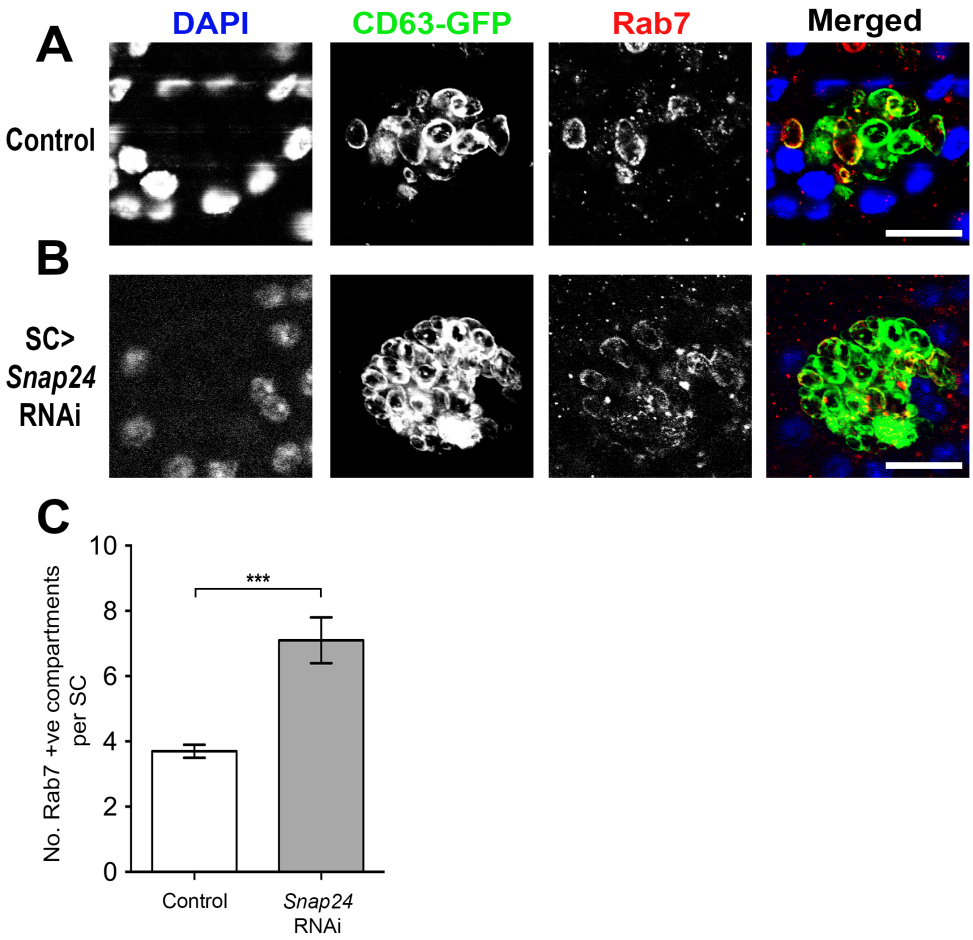


Figure 4.25 Snap24 control the number of Rab7 positive compartments.

Rab7 normally lines 3-4 compartments in 8-day-old SCs expressing CD63-GFP (**A, C**). **B)** Knockdown of *Snap24* significantly increases the number of Rab7 positive compartments **(C)**. *** P<0.001, Mann-Whitney *U* test, n=10. Scale bar is 10 µm.

4.2.3.3 V-ATPases control fusion of intracellular compartments and maturation of endolysosomal compartments in SCs

To test if SCs endogenously express the V-ATPase complex, we imaged flies expressing a tagged version of the VhaSFD subunit under its endogenous promoter. Interestingly, in these flies, there was a GFP positive signal throughout the SCs (Figure 4.26). Another DPhil student, Ben Kroeger, has tested a gene trap for Vha55, which localised on the limiting membrane of acidic compartments, suggesting that SCs normally express multiple components of the V-ATPase complex.

We performed an RNAi screen of all major V-ATPase subunits involved in exosome secretion and imaged SCs live after 8 days using confocal microscopy. Silencing of Vha26, Vha55, Vha68.2, and M9.7-1 all increased the number of non-acidic compartments (Figure 4.27B, C, D, E, Figure 4.28A), suggesting that all these subunits are involved in the membrane regulation function of the V-ATPase complex. The number of acidic MVBL compartments decreased when Vha26 was silenced and increased when Vha68.2 and VhaM9.7-1 knocked-down (Figure 4.28D), suggesting that these two subunits may have specialised roles in control endolysosomal trafficking.

Interestingly, we observed mixed results when measuring the size of the largest MVBL when V-ATPase function was perturbed. For Vha68.2 and Vha26 the MVBLs became smaller, whilst for VhaM9.7-1 this compartment was larger than aged matched controls (Figure 4.28E). In all cases where the V-ATPase subunits were silenced, there were increased levels of luminal CD63-GFP in the largest acidic compartments (Figure 4.28C), suggesting that the V-ATPase complex is involved in endolysosomal maturation.

In conclusion, SCs normally express the V-ATPase complex, which is involved in the fusion of non-acidic and acidic compartments and is required for the maturation of MVBLs.

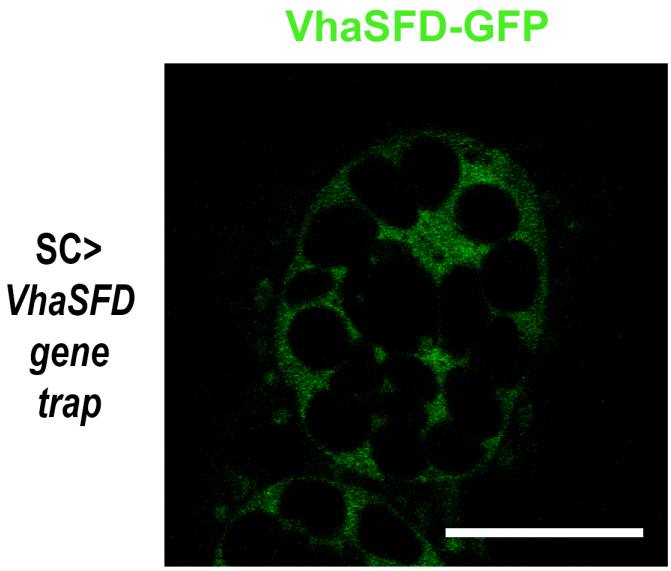


Figure 4.26 V-ATPase is normally expressed in SCs.

In 3-day-old SCs expressing the V-ATPase subunit, VhaSFD, GFP signal is seen throughout SCs. Ben Kroeger has used a gene trap for Vha55 and shown that it is also expressed by SCs and localises to acidic compartments. Scale bar is 10 μm.

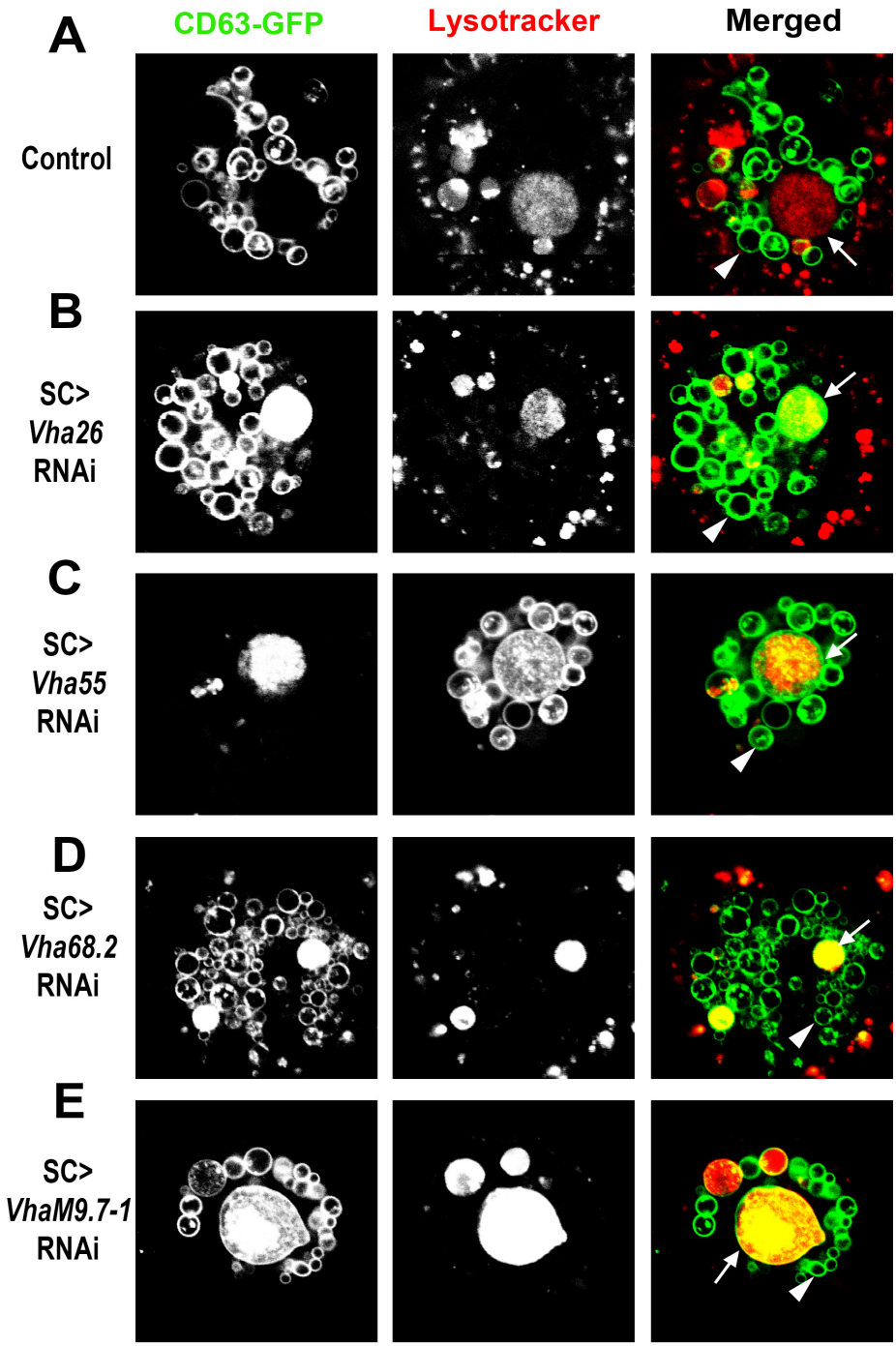


Figure 4.27 Trafficking analysis of V-ATPase knockdown.

Live confocal imaging of 8-day-old SCs expressing CD63-GFP **(A)** and RNAi against Vha26 **(B)**, Vha55 **(C)**, Vha68.2 **(D)** or VhaM9.7-1 **(E)**.

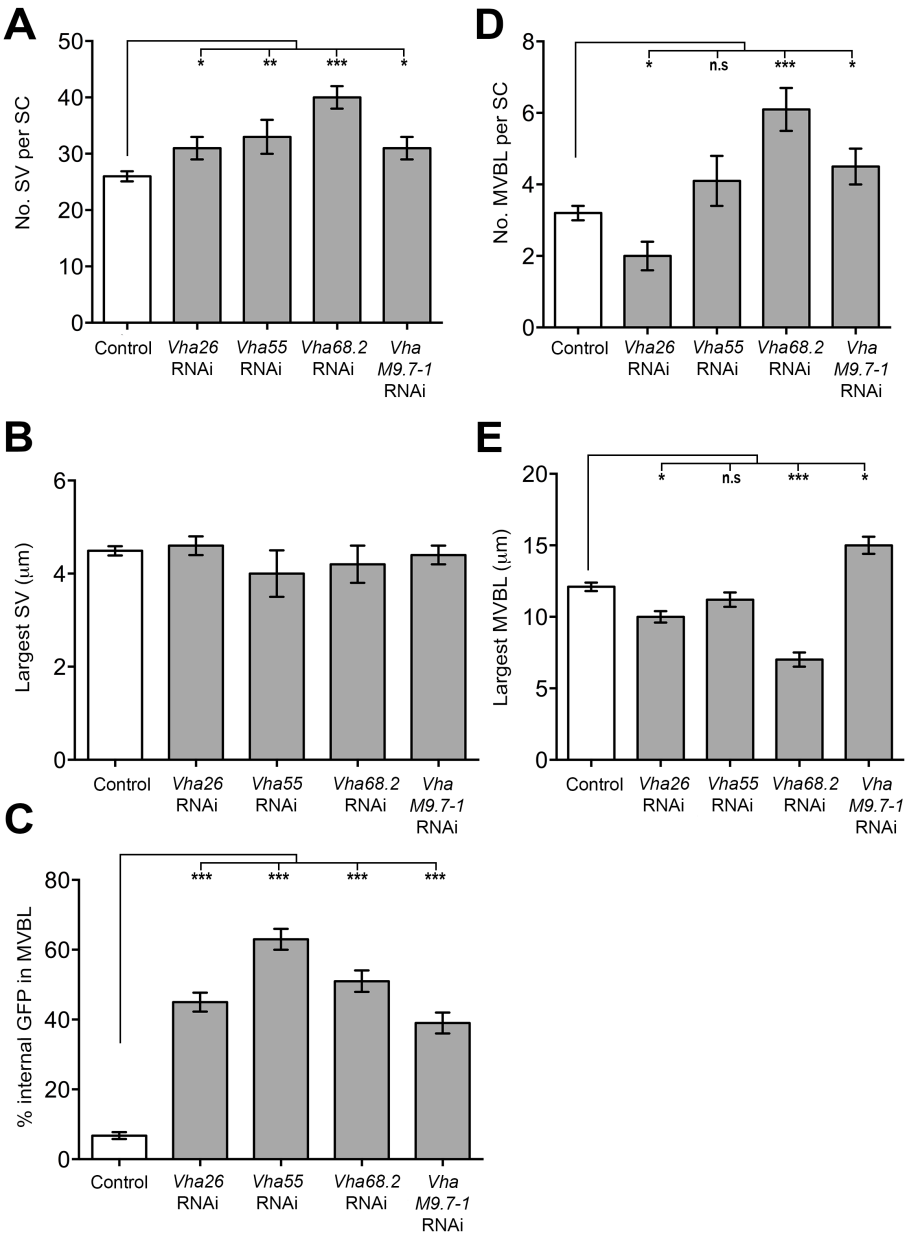


Figure 4.28 Trafficking quantification for V-ATPase knockdown.

Silencing subunits of the V-ATPase complex results in an increase in the number SVs **(A)**, whilst changes to MVBL numbers are more variable **(D)**. The size of the SVs does not change significantly **(B)**. The size of MVBL is reduced when Vha26 or Vha68.2 are silenced, and bigger in VhaM9.7-1 RNAi expressing SCs **(E)**. *P<0.05, **<0.01, ***<0.001, Kruskal-Wallis test, n=10.

4.2.4 Rab GTPases, SNAREs and V-ATPases control SC growth

As mentioned previously, the endolysosomal compartment is a major hub for growth regulation via the mTORC1 signalling cascade (Betz and Hall, 2013). Our observations that endolysosomal compartments appear smaller and less mature when Rab GTPases, SNARE proteins and the V-ATPases are knocked down prompted us test if the growth of the cells is altered.

Growth was assessed by measuring the total area of SC nuclei relative to MCs at 6 days (see Section 2.14). This method has previously been used before to evaluate growth in the AG and other systems. Knockdown of the Rab5, Rab7, Rab11 and Rab35 proteins, which control endolysosomal maturation, caused a significant reduction in SC nuclear size (Figure 4.29A, B, C, D, E, Figure 4.30), indicating that this set of Rabs also control SC growth. Overexpressing Rab11 also reduced SC growth.

When the SNARE, Snap24, was silenced, the growth of SCs decreased (Figure 4.30). Similarly, the growth of SCs was decreased when Vha55 and Vha68.2 were knocked down (Figure 4.30). This suggests that many of the genes that alter endolysosomal maturation also reduce cell growth.

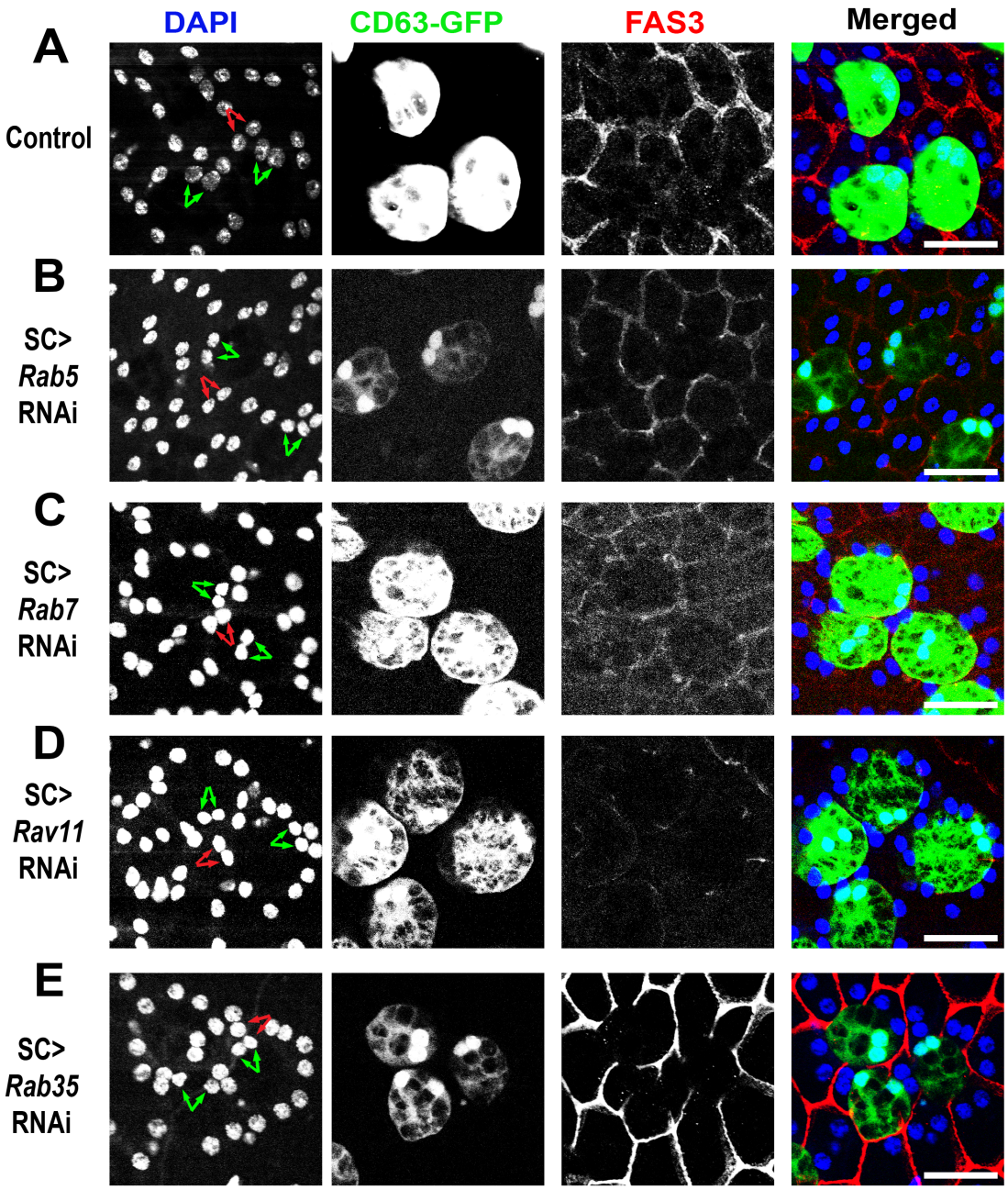


Figure 4.29 Rab GTPases control SC growth.

Accessory glands (AGs) from 6-day-old controls **(A)** and males expressing RNAi targeting *Rab5* **(B)**, *Rab7* **(C)**, Rab11 **(D)** or Rab35 **(E)** under the control of esgF/O^{ts} after temperature shift at eclosion. AGs were dissected, fixed and imaged by confocal microscopy. Glands were stained with DAPI (blue) to mark nuclei and an anti-Fas3 antibody (red) to mark cell boundaries. SCs express nuclear GFP, which is also present in the cytosol. Pairs of nuclei from binucleate SCs and MCs are indicated by green and red arrows respectively. Scale bar is 10 µm.

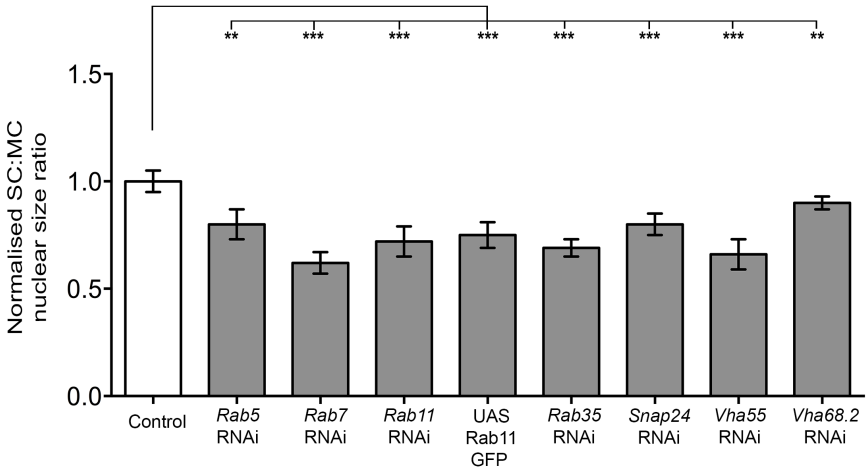


Figure 4.30 Rab GTPases, Snap24 and the V-ATPase complex control SC growth.

Bar chart showing SC nuclear size relative to that of MC neighbours for glands expressing different transgenes in SCs under esgF/O^{ts} control, normalized to the ratio for controls. Note that all manipulations that perturb SC trafficking also significantly reduce SC nuclear size. **P<0.01, ***<0.001, Kruskal-Wallis test, n=10.

4.3 Discussion

In this chapter I provide evidence that Rab GTPases, SNARE proteins and the V-ATPase complex regulate exosome secretion, and they do so by controlling distinct trafficking and fusion events in SCs. Moreover, I show that male-derived exosomes are crucial for reprogramming the female post-mating behaviour. Indeed, these findings have materialised because the AG has a large lumen to permit counting of exosome before and after genetic manipulation. Likewise, the large intracellular compartments of SCs enable scoring specific trafficking events reliable, thus providing a platform to dissect out the function of genes.

4.3.1 Regulation of exosome biogenesis

In order to assess if SCs produce and secrete exosome, we expressed the classical exosome marker CD63-GFP. The Wilson lab has previously shown that CD63-GFP is found in the AG lumen only when SCs, not MCs, express this construct, suggesting that SCs are the only epithelial cell type capable of secreting CD63-GFP positive exosome. Importantly, we do not believe that the exosome-like puncta observed in the AG lumen are a products of shedding from the plasma membrane because A) we found CD63-GFP inside MVBL, the site of ILV production, but also in SVs, potentially highlighting a non-MVBL based mechanism of exosome formation, and B) the release of exosomes is dependent known regulators of mammalian exosome secretion such as Rab7, 11, 27, and 35 as well as components of the ESCRT complex (Colombo et al., 2014).

We also found that regulators of membrane fusion such as Snap24, Synaptobrevin, Syntaxin1a and subunits of the V-ATPase complex are also involved in exosome secretion, therefore indicating that fusion events are required for SC secretion. Studies in yeast show that VAMP7 (equivalent to Snap24 in *Drosophila*) interacts with Rab7

and controls it's docking on endolysosomal compartments (Pryor et al., 2004). Interestingly, the downstream effector of Rab7, Rab-interacting lysosomal protein (RILP), recruits components of the V-ATPase complex to the late endosome/MVBL complex and is needed for its stability (De Luca et al., 2014), coupling Rab activation with SNARE and V-ATPase function.

Although the *Drosophila* seminal fluid has been shown to contain numerous proteins that control the female PMR, most of these are derived from MCs. However, recently it has emerged that perturbing development of SCs causes long-term behavioural changes in females (Gligorov et al., 2013). We show for the first time that SC-derived exosome are crucial for re-programming the females PMR. Indeed, Corrigan et al 2014 illustrates that male-derived exosomes fuse to both sperm and the epithelial cells of the female reproductive tract, potentially providing a platform for exosome-mediated signalling. It would be interesting to test what the changes in gene expression are in females mated to control males versus those incapable of transferring exosomes.

4.3.2 Biogenesis of SVs and endolysosomal maturation and growth by Rab GTPases

By studying the cell biology of SCs after silencing or overexpressing Rab GTPases, I showed that Rab11 seems to control directional trafficking of SVs towards endolysosomal compartments, whilst Rab7 is key to the formation and maintenance of the endolysosomal system. Interestingly, Rab35, which resides on small vesicles separate from those marked by Rab7 or Rab11, is also involved in SV trafficking and the maintenance of endolysosomal compartments once it has formed.

Previous reports suggest that as well as being involved in recycling of proteins; Rab11 also participates in trafficking from early endosomes to the *trans*-Golgi network (Wilcke et al., 2000). Although we could not confirm this in SCs because of the lack of GFP-

tagged markers, over-expressing Rab11 did not change the size of SVs suggesting that outward trafficking from the Golgi is not hindered. In another study, Phosphatase and tensin homologue deleted on chromosome 10 (PTEN) was shown to promote EGFR trafficking from early to late endosomes by dephosphorylating Rab7 (Shinde and Maddika, 2016). Consequently, this stimulates the localisation of Rab7 on MVBL compartments from where it controls maturation. It will be important to test if the function of PTEN in SCs and check if it controls the phosphorylation status of other Rabs such as Rab35.

In many cases, perturbing the function of the aforementioned Rabs resulted in significant accumulation of CD63-GFP inside the largest acidic compartment, leading us to propose their involvement in the maturation of the endolysosomes. Acidic compartments are central to nutritional sensing because are reported to be the first place where Amino acids spawn under autophagy (Betz and Hall, 2013). This leads to the recruitment of mTORC1 to the surface of endolysosomal compartments and initiates cell growth. We propose a model whereby the maturation status of the endolysosomal compartments may affect mTORC1 signalling and SC growth.

Knockdown of Rab7 caused a reduction in SCs growth but massively increased the number of small SVs, effectively uncoupling these two processes. One must ask the question – is there a second form of mTORC1 signalling that is independent of the endolysosomal system? It will be crucial in the future to test the requirement of mTORC1 signalling when Rab7 is silenced in SCs.

4.3.3 Fusion regulation by SNARE protein and the V-ATPase complex

Loss of function of synaptobrevin and syntaxin1a essentially produce the same phenotype: increase in SVs but not MVBLs numbers, suggesting that these two SNARE proteins potentially couple to control SV fusion. Interestingly, reconstitution studies on liposomes suggest that synaptobrevin and synaxtin form a stable binary via their transmembrane domain.

In the *Drosophila* larval salivary gland, phosphatidylinositol 4-kinase type 2 (PI4KII) mutants displayed aberrant accumulation of Snap24 on late endosomes leading to smaller glue granules (Burgess et al., 2012). The authors concluded that PI4KII is involved in the fusion of secretory glue granules and controls recycling of Snap24 to the TGN via late endosomes. Interestingly, Snap24 knockdown increased both SVs and acidic compartments. SCs expressing Snap24 RNAi accumulated Rab7 positive endosomes, suggesting that this SNARE is involved in their fusion. Future experiments should be steered towards understand the role of PI4KII in SCs and its association to Snap24 localisation.

In accordance to their reported roles as regulators of membrane fusion, we found the V-ATPase complex is involved in trafficking of SVs potentially by controlling their homotypic fusion or to the MVBL. Unfortunately, when we tried using pH-sensitive dyes to uncouple the fusion and proton pumping function of the V-ATPase, we could not detect significant changes in acidity after V-ATPase silencing (in collaboration with Ben Kroeger). It will be important to understand how proton pumping and fusion by the V-ATPase is coupled *in vivo*.

5. BMP signalling controls SC growth, exosome secretion and dense-core granule biogenesis (Results III)

5.1 Introduction

A long-term interest of the Wilson lab has been to understand how BMP signalling affects SC growth, trafficking and function. Initially, Aaron Leiblich demonstrated that BMP signalling controls SC growth and migration (Leiblich et al., 2012). Laura Corrigan then built upon these findings and provided evidence, some through collaborative work with me, that this pathway is also involved in SC exosome secretion, and that the nano-sized vesicles produced function to control the female PMR (Corrigan et al., 2014). In both cases, BMP signalling was crucially important to regulate aspects of SC biology and fly physiology. Having investigated the function of Rab proteins in specifying specific secretory compartments in SCs, I turned my attention to how BMP signalling components are trafficked into different Rab compartments, the source of the BMP ligand controlling SC biology, and how this signalling cascade controls the formation and secretion of Rab11-positive dense-core granule (DCG) compartments.

5.1.1 Overview of BMP signalling

BMPs were first recognised by their ability to induce bone formation at ectopic sites in rats. Since then, the BMP signalling cascade has been reported to control many aspects of cell biology and physiology. Some of these include patterning the dorsal-ventral axis (Lynch and Roth, 2011), establishing morphogen gradients (Ashe, 2005), controlling cell fate decisions, migration and proliferation (Rahman et al., 2015, Varga and Wrana, 2005). In mammals there are over 20 BMPs, some of which have distinct function.

The activation of the pathway is achieved once two BMP ligand bind to two transmembrane serine-threonine kinases receptors, resulting in Smad-mediated changes in transcription (Wang et al., 2014). At the plasma membrane, ligand binding induces the phosphorylation of the Type I receptor by the Type II receptor.

Subsequently, the Type I receptor relays this signal downstream by phosphorylating Receptor-Smads (R-Smads), leading to the formation of a heterodimeric complex after coupling with Co-Smads (Wang et al., 2014). This complex is capable of shuttling the nucleus, binding to DNA and initiating the transcription of BMP-responsive genes (Figure 5.1). Interestingly, one class of these genes are anti-Smads, which negatively regulate the pathway (Kawabata and Miyazono, 1999). Therefore, activation of the pathway can in effect leads to its own inhibition via a negative feedback loop.

5.1.2 BMP signalling in flies

In fruit flies, the BMP pathway is less complex in terms of the number of ligands, receptors and Smads, but the signalling machinery remains conserved (Ashe, 2005). There are three BMP ligands in *Drosophila*. Decapentaplegic (Dpp) is homologous to BMP2 and BMP4, Glass bottom boat (Gbb) is more closely related to BMP5-8 and Screw (Scw) is a more distant BMP relative (Hamaratoglu et al., 2014). Flies possess two Type I receptors, Thickveins (Tkv) and Saxophone (Sax), and two Type II receptors, Wishful thinking (Wit) and punt (Put) (Hamaratoglu et al., 2014). The downstream R-Smads are Mad and Smox, which couples to a single co-Smad, Medea (Med). *Daughters against Dpp* (*Dad*) is one transcriptional target of BMP signaling. The Dad protein functions as an anti-Smad to shut down signaling by binding to Type I receptors and blocking activation of Mad (Figure 5.1) (Tsuneizumi et al., 1997).

The *Dpp* ligand can dimerise with itself or form heterodimers with *Gbb* or *Screw*. Dpp has been shown to have a higher affinity for *Tkv* than *Punt,* whilst Gbb binds the *Wit* and *Sax* receptor. Depending on the combination of ligand-receptor complex and the cell type, Dpp-dependent BMP signalling can have multiple functions. During embryogenesis, it controls migration of tracheal cells, as it does in developing adult abdominal epithelial cells (Vincent et al., 1997). In the wing disc, BMP signalling is

required for growth, proliferation and dorsal-ventral patterning (Raftery and Umulis, 2013). Interestingly, at the neuromuscular junction (NMJ), Gbb-dependent signalling is involved in retrograde control of synaptic growth. The components of the extracellular matrix are also crucial for regulated BMP signalling. Sawala et al 2015 showed that the α-integrin subunit is one of the target genes for BMP signalling. In the same study integrins were shown to interact with BMP receptors to potentiate downstream signalling, thus participating in a positive feedback loop (Sawala et al., 2015).

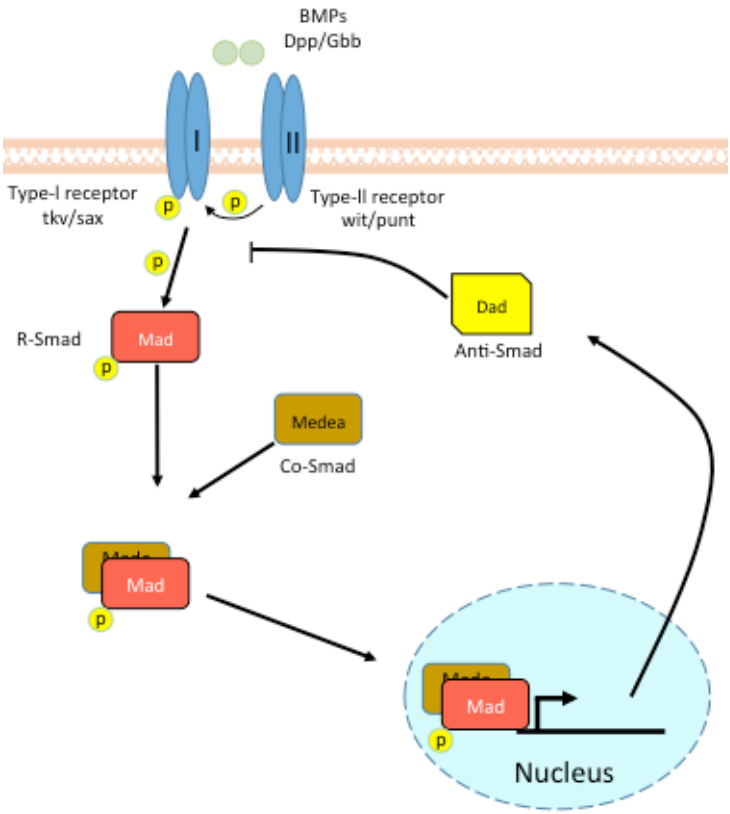


Figure 5.1 BMP signalling in mammals and flies.

Activation of BMP receptors by ligand binding results in the Type-II receptor phosphorylating the Type-I receptor, the latter then phosphorylates the R-Smad, Mad, leading to its coupling with Co-Smad, Medea. This complex now translocates to the nucleus to regulate gene expression. One of the target genes for the BMP pathway is Anti-Smad. The homolog of this in flies is is Dad, which negatively regulates the pathway.

5.1.3 BMP signalling in controlling secretion

One aspect of BMP signalling that remains poorly understood is how it controls cell secretion. In mammalian dendritic cells (DC), BMP signalling is proposed to control DC maturation and stimulate the release of several cytokines (Martinez et al., 2011). Exactly how it achieves this remains to be determined.

An important study in 2007 showed that the mouse BMP4 ligand (a homologue of Dpp in flies) associates strongly with the BMP type 1a receptor (Bmpr1a) (Goulley et al., 2007). Interestingly, mice with attenuated BMP signalling developed diabetes as a result of impaired insulin secretion from pancreatic β cells. BMP signalling was shown to increase the expression of known regulators of exocytosis such as Snap25 (Goulley et al., 2007). Additionally, the authors provided evidence that ectopic expression of BMP4 in β cells promoted glucose-stimulated insulin secretion, potentially highlighting a β cell-mediated feedback loop involved in this process. As mentioned previously, the Wilson lab has also shown that BMP signalling plays a crucial role in SC-dependent growth, migration and exosome secretion.

5.1.4 Dense-cored granule biogenesis

In EM micrographs, SCs appear to have numerous compartments containing a central electron-dense core region. I have shown section 3.2.4 that Rab11 selectively marks these compartments. In highly secretory cells, bioactive molecules are usually packaged inside DCGs and are secreted in a regulated manner. As mentioned previously (Section 1.3), the biogenesis of DCGs involves a step-wise trafficking of cargos through the Golgi complex, finally ending at the TGN, where budding of immature DCGs takes place (see Section1.3).

Much work has been focused on understanding the regulators that participate in DCG biogenesis. Granins are a class of proteins highly enriched in DCGs and are suggested to be involved in generating the driving force for DCG budding at the TGN (Kim et al., 2006). Moreover, roles for lipids have also been described in controlling DCG biogenesis and constitutive secretion, whilst its involvement in regulated secretion remains more ambiguous (Kim et al., 2006). Once immature DCGs have formed, they undergo a maturation program involving intraluminal Ca^{2+} ions and acidification (Wu et al., 2001).

DCGs can be secreted constitutively by many cell types, but in specialised secretory cells they are much more highly secreted after a specific signal (Morvan and Tooze, 2008). Indeed, how the cell distinguishes DCGs undergoing constitutive or regulated secretion remains a mystery, although it probably involves certain aspects of DCG maturation or identity. Moreover, the signalling pathways that are involved in replenishing the pool of DCGs that are lost during secretion are poorly characterised.

5.1.5 Aims

In my final chapter, I focus on characterising how BMP signalling components are trafficked in SCs and how this cascade is involved in DCG biogenesis. To do this, I:

1. Screen the central components of the BMP signalling pathway for functions in SC trafficking and growth.
2. Characterise the trafficking of BMP signalling components in SCs.
3. Dissect the mechanisms by which BMP signalling is activated in SCs and how these are involved in DCG biogenesis and secretion.

I conclude that autocrine BMP signalling plays a central role in increasing the rate of DCG core compartment formation following DCG release during mating, therefore matching DCG replenishment to regulated secretion. I discuss potential parallels with other cells involved in regulated secretion in mammals and flies. Much of this work has recently been accepted for publication in PLoS Genetics (Redhai et al. 2016).

5.2 Results

5.2.1 All components of the BMP signalling pathway are involved in SC growth and trafficking

5.2.1.1 BMP signalling controls growth

The Wilson lab has already shown that the BMP signalling pathway is important in controlling SC growth because overexpression of the negative regulator, Dad, or RNAi-mediated knockdown of *Medea* (*Med*) inhibits growth. By contrast, expressing a constitutively activated form of the Type I BMP receptor Thick veins, Tkv (Tkv^{ACT}), containing a Q199D substitution, promoted growth in SCs (Leiblich et al., 2012).

To test whether all core components of the BMP cascade are required to control SC growth, each constituent was knocked down with two independent RNAi, most of which have been used in other tissues to analyse BMP signalling (see Materials and Methods). Silencing of both Type I and both Type II receptors significantly decreased the relative SC:MC and absolute SC nuclear size compared to controls (Figure 5.2A, B; and Redhai et al., 2016). As reported previously, downregulation of BMP signalling by knockdown of *Med* or *Mad*, or by overexpressing Dad also significantly inhibited SC nuclear growth, while overexpression of Tkv^{ACT} increased growth and size of cells, confirming that all components of the BMP pathway are involved in SC growth control (Figure 5.2A, B). Importantly, when the same UAS-constructs were present without a GAL4 driver, the growth of SCs was not changed (Figure 5.3).

Since SCs only represent a small population of epithelial cells in the AG, we could not reliably confirm the level of knockdown by RT-PCR of total AG mRNA (Data not shown). However, staining SCs expressing *wit* RNAi with an antibody against Wit

drastically suppressed the distinct staining pattern observed in control SCs, demonstrating strong knockdown efficiency in this experiment. (Figure 5.4A, B).

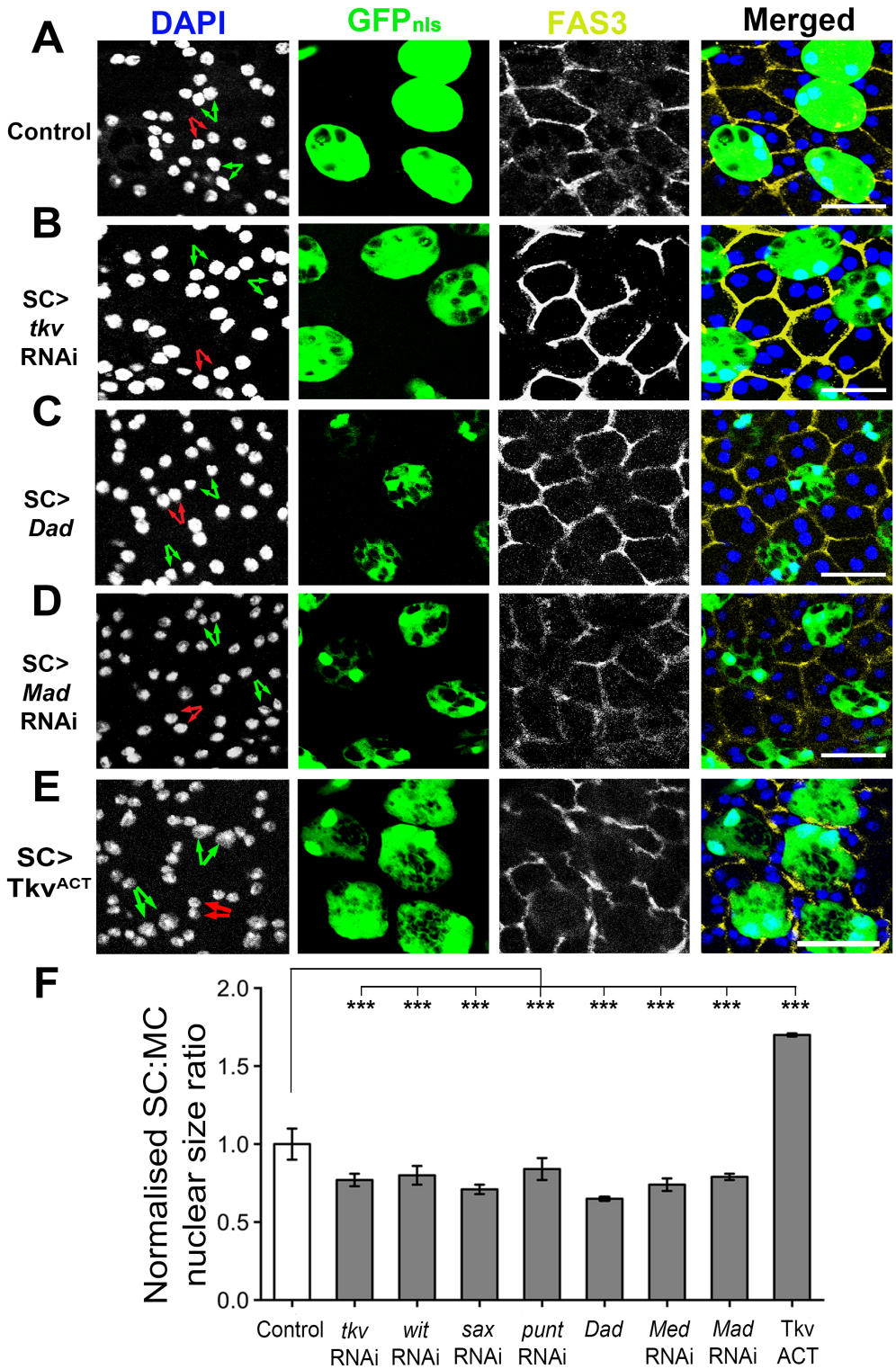


Figure 5.2 All BMP signalling components regulate SC growth.

A) Accessory glands (AGs) from 6-day-old controls **(A)** and males expressing RNAi targeting *tkv* **(B)**, or *Mad* **(D)** or expressing the BMP signalling antagonist *Dad* **(C)**, or a constitutive active form of the Tkv receptor (Tkv^{ACT}) **(E)** in adult SCs under the control of $esgF/O^{ts}$ after temperature shift at eclosion. **F)** Bar chart showing SC nuclear size relative to that of MC neighbours for glands expressing different transgenes in SCs under $esgF/O^{ts}$ control, normalized to the ratio for controls. Note that all manipulations that decrease BMP signalling significantly reduce SC nuclear size. ***P<0.001, Kruskal-Wallis test, n=10. Scale bar for all images is 20 μm.

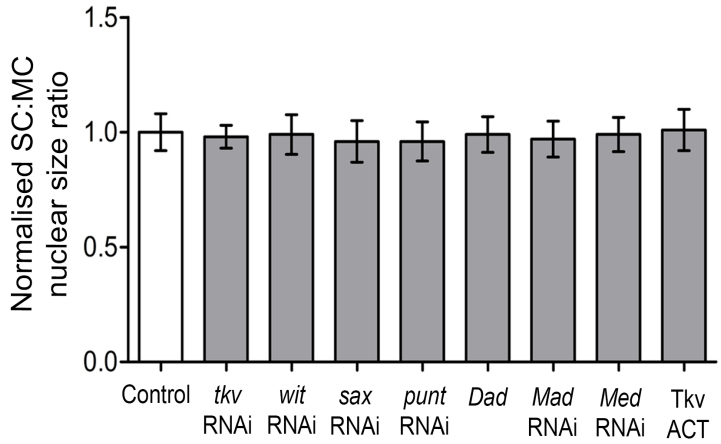


Figure 5.3 Expression of transgene in SCs requires GAL4 driver.

Flies carrying UAS-transgenes used in this study do not affect the SC:MC nuclear size ratio in the absence of an SC-specific driver. Kruskal-Wallis test, n=10.

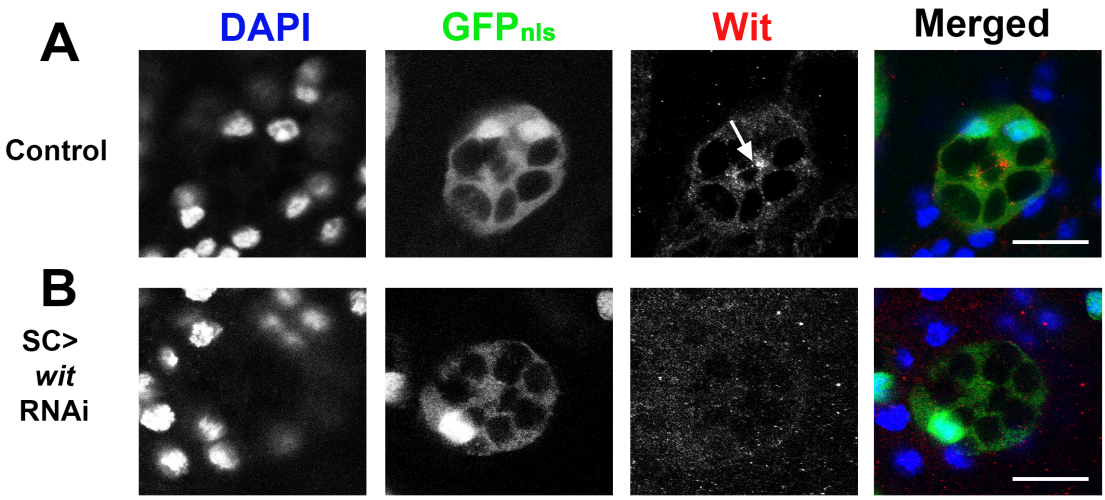


Figure 5.4 RNAi induces strong knockdown.

SC-specific knockdown of *wit* for 6 days using the esgF/O^{ts} driver line eliminates anti-Wit antibody staining in SCs **(B)** compared to control (**A**, arrow). Glands were stained with DAPI (blue) to mark nuclei. Gain settings on confocal are increased in **(B)** to demonstrate absence of specific signal. Scale bar is 10 μm.

5.2.1.2 BMP signalling control SC trafficking, MVBL maturation and exosome secretion

Corrigan et al (2014) previously showed that inhibiting BMP signalling by overexpressing Dad caused a reduction in SV numbers, the formation of an immature MVBL and decreased exosome secretion. Conversely, activating the pathway increased the number of SVs and manifested in the formation of a single massive lysosomal compartment containing no internal fluorescent CD63-GFP.

To test if other components of the BMP signalling cascade are involved in these processes, SCs were imaged live after 6 days of RNAi or other transgene induction. I found that RNAi knockdown of *tkv*, *put*, *wit*, *Mad*, or *Med* resulted in an overall decrease in SV number, whilst Tkv^{ACT} expression produced an increase (Figure 5.5A, B, C, D, E, F). Surprisingly, silencing of *sax* increased SV numbers, presumably because this receptor has a different effect to the other signalling components on one or more aspects of SC membrane trafficking, as previously reported by (Bangi and Wharton, 2006).

As shown previously in control SCs, when imaged at its greatest diameter, usually less than 10% of the total area of the largest MVBL compartment contains fluorescent CD63-GFP constitutes in living SCs. Silencing any BMP signalling component resulted in significantly increased accumulation of fluorescent CD63-GFP inside this lysosome-like compartment (Figure 5.5G). Conversely, Tkv^{ACT} expression reduced the GFP signal, supporting the idea that BMP signalling promotes lysosomal maturation in SCs. Moreover, the largest MVBL was often smaller in size when BMP signalling was inhibited, except with *punt* RNAi, where the size of this compartment was not affected (Figure 5.5H). Tkv^{ACT} expression greatly increased the size of the largest MVBL, consistent with the idea that the BMP signalling cascade drives trafficking into this compartment.

Knockdown of all BMP receptors, *Mad* or *Med,* or overexpression of Dad in adult SCs resulted in a reduction in CD63-GFP-positive puncta in the AG lumen, demonstrating that all BMP components are involved in exosome secretion (Figure 5.5I). Unfortunately, in flies expressing Tkv^{ACT}, I observed massive build-up of CD63-GFP-positive debris in the AG lumen, consistent with previous observations, making it impossible to estimate the levels of exosome secretion.

In conclusion, all components of the BMP signalling pathway are required to maintain normal SV number, promote endolysosomal maturation and drive exosome secretion.

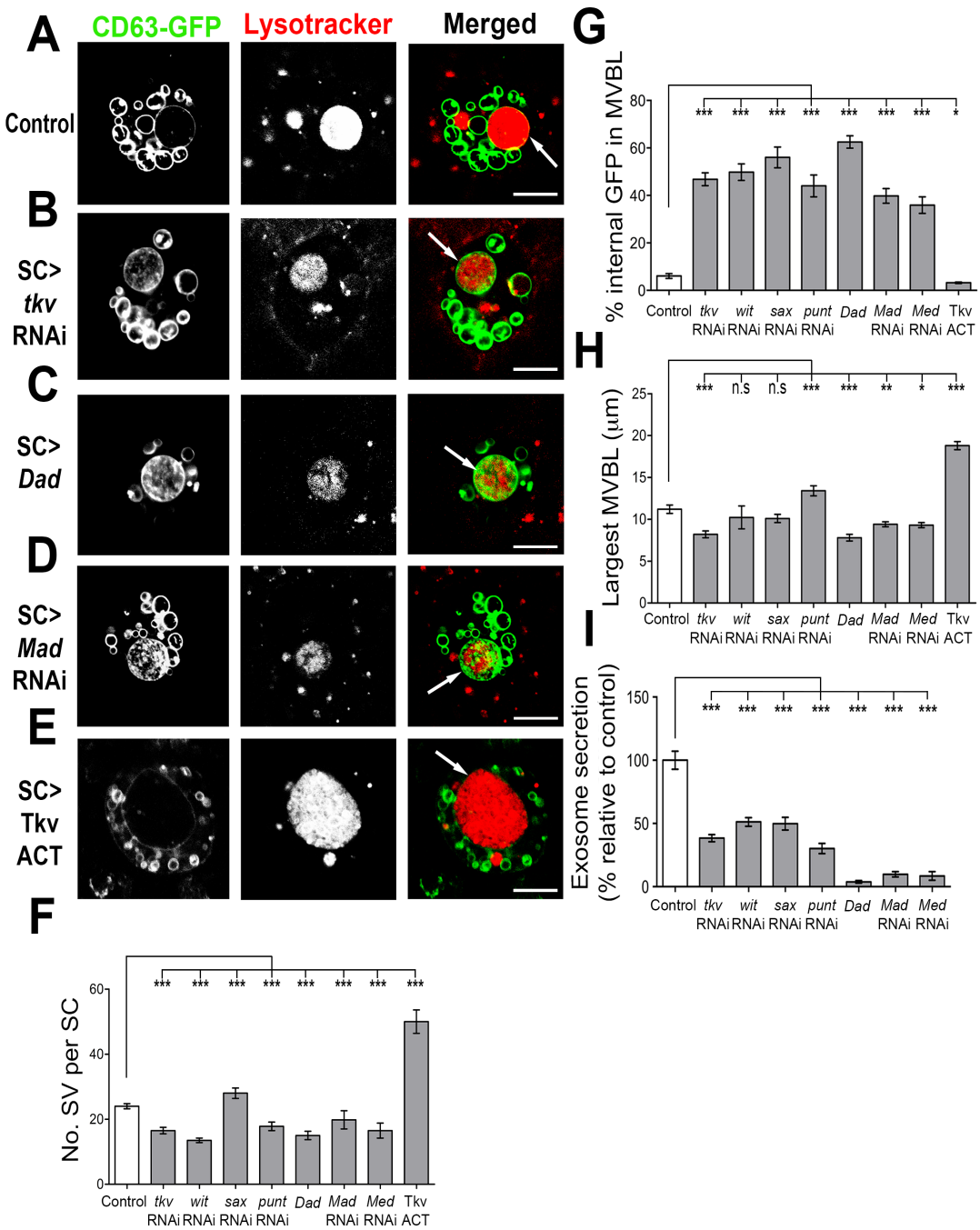

A
CD63-GFP
Lysotracker
Merged
Control
B
SC> tkv RNAi
C
SC> Dad
D
SC> Mad RNAi
E
SC> Tkv ACT
F
No. SV per SC
Control tkv RNAi wit RNAi sax RNAi punt RNAi Dad Mad RNAi Med RNAi Tkv ACT
G
% internal GFP in MVBL
H
Largest MVBL (μm)
n.s
I
Exosome secretion (% relative to control)

Figure 5.5 Multiple BMP signalling components in SCs regulate numbers of SVs, endolysosomal maturation, largest MVBL size and exosome secretion.

Live imaging of SCs from 6-day-old males expressing CD63-GFP and either no additional transgene (**A**), or RNAi against *tkv* **(B)** or *Mad* **(D)**, or overexpressing *Dad* **(C)** or an activated form of the *Tkv* receptor (Tkv^{ACT}; **E**) throughout adulthood and stained with Lysotracker. Images represent a single z-plane, so do not show all SVs. **F**) The number of large CD63-GFP-positive SVs (>1µm diameter) per SC was counted. **G**) In control glands **(A)**, GFP fluorescence is largely undetectable in the lumen of the largest, most mature MVBL (arrow). However, inhibiting of BMP signalling, results in significant accumulation of GFP fluorescent signal in the MVBL lumen. **H**) Reducing BMP signalling often reduces the diameter of the largest MVBL, while activating the pathway (by overexpressing Tkv^{ACT}) increases the diameter. **I)** Inhibiting BMP signalling in SCs reduces the number of CD63-GFP-positive exosomes inside the AG lumen. *P<0.05, **P<0.01, ***P<0.001, Kruskal-Wallis test, n=10. Scale bar for all images is 10 µm.

5.2.1.3 Dpp is the predominant ligand controlling BMP signalling in SCs

There are three BMP ligands in *Drosophila*, two of which, Dpp and Gbb, are closely related to BMPs found in mammals. The third ligand, Scw, was not investigated because it does not seem to be expressed in the AG (Sitnik et al., 2016). Knocking down *dpp* or *gbb* in MCs did not change their nuclear size (Redhai et al 2016). However, when *dpp*, but not *gbb*, was silenced in SCs, I saw a significant reduction in growth (Figure 5.6A, E). The role for Dpp in SC growth was further supported by the finding that Dpp-GFP overexpression in SCs also promotes nuclear growth and cell size (Figure 5.6B, E). No such change was observed when overexpressing Gbb-GFP (Figure 5.6E). Interestingly, expressing Dpp-GFP in MCs did not affect their nuclear size, but did increase SC growth, suggesting that SCs can respond to exogenous Dpp (Figure 5.6C, F). Expressing Gbb-GFP in MCs caused a significant reduction of SC growth (Figure 5.6F), perhaps because Gbb, which is expressed in AGs, has an antagonistic role in growth control that is not detected by knockdown experiments in a single cell type. I conclude that Dpp is the main ligand controlling BMP-regulated growth control in SCs.

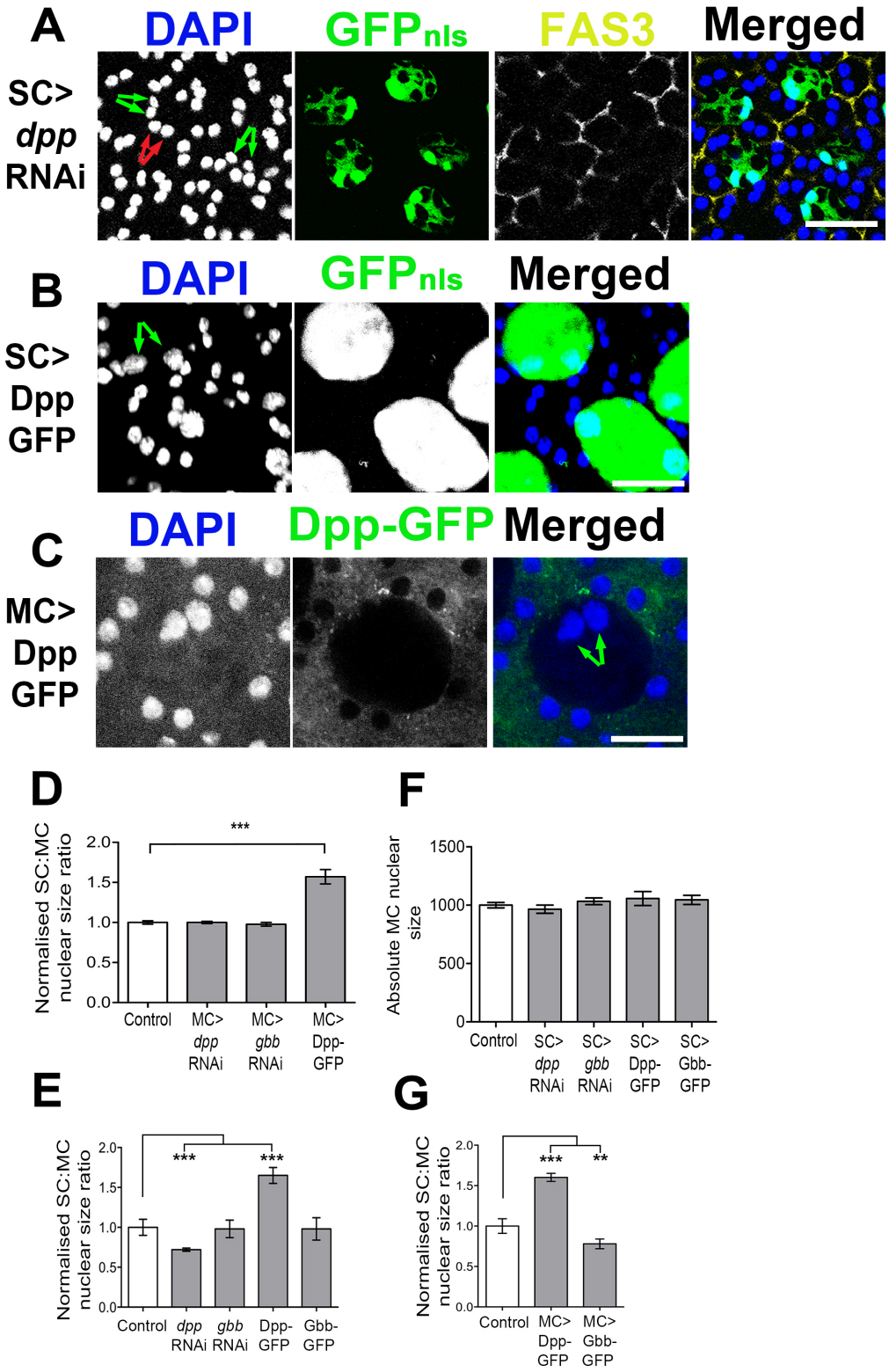

A
DAPI
GFPnls
FAS3
Merged
SC>
dpp
RNAi
B
DAPI
GFPnls
Merged
SC>
Dpp
GFP
C
DAPI
Dpp-GFP
Merged
MC>
Dpp
GFP
D
Normalised SC:MC nuclear size ratio
2.0
1.5
1.0
0.5
0.0
***
Control
MC> dpp RNAi
MC> gbb RNAi
MC> Dpp-GFP
F
Absolute MC nuclear size
1500
1000
500
0
Control
SC> dpp RNAi
SC> gbb RNAi
SC> Dpp-GFP
SC> Gbb-GFP
E
Normalised SC:MC nuclear size ratio
2.0
1.5
1.0
0.5
0.0
***
***
Control
dpp RNAi
gbb RNAi
Dpp-GFP
Gbb-GFP
G
Normalised SC:MC nuclear size ratio
2.0
1.5
1.0
0.5
0.0
***
**
Control
MC> Dpp-GFP
MC> Gbb-GFP

Figure 5.6 Dpp regulates SC growth in the AG.

Image of SCs from 6-day-old males expressing *dpp* RNAi **(A)** or Dpp-GFP **(B)** under the control of esgF/O^{ts} after temperature shift at eclosion and stained for Fas3 (yellow only in **A**) and DAPI (blue). Note that in that *dpp* RNAi reduces the size of SCs nuclei (green arrows) relative to MCs (red arrows), whilst overexpressing Dpp-GFP increases nuclear size (**B**, green arrow). **C)** Main cell expression of Dpp-GFP for 6 days induces growth in SCs (green arrows). **D)** Graph showing that MC nuclear size is unchanged when Dpp RNAi or Gbb RNAi are expressed in MCs, but increased when MC overexpress Dpp-GFP. **E)** Graph showing that Main cell nuclei are not affect by SC expression of transgenes. **F)** Quantification of A and B, highlighting Dpp, not Gbb, regulates SC growth. **G)** Expression of Dpp-GFP in Main cells increases SC growth, whilst Gbb-GFP reduces SC growth. ***P<0.001, Kruskal-Wallis test, n=10. Scale bar for A, B is 20 µm and for C its 10 µm.

5.2.1.4 Dpp regulates BMP signalling via an autocrine feedback loop

To test if SCs or any other cell type in the AG normally expresses Dpp, we used a previously characterised *dpp*-GAL4 transgene, dpp^{blk}-GAL4, which recapitulates endogenous *dpp* expression in several developmental scenarios (Staehling-Hampton et al., 1994, Morimura et al., 1996). Flies carrying dpp^{blk}-GAL4 and UAS-GFP displayed a specific GFP signal in SCs (Figure 5.7A), suggesting that Dpp is normally synthesised exclusively by SCs in the AG.

Since knocking down Dpp in SCs caused a reduction in nuclear growth, I hypothesised that it may signal via autocrine signalling. To address this question, I produced SC mosaic clones expressing *dpp*-RNAi using the esgF/O^{ts} system. Growth of SCs expressing *dpp*-RNAi (GFP-positive) was most severely reduced, whilst SCs not expressing the RNAi (GFP-negative) were also affected, albeit to a lesser extent (Figure 5.7B, C). Conversely, mosaic overexpression of UAS-*dpp-GFP* increased nuclear growth only in SCs expressing this construct (Figure 5.7C). In conclusion, SC-specific Dpp appears to predominantly control cell-autonomous, autocrine BMP signalling, although it also exerts some paracrine effects.

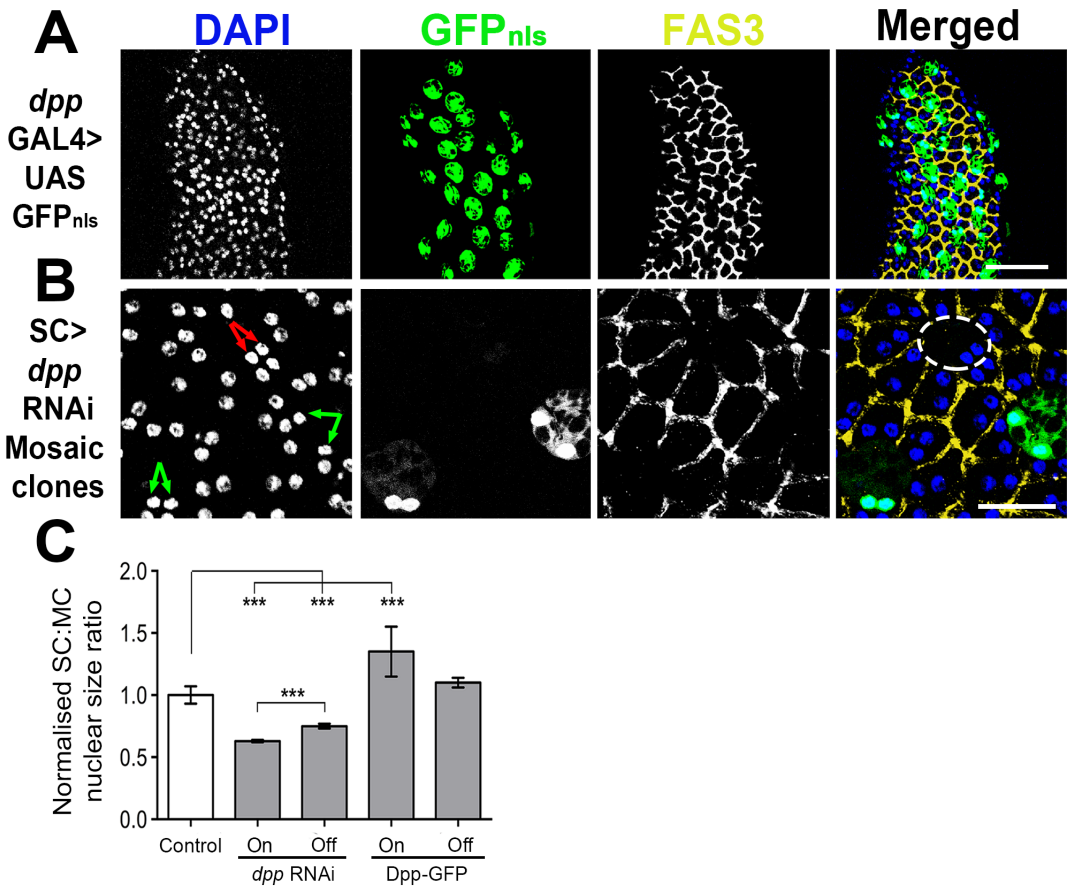


Figure 5.7 Autocrine Dpp signalling controls SC growth.

A) *dpp*^{blk}-GAL4 drives expression of a UAS-coupled nuclear GFP exclusively in SCs of the AG. **B)** Mosaic expression of *dpp*-RNAi or Dpp-GFP in a subset of SCs has a stronger effect on nuclear growth in expressing cells (on – green arrows) than in non-expressing (off – red arrows; white dashed circle) SCs, although *dpp* knockdown also reduces growth in the latter **(C)**. *w; esg-GAL4 tub-GAL80*^{ts} *UAS-FLP; UAS-GFP*$_{nls}$ *actin>FRT>CD2>FRT>GAL4* was used to generate mosaic clones of SCs expressing *Dpp*-RNAi (**B**, BI 33618). ***P<0.001, Kruskal-Wallis test, n=10. Scale bar for A is 50 µm, for B is 20 µm.

5.2.1.5 Dpp controls SV numbers, MVBL maturation and exosome release

To test whether Dpp affects membrane trafficking events, it was silenced in SCs and the resulting cells imaged live. As for other BMP signalling components, knockdown of *dpp* resulted in fewer SVs, prevented endolysosomal maturation and inhibited exosome secretion (Figure 5.8B, C, D, F). Interestingly, the size of the largest acidic compartment was increased with one RNAi but unaffected by the other (Figure 5.8E), suggesting that like *punt*, Dpp affects the lysosome-like compartment of SCs in a different way to other BMP signalling components.

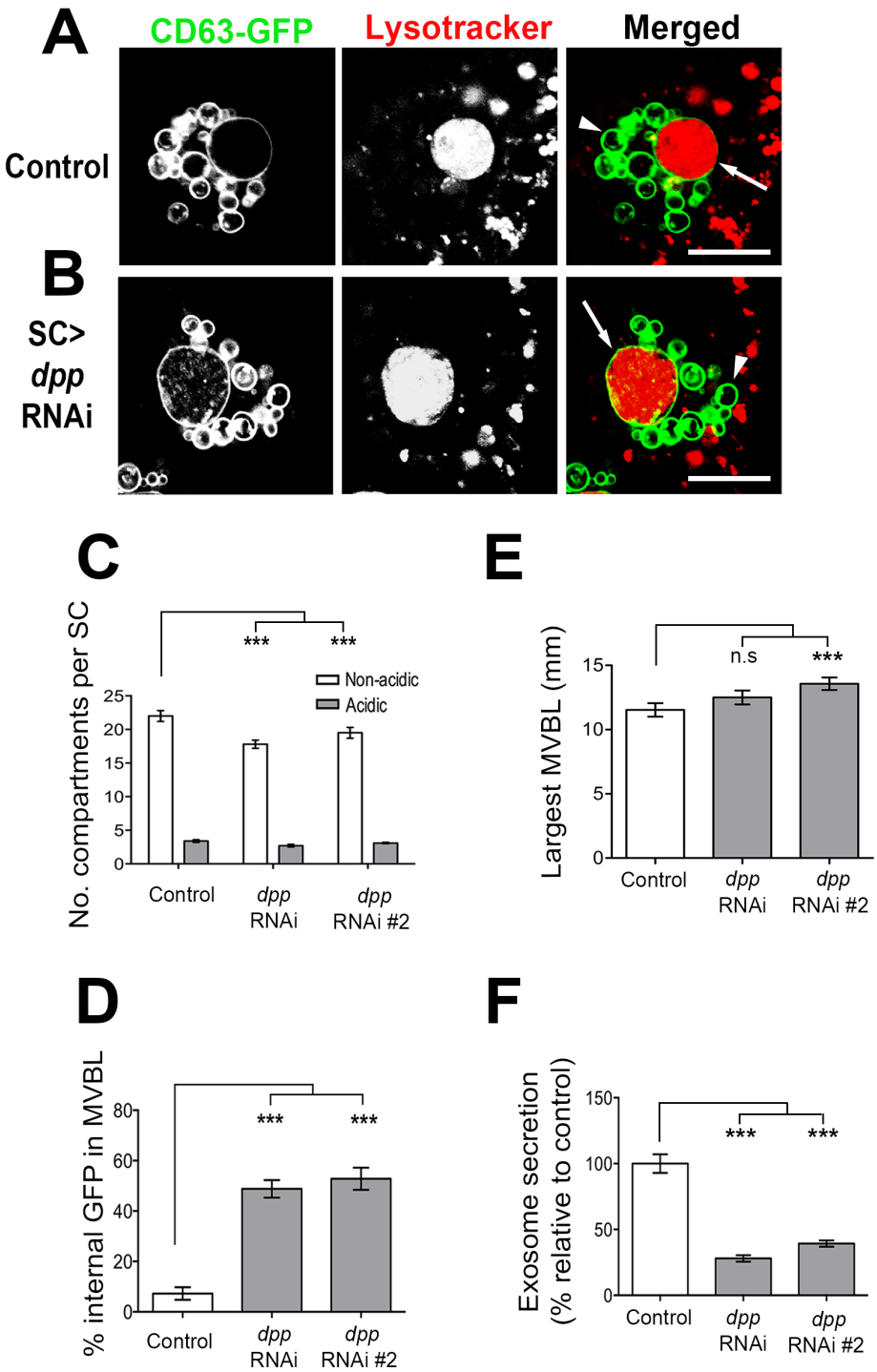


Figure 5.8 Dpp regulates SC trafficking.

6-day-old SCs expressing CD63-GFP with no additional transgene **(A)** or *dpp*-RNAi **(B)** using the *dsx*-GAL4 driver reduces non-acidic SV number **(C)** (eg., marked by arrowhead) and increases GFP fluorescence in largest MVBL (arrow; stained with Lysotracker Red) compared to controls **(D)**. Knockdown of *dpp* either results in a small increase in the size of the largest MVBL or no significant size change **(E)**, and reduces exosome secretion **(F)**. ***P<0.001, Kruskal-Wallis test, n=10. Scale bar is 10 μm.

5.2.2 Trafficking of BMP signalling components

5.2.2.1 SCs endogenously express BMP receptors

Having shown that BMP signalling is crucial for controlling SC trafficking and growth and that this is dependent on a Dpp autocrine feedback loop, I turned my attention to characterising the localisation of BMP components in the hope of understanding how signalling and trafficking are coupled together.

To determine where BMP receptors are localised, I first expressed a yellow fluorescent protein- (YFP-) tagged *tkv* gene trap line, $tkv^{CPTI002487}$. Expression was observed in all SCs, where YFP was seen to be present on the plasma membrane as well as small intracellular compartments distinct from the large SVs (Figure 5.9). Moreover, I stained SCs with an antibody against the Type II BMP receptor Wishful Thinking (Wit), which forms a heterodimer with Type I receptors. Wit was also found on the plasma membrane and on a subset of the Tkv-YFP-positive intracellular compartments, suggesting that both receptors are trafficked via the same route (Figure 5.9), potentially after endocytosis. Unfortunately, we did not have the necessary tools to characterise wild type Sax and Punt expression. In conclusion, SCs endogenously express both Type I and Type II receptors, which reside on the same intracellular compartments in SCs.

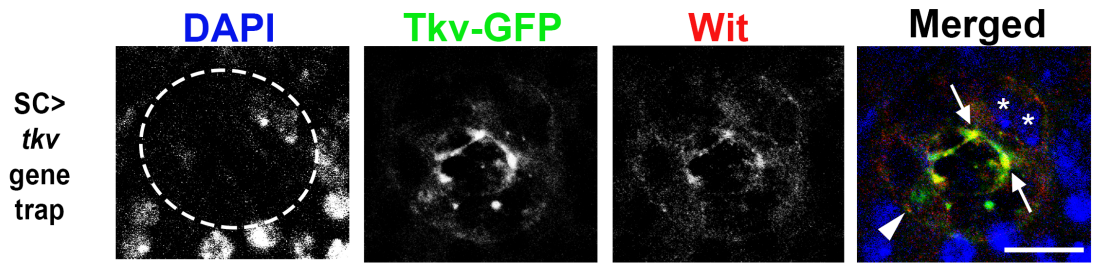


Figure 5.9 SCs endogenously express BMP receptors.

SC (circled) expressing a gene trap for the BMP type I receptor *tkv*, and stained with an antibody against the BMP type II receptor Wit. These receptors are present both on the plasma membrane (arrowhead) and co-localise in intracellular compartments (arrow). DAPI marks nuclei blue in SCs (asterisks) and surrounding non-expressing MCs. Scale bar is 10 μm.

5.2.2.2 Dpp is trafficked to dense-core granules

To characterise where BMP ligands are localised, GFP tagged versions of both Gbb and Dpp were expressed in SCs. In these cells, Gbb-GFP appeared to be in intracellular compartment distinct from the larger SV, but reminiscent of compartments marked by Rab35 (Figure 5.10). To test if Gbb is present on Rab35 compartments, SCs expressing Rab35-GFP were stained with an anti-Gbb antibody. Indeed, in these SCs, Gbb was found to co-localise with Rab35 (Figure 5.10). Therefore, although *gbb* knockdown in SCs with an RNAi that has been shown to be functional in other cell types (Beckwith et al., 2013), does not affect SC growth, the Gbb ligand does appear to be present in these cells.

Where does Dpp localised? To answer this question, SCs expressing Dpp-GFP were imaged live. Dpp-GFP was concentrated in spherical structures resembling DCGs, but was typically absent from acidic MVBLs (Figure 5.11A). To confirm that Dpp resides inside DCG comparmtnets, SCs expressing Dpp-GFP were co-stained with ANCE. In these cells, Dpp co-localised with ANCE (Figure 5.11B), suggesting that it is packaged inside DCGs in SCs.

Dpp-GFP was also seen in the AG lumen in small puncta and fibril-like structures (Figure 5.11E). This secreted Dpp may be involved in the paracrine effects of this ligand. Expressing this construct for even a short period of time (3 days) caused SCs to grow. Therefore, to rule out that the localisation of Dpp-GFP was a product of long-term overexpression of this protein, I performed short pulse-chase experiments. Interestingly, a one-hour pulse of Dpp-GFP was chased into DCG structures containing ANCE over a subsequent 12 hour period (Figure 5.11C).

In SCs expressing both CD63-GFP and Dpp-RFP, Dpp was found to be inside CD63 positive SVs (Figure 5.11D). In conclusion, Dpp-GFP is trafficked to Rab11- and ANCE-positive DCG compartments.

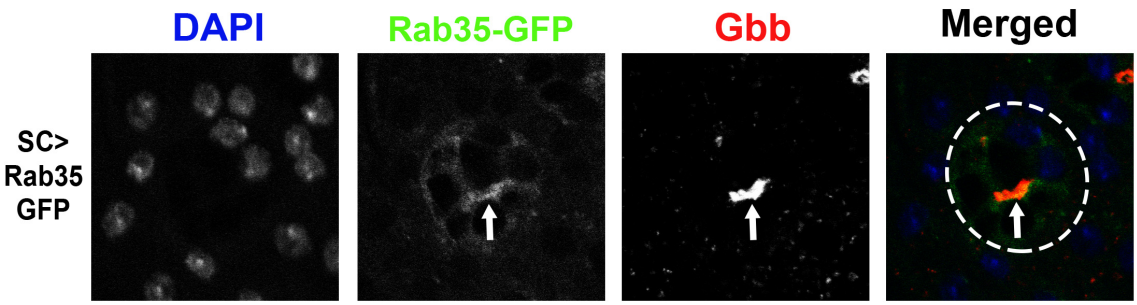


Figure 5.10 Gbb localises to Rab35 compartments.

3-day-old SCs expressing Rab35-GFP (green) and stained with an antibody raised against Gbb (red). Notice that Gbb co-localises with Rab35-GFP (arrow). Scale bar is 10 μm.

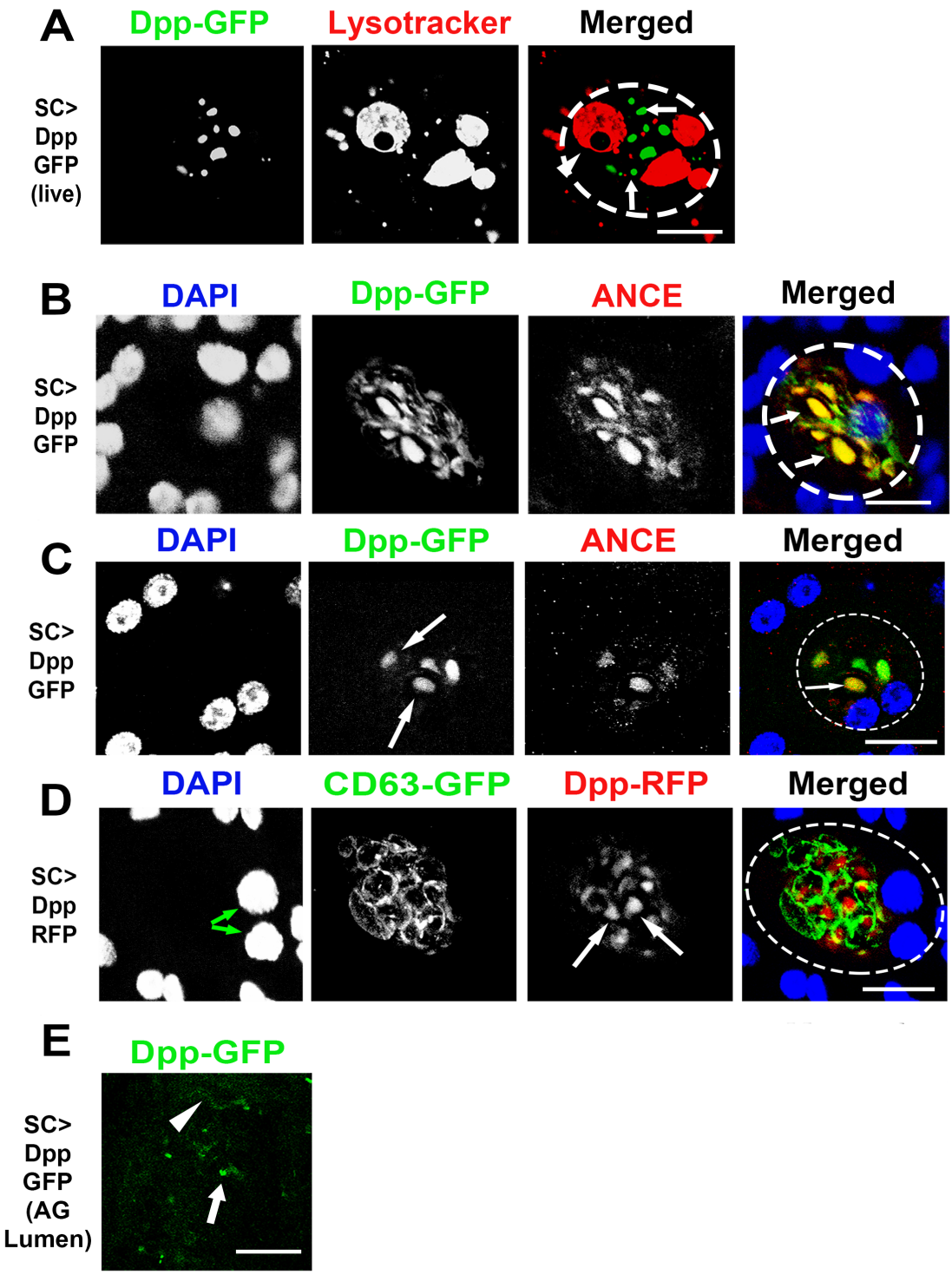

A
Dpp-GFP
Lysotracker
Merged
SC>
Dpp
GFP
(live)
B
DAPI
Dpp-GFP
ANCE
Merged
SC>
Dpp
GFP
C
DAPI
Dpp-GFP
ANCE
Merged
SC>
Dpp
GFP
D
DAPI
CD63-GFP
Dpp-RFP
Merged
SC>
Dpp
RFP
E
Dpp-GFP
SC>
Dpp
GFP
(AG
Lumen)

Figure 5.11 Dpp is localised inside dense-cored granules.

A) Live image of Dpp-GFP-expressing SC stained with Lysotracker Red to identify acidic compartments. Note that Dpp-GFP localises to spherical structures (arrows) that are distinct from acidic compartments (arrowhead). **B)** Image of fixed SC, stained with anti-ANCE antibody (red) and DAPI (blue) after 24 h pulse of Dpp-GFP expression, reveals co-localisation of GFP fluorescence with ANCE-positive DCGs (arrows). **C)** Dpp-GFP expressed in a one-hour pulse in adult males previously aged for 3 days at 25^{o}C after eclosion is chased into a number of ANCE positive compartments (arrows). **D)** Males aged for 3 days were dissected and fixed after a 24 h pulse of CD63-GFP and Dpp-RFP, and SCs imaged. Dpp-positive cores (white arrows) are observed inside CD63-GFP-positive compartments. Note the increase in SC nuclear size (green arrows) even after one day of Dpp-RFP expression. **E)** GFP-positive puncta (arrow) and filaments (arrowhead) are detected in the AG lumen when Dpp-GFP is expressed in SCs. Scale bar A-D is 10 μm and for E is 20 μm.

5.2.2.3 Glycophosphatidylinositol-anchored form of GFP mark DCGs

Since overexpressing Dpp-GFP in SCs over extended periods had a significant effect on membrane trafficking and cell growth, we investigated alternative markers to label DCG compartments in living cells. Having previously used a variety of different intracellular markers, the Wilson lab had shown that a *spitz*-GAL4 expression of UAS-regulated GFP-GPI, a form of GFP that binds to the outer leaflet of lipid bilayers via a glycophosphatidylinositol (GPI) anchor, is also present on the limiting membrane of DCG compartments and concentrated inside DCGs (L. Corrigan, DPhil thesis; M. Wainwright, B. Kroeger and F. Castellanos, pers. comm.).

To verify that GFP-GPI localises to the cores of DCGs, I co-stained GFP-GPI-expressing SCs with ANCE. This revealed that both proteins co-localise inside DCG compartments (Figure 5.12), highlighting that GFP-GPI is a good marker for studying DCG regulation.

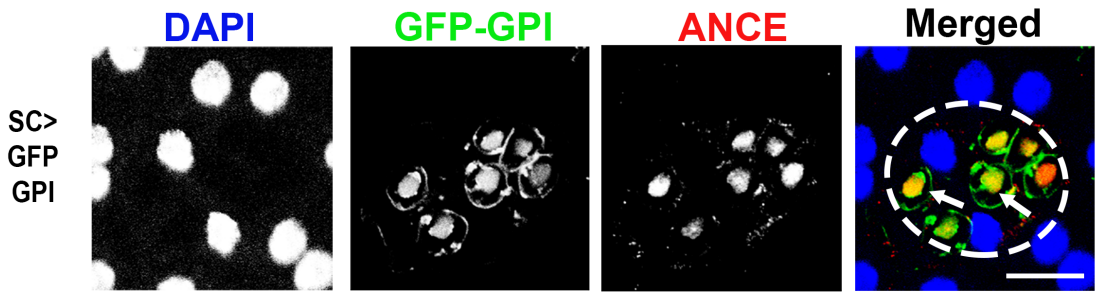


Figure 5.12 GPI-GFP marks dense-cored granules.

Fixed 6-day-old SC expressing GFP-GPI and stained with anti-ANCE (red) and DAPI (blue), showing co-localisation of ANCE and GFP in DCGs (arrows).

5.2.2.4 Driver specific effects on SC expression

We found it difficult to make a fly line containing both UAS-*GFP-GPI* and *dsx*-GAL4, and therefore we combined the GFP-GPI transgene with a ubiquitously expressed GAL80^{ts} construct and *spitz*-GAL4 (*spi*-GAL4), which drives GAL4 expression strongly and specifically in SCs of the AG.

By taking this approach, I was therefore employing a third SC GAL4 driver to study gene function in SCs. *dsx*-GAL4 had been used by me and others to drive CD63-GFP expression and highlight intracellular compartments (Corrigan et al., 2014), while esgF/O^{ts} flies were used for growth analysis (Leiblich et al., 2012), and now *spitz*-GAL4>UAS-*GFP-GPI* males were being taken to mark DCGs and study their trafficking in SCs. Although this approach had the advantage of reducing the likelihood that observed phenotypes were not merely resulting from GAL4 expression in another cell type within the male, it did raise the issue of whether the different drivers were producing similar levels of transgene expression in SCs.

To test this, I overexpressed selected transgenes using all three drivers and measured SC nuclear size. *spi*-GAL4 induced similar nuclear growth phenotypes to *dsx*-GAL4 and esgF/O^{ts} when combined with UAS-*Dad* and UAS-*Tkv^{ACT}* constructs (Figure 5.13A). It also has a similar effect to *dsx*-GAL4 on largest MVBL size when combined with these regulators of BMP signalling (Figure 5.13B). These data indicate that *spi*-GAL4 promotes UAS-dependent gene expression at roughly the same level as the other two drivers.

I also explored the effects of GFP-GPI overexpression in SCs. In virgin 3-day-old males, GFP-GPI expressed under *spi*-GAL4 control from eclosion onwards marked the same number of DCGs as ANCE in control flies and as Rab11-YFP in *tub-Rab11*-

YFP males (Figure 5.13C). Furthermore, GFP-GPI overexpression with *spi*-GAL4 did not significantly affect SC nuclear growth or MVBL numbers over the first six days of adulthood compared to other genotypes (Figure 5.13D, F). However, it did increase the size of the largest MVBL when compared to SCs from w^{1118} control males, albeit to a lesser extent than CD63-GFP overexpression (Figure 5.13E). Interestingly, even the esgF/O^{ts} line, which does not express a membrane-targeted version of GFP increased largest MVBL size, but the not other properties of SCs like nuclear growth. Aside from the change in MVBL size, I conclude that the *spi*-GAL4 UAS-*GFP-GPI* reporter line has no obvious effect on normal SC biology, even after 6 days of GAL4 induction in adults.

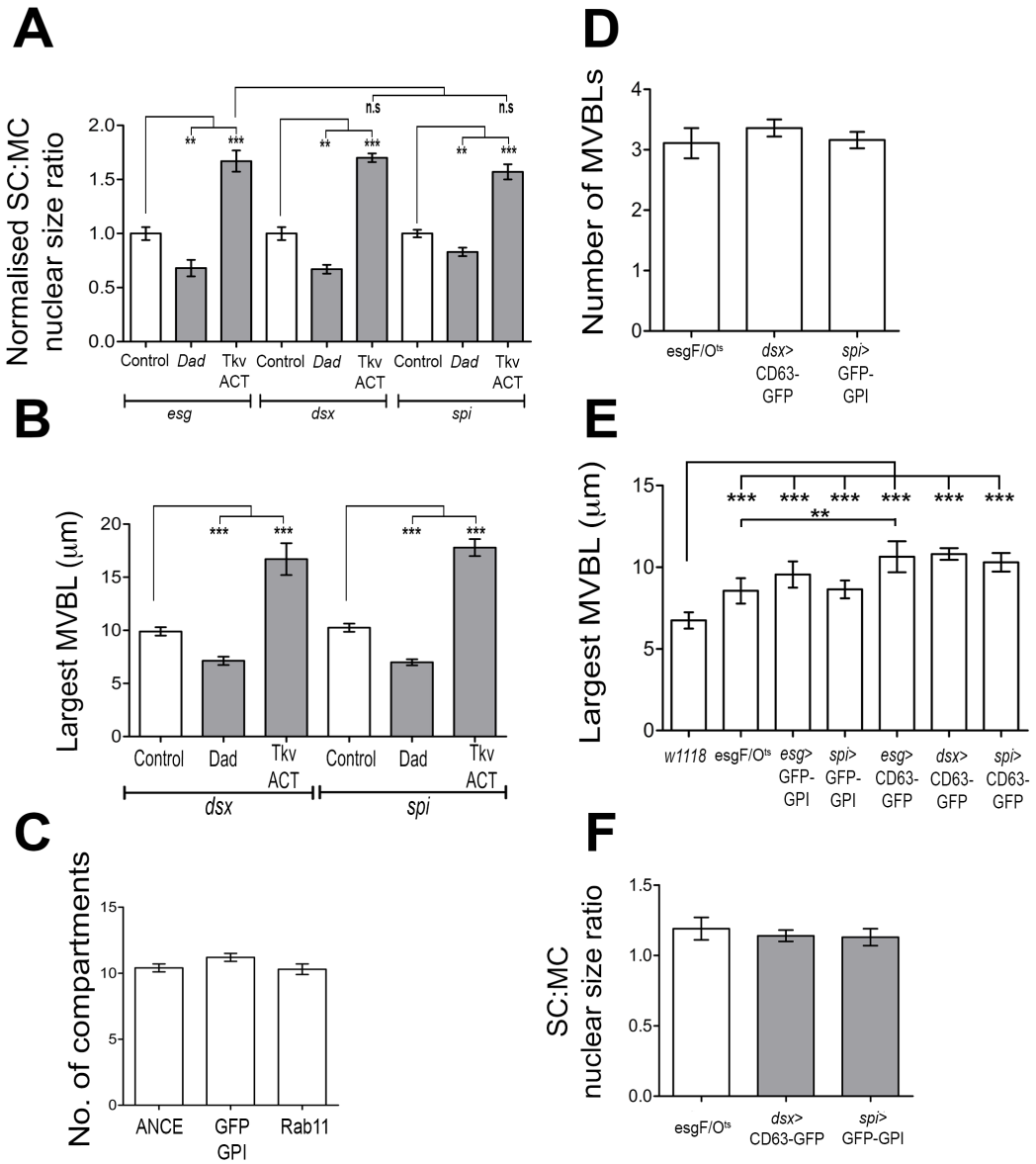

A
Normalised SC:MC nuclear size ratio
2.0
1.5
1.0
0.5
0.0
n.s
n.s
**
***
Control
Dad
Tkv ACT
esg
dsx
spi
B
Largest MVBL (μm)
20
15
10
5
0
Control
Dad
Tkv ACT
dsx
spi
C
No. of compartments
15
10
5
0
ANCE
GFP GPI
Rab11
D
Number of MVBLs
4
3
2
1
0
esgF/O^ts
dsx> CD63-GFP
spi> GFP-GPI
E
Largest MVBL (μm)
15
10
5
0
w1118
esgF/O^ts
esg> GFP-GPI
spi> GFP-GPI
esg> CD63-GFP
dsx> CD63-GFP
spi> CD63-GFP
F
SC:MC nuclear size ratio
1.5
1.0
0.5
0.0
esgF/O^ts
dsx> CD63-GFP
spi> GFP-GPI

Figure 5.13 SC GAL4 drivers drive expression of UAS construct at similar levels.

A) Driving expression of Dad and Tkv^{ACT} in adult SCs for 6 days with esgF/O^{ts}, *dsx*-GAL4 and *spi*-GAL4 produces similar effects on SC nuclear growth. **B)** Expressing Dad and Tkv^{ACT} in SCs using either the *dsx*-GAL4 or *spi*-GAL4 driver produces a similar effect on the size of the largest MVBL. **C)** Bar chart shows number of large compartments per cell labelled by anti-ANCE, GFP-GPI *w; spi-GAL4 tub-GAL80^{ts} UAS-GFP-GPI* line) or Rab11-YFP (*tub-Rab11-YFP* line). Counts were made in independent experiments using 3-day-old virgin males and do not differ significantly. **D)** The number of MVBLs per SCs was counted in 6-day-old flies expressing either esgF/O^{ts}, *dsx*-GAL4 or *spi*-GAL4, showing no significant change. **E)** The diameter of the largest MVBL in SCs from 6-day-old males is increased compared to wild type cells using *spi-GAL4,* esgF/O^{ts} *to drive UAS-GFP-GPI* expression and in esgF/O^{ts}, *dsx*-GAL4*, spi*-GAL4 driving *UAS-CD63-GFP* expression*.* **F)** The esgF/O^{ts}, *dsx*-GAL4 UAS-*CD63-GFP* and *spi*-GAL4 UAS-*GFP-GPI* lines all produce SCs with equivalent nuclear size when expression is induced for 6 days immediately after eclosion. Kruskal-Wallis test, n=10.

5.2.2.5 CD63-GFP expression induces formation of DCGs

In undertaking this analysis, I noticed that in CD63-GFP-expressing SCs, the total number of SVs was much greater than the number of DCG compartments in GFP-GPI-expressing cells, and that the former compartments appeared smaller than the latter. To determine if CD63-GFP overexpression changes DCG numbers, we co-expressed this transgene with GFP-GPI. This combination increased the number of GFP-GPI-positive DCGs in SCs from 6-day-old males by about 50% (Figure 5.14 B, C), suggesting that although there are no obvious defects in compartment identity in CD63-GFP-overexpressing SCs, the number of large non-acidic compartments is increased. This perhaps reflects an increased rate of trafficking through the secretory and endolysosomal systems. However, in these SCs there were still compartments that were not acidic and GFP-GPI-negative, suggesting that there is a population of non-acidic SVs that do not have dense core granules and whose Rab signature is yet to be determined.

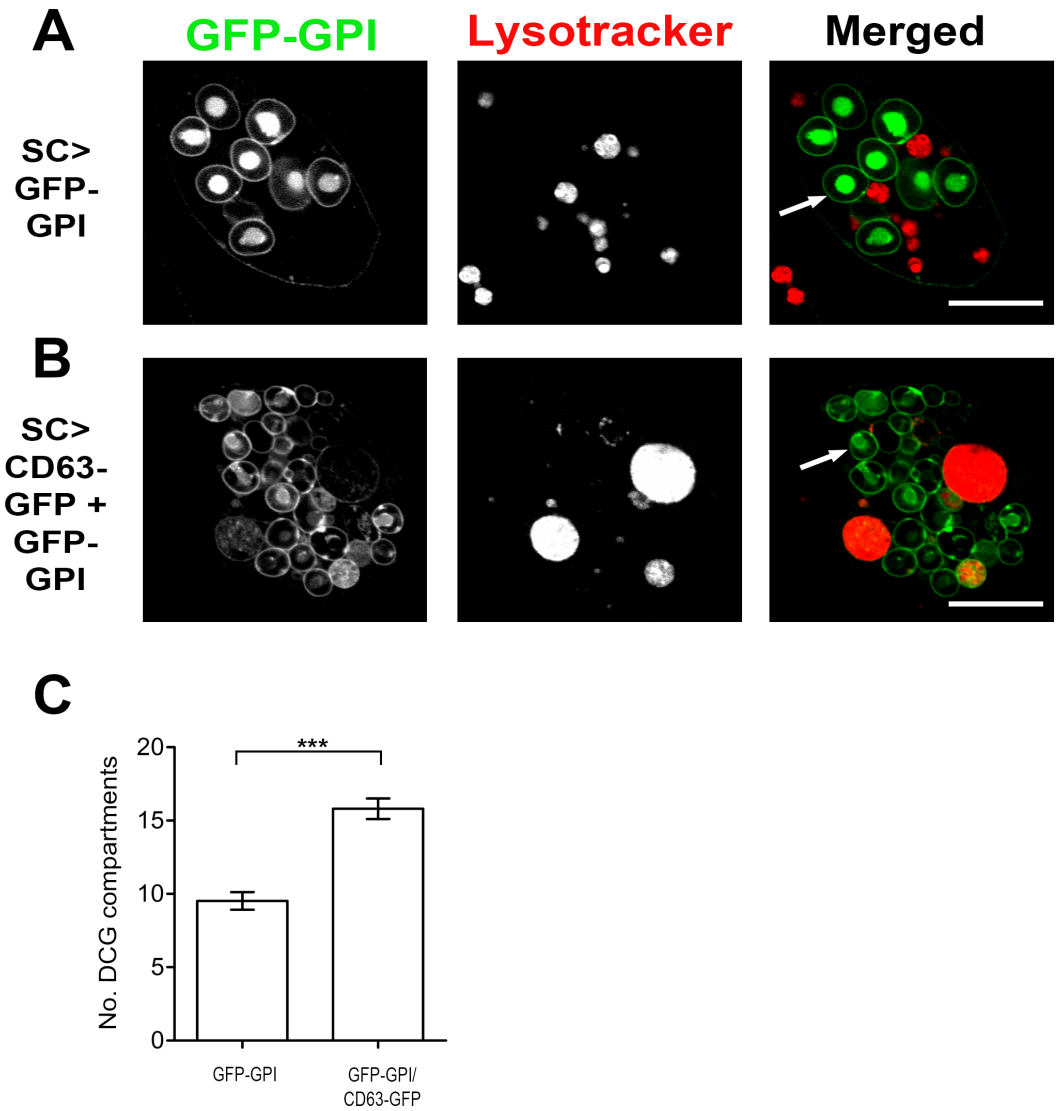


Figure 5.14 CD63-GFP expression induces formation of dense-cored compartments.

SCs from 6-day-old *spi*-GAL4 UAS-*GFP-GPI* **(A)** and *spi*-GAL4 UAS-*GFP-GPI* UAS-*CD63-GFP* **(B)** males stained with Lysotracker Red to mark acidic compartments. **C)** Such co-expression of CD63-GFP with GFP-GPI for 6 days following eclosion produces SCs with increased numbers of GFP-GPI-positive DCG compartments compared to controls. ***P<0.001, Mann-Whitney *U* test, n=10. Scale bar is 10 µm.

5.2.3 Mating-dependent DCG release

5.2.3.1 BMP signalling controls DCG numbers

I have already shown BMP signalling controls the number of CD63-positive SVs. To test more directly whether BMP signalling controls the number of DCGs, which carry Dpp, the GFP-GPI marker was used, which unlike CD63-GFP, does not noticeably affect DCG numbers in SCs when overexpressed.

Inhibiting the BMP pathway by knockdown of *dpp*, BMP receptors, *Mad* or *Med*, or by overexpression of *Dad* in adult SCs reduced the number of DCGs by about 20%, except in the case of *sax*, which also has a unique effect on SV number (Figure 5.15A, B, C). Similar results were observed when BMP receptors and *Med* and *Mad* were knocked down (Figure, 5.15C). These results suggest that BMP signalling controls the biogenesis of DCG compartments.

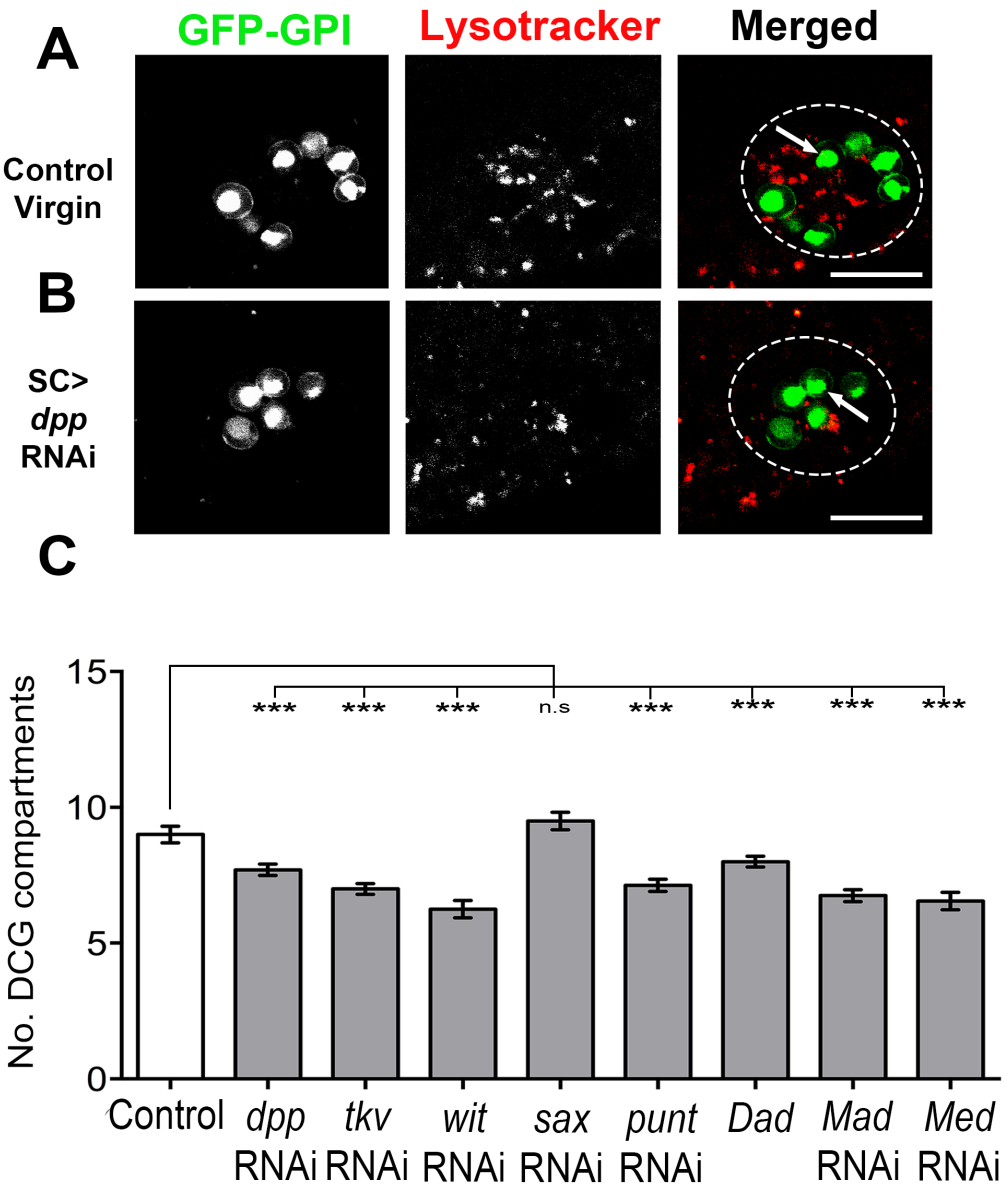


Figure 5.15 BMP signalling regulates dense-core granule numbers.

Single z-plane images of SCs from 6-day-old virgin males labelled with GFP-GPI, either co-expressing **(B)** or not expressing *dpp*-RNAi **(A)**. Reducing Dpp signalling decreases the number of labelled DCGs (arrow). **C)** Graph showing that the number of GFP-GPI-labelled DCGs in SCs from 6-day-old *w; spi-GAL4 tub-GAL80^{ts} UAS-GFP-GPI* virgin males is reduced when BMP signalling components other than *sax* are knocked down post-eclosion. ***P<0.001, Kruskal-Wallis test, n=10. Scale bar is 10 µm.

5.2.3.2 Mating triggers release of DCGs

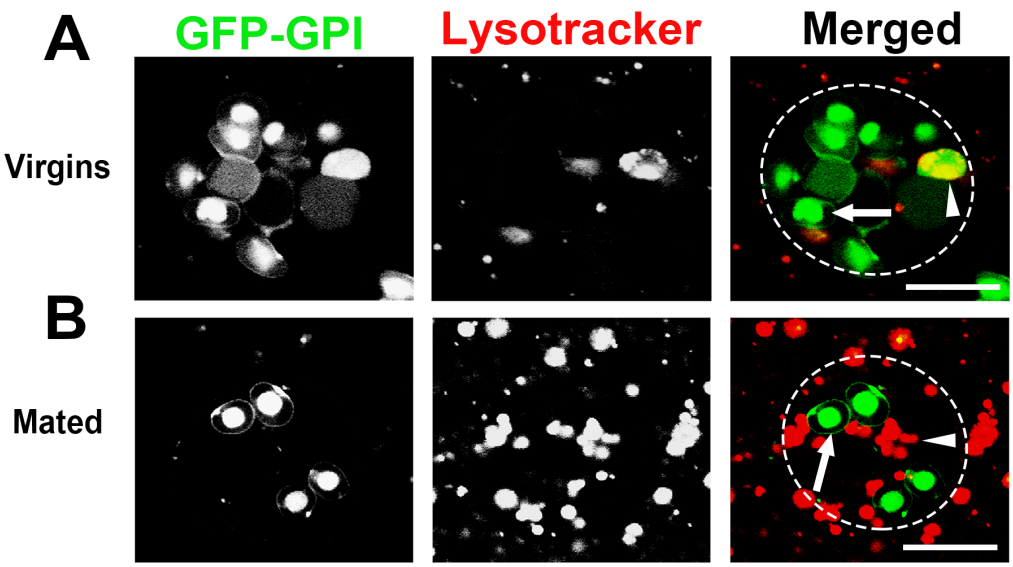
One important role for regulated secretion is to respond to physiological requirements. We hypothesised that during mating, SCs might release more DCGs to replenish AG luminal contents transferred to females. To test this, I imaged GFP-GPI-expressing SCs of 6-day-old males immediately after a single mating. Interestingly, roughly four GFP-positive DCG compartments were lost (Figure 5.16B, C), indicating that DCGs are secreted during mating.

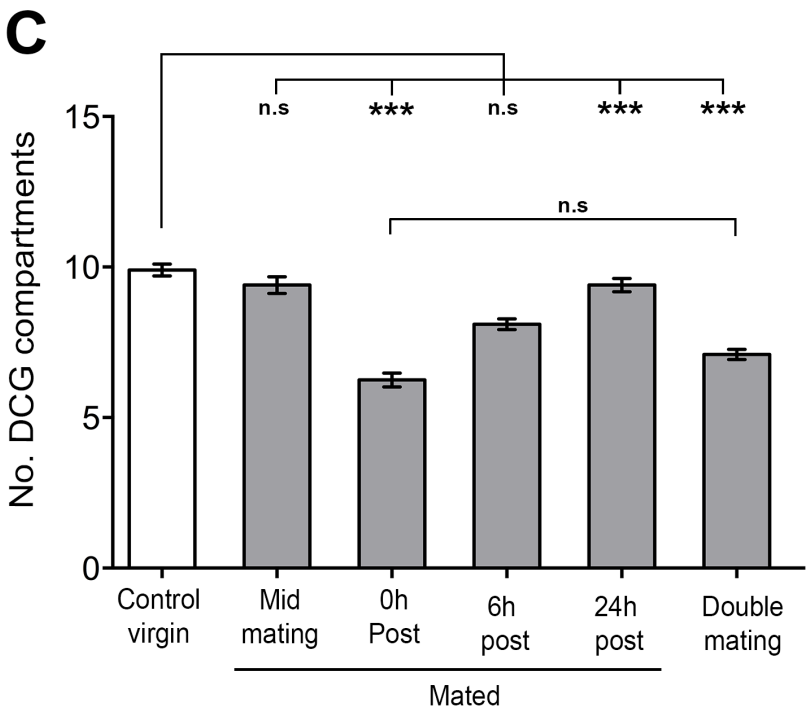
SCs in theory should have a mechanism for replenishing the compartments secreted during mating as rapidly as possible to prepare for subsequent matings. To investigate this, I mated males once and dissected them at specific time-points after this event. Approximately two DCGs were replenished within 6 h and by 24 h, the original number of DCGs was restored (Figure 5.16C).

To test if males are capable of releasing more than four DCG compartments per mating, males where mated twice within a 2 h period. Interestingly, I did not observe a further reduction in DCG numbers compared to singly mated males (Figure 5.16C), indicating that the DCGs that are left over after the first mating cannot be secreted, perhaps because they are immature. Previous reports suggest that AG luminal contents are only transferred to females during the second half of the ~20 min mating process. Males separated after only 8 minutes of mating did not show a significant reduction in GFP-GPI-positive DCGs (Figure 5.16C), suggesting that secretion coincides with transfer of AG luminal content to females.

When males mate, part of the AG luminal content is transferred to females (Corrigan et al., 2014). To test if SC expressed GFP-GPI is transferred to females, I performed Western blots (in collaboration with Sumeth Perera) to analyse proteins from

reproductive tracts of females mated with males expressing GFP-GPI in SCs. An anti-GFP antibody produced a specific signal of the same size as GFP-GPI in female reproductive tract lysates only when mated with males expressing this transgene (Figure 5.16D). Therefore, consistent with previous findings using the DCG marker ANCE (Corrigan et al., 2014), the DCG-localised GFP-GPI is transferred to females during mating. Since Dpp is also contained in DCGs, it is plausible that it may also be transferred to females during mating. It would be extremely interesting to test if male-donated Dpp can stimulate BMP signalling in females.


A
GFP-GPI
Lysotracker
Merged
Virgins
B
Mated


C
n.s
***
n.s
***
***
n.s
No. DCG compartments
15
10
5
0
Control virgin
Mid mating
0h Post
6h post
24h post
Double mating
Mated

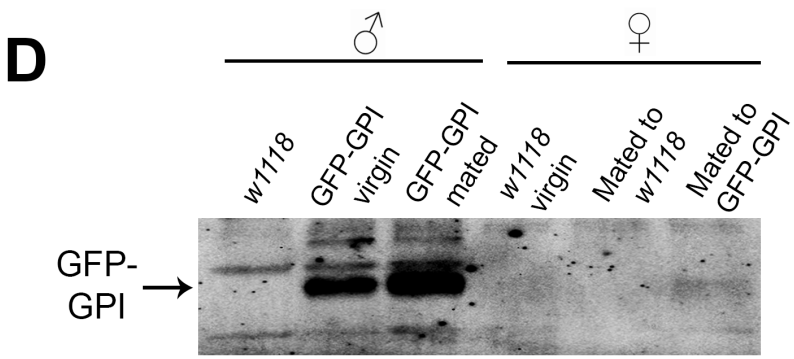

D
♂
♀
w1118
GFP-GPI virgin
GFP-GPI mated
w1118 virgin
Mated to w1118
Mated to GFP-GPI
GFP-GPI

Figure 5.16 Mating stimulates the release of dense-cored granules.

Immediately after mating, living 6-day-old SCs have less GFP-GPI-labelled DCGs **(B)** than virgins **(A).** Image shows a single z-plane of gland stained with Lysotracker Red; not all compartments are in the focal plane. **C)** Graph shows number of GFP-GPI-positive DCG compartments in virgin and mated males (Double is twice mated in 2 h), and at different times after single mating in control SCs. **D)** Western blot probed with anti-GFP antibody, performed in collaboration with Sumeth Perera . AG extracts from either w^{1118} males, or virgin and mated *w; spi-GAL4 tub-GAL80^{ts} UAS-GFP-GPI* males were analysed. Females were either virgins or mated to w^{1118} males or SC>GFP-GPI-expressing males. ***P<0.001, Kruskal-Wallis test, n=10. Scale bar is 10 μm.

5.2.3.3 Readout for BMP activation

Because DCG compartments contain the Dpp ligand, we wondered if mating-dependent secretion of these compartments is coupled with the activation of BMP signalling in SCs. Activation of BMP signalling leads to phosphorylation of cytosolic SMAD proteins, which then translocate to the nucleus to regulate gene transcription. Nuclear staining with a phospho-specific Mad antibody is a commonly used readout for BMP pathway activity in flies (Cao, 2006).

To test if pMad is a reliable readout for BMP signalling, I stained control SCs and SCs overexpressing either Dpp-GFP or Tkv^{ACT} in SCs with anti-pMAD. In wild type AGs, about 9% of SCs were stained with the anti-pMad antibody in 3-day-old virgin males; this increased to 21% in 6-day-old flies, suggesting that aging increases BMP signalling in SCs, presumably as a result of increased consituative secretion. Both Dpp-GFP or Tkv^{ACT} induced detectable nuclear pMad staining in all SCs, while no nuclear pMad staining was observed in SCs overexpressing Dad or *Dpp* RNAi (Figure 5.17A, B, C, D, F). Moreover, pMAD signal was also severely reduced when BMP receptors or downstream Smads were silenced (Figure 5.17F). Interestingly, in mosaic clones of SCs expressing Dpp-GFP, pMAD was only seen in those cells expressing this transgene, providing good evidence that Dpp is able to induce BMP activation (Figure 5.17E). Additionally, MC-specific expression of Dpp had no effect on MCs themselves, but increased pMad levels in SCs (Redhai *et al*., 2016). In conclusion, pMAD staining faithfully marks BMP activity and can be used as a readout.

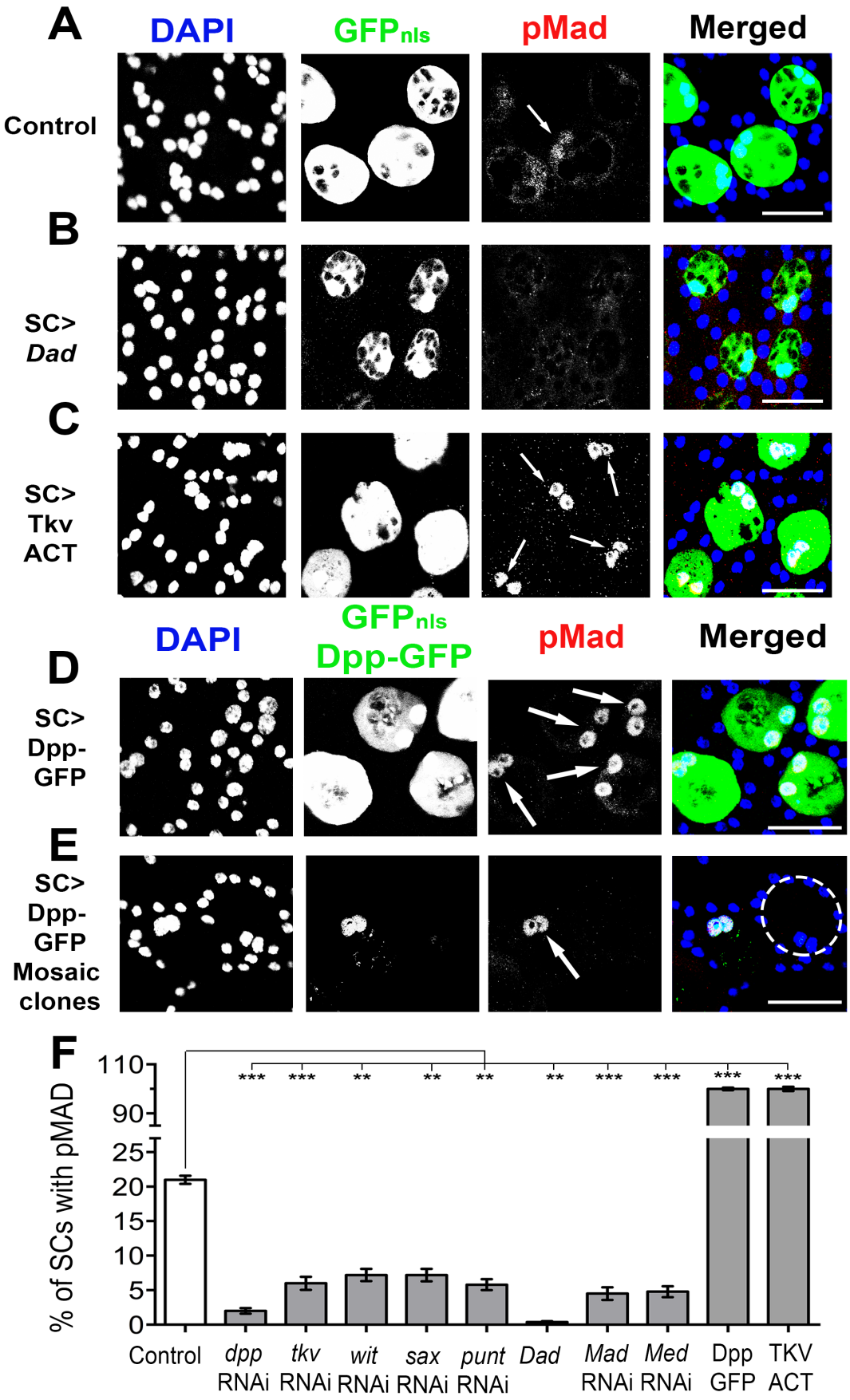

A
DAPI
GFPnls
pMad
Merged
Control
B
SC>
Dad
C
SC>
Tkv
ACT
DAPI
GFPnls
Dpp-GFP
pMad
Merged
D
SC>
Dpp-
GFP
E
SC>
Dpp-
GFP
Mosaic
clones
F
% of SCs with pMAD
110
90
25
20
15
10
5
0
***
***
**
**
**
**
***
***
***
***
Control
dpp RNAi
tkv RNAi
wit RNAi
sax RNAi
punt RNAi
Dad
Mad RNAi
Med RNAi
Dpp GFP
TKV ACT

Figure 5.17 pMAD is a reliable readout for BMP activation.

A-C) SCs from 6-day-old virgin males expressing either Dad **(B),** activated Tkv **(C)** or no BMP signalling regulator **(A)** stained with pMad antibody (arrow), revealing different BMP signalling activities. **D)** 6-day-old SCs expressing Dpp-GFP from eclosion or in mosaic clones **(E)** and stained with pMAD antibody. Notice that in mosaic clones pMAD (arrow) is only seen in non-expressing cells (dashed circle). **F)** Graph showing the proportion of SCs that contain pMad-positive nuclei in 6-day-old esgF/O^{ts} virgin males expressing RNAi against different BMP signalling components after eclosion. ***P<0.001, Kruskal-Wallis test, n=10. Scale bar is 20 μm.

5.2.3.4 Mating-dependent DCG secretion is coupled to BMP activation

Since mating stimulates the release of DCG, I tested if mating flies activates BMP signalling in SCs via secreting DCG-containing Dpp. To test this hypothesis, control 3- and 6-day-old esgF/O^{ts} males were mated and their AGs immediately dissected and stained for pMad.

As discussed above, in virgin flies dissected at 6 days, approximately 20% of SCs had a pMAD signal, presumably because of constitutive DCG secretion (Figure 5.18A, C). Although I observed no significant change in nuclear pMad staining between virgins and males separated 8 min into mating (Figure 5.18C), there was a significant increase in the number of pMad-positive SCs immediately after mating to approximately 50% in flies dissected at 6 days (Figure 5.18B). Similar results were obtained for experiments done with 3-day-old flies (Redhai et al 2016). This suggests that Dpp packaged in DCGs can stimulate mating-dependent BMP signalling.

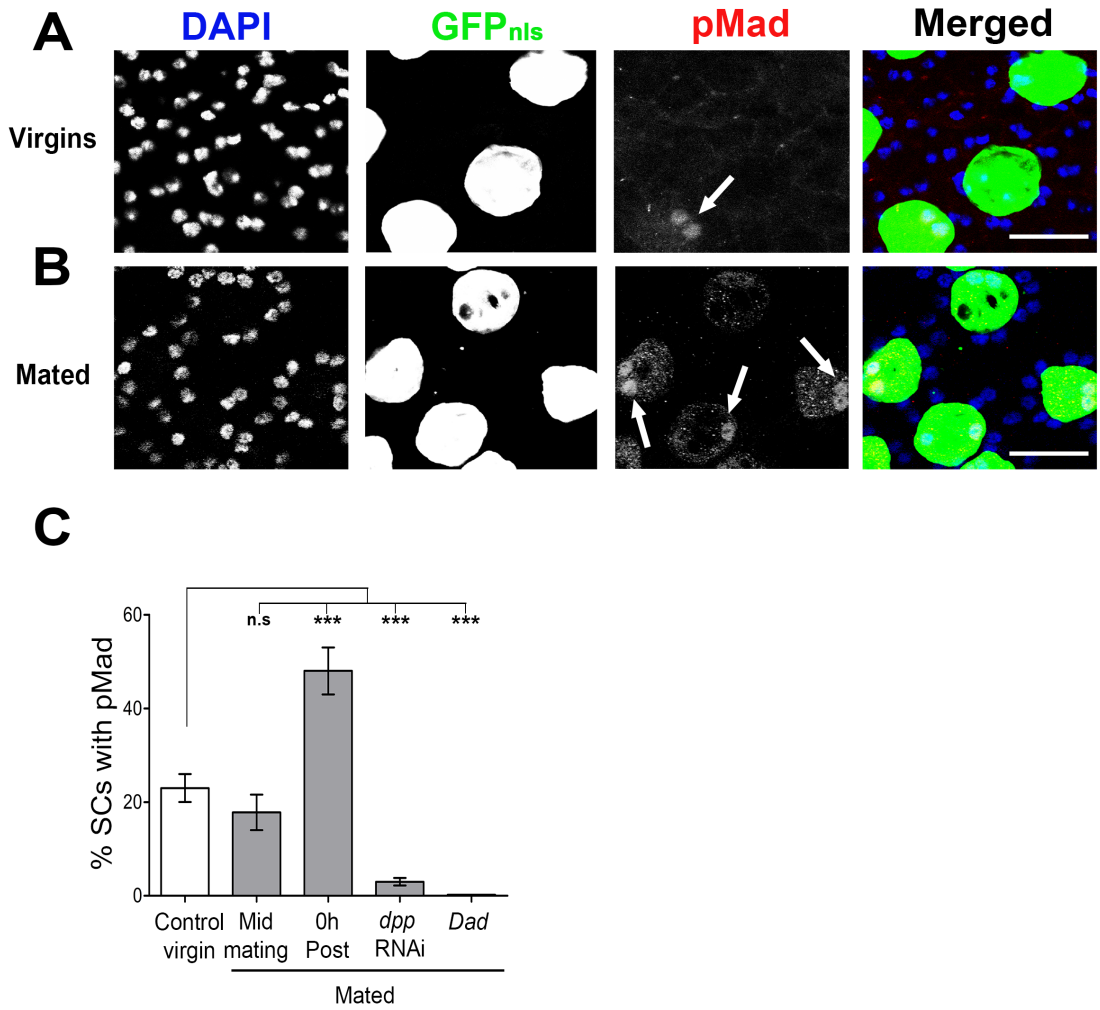


Figure 5.18 Mating results in BMP activation in SCs.

SCs from 6-day-old esgF/O^{ts} virgin males **(A)** and from males immediately after mating **(B)** were fixed and stained with an anti-pMad antibody (red) and DAPI (blue), revealing that the proportion of SCs with detectable nuclear pMad is higher in mated animals. **C)** Graph shows proportion of SCs with nuclear pMad in 6-day-old virgin, and mated males (dissected 8 min into mating [Mid] and immediately after mating), and mated males expressing *dpp*-RNAi and Dad in SCs from eclosion onwards, the latter was performed in collaboration with Josephine Hellberg. ***P<0.001, Kruskal-Wallis test, n=10. Scale bar is 20 μm.

5.2.3.5 BMP signalling control mating-dependent DCG secretion

As mentioned previously, BMP signalling is required for normal biogenesis of DCGs and for mating-dependent activation of pMAD signalling. To test if BMP signalling is also involved in mating-dependent DCG secretion, I imaged the AGs of flies expressing either Dpp RNAi or overexpressing Dad immediately after mating.

There was no change observed in DCG numbers between mated and virgin flies when BMP signalling was inhibited by *dpp* knockdown or Dad overexpression (Figure 5.19), suggesting that DCG release is blocked, perhaps because the compartments have failed to mature normally. Indeed, when flies expressing these two constructs were mated, the number of pMAD-positive SCs was drastically lower than mated controls (Figure 5.18C). In conclusion, BMP signalling is needed for DCG release and autocrine BMP activation during mating.

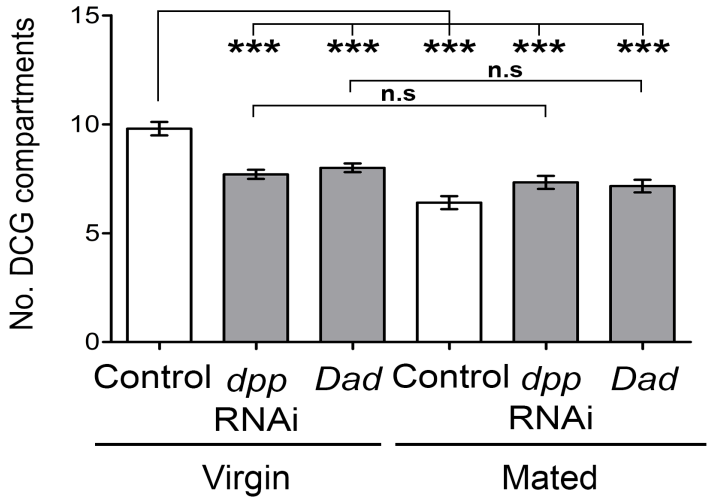


Figure 5.19 BMP signalling is involved in the release of dense-cored compartments.

Graph showing number of GFP-GPI-positive DCGs in SCs from either 6-day-old virgin or mated control flies or flies in which BMP signalling is inhibited. There is no decrease in DCG number in SCs expressing either *dpp*-RNAi or *Dad* after mating. ***P<0.001, Kruskal-Wallis test, n=10.

5.2.3.6 SNARE-mediated fusion events control DCG secretion

SNARE proteins are major regulators of DCG compartment fusion to the plasma membrane in other cell types. In the *Drosophila* salivary gland, the granule-associated SNARE, SNAP24, a homologue of mammalian SNAP25, is involved in glue granule release (Burgess et al., 2012). To test if SNAP24 has a role in controlling DCG secretion from SCs, I expressed two RNAi targeting *Snap24* in adult SCs. This significantly increased the number of GFP-GPI-positive DCGs (Figure 5.20A), suggesting that SNARE-mediated fusion events are required for normal DCG release in virgin males.

To test if SNAP24 is also involved in mating-dependent DCG secretion, *Snap24* RNAi-expressing flies were mated and dissected immediately after. Interestingly, the difference in DCG numbers was found between virgin males and mated males expressing *Snap24* RNAi (Figure 5.20C), suggesting that DCGs are secreted during mating in a SNAP24-dependent process.

If SNAP24 prevents DCG release both in virgin and mated flies, one prediction would be that SC growth, which is dependent on BMP signalling, would be stunted. Indeed, when measuring the nuclear size of SCs expressing *Snap24* RNAi in virgin flies, I observed a significant decrease when compared to controls (Figure 4.30). Moreover, staining *Snap24* RNAi-expressing SCs after mating revealed a decrease in pMAD signal compared to mated control flies (Figure 5.20B), suggesting that Snap24-mediated fusion events are necessary for activation of mating-dependent DCG secretion and SC growth.

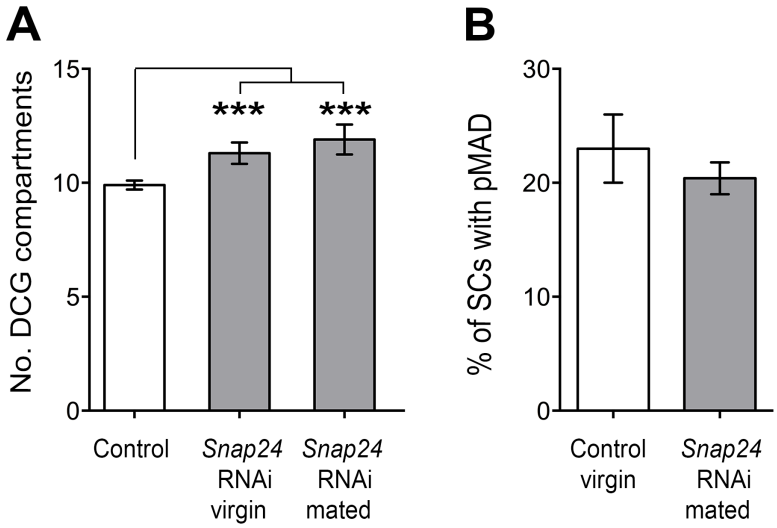


Figure 5.20 Snap24 regulated mating-dependent dense-core granule secretion.

A) SCs expressing GFP-GPI with no additional transgene (control) or *Snap24* RNAi in virgin and mated flies. Note that the DCG numbers increase in virgin males expressing *Snap24* RNAi when compared to virgin control but no change is observed when comparing to mated flies expressing *Snap24* RNAi. **B)** The percentage of pMAD positive SCs does not change in mated flies expressing *Snap24* compared to virgin controls. ***P<0.001, Mann-Whitney *U* test, n=10.

5.2.4 BMP regulation of DCG replenishment

5.2.4.1 Mating stimulates the formation of DCGs

As mentioned previously, the DCG compartments released during mating are fully replenished after 24 h, with one new DCG being formed every 6 h. One explanation for the rapid replenishment of DCGs after mating is that BMP signalling upregulates biosynthesis of new DCG compartments. To test this, I performed a series of time-limited experiments using pulses of GFP-GPI expression. A 16 h pulse of GFP-GPI labelled 3 ± 0.1 DCG compartments in virgin males (Figure 5.21A, D), consistent with a biogenesis rate of about one DCG compartment per 6 hours. Interestingly, if mating ensued after the 16 h expression of GFP-GPI, the number of DCG compartments did not significantly change from virgin counts, indicating that these early labelled compartments are not capable of undergoing secretion (Figure 5.21C). When the 16 h GFP-GPI pulse occurred immediately after mating, there was a significant increase in the number of labelled DCGs to 4.1 +/- 0.1, supporting a model whereby mating accelerates formation of new DCGs (Figure 5.21B, D).

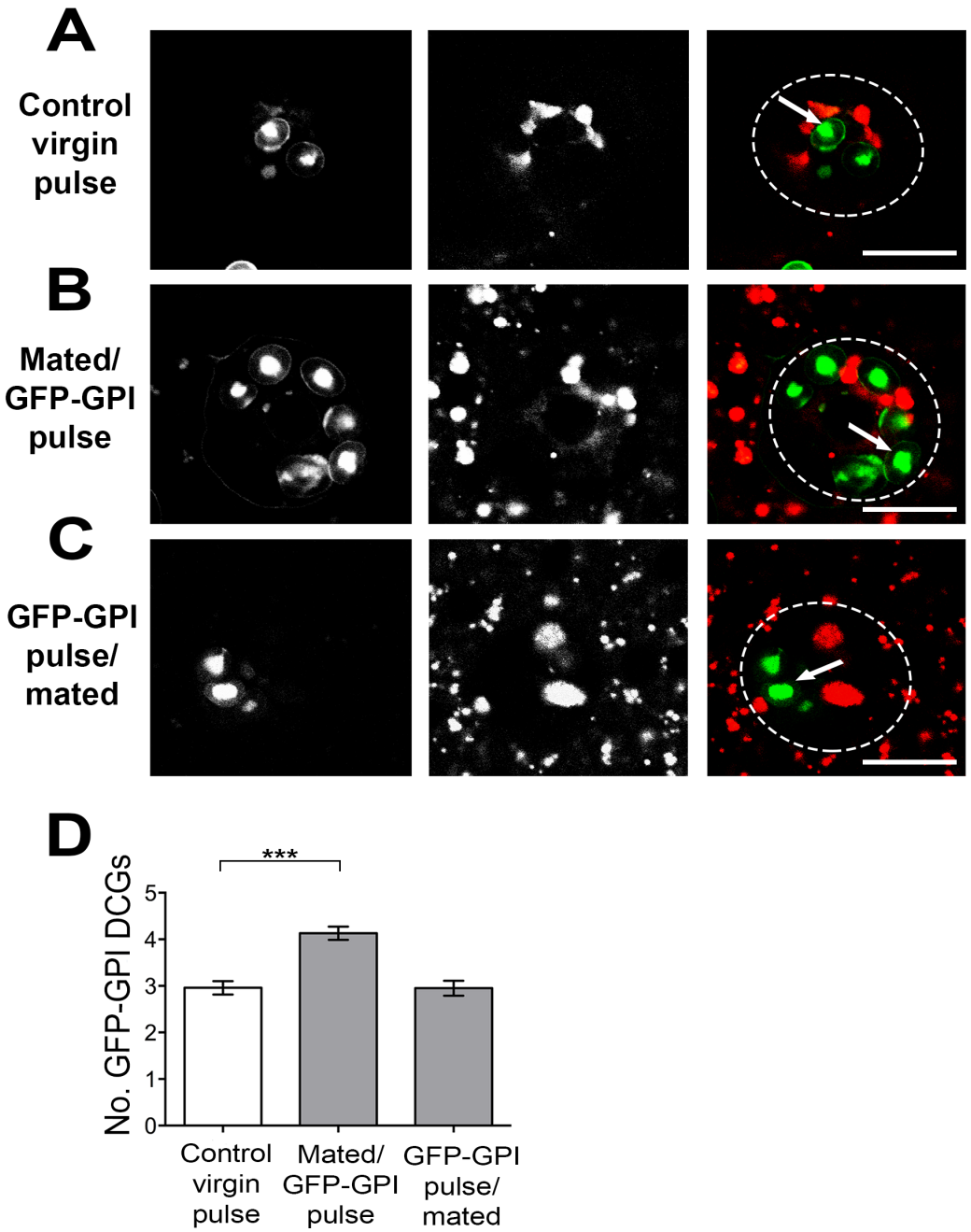


Figure 5.21 Mating accelerates the formation of dense-core granules.

6-day-old males were shifted to 28°C to induce GFP-GPI expression for 16 hrs in virgins **(A)** or immediately after **(B)** or before **(C)** mating. Their AGs were dissected and imaged; each image is from a single z-plane. **D)** Graph showing DCG number after a 16 h pulse of GFP-GPI in SCs from 6-day-old males, as in A-C above. The *w; spi-GAL4 tub-GAL80^{ts} UAS-GFP-GPI* flies were used to generate data in **(D)**. ***P<0.001, Kruskal-Wallis test, n=10. Scale bar is 10 µm.

5.2.4.2 Immature DCGs are not secreted during mating

The results mentioned above can be interpreted in another way in which some DCG compartments formed during the 16 h pulse are secreted in virgins, but not after mating. Interestingly, immature DCGs are typically not secreted in mammals, but must undergo a stepwise maturation process involving luminal acidification by the V-ATPase and selective removal of non-DCG proteins prior to exocytosis (Kim et al., 2006).

To test whether pulse-labelled DCG compartments could be secreted from SCs upon mating, I induced GFP-GPI for 16 h before mating, then dissected the AGs immediately after mating and counted the number of DCGs. I did not observe any decrease in the number of labelled DCG compartments, indicating that GFP-GPI is trafficked over a 16 h period to new immature compartments, which cannot be immediately secreted (Figure 5.21D). We hypothesise that pulse-labelled DCGs cannot be secreted because they have not reached full maturity. This is consistent with the previous data I presented showing that doubly mated males do not release additional DCGs (Figure 5.19).

5.2.4.3 DCG replenishment is dependent on BMP signalling

I have already shown that BMP signalling is important for DCG biogenesis and mating-dependent secretion of DCGs. To assess whether the acceleration of DCG biosynthesis after mating involved BMP signalling, I co-overexpressed Dad during a 24 h GFP-GPI pulse to test whether this might induce sufficient inhibition of signalling to affect new DCG formation (Figure 5.22A). Mating control flies 8 h after starting a 24 h GFP-GPI pulse increased DCG numbers when compared to virgins expressing GFP-GPI for the same duration (Figure 5.22C, E; 4.4 ± 0.16 DCG in virgins versus 6.2 ± 0.18 DCG in mated flies). When Dad was co-expressed with GFP-GPI in virgin flies for 24 h, the number of labelled DCGs was significantly reduced (Figure 5.22D, E),

suggesting that BMP signalling is required for biogenesis of new immature DCGs in virgin males.

When I overexpressed GFP-GPI with Dad for 8 h in SCs of males, mated these flies once and then continued the pulse for a further 16 h (24 h in total), I observed a marked decrease in the number of labelled DCGs in comparison to mated control flies (Figure 5.22E). The number of marked DCGs was slightly higher than in Dad-expressing virgins, presumably because BMP signalling is not fully inhibited by a 24 h pulse of Dad. However, the difference between mated and virgin DCG numbers in Dad-expressing versus control males was significantly reduced (Figure 5.22F), demonstrating that BMP signalling is required to drive increased biosynthesis of new DCGs after mating.

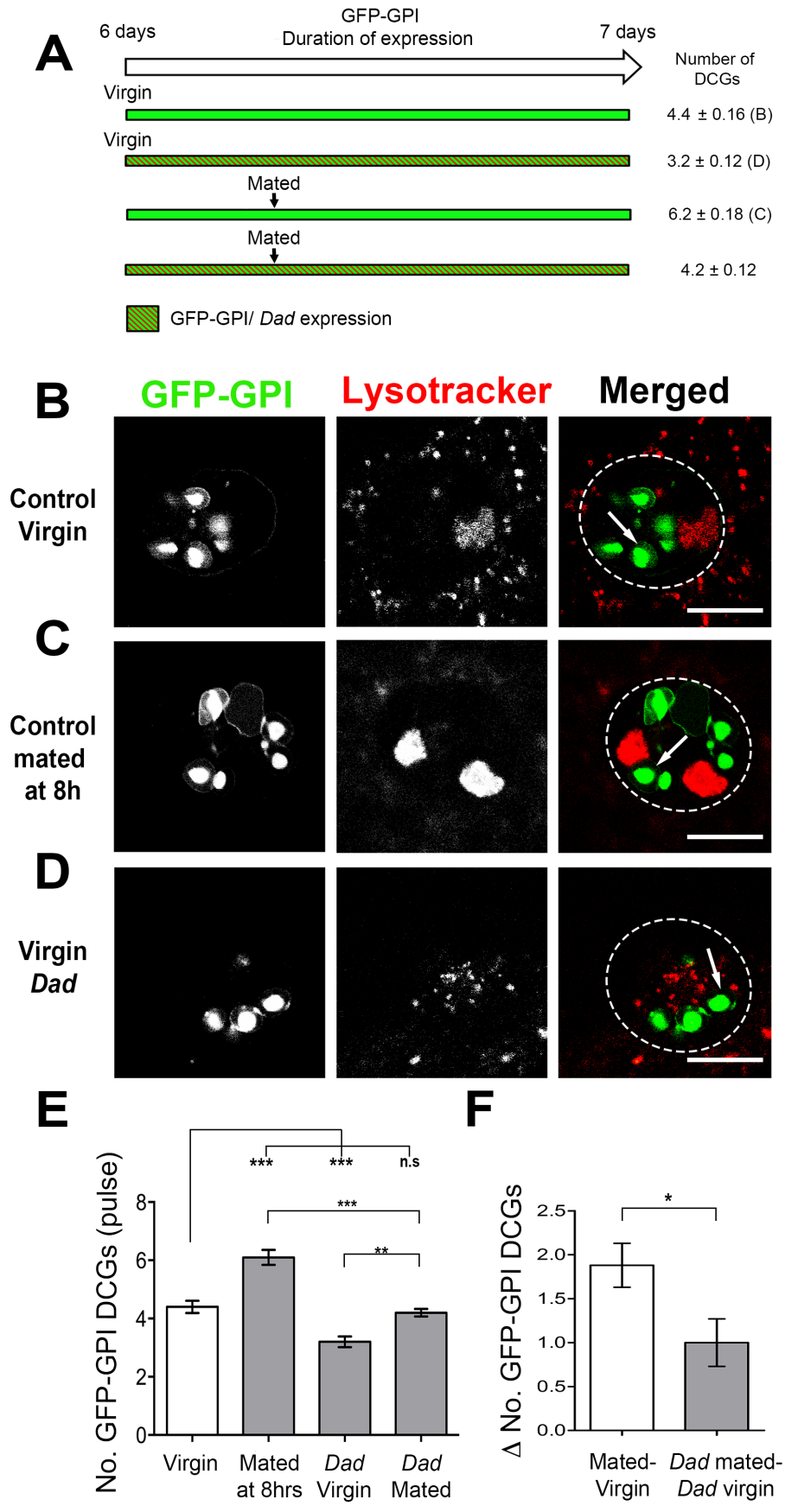

A
6 days
GFP-GPI
Duration of expression
7 days
Number of DCGs
Virgin
4.4 ± 0.16 (B)
Virgin
3.2 ± 0.12 (D)
Mated
6.2 ± 0.18 (C)
Mated
4.2 ± 0.12
GFP-GPI/ Dad expression
B
GFP-GPI
Lysotracker
Merged
Control Virgin
C
Control mated at 8h
D
Virgin Dad
E
No. GFP-GPI DCGs (pulse)
***
***
n.s
***
**
Virgin
Mated at 8hrs
Dad Virgin
Dad Mated
F
Δ No. GFP-GPI DCGs
*
Mated-Virgin
Dad mated-Dad virgin

Figure 5.22 Rapid replenishment of DCGs after mating is BMP-dependent.

A. Schematic representation of pulse-chase experiments shown in B-F, indicating the duration of GFP-GPI and *Dad* overexpression and timings of mating events. **B-D**. 6-day-old flies were shifted to 28.5^{0}C for 24 h to allow expression of GFP-GPI in virgins **(B)** or in males mated 8 h after the start of the pulse **(C)**. The number of GFP-GPI-labelled DCGs in SCs was reduced in virgin males co-expressing Dad **(D)**. **E)** Graph shows a significant increase in the number of labelled DCGs if males are mated at 8h during a 24 h GFP-GPI pulse. The number of DCGs labelled in virgin and mated males is reduced if *Dad* is co-expressed. **(F)**. The increase in labelled compartments after mating is also reduced by Dad co-expression. The *w; spi-GAL4 tub-GAL80^{ts} UAS-GFP-GPI* flies were used to generate data in **(E)**. *P<0.05, ***P<0.001, Kruskal-Wallis test, n=15. Scale bar in B-D, 10 µm.

5.3 Discussion

In my final result chapter, I provide evidence that BMP signalling is important for controlling SV trafficking, MVBL maturation, exosome secretion and growth in SCs. SCs package the BMP ligand, Dpp, inside DCGs, approximately four of which are secreted immediately during mating to activate autocrine BMP signalling. Interestingly, I show that mating flies also increases the formation of new DCG compartments in a BMP dependent process, and therefore matches elevated secretion with the increased formation of new DCGs (Figure 5.23).

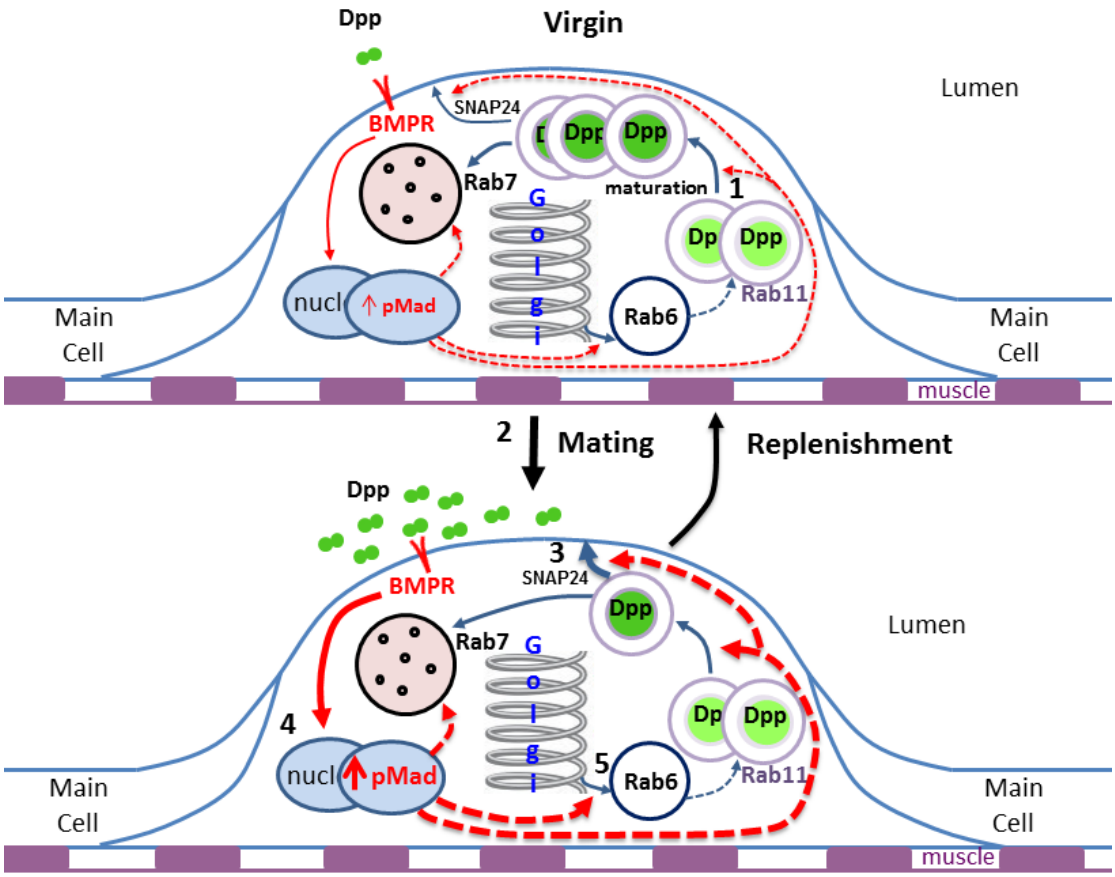


Figure 5.23 Model to explain autocrine regulation of DCG replenishment by BMP signalling in SCs.

Schematics of a single SC immediately before and after mating. **(1)** In virgin males, Dpp is trafficked to and stored in Rab11 positive DCGs, potentially via immature Rab6 compartments. Sporadic release of these DCGs activates BMP signalling, and sustains a basal level of growth, DCG biogenesis and exosome secretion. **(2)** During mating, about 4 mature DCGs are released **(3)**, resulting in an increase in BMP signalling **(4)**, primarily via an autocrine mechanism and probably in pulses. SNAP24-mediated dependent secretion is essential to elicit the activation of mating-induced BMP activation. This stimulates growth, but also increases biosynthesis of new Rab11 positive DCGs, possibly via Rab6 compartments (**5**; solid arrow), ensuring that the total number of DCGs is fully replenished within 24 h. Dashed arrows highlight other parts of the secretory/endolysosomal system that might be affected by altered BMP signalling.

5.3.2 BMP signalling controls compartment biogenesis, endolysosomal trafficking, exosome secretion and growth in SCs

Building upon previous findings by the Wilson lab, I have shown that all components of the BMP pathway are involved in maintaining SV numbers, the maturation of endolysosomal compartments, exosome secretion and growth. The compartment phenotypes induced by blocking BMP signalling are consistent with a general reduction in membrane flux through the secretory and endosomal systems in SCs, and I have shown that new DCG biogenesis is stimulated by BMP signalling.

Because multiple receptors are involved in this process, this suggests that heterodimeric BMP receptors function in a non-redundant manner in SCs. Both Type I and Type II receptors have previously been shown to act non-redundantly in other *Drosophila* cell types (Bangi and Wharton, 2006, Marmion et al., 2013). Interestingly, knockdown of different BMP receptors produce different effects; most notably *sax* RNAi did not reduce SV or DCG number in the same way as inhibiting other BMP signalling components. Indeed, Sax has previously been reported to have both positive and negative effects on BMP signalling through its different responses to Dpp and Gbb ligands (Bangi and Wharton, 2006). One possibility is that Sax is involved in specific interactions with Gbb in SCs. Indeed, to assess this, future experiments should be aimed at creating transgenic flies carrying silencing vectors against both *Sax* and *Gbb*.

Although Gbb is trafficked into Rab35-positive compartments in SCs, my knockdown analyses did not reveal a function for Gbb in SC growth, although it appears to be expressed strongly in the AG. Although the knockdown RNAi constructs have been used successfully in other cell types, I did not see a reduction in SC-specific Gbb

antibody staining in these experiments or in experiments where *gbb* was knocked down in other AG cell types (data not shown). Therefore, the source of Gbb in the AG remains unknown. Future experiments should be directed towards understanding the role of Gbb in SC BMP signalling. I speculate that unlike the growth-promoting ligand Dpp, Gbb produced in multiple AG cell types may have an antagonistic role, since overexpressing it in MCs caused a decrease in SC growth, even though this fusion protein was not internalised within SCs.

Dpp and the signalling it induces regulates SC nuclear size. Although in some *Drosophila* post-mitotic cells, like larval salivary gland cells and ovarian follicle cells, nuclear growth is achieved through endoreplication of the genome, nuclei can also grow in other organs, such as the eye, without replicating the genome (Gao and Pan, 2001). The Wilson has previously shown that bromodeoxyuridine (BrdU) does not label SCs (Leiblich et al., 2012), indicating that SC growth may not be achieved through new DNA synthesis, although the BrdU labelling technique may be insufficiently sensitive to detect low levels of endoreplication in these experiments.

A long-standing hypothesis in the Wilson lab has been trying to link the maturation status of endolysosomal compartments with SC growth and to determine whether mechanistic Target of Rapamycin Complex 1 (mTORC1) signalling, which is activated at the surface of MVBL compartments in other cell types (Betz and Hall, 2013), is involved in this process. Although I have not investigated this relationship, it is currently being tested by other members of the lab. Therefore, it remains to be seen whether defective maturation of late endosomes and lysosomes underlies the inhibition of SC growth observed after BMP signalling blockade.

5.3.3 Using different GAL4 drivers to study SC function

I have shown that adult SCs from virgin males consistently contain approximately 10 Rab11-positive DCG compartments, as well as a number of other non-acidic compartments that do not contain DCGs and whose Rab signature is yet to be established (Figure 3.14). Indeed, these other compartments can be visualised using the CD63-GFP marker, which also labels DCG compartments and MVBLs. However, analysing the expression of CD63-GFP in adult SCs for 6 days, suggests that this marker increases the number of SVs and DCG compartments, and the MVBL size. This means that the normal number of SVs in SCs remains to be accurately determined, because other markers we have employed to date do not mark all SVs.

Since I was using different GAL4 drivers to drive markers for different SC compartments, I also tested whether the strength of the driver might explain the changes induced by CD63-GFP. esgF/O^{ts}, *dsx*-GAL4 and *spi*-GAL4 all produced similar effects on SC nuclear growth, and secretory and endolysosomal trafficking when used to drive different transgenes affecting BMP signalling, suggesting that they induce comparable levels of overexpression. However, these experiments indicated that all three transgenic lines I employed to study SC cell biology increase the size of the largest lysosome-like compartment, perhaps because this compartment plays a role in degrading the proteins induced by these driver lines. Importantly, none of the driver lines appeared to alter the identity of compartments within SCs, and for the esgF/O^{ts} and *spitz*-GAL4>UAS-*GFP-GPI* lines, no other detectable differences were observed compared to wild type flies, suggesting that they are powerful tools to study the molecular genetic regulation of SC biology in the AG.

5.3.4 DCG formation and release is coupled to mating

In flies, mating lasts roughly 20 min. I have shown that approximately four DCG compartments are lost from SCs during the second half of this period. Knockdown experiments revealed that both constitutive and regulated secretion of DCGs is dependent on the SNARE protein, SNAP24, which has been shown to control regulated secretion from the fly salivary gland (Niemeyer and Schwarz, 2000). This function appears to be very broadly conserved in evolution, since the mammalian SNAP24 homologue, SNAP-25, is also implicated in insulin secretion from rat pancreatic β-cells and DCG release from other secretory cells (Nagamatsu et al., 1999).

In addition to initiating the release of DCGs, mating also accelerates the formation of new DCG compartments. This process is dependent on autocrine BMP signalling since blocking the pathway reduces the rate of new DCG biogenesis. Evidence from other systems suggests that autocrine BMP signalling may provide a general mechanism for control of DCG biogenesis rates in response to regulated secretion. For example, in the *Drosophila* neuromuscular junction, neuronal Gbb synthesis is required for normal synaptic secretion (Nahm et al., 2010). Additionally, mammalian pancreatic β-cell signalling by the Dpp orthologue, BMP4, has been implicated in regulating glucose-stimulated insulin secretion via the BMP receptor BMPR1A (Goulley et al., 2007). This study lacked mosaic analysis to test the role of cell-autonomous signalling, and it will now be important to assess whether this signalling is truly autocrine and if it could also match DCG biogenesis to secretion. This is particularly important given the significance of secretory mis-regulation in some forms of diabetes.

5.3.5 Mating-dependent DCG release is accompanied by autocrine BMP activation

Staining with an anti-pMad antibody revealed the sporadic activation of BMP signalling in SCs, probably as a result of constitutive secretion of DCGs. In mated flies, there was a significant increase in the number of pMad-positive SCs at both 3 and 6 days. Although it seems that all SCs release DCGs during mating and that overexpressing Dpp-GFP in SCs can activate BMP signalling in all expressing cells, only about 50% of SCs from mated males contain nuclear pMad at any specific time, suggesting that activation after DCG release may be short-lived.

Interestingly, the Wilson lab has previously found that a *Dad-GFP* transgene, which has been used as a BMP signalling reporter in other *Drosophila* cell types, is active in all SCs and at lower levels in MCs (Leiblich et al., 2012). Its expression was not obviously increased by mating. It is unclear if this reporter activity reflects cumulative activation of BMP signalling in SCs and/or non-BMP-dependent expression. However, since normal SC growth is primarily regulated cell-autonomously by BMP signalling, it seems likely that autocrine BMP signalling is independently activated in a pulsatile way in each individual SC as adults age.

5.3.6 BMP receptor localisation

Given the autocrine and secretion-dependent nature of BMP signalling in SCs, it is critical that Dpp is separated from its receptors prior to release. We found that at least one Type I and one Type II receptor (Tkv and Wit respectively) are trafficked to compartments that are distinct from the Rab11-positive DCGs, where Dpp is packaged. Interestingly, work in *C. elegans* has shown that Type I and Type II receptors are separated after endocytosis, potentially terminating signalling (Gleason

et al., 2014). Our analysis suggests that Tkv and Wit may be in the same intracellular compartments in SCs, but their separation from Dpp presumably prevents continued activation.

5.3.7 Regulation of DCG compartments by BMP signalling

I have shown that in addition to regulating SV numbers, the BMP pathway is crucially important for biogenesis of normal numbers of DCG compartments as well. Indeed, blocking BMP signalling in SCs reduces biogenesis of new DCG compartments in both virgin and mated males, but also inhibits release of DCGs. These complex effects may explain why the number of DCGs in knockdown cells is only reduced by about 20%. One hypothesis to explain why DCGs are not released when BMP signalling is inhibited is that this signalling is needed for the secretion of DCGs. However, my current model is that BMP signalling regulates the maturation of DCGs, preparing them to be released upon stimulation. Newly-formed DCGs that are labelled during a 16 h GFP-GPI pulse are not released during mating, suggesting that only mature compartments are secreted in a regulated fashion. This type of mechanism is mirrored in mammalian DCG secretion (Kim et al., 2006). Indeed, since additional DCGs are not released after a second mating, only about four DCGs normally appear to be sufficiently mature to be released. To discriminate the maturity of DCGs in SCs, new markers will need to be developed in the future.

My data support a model in which DCG-loaded Dpp acts primarily as an autocrine signal that matches regulated release of DCG compartments to new biogenesis. Upon mating, the rate of biogenesis is increased in a BMP-dependent fashion, so that two of the four DCGs lost at mating are replaced within 6 h and complete recovery of the DCG pool is achieved by 24 h.

How could BMP signalling be driving elevated rates of DCG biogenesis? Downstream Smad signalling primarily regulates gene transcription. Previous studies in pancreatic β-cells have revealed that BMP signalling induces insulin secretion and increases levels of many transcripts associated with the secretory process, such as the *Snap24* homologue, *SNAP25* (Goulley et al., 2007). Pheochromocytoma cells also express higher levels of the DCG assembly protein Chromogranin A in response to secretion (Tang et al., 1997). Since SCs constitute only a small proportion of cells in the AG, I was not been able to use qRT-PCR to determine if *Snap24* are induced by mating or BMP signalling activation. Therefore, it remains to be seen how changes of SC-specific BMP target genes are affect by physiological functions such as mating.

One key question that now needs to be addressed is how DCG secretion is stimulated upon mating. One possibility is that during mating, DCG compartments docked close to the SC plasma membrane are released after experiencing the physical forces induced by peristaltic movement of the muscular sheath surrounding the AG. Alternatively, a neuropeptide circuit has recently been identified in males that is critical for sperm and seminal fluid transfer and innervates cells in the AG (Tayler et al., 2012). It will be important to test whether this circuit makes connections with SCs or can stimulate DCG secretion through diffusion of the neurotransmitter(s) it releases.

6. Summary of results & concluding remarks

6.1 Summary of findings

The majority of the discussion for my specific findings has been included within the individual result chapters, so I will not repeat this here. Instead I will focus on summarising the overall conclusions from my work and setting it in the wider context of basic research in the areas of secretory and reproductive biology.

The research I have conducted during my DPhil has helped establish SCs as a new *in vivo* model to study many complex aspects of cell biology, including, membrane trafficking, secretion and growth regulation. My results have been used for several successful grant applications, particularly to the BBSRC. Moreover, my data has featured in a second author publication in JCB (Corrigan et al. 2014) and also in my first author paper in PLOS Genetics (Redhai et al. 2016).

6.1.1 Summary of results

In my first Results chapter, I show that different Rab signatures mark the intracellular compartments of SCs. For example, Rab11 marks DCG compartments, but a subset of these is also marked by Rab6 and Rab7. Interestingly, acidic MVBLs appear to be exclusively marked by Rab7, whilst Rab5 highlights a population of small early endosomes. Interestingly, Rab35 also marks another set of small compartments carrying the BMP ligand Gbb. These latter compartments merit further investigation as an additional source of biomolecules that could be secreted from SCs into the AG lumen. Furthermore, using RNAi against regulators of Golgi trafficking and pulse-chase experiments, I show that the formation of DCG compartments in part stems from the Golgi and that the traffic of some membrane proteins terminates in MVBLs.

In my second Results chapter, I focus on understanding how different Rab proteins, SNAREs and the multimeric V-ATPase regulate SC trafficking and exosome secretion.

Using overexpression and knockdown of Rab proteins, I show that Rab11 is required to maintain DCG compartments and restricts the trafficking of their contents towards MVBLs, while Rab7 is a key regulator in the biogenesis of MVBL compartments. Rab35 seems to promote fusion of SVs with MVBLs, expansion of MVBLs and the size of SVs, though the mechanisms involved are unclear, given that Rab35 does not appear to mark these compartments. Both Rab7 and Rab35 are also involved in maintaining the MVBL compartments once they have formed. Additionally, I show that SNAREs and the V-ATPase also appear to be involved in the fusion of intracellular compartments and in maintaining SC growth. Interestingly, I demonstrate that Rab proteins, SNAREs and V-ATPases are crucial for secreting exosomes. Indeed, using genetic tools to manipulate Rabs that control exosome secretion, I provide evidence that male-derived exosomes regulate the female PMR *in vivo*.

Having characterised the intracellular compartments of SCs and identified specific interactions between them, my attention turned to how their formation and secretion might be regulated in normal adult AGs. Previous evidence from the lab had already suggested a role for BMP signalling in controlling SC growth, exosome secretion and the number and size of secretory compartments, so I initiated a detailed analysis of the mechanisms involved. In my last Results chapter, I show that the BMP ligand Dpp is packaged inside DCGs and is the main regulator of autocrine BMP signalling. Mating stimulates the release of DCGs, which involves fusion events regulated by SNAP24. The DCGs secreted during mating are fully replenished within 24 h and therefor priming the SCs for another round of secretory events. Interestingly, mating coincides with increased activation of BMP signalling, presumably as a result of the secretion of Dpp-containing DCGs. The maturity of these compartments seems to be important for release because early pulse-labelled DCGs are not released after mating. SCs increase the biogenesis of new DCGs after mating in a BMP-dependent process. Therefore, the increased secretion of DCG compartments during mating is matched

by an increased rate of DCG replenishment through a predominantly autocrine BMP signalling mechanism.

6.2 Cell biological implications and future studies

6.2.1 The importance of visualising intracellular compartments

In establishing the SC as a new *in vivo* genetic system to study secretion, we have uncovered many hidden beauties of the underlying cell biology that have previously been very difficult to model using other systems. For example, visualising live fusion events between MVBLs and secretory compartments, and the tubular structures that emanate from these compartments provides a platform for exchanging material, whose regulation we can now study in greater detail. Laura Corrigan was able to observe intraluminal vesicle formation *in vivo* for the first time using SCs and provide the first evidence that ILVs inside MVBLs are involved in acidifying these compartments (Corrigan et al. 2014). Because the intracellular compartments of SCs are so large, I was given a unique opportunity in my studies to probe the regulation of membrane trafficking and secretion. In addition, the highly regulated release of DCGs at mating provided a dual assay to study regulated and constitutive secretion from SCs.

The level of resolution that can be obtained by studying SCs was at times a hidden curse. SCs are acutely sensitive to the modulation of membrane trafficking and compartment identity regulators, so I frequently uncovered variable and/or unpredictable phenotypes with constructs widely used in the field. For example, expressing Rab DN/CA constructs often did not give consistent phenotypes, and DN phenotypes frequently did not match knockdown phenotypes for the same Rabs. Recently the field has tried to move away from using such constructs, because there is no guarantee that they are truly acting as DN/ CA when overexpressed at high levels.

In data I do not present, expression of many GFP-tagged overexpression constructs used to mark late endosomal and lysosomal compartments in other *Drosophila* cells greatly expanded the lysosome-like compartment in SCs, making these markers inappropriate for further study. Both I and others have since employed a number of gene trap constructs to further investigate SC compartment biology, including the newly established set of *Drosophila Rab* gene traps. Although even these can induce mild phenotypes, they are allowing us to visualise events such as compartment, DCG and exosome biogenesis and secretion in unparalleled detail over extended periods of time.

6.2.2 The potential of multiple mTORC1 signalling hub

By using RNAi, I have shown that Rab7, a key gene implicated in melanoma progression, where late endosomal and lysosomal compartments appear to play specialised roles in secretion (Alonso-Curbelo et al., 2014), is crucial for the biogenesis of MVBLs. Surprisingly, in *Rab7* knockdown SCs, we saw a massive build-up of SVs but the overall growth of SCs was stunted. Since mTORC1 signalling is thought to be dependent on MVBL compartments, we propose that Rab7 may uncouple nuclear, and potentially cytosolic, growth from membrane biogenesis. Indeed, silencing Rab7 prevents the formation of MVBLs, favouring an 'alternative' form of mTORC1 signalling that is not controlled at the surface of MVBLs, which has been postulated in collaborative work between the Goberdhan and Wilson labs, as well as others groups. Identifying this alternative mTORC1 signalling is currently one of the main focuses of the Wilson Lab and if it materialises, it would make a significant contribution to the field, providing the first *in vivo* evidence for multiple mTORC1 signalling hubs in secretory cells.

6.2.3 Implications for the exosome field

Exosomes are postulated to be major signalling entities, sometimes harbouring both proteins and genetic material, which can initiate signalling in receipt cells (Colombo et al., 2014). However, the exosome field has been dogged by three major problems. First, most of the key studies in the area have been undertaken in cell culture, usually with cancer cell lines, raising the question of whether these entities are physiologically relevant. Second, there are currently no genetic manipulations that specifically block exosome secretion, making it difficult to test the physiological importance of exosome signalling. And third, assays for exosome function typically involve addition of very large numbers of exosomes that may not reflect normal biological situations.

My collaborative work with Laura Corrigan has established a powerful new model to study *in vivo* exosome secretion. I provide evidence that exosomes are capable of signalling between organisms, since blocking their production in male flies, causes female to court more frequently. Interestingly, prostasomes, prostate-derived exosomes, are also present in human semen and *in vitro*, they can fuse with sperm to provide calcium-signalling tools needed for sperm motility (Park et al., 2011).

To robustly demonstrate the physiological roles of SC exosomes, new genetic manipulations that more specifically block exosome secretion are required. However, the SC system provides an important new tool to characterise the cell biology of exosome biogenesis and therefore define such manipulations. In this regard, confocal imaging by both Laura Corrigan and myself revealed some time ago the presence of CD63-GFP staining inside Rab11-positive DCG compartments in SCs. Exosomes are classically thought to be produced in Rab7-positive MVBL compartments. However, subsequent work using super-resolution microscopy, particularly from another DPhil student in the lab, Ben Kroeger, has demonstrated that exosomes are formed in

Rab11-positive compartments, and collaborative studies with the Goberdhan lab have shown that this mechanism is evolutionarily conserved from fly to human. This programme of work is now expanding with funding from CRUK.

Exosomes are also considered to be involved in cancer progression and in priming distant sites for metastatic invasion. Having established that SNAREs and V-ATPases, as well as Rabs, are involved in CD63-positive exosome release, it would be interesting to test if these functions are conserved in mammals, including humans, with the aim of targeting them in disease states.

6.2.4 Implications for the field of regulated secretion

BMP signalling is important for various aspects of SC biology. An interesting observation is that the BMP2/4 ligand, Dpp, is packaged inside DCGs. The contents of DCG compartments are secreted into the AG lumen and transferred to females during mating. If Dpp is also transferred to females, it would be fascinating to test if it can initiate signalling in females. One scenario could be that Dpp is involved in instigating signalling at the neuronal level in females to regulate her behaviour towards other males. Interestingly, data not shown in my thesis suggest that Dpp might also be carried on vesicles inside DCG compartments. It will be interesting to explore further whether exosomes might be involved in Dpp signalling in this system, and if so, how exosome and DCG loading are regulated.

DCG secretion is important for many aspects of cell biology and physiology. For example, in β-cells, insulin is packaged into DCGs and secreted in response to BMP signalling (Goulley et al., 2007), highlighting parallels between this system and the fly AG. It will be important to check if BMP2/4 are also packaged inside DCGs in β-cells

and if it can initiate autocrine BMP signalling from this location upon stimulation of secretion.

Another key question is how are the DCGs formed in SCs? My work has identified large Rab6-positive compartments, some of which presumably do not contain DCGs, as well as large Rab11-positive containing DCG compartments, some of which are also co-labelled with Rab6. Rab6 is a key regulator of trafficking out of the Golgi in other cell types (Martinez et al., 1994). Without disclosing too much unpublished work, Ben Kroeger and Felix Castellanos in the Wilson Lab have provided evidence that Rab6-positive compartments are the place that DCG-containing compartments begin to be generated. Indeed, in this model, proteins destined for DCGs would traffic through the Golgi and concentrate in Rab6-positive compartments that bud from the TGN and mature into Rab11 positive DCG compartments. Real-time imaging of these events should permit the first *in vivo* analysis of DCG formation in eukaryotic cells and allow us to define the molecular mechanisms involved.

6.3 Concluding remarks

I arrived at the Wilson lab after three years of undergraduate studies, not having any experience with fruit flies. Over the past four years I have learnt a great deal on how *Drosophila* genetics is used to better understand different aspects of cell biology, and how cell biological mechanisms ultimately connect to physiological functions. I was given the freedom to research in a broad range of areas, and in trying to establish the AG as a new secretory model, I stumbled across a fascinating bunch of cells – the secondary cells. Characterising them not only gave me a lesson in how to steer through difficult tasks, but also taught me how to build a research project around a set of entirely novel and not instantly connected, observations, a skill that I will carry for the foreseeable future.

One of the initial goals of my study was to marry the field of membrane trafficking with growth-promoting signalling pathways. But having characterised SC compartments using different Rab GTPases, I was lucky to find that DCGs are loaded with Dpp – the major ligand involved in BMP signalling in SCs. Indeed, this ligand is secreted during mating where it activates autocrine BMP signalling to increase the formation of new DCGs and replenish the lost compartments. This truly fascinated me, partly because a simple mechanism like this ensured that SCs maintain their reproductive functions under different physiological scenarios and through exosomes gave male fruit flies a potential upper hand in the battle of the sexes.

The Wilson lab now has numerous collaborations to translate findings in *Drosophila* to mammalian systems. Indeed, it is through these collaborations that we have started to find conserved roles for the regulators of SC exosome secretion in human cancer cell lines. By using *Drosophila*, one can easily manipulate a complete set of candidate genes at will and subsequently test those that are highlighted in other systems for conversed roles. Fittingly, this is partly the reason I enjoy working with fruit flies.

I would like to thank the readers for taking the time to work through my thesis. I have thoroughly enjoyed my time as a DPhil student in the Wilson lab and I hope you can share my enthusiasm for the research that has emerged over the past four years.

7. References

ABERLE, H., HAGHIGHI, A. P., FETTER, R. D., MCCABE, B. D., MAGALHAES, T. R. & GOODMAN, C. S. 2002. wishful thinking encodes a BMP type II receptor that regulates synaptic growth in Drosophila. *Neuron,* 33**,** 545-58.

ADAMS, M. D., CELNIKER, S. E., HOLT, R. A., EVANS, C. A., GOCAYNE, J. D., AMANATIDES, P. G., SCHERER, S. E., LI, P. W., HOSKINS, R. A., GALLE, R. F., GEORGE, R. A., LEWIS, S. E., RICHARDS, S et al. 2000. The genome sequence of Drosophila melanogaster. *Science,* 287**,** 2185-95.

ALARCON, C., ZAROMYTIDOU, A. I., XI, Q., GAO, S., YU, J., FUJISAWA, S., BARLAS, A., MILLER, A. N., MANOVA-TODOROVA, K., MACIAS, M. J., SAPKOTA, G., PAN, D. & MASSAGUE, J. 2009. Nuclear CDKs drive Smad transcriptional activation and turnover in BMP and TGF-beta pathways. *Cell,* 139**,** 757-69.

ALONSO-CURBELO, D., RIVEIRO-FALKENBACH, E., PEREZ-GUIJARRO, E., CIFDALOZ, M., KARRAS, P., OSTERLOH, L., MEGIAS, D., CANON, E., CALVO, T. G., OLMEDA, D., GOMEZ-LOPEZ, G et al. 2014. RAB7 controls melanoma progression by exploiting a lineage-specific wiring of the endolysosomal pathway. *Cancer Cell,* 26**,** 61-76.

APGER-MCGLAUGHON, J. & WOLFNER, M. F. 2013. Post-mating change in excretion by mated Drosophila melanogaster females is a long-term response that depends on sex peptide and sperm. *J Insect Physiol,* 59**,** 1024-30.

ASHE, H. L. 2005. BMP signalling: synergy and feedback create a step gradient. *Curr Biol,* 15**,** R375-7.

BABST, M. 2011. MVB vesicle formation: ESCRT-dependent, ESCRT-independent and everything in between. *Curr Opin Cell Biol,* 23**,** 452-7.

BAIETTI, M. F., ZHANG, Z., MORTIER, E., MELCHIOR, A., DEGEEST, G., GEERAERTS, A., IVARSSON, Y., DEPOORTERE, F., COOMANS, C., VERMEIREN, E., ZIMMERMANN, P. & DAVID, G. 2012. Syndecan-syntenin-ALIX regulates the biogenesis of exosomes. *Nat Cell Biol,* 14**,** 677-85.

BAIRATI, A. 1986. Structure and ultrastructure of the male reproductive system in Drosophila melanogaster Meig. 2. The genital duct and accessory glands. *Monitore Zoologico Italiano - Italian Journal Of Zoology* 2.

BANGI, E. & WHARTON, K. 2006. Dual function of the Drosophila Alk1/Alk2 ortholog Saxophone shapes the Bmp activity gradient in the wing imaginal disc. *Development,* 133**,** 3295-303.

BARON, R., NEFF, L., LOUVARD, D. & COURTOY, P. J. 1985. Cell-mediated extracellular acidification and bone resorption: evidence for a low pH in resorbing lacunae and localization of a 100-kD lysosomal membrane protein at the osteoclast ruffled border. *J Cell Biol,* 101**,** 2210-22.

BARR, F. & LAMBRIGHT, D. G. 2010. Rab GEFs and GAPs. *Curr Opin Cell Biol,* 22**,** 461-70.

BARR, F. A. 2013. Review series: Rab GTPases and membrane identity: causal or inconsequential? *J Cell Biol,* 202**,** 191-9.

BECKETT, K., MONIER, S., PALMER, L., ALEXANDRE, C., GREEN, H., BONNEIL, E., RAPOSO, G., THIBAULT, P., LE BORGNE, R. & VINCENT, J. P. 2013. Drosophila S2 cells secrete wingless on exosome-like vesicles but the wingless gradient forms independently of exosomes. *Traffic,* 14**,** 82-96.

BECKWITH, E. J., GOROSTIZA, E. A., BERNI, J., REZAVAL, C., PEREZ-SANTANGELO, A., NADRA, A. D. & CERIANI, M. F. 2013. Circadian period integrates network information through activation of the BMP signaling pathway. *PLoS Biol,* 11**,** e1001733.

BELENKAYA, T. Y., HAN, C., YAN, D., OPOKA, R. J., KHODOUN, M., LIU, H. & LIN, X. 2004. Drosophila Dpp morphogen movement is independent of dynamin-mediated endocytosis but regulated by the glypican members of heparan sulfate proteoglycans. *Cell,* 119**,** 231-44.

BELLEN, H. J., TONG, C. & TSUDA, H. 2010. 100 years of Drosophila research and its impact on vertebrate neuroscience: a history lesson for the future. *Nat Rev Neurosci,* 11**,** 514-22.

BERTRAM, M. J., AKERKAR, G. A., ARD, R. L., GONZALEZ, C. & WOLFNER, M. F. 1992. Cell type-specific gene expression in the Drosophila melanogaster male accessory gland. *Mech Dev,* 38**,** 33-40.

BETZ, C. & HALL, M. N. 2013. Where is mTOR and what is it doing there? *J Cell Biol,* 203**,** 563-74.

BILODEAU, P. S., URBANOWSKI, J. L., WINISTORFER, S. C. & PIPER, R. C. 2002. The Vps27p Hse1p complex binds ubiquitin and mediates endosomal protein sorting. *Nat Cell Biol,* 4**,** 534-9.

BISWAS, P., TAMBUSSI, G. & LAZZARIN, A. 2007. Access denied? The status of co-receptor inhibition to counter HIV entry. *Expert Opin Pharmacother,* 8**,** 923-33.
BLOTT, E. J. & GRIFFITHS, G. M. 2002. Secretory lysosomes. *Nat Rev Mol Cell Biol,* 3**,** 122-31.
BRAND, A. H. & PERRIMON, N. 1993. Targeted gene expression as a means of altering cell fates and generating dominant phenotypes. *Development,* 118**,** 401-15.
BRANDIZZI, F. & BARLOWE, C. 2013. Organization of the ER-Golgi interface for membrane traffic control. *Nat Rev Mol Cell Biol,* 14**,** 382-92.
BUCCI, C., THOMSEN, P., NICOZIANI, P., MCCARTHY, J. & VAN DEURS, B. 2000. Rab7: a key to lysosome biogenesis. *Mol Biol Cell,* 11**,** 467-80.
BUDNIK, V., RUIZ-CANADA, C. & WENDLER, F. 2016. Extracellular vesicles round off communication in the nervous system. *Nat Rev Neurosci,* 17**,** 160-72.
BURGESS, J., DEL BEL, L. M., MA, C. I., BARYLKO, B., POLEVOY, G., ROLLINS, J., ALBANESI, J. P., KRAMER, H. & BRILL, J. A. 2012. Type II phosphatidylinositol 4-kinase regulates trafficking of secretory granule proteins in Drosophila. *Development,* 139**,** 3040-50.
BURGESS, T. L. & KELLY, R. B. 1987. Constitutive and regulated secretion of proteins. *Annu Rev Cell Biol,* 3**,** 243-93.
CAI, H., REINISCH, K. & FERRO-NOVICK, S. 2007. Coats, tethers, Rabs, and SNAREs work together to mediate the intracellular destination of a transport vesicle. *Dev Cell,* 12**,** 671-82.
CAO, J., BRETT J. PELLOCK*, KRISTIN WHITE, AND LAUREL A. RAFTERY. 2006. A commercial phospho-Smad antibody detects endogenous BMP signaling in
Drosophila tissues. . *Dros. Inf. Serv,* 89.
CHAPMAN, T., BANGHAM, J., VINTI, G., SEIFRIED, B., LUNG, O., WOLFNER, M. F., SMITH, H. K. & PARTRIDGE, L. 2003. The sex peptide of Drosophila melanogaster: female post-mating responses analyzed by using RNA interference. *Proc Natl Acad Sci U S A,* 100**,** 9923-8.
CHEN, X. & WANG, Z. 2001. Regulation of epidermal growth factor receptor endocytosis by wortmannin through activation of Rab5 rather than inhibition of phosphatidylinositol 3-kinase. *EMBO Rep,* 2**,** 842-9.
CHEN, Y. A. & SCHELLER, R. H. 2001. SNARE-mediated membrane fusion. *Nat Rev Mol Cell Biol,* 2**,** 98-106.
COLOMBO, M., RAPOSO, G. & THERY, C. 2014. Biogenesis, secretion, and intercellular interactions of exosomes and other extracellular vesicles. *Annu Rev Cell Dev Biol,* 30**,** 255-89.
CORRIGAN, L., REDHAI, S., LEIBLICH, A., FAN, S. J., PERERA, S. M., PATEL, R., GANDY, C., WAINWRIGHT, S. M., MORRIS, J. F., HAMDY, F., GOBERDHAN, D. C. & WILSON, C. 2014. BMP-regulated exosomes from Drosophila male reproductive glands reprogram female behavior. *J Cell Biol,* 206**,** 671-88.
COSTA-SILVA, B., AIELLO, N. M., OCEAN, A. J., SINGH, S., ZHANG, H., THAKUR, B. K., BECKER, A., HOSHINO, A., MARK, M. T., MOLINA, H., XIANG, J., ZHANG, T., THEILEN, T. M., GARCIA-SANTOS, G., WILLIAMS, C., ARARSO, Y., HUANG, Y., RODRIGUES, G., SHEN, T. L et al. 2015. Pancreatic cancer exosomes initiate pre-metastatic niche formation in the liver. *Nat Cell Biol,* 17**,** 816-26.
COUTURIER, L., TRYLINSKI, M., MAZOUNI, K., DARNET, L. & SCHWEISGUTH, F. 2014. A fluorescent tagging approach in Drosophila reveals late endosomal trafficking of Notch and Sanpodo. *J Cell Biol,* 207**,** 351-63.
D'SOUZA-SCHOREY, C. & CHAVRIER, P. 2006. ARF proteins: roles in membrane traffic and beyond. *Nat Rev Mol Cell Biol, 7***,** 347-58.
DANI, N., NAHM, M., LEE, S. & BROADIE, K. 2012. A targeted glycan-related gene screen reveals heparan sulfate proteoglycan sulfation regulates WNT and BMP trans-synaptic signaling. *PLoS Genet,* 8**,** e1003031.
DE LUCA, M., COGLI, L., PROGIDA, C., NISI, V., PASCOLUTTI, R., SIGISMUND, S., DI FIORE, P. P. & BUCCI, C. 2014. RILP regulates vacuolar ATPase through interaction with the V1G1 subunit. *J Cell Sci,* 127**,** 2697-708.
DE MATTEIS, M. A. & LUINI, A. 2008. Exiting the Golgi complex. *Nat Rev Mol Cell Biol,* 9**,** 273-84.
DERETIC, V. 2005. Ay, there's the Rab: organelle maturation by Rab conversion. *Dev Cell,* 9**,** 446-8.
DI GUGLIELMO, G. M., BAASS, P. C., OU, W. J., POSNER, B. I. & BERGERON, J. J. 1994. Compartmentalization of SHC, GRB2 and mSOS, and hyperphosphorylation of Raf-1 by EGF but not insulin in liver parenchyma. *EMBO J,* 13**,** 4269-77.
DIKEAKOS, J. D. & REUDELHUBER, T. L. 2007. Sending proteins to dense core secretory granules: still a lot to sort out. *J Cell Biol,* 177**,** 191-6.
DOHERTY, G. J. & MCMAHON, H. T. 2009. Mechanisms of endocytosis. *Annu Rev Biochem,* 78**,** 857-902.

DONALDSON, J. G. & JACKSON, C. L. 2011. ARF family G proteins and their regulators: roles in membrane transport, development and disease. *Nat Rev Mol Cell Biol,* 12**,** 362-75.
DUFFY, J. B. 2002. GAL4 system in Drosophila: a fly geneticist's Swiss army knife. *Genesis,* 34**,** 1-15.
DUNST, S., KAZIMIERS, T., VON ZADOW, F., JAMBOR, H., SAGNER, A., BRANKATSCHK, B., MAHMOUD, A., SPANNL, S., TOMANCAK, P., EATON, S. & BRANKATSCHK, M. 2015. Endogenously tagged rab proteins: a resource to study membrane trafficking in Drosophila. *Dev Cell,* 33**,** 351-65.
EMR, S., GLICK, B. S., LINSTEDT, A. D., LIPPINCOTT-SCHWARTZ, J., LUINI, A., MALHOTRA, V., MARSH, B. J., NAKANO, A., PFEFFER, S. R., RABOUILLE, C., ROTHMAN, J. E., WARREN, G. & WIELAND, F. T. 2009. Journeys through the Golgi--taking stock in a new era. *J Cell Biol,* 187**,** 449-53.
FADER, C. M., SANCHEZ, D. G., MESTRE, M. B. & COLOMBO, M. I. 2009. TI-VAMP/VAMP7 and VAMP3/cellubrevin: two v-SNARE proteins involved in specific steps of the autophagy/multivesicular body pathways. *Biochim Biophys Acta,* 1793**,** 1901-16.
FALCON-PEREZ, J. M., NAZARIAN, R., SABATTI, C. & DELL'ANGELICA, E. C. 2005. Distribution and dynamics of Lamp1-containing endocytic organelles in fibroblasts deficient in BLOC-3. *J Cell Sci,* 118**,** 5243-55.
FALGUIERES, T., LUYET, P. P., BISSIG, C., SCOTT, C. C., VELLUZ, M. C. & GRUENBERG, J. 2008. In vitro budding of intralumenal vesicles into late endosomes is regulated by Alix and Tsg101. *Mol Biol Cell,* 19**,** 4942-55.
FARES, H. & GREENWALD, I. 2001. Genetic analysis of endocytosis in Caenorhabditis elegans: coelomocyte uptake defective mutants. *Genetics,* 159**,** 133-45.
FARHAN, H. & RABOUILLE, C. 2011. Signalling to and from the secretory pathway. *J Cell Sci,* 124**,** 171-80.
FORGAC, M. 2007. Vacuolar ATPases: rotary proton pumps in physiology and pathophysiology. *Nat Rev Mol Cell Biol,* 8**,** 917-29.
FRANCH-MARRO, X., WENDLER, F., GUIDATO, S., GRIFFITH, J., BAENA-LOPEZ, A., ITASAKI, N., MAURICE, M. M. & VINCENT, J. P. 2008. Wingless secretion requires endosome-to-Golgi retrieval of Wntless/Evi/Sprinter by the retromer complex. *Nat Cell Biol,* 10**,** 170-7.
FRANCOIS, V., SOLLOWAY, M., O'NEILL, J. W., EMERY, J. & BIER, E. 1994. Dorsal-ventral patterning of the Drosophila embryo depends on a putative negative growth factor encoded by the short gastrulation gene. *Genes Dev,* 8**,** 2602-16.
FRESCAS, D., MAVRAKIS, M., LORENZ, H., DELOTTO, R. & LIPPINCOTT-SCHWARTZ, J. 2006. The secretory membrane system in the Drosophila syncytial blastoderm embryo exists as functionally compartmentalized units around individual nuclei. *J Cell Biol,* 173**,** 219-30.
FUKUDA, M. 1991. Lysosomal membrane glycoproteins. Structure, biosynthesis, and intracellular trafficking. *J Biol Chem,* 266**,** 21327-30.
FUTTER, C. E., PEARSE, A., HEWLETT, L. J. & HOPKINS, C. R. 1996. Multivesicular endosomes containing internalized EGF-EGF receptor complexes mature and then fuse directly with lysosomes. *J Cell Biol,* 132**,** 1011-23.
GALBRAITH, C. G. & GALBRAITH, J. A. 2011. Super-resolution microscopy at a glance. *J Cell Sci,* 124**,** 1607-11.
GAO, X. & PAN, D. 2001. TSC1 and TSC2 tumor suppressors antagonize insulin signaling in cell growth. *Genes Dev,* 15**,** 1383-92.
GARCIA-DEL PORTILLO, F., STEIN, M. A. & FINLAY, B. B. 1997. Release of lipopolysaccharide from intracellular compartments containing Salmonella typhimurium to vesicles of the host epithelial cell. *Infect Immun,* 65**,** 24-34.
GIDON, A., BARDIN, S., CINQUIN, B., BOULANGER, J., WAHARTE, F., HELIOT, L., DE LA SALLE, H., HANAU, D., KERVRANN, C., GOUD, B. & SALAMERO, J. 2012. A Rab11A/myosin Vb/Rab11-FIP2 complex frames two late recycling steps of langerin from the ERC to the plasma membrane. *Traffic,* 13**,** 815-33.
GLEASON, R. J., AKINTOBI, A. M., GRANT, B. D. & PADGETT, R. W. 2014. BMP signaling requires retromer-dependent recycling of the type I receptor. *Proc Natl Acad Sci U S A,* 111**,** 2578-83.
GLIGOROV, D., SITNIK, J. L., MAEDA, R. K., WOLFNER, M. F. & KARCH, F. 2013. A novel function for the Hox gene Abd-B in the male accessory gland regulates the long-term female post-mating response in Drosophila. *PLoS Genet,* 9**,** e1003395.
GOBERDHAN, D. C., WILSON, C. & HARRIS, A. L. 2016. Amino Acid Sensing by mTORC1: Intracellular Transporters Mark the Spot. *Cell Metab,* 23**,** 580-9.
GOH, L. K. & SORKIN, A. 2013. Endocytosis of receptor tyrosine kinases. *Cold Spring Harb Perspect Biol,* 5**,** a017459.
GOLDENRING, J. R. 2013. A central role for vesicle trafficking in epithelial neoplasia: intracellular highways to carcinogenesis. *Nat Rev Cancer,* 13**,** 813-20.

GONZALEZ-GAITAN, M. & JACKLE, H. 1999. The range of spalt-activating Dpp signalling is reduced in endocytosis-defective Drosophila wing discs. *Mech Dev,* 87**,** 143-51.
GOOD, M. C., ZALATAN, J. G. & LIM, W. A. 2011. Scaffold proteins: hubs for controlling the flow of cellular information. *Science,* 332**,** 680-6.
GOULLEY, J., DAHL, U., BAEZA, N., MISHINA, Y. & EDLUND, H. 2007. BMP4-BMPR1A signaling in beta cells is required for and augments glucose-stimulated insulin secretion. *Cell Metab,* 5**,** 207-19.
GRANT, B. D. & DONALDSON, J. G. 2009. Pathways and mechanisms of endocytic recycling. *Nat Rev Mol Cell Biol,* 10**,** 597-608.
GROSS, J. C., CHAUDHARY, V., BARTSCHERER, K. & BOUTROS, M. 2012. Active Wnt proteins are secreted on exosomes. *Nat Cell Biol,* 14**,** 1036-45.
GROSSHANS, B. L., ORTIZ, D. & NOVICK, P. 2006. Rabs and their effectors: achieving specificity in membrane traffic. *Proc Natl Acad Sci U S A,* 103**,** 11821-7.
GUREVICH, V. V., DION, S. B., ONORATO, J. J., PTASIENSKI, J., KIM, C. M., STERNE-MARR, R., HOSEY, M. M. & BENOVIC, J. L. 1995. Arrestin interactions with G protein-coupled receptors. Direct binding studies of wild type and mutant arrestins with rhodopsin, beta 2-adrenergic, and m2 muscarinic cholinergic receptors. *J Biol Chem,* 270**,** 720-31.
HAAS, A. K., FUCHS, E., KOPAJTICH, R. & BARR, F. A. 2005. A GTPase-activating protein controls Rab5 function in endocytic trafficking. *Nat Cell Biol,* 7**,** 887-93.
HAMARATOGLU, F., AFFOLTER, M. & PYROWOLAKIS, G. 2014. Dpp/BMP signaling in flies: from molecules to biology. *Semin Cell Dev Biol,* 32**,** 128-36.
HEIFETZ, Y., VANDENBERG, L. N., COHN, H. I. & WOLFNER, M. F. 2005. Two cleavage products of the Drosophila accessory gland protein ovulin can independently induce ovulation. *Proc Natl Acad Sci U S A,* 102**,** 743-8.
HIESINGER, P. R., FAYYAZUDDIN, A., MEHTA, S. Q., ROSENMUND, T., SCHULZE, K. L., ZHAI, R. G., VERSTREKEN, P., CAO, Y., ZHOU, Y., KUNZ, J. & BELLEN, H. J. 2005. The v-ATPase V0 subunit a1 is required for a late step in synaptic vesicle exocytosis in Drosophila. *Cell,* 121**,** 607-20.
HOU, J. C., MIN, L. & PESSIN, J. E. 2009. Insulin granule biogenesis, trafficking and exocytosis. *Vitam Horm,* 80**,** 473-506.
HOWE, C. L., VALLETTA, J. S., RUSNAK, A. S. & MOBLEY, W. C. 2001. NGF signaling from clathrin-coated vesicles: evidence that signaling endosomes serve as a platform for the Ras-MAPK pathway. *Neuron,* 32**,** 801-14.
HSU, C., MOROHASHI, Y., YOSHIMURA, S., MANRIQUE-HOYOS, N., JUNG, S., LAUTERBACH, M. A., BAKHTI, M., GRONBORG, M., MOBIUS, W., RHEE, J., BARR, F. A. & SIMONS, M. 2010. Regulation of exosome secretion by Rab35 and its GTPase-activating proteins TBC1D10A-C. *J Cell Biol,* 189**,** 223-32.
HUBER, L. A., PIMPLIKAR, S., PARTON, R. G., VIRTA, H., ZERIAL, M. & SIMONS, K. 1993. Rab8, a small GTPase involved in vesicular traffic between the TGN and the basolateral plasma membrane. *J Cell Biol,* 123**,** 35-45.
HUMPHRIES, W. H. T., SZYMANSKI, C. J. & PAYNE, C. K. 2011. Endo-lysosomal vesicles positive for Rab7 and LAMP1 are terminal vesicles for the transport of dextran. *PLoS One,* 6**,** e26626.
HUOTARI, J. & HELENIUS, A. 2011. Endosome maturation. *EMBO J,* 30**,** 3481-500.
HURST, D., RYLETT, C. M., ISAAC, R. E. & SHIRRAS, A. D. 2003. The drosophila angiotensin-converting enzyme homologue Ance is required for spermiogenesis. *Dev Biol,* 254**,** 238-47.
HURTADO-LORENZO, A., SKINNER, M., EL ANNAN, J., FUTAI, M., SUN-WADA, G. H., BOURGOIN, S., CASANOVA, J., WILDEMAN, A., BECHOUA, S., AUSIELLO, D. A., BROWN, D. & MARSHANSKY, V. 2006. V-ATPase interacts with ARNO and Arf6 in early endosomes and regulates the protein degradative pathway. *Nat Cell Biol,* 8**,** 124-36.
HUTAGALUNG, A. H. & NOVICK, P. J. 2011. Role of Rab GTPases in membrane traffic and cell physiology. *Physiol Rev,* 91**,** 119-49.
JACQUEMET, G., HAMIDI, H. & IVASKA, J. 2015. Filopodia in cell adhesion, 3D migration and cancer cell invasion. *Curr Opin Cell Biol,* 36**,** 23-31.
JAHN, R. & SCHELLER, R. H. 2006. SNAREs--engines for membrane fusion. *Nat Rev Mol Cell Biol,* 7**,** 631-43.
JEAN, S. & KIGER, A. A. 2012. Coordination between RAB GTPase and phosphoinositide regulation and functions. *Nat Rev Mol Cell Biol,* 13**,** 463-70.
JEKELY, G., SUNG, H. H., LUQUE, C. M. & RORTH, P. 2005. Regulators of endocytosis maintain localized receptor tyrosine kinase signaling in guided migration. *Dev Cell,* 9**,** 197-207.
JIANG, H., PATEL, P. H., KOHLMAIER, A., GRENLEY, M. O., MCEWEN, D. G. & EDGAR, B. A. 2009. Cytokine/Jak/Stat signaling mediates regeneration and homeostasis in the Drosophila midgut. *Cell,* 137**,** 1343-55.

JONEK, J., KONECKI, J., GRZYBEK, H. & OKKOWSKI, Z. 1971. Electron microscopical studies on the lysosomes and the Golgi apparatus in the motoneurons of spinal cords of mice under physiological and pathological conditions. *Histochemie,* 26**,** 28-34.
JORDENS, I., WESTBROEK, W., MARSMAN, M., ROCHA, N., MOMMAAS, M., HUIZING, M., LAMBERT, J., NAEYAERT, J. M. & NEEFJES, J. 2006. Rab7 and Rab27a control two motor protein activities involved in melanosomal transport. *Pigment Cell Res,* 19**,** 412-23.
KAETHER, C. & GERDES, H. H. 1995. Visualization of protein transport along the secretory pathway using green fluorescent protein. *FEBS Lett,* 369**,** 267-71.
KALB, J. M., DIBENEDETTO, A. J. & WOLFNER, M. F. 1993. Probing the function of Drosophila melanogaster accessory glands by directed cell ablation. *Proc Natl Acad Sci U S A,* 90**,** 8093-7.
KATZMANN, D. J., BABST, M. & EMR, S. D. 2001. Ubiquitin-dependent sorting into the multivesicular body pathway requires the function of a conserved endosomal protein sorting complex, ESCRT-I. *Cell,* 106**,** 145-55.
KAVALALI, E. T. 2015. The mechanisms and functions of spontaneous neurotransmitter release. *Nat Rev Neurosci,* 16**,** 5-16.
KAWABATA, M. & MIYAZONO, K. 1999. Signal transduction of the TGF-beta superfamily by Smad proteins. *J Biochem,* 125**,** 9-16.
KIM, E., GORAKSHA-HICKS, P., LI, L., NEUFELD, T. P. & GUAN, K. L. 2008. Regulation of TORC1 by Rag GTPases in nutrient response. *Nat Cell Biol,* 10**,** 935-45.
KIM, T., GONDRE-LEWIS, M. C., ARNAOUTOVA, I. & LOH, Y. P. 2006. Dense-core secretory granule biogenesis. *Physiology (Bethesda),* 21**,** 124-33.
KIM, T., TAO-CHENG, J. H., EIDEN, L. E. & LOH, Y. P. 2001. Chromogranin A, an "on/off" switch controlling dense-core secretory granule biogenesis. *Cell,* 106**,** 499-509.
KLINKERT, K. & ECHARD, A. 2016. Rab35 GTPase: A Central Regulator of Phosphoinositides and F-actin in Endocytic Recycling and Beyond. *Traffic,* 17**,** 1063-77.
KNOCK, E., PEREIRA, J., LOMBARD, P. D., DIMOND, A., LEAFORD, D., LIVESEY, F. J. & HENDRICH, B. 2015. The methyl binding domain 3/nucleosome remodelling and deacetylase complex regulates neural cell fate determination and terminal differentiation in the cerebral cortex. *Neural Dev,* 10**,** 13.
KOLES, K., NUNNARI, J., KORKUT, C., BARRIA, R., BREWER, C., LI, Y., LESZYK, J., ZHANG, B. & BUDNIK, V. 2012. Mechanism of evenness interrupted (Evi)-exosome release at synaptic boutons. *J Biol Chem,* 287**,** 16820-34.
KOUREMBANAS, S. 2015. Exosomes: vehicles of intercellular signaling, biomarkers, and vectors of cell therapy. *Annu Rev Physiol,* 77**,** 13-27.
KOWAL, J., ARRAS, G., COLOMBO, M., JOUVE, M., MORATH, J. P., PRIMDAL-BENGTSON, B., DINGLI, F., LOEW, D., TKACH, M. & THERY, C. 2016. Proteomic comparison defines novel markers to characterize heterogeneous populations of extracellular vesicle subtypes. *Proc Natl Acad Sci U S A,* 113**,** E968-77.
KUBLI, E. & BOPP, D. 2012. Sexual behavior: how Sex Peptide flips the postmating switch of female flies. *Curr Biol,* 22**,** R520-2.
LAWE, D. C., PATKI, V., HELLER-HARRISON, R., LAMBRIGHT, D. & CORVERA, S. 2000. The FYVE domain of early endosome antigen 1 is required for both phosphatidylinositol 3-phosphate and Rab5 binding. Critical role of this dual interaction for endosomal localization. *J Biol Chem,* 275**,** 3699-705.
LEIBLICH, A., MARSDEN, L., GANDY, C., CORRIGAN, L., JENKINS, R., HAMDY, F. & WILSON, C. 2012. Bone morphogenetic protein- and mating-dependent secretory cell growth and migration in the Drosophila accessory gland. *Proc Natl Acad Sci U S A,* 109**,** 19292-7.
LEVINE, T. P., DANIELS, R. D., WONG, L. H., GATTA, A. T., GERONDOPOULOS, A. & BARR, F. A. 2013. Discovery of new Longin and Roadblock domains that form platforms for small GTPases in Ragulator and TRAPP-II. *Small GTPases,* 4**,** 62-9.
LEWIS, M. J., NICHOLS, B. J., PRESCIANOTTO-BASCHONG, C., RIEZMAN, H. & PELHAM, H. R. 2000. Specific retrieval of the exocytic SNARE Snc1p from early yeast endosomes. *Mol Biol Cell,* 11**,** 23-38.
LI, L., KIM, E., YUAN, H., INOKI, K., GORAKSHA-HICKS, P., SCHIESHER, R. L., NEUFELD, T. P. & GUAN, K. L. 2010. Regulation of mTORC1 by the Rab and Arf GTPases. *J Biol Chem,* 285**,** 19705-9.
LIEGEOIS, S., BENEDETTO, A., GARNIER, J. M., SCHWAB, Y. & LABOUESSE, M. 2006. The V0-ATPase mediates apical secretion of exosomes containing Hedgehog-related proteins in Caenorhabditis elegans. *J Cell Biol,* 173**,** 949-61.
LLOYD, T. E., ATKINSON, R., WU, M. N., ZHOU, Y., PENNETTA, G. & BELLEN, H. J. 2002. Hrs regulates endosome membrane invagination and tyrosine kinase receptor signaling in Drosophila. *Cell,* 108**,** 261-9.

LO, RS & MASSGUE, J. 1999. UBIQUITIN-DEPENDENT DEGRADATION OF TGF-BETA-ACTIVATED SMAD2. *Nat Cell Bio*: 1(8):472-8.
LOBB, R. J., BECKER, M., WEN, S. W., WONG, C. S., WIEGMANS, A. P., LEIMGRUBER, A. & MOLLER, A. 2015. Optimized exosome isolation protocol for cell culture supernatant and human plasma. *J Extracell Vesicles,* 4**,** 27031.
LOCK, J. G. & STOW, J. L. 2005. Rab11 in recycling endosomes regulates the sorting and basolateral transport of E-cadherin. *Mol Biol Cell,* 16**,** 1744-55.
LUZIO, J. P., GRAY, S. R. & BRIGHT, N. A. 2010. Endosome-lysosome fusion. *Biochem Soc Trans,* 38**,** 1413-6.
LUZIO, J. P., PRYOR, P. R. & BRIGHT, N. A. 2007. Lysosomes: fusion and function. *Nat Rev Mol Cell Biol,* 8**,** 622-32.
LYNCH, J. A. & ROTH, S. 2011. The evolution of dorsal-ventral patterning mechanisms in insects. *Genes Dev,* 25**,** 107-18.
MARMION, R. A., JEVTIC, M., SPRINGHORN, A., PYROWOLAKIS, G. & YAKOBY, N. 2013. The Drosophila BMPRII, wishful thinking, is required for eggshell patterning. *Dev Biol,* 375**,** 45-53.
MAROIS, E., MAHMOUD, A. & EATON, S. 2006. The endocytic pathway and formation of the Wingless morphogen gradient. *Development,* 133**,** 307-17.
MARTINEZ, O., SCHMIDT, A., SALAMERO, J., HOFLACK, B., ROA, M. & GOUD, B. 1994. The small GTP-binding protein rab6 functions in intra-Golgi transport. *J Cell Biol,* 127**,** 1575-88.
MARTINEZ, V. G., HERNANDEZ-LOPEZ, C., VALENCIA, J., HIDALGO, L., ENTRENA, A., ZAPATA, A. G., VICENTE, A., SACEDON, R. & VARAS, A. 2011. The canonical BMP signaling pathway is involved in human monocyte-derived dendritic cell maturation. *Immunol Cell Biol,* 89**,** 610-8.
MASSAGUE, J. 2012. TGFbeta signalling in context. *Nat Rev Mol Cell Biol,* 13**,** 616-30.
MATSUI, Y., KIKUCHI, A., ARAKI, S., HATA, Y., KONDO, J., TERANISHI, Y. & TAKAI, Y. 1990. Molecular cloning and characterization of a novel type of regulatory protein (GDI) for smg p25A, a ras p21-like GTP-binding protein. *Mol Cell Biol,* 10**,** 4116-22.
MEHDIANI, A., MAIER, A., PINTO, A., BARTH, M., AKHYARI, P. & LICHTENBERG, A. 2015. An innovative method for exosome quantification and size measurement. *J Vis Exp***,** 50974.
MELDOLESI, J., CHIEREGATTI, E. & LUISA MALOSIO, M. 2004. Requirements for the identification of dense-core granules. *Trends Cell Biol,* 14**,** 13-9.
MERCER, J., SCHELHAAS, M. & HELENIUS, A. 2010. Virus entry by endocytosis. *Annu Rev Biochem,* 79**,** 803-33.
MERZ, A. J. 2015. What are the roles of V-ATPases in membrane fusion? *Proc Natl Acad Sci U S A,* 112**,** 8-9.
MICHEL, M., RAABE, I., KUPINSKI, A. P., PEREZ-PALENCIA, R. & BOKEL, C. 2011. Local BMP receptor activation at adherens junctions in the Drosophila germline stem cell niche. *Nat Commun,* 2**,** 415.
MIRONOV, A. A., BEZNOUSSENKO, G. V., POLISHCHUK, R. S. & TRUCCO, A. 2005. Intra-Golgi transport: a way to a new paradigm? *Biochim Biophys Acta,* 1744**,** 340-50.
MITTELBRUNN, M., VICENTE-MANZANARES, M. & SANCHEZ-MADRID, F. 2015. Organizing polarized delivery of exosomes at synapses. *Traffic,* 16**,** 327-37.
MORGAN, T. H. 1910. Sex Limited Inheritance in Drosophila. *Science,* 32**,** 120-2.
MORGAN, T. H. 1911a. Chromosomes and Associative Inheritance. *Science,* 34**,** 636-8.
MORGAN, T. H. 1911b. Random Segregation Versus Coupling in Mendelian Inheritance. *Science,* 34**,** 384.
MORIMURA, S., MAVES, L., CHEN, Y. & HOFFMANN, F. M. 1996. decapentaplegic overexpression affects Drosophila wing and leg imaginal disc development and wingless expression. *Dev Biol,* 177**,** 136-51.
MORVAN, J. & TOOZE, S. A. 2008. Discovery and progress in our understanding of the regulated secretory pathway in neuroendocrine cells. *Histochem Cell Biol,* 129**,** 243-52.
MULLER, H. J. 1946. Thomas Hunt Morgan 1866-1945. *Science,* 103**,** 550-1.
NAGAMATSU, S., NAKAMICHI, Y., YAMAMURA, C., MATSUSHIMA, S., WATANABE, T., OZAWA, S., FURUKAWA, H. & ISHIDA, H. 1999. Decreased expression of t-SNARE, syntaxin 1, and SNAP-25 in pancreatic beta-cells is involved in impaired insulin secretion from diabetic GK rat islets: restoration of decreased t-SNARE proteins improves impaired insulin secretion. *Diabetes,* 48**,** 2367-73.
NAHM, M., KIM, S., PAIK, S. K., LEE, M., LEE, S., LEE, Z. H., KIM, J., LEE, D., BAE, Y. C. & LEE, S. 2010. dCIP4 (Drosophila Cdc42-interacting protein 4) restrains synaptic growth by inhibiting the secretion of the retrograde Glass bottom boat signal. *J Neurosci,* 30**,** 8138-50.
NELLEN, D., BURKE, R., STRUHL, G. & BASLER, K. 1996. Direct and long-range action of a DPP morphogen gradient. *Cell,* 85**,** 357-68.

NIELSEN, E., CHRISTOFORIDIS, S., UTTENWEILER-JOSEPH, S., MIACZYNSKA, M., DEWITTE, F., WILM, M., HOFLACK, B. & ZERIAL, M. 2000. Rabenosyn-5, a novel Rab5 effector, is complexed with hVPS45 and recruited to endosomes through a FYVE finger domain. *J Cell Biol,* 151**,** 601-12.

NIEMEYER, B. A. & SCHWARZ, T. L. 2000. SNAP-24, a Drosophila SNAP-25 homologue on granule membranes, is a putative mediator of secretion and granule-granule fusion in salivary glands. *J Cell Sci,* 113 (Pt 22)**,** 4055-64.

NISHI, T. & FORGAC, M. 2002. The vacuolar (H+)-ATPases--nature's most versatile proton pumps. *Nat Rev Mol Cell Biol,* 3**,** 94-103.

NOVICK, P., FERRO, S. & SCHEKMAN, R. 1981. Order of events in the yeast secretory pathway. *Cell,* 25**,** 461-9.

NOVICK, P., FIELD, C. & SCHEKMAN, R. 1980. Identification of 23 complementation groups required for post-translational events in the yeast secretory pathway. *Cell,* 21**,** 205-15.

OKSVOLD, M. P., SKARPEN, E., WIEROD, L., PAULSEN, R. E. & HUITFELDT, H. S. 2001. Re-localization of activated EGF receptor and its signal transducers to multivesicular compartments downstream of early endosomes in response to EGF. *Eur J Cell Biol,* 80**,** 285-94.

OSTROWSKI, M., CARMO, N. B., KRUMEICH, S., FANGET, I., RAPOSO, G., SAVINA, A., MOITA, C. F., SCHAUER, K., HUME, A. N., FREITAS, R. P., GOUD, B., BENAROCH, P., HACOHEN, N., FUKUDA, M., DESNOS, C., SEABRA, M. C., DARCHEN, F., AMIGORENA, S., MOITA, L. F. & THERY, C. 2010. Rab27a and Rab27b control different steps of the exosome secretion pathway. *Nat Cell Biol,* 12**,** 19-30; sup pp 1-13.

PALFY, M., REMENYI, A. & KORCSMAROS, T. 2012. Endosomal crosstalk: meeting points for signaling pathways. *Trends Cell Biol,* 22**,** 447-56.

PANDEY, U. B. & NICHOLS, C. D. 2011. Human disease models in Drosophila melanogaster and the role of the fly in therapeutic drug discovery. *Pharmacol Rev,* 63**,** 411-36.

PARK, K. H., KIM, B. J., KANG, J., NAM, T. S., LIM, J. M., KIM, H. T., PARK, J. K., KIM, Y. G., CHAE, S. W. & KIM, U. H. 2011. Ca2+ signaling tools acquired from prostasomes are required for progesterone-induced sperm motility. *Sci Signal,* 4**,** ra31.

PATEL, N. H., SNOW, P. M. & GOODMAN, C. S. 1987. Characterization and cloning of fasciclin III: a glycoprotein expressed on a subset of neurons and axon pathways in Drosophila. *Cell,* 48**,** 975-88.

PENG, J., CHEN, S., BUSSER, S., LIU, H., HONEGGER, T. & KUBLI, E. 2005. Gradual release of sperm bound sex-peptide controls female postmating behavior in Drosophila. *Curr Biol,* 15**,** 207-13.

PENHEITER, S. G., MITCHELL, H., GARAMSZEGI, N., EDENS, M., DORE, J. J., JR. & LEOF, E. B. 2002. Internalization-dependent and -independent requirements for transforming growth factor beta receptor signaling via the Smad pathway. *Mol Cell Biol,* 22**,** 4750-9.

PFEFFER, S. & AIVAZIAN, D. 2004. Targeting Rab GTPases to distinct membrane compartments. *Nat Rev Mol Cell Biol,* 5**,** 886-96.

PFEFFER, S. R. 2001. Rab GTPases: specifying and deciphering organelle identity and function. *Trends Cell Biol,* 11**,** 487-91.

PINAR, M., ARST, H. N., JR., PANTAZOPOULOU, A., TAGUA, V. G., DE LOS RIOS, V., RODRIGUEZ-SALARICHS, J., DIAZ, J. F. & PENALVA, M. A. 2015. TRAPPII regulates exocytic Golgi exit by mediating nucleotide exchange on the Ypt31 ortholog RabERAB11. *Proc Natl Acad Sci U S A,* 112**,** 4346-51.

PLUTNER, H., COX, A. D., PIND, S., KHOSRAVI-FAR, R., BOURNE, J. R., SCHWANINGER, R., DER, C. J. & BALCH, W. E. 1991. Rab1b regulates vesicular transport between the endoplasmic reticulum and successive Golgi compartments. *J Cell Biol,* 115**,** 31-43.

POEA-GUYON, S., AMMAR, M. R., ERARD, M., AMAR, M., MOREAU, A. W., FOSSIER, P., GLEIZE, V., VITALE, N. & MOREL, N. 2013. The V-ATPase membrane domain is a sensor of granular pH that controls the exocytotic machinery. *J Cell Biol,* 203**,** 283-98.

POLS, M. S. & KLUMPERMAN, J. 2009. Trafficking and function of the tetraspanin CD63. *Exp Cell Res,* 315**,** 1584-92.

POTERYAEV, D., DATTA, S., ACKEMA, K., ZERIAL, M. & SPANG, A. 2010. Identification of the switch in early-to-late endosome transition. *Cell,* 141**,** 497-508.

PROGIDA, C., COGLI, L., PIRO, F., DE LUCA, A., BAKKE, O. & BUCCI, C. 2010. Rab7b controls trafficking from endosomes to the TGN. *J Cell Sci,* 123**,** 1480-91.

PRYOR, P. R., MULLOCK, B. M., BRIGHT, N. A., LINDSAY, M. R., GRAY, S. R., RICHARDSON, S. C., STEWART, A., JAMES, D. E., PIPER, R. C. & LUZIO, J. P. 2004. Combinatorial SNARE complexes with VAMP7 or VAMP8 define different late endocytic fusion events. *EMBO Rep,* 5**,** 590-5.

PULIPPARACHARUVIL, S., AKBAR, M. A., RAY, S., SEVRIOUKOV, E. A., HABERMAN, A. S., ROHRER, J. & KRAMER, H. 2005. Drosophila Vps16A is required for trafficking to lysosomes and biogenesis of pigment granules. *J Cell Sci,* 118**,** 3663-73.
RAM, K. R. & WOLFNER, M. F. 2007. Sustained post-mating response in Drosophila melanogaster requires multiple seminal fluid proteins. *PLoS Genet,* 3**,** e238.
RAFTERY, L & UMULIS, D. 2012. Regulation of BMP activity and range in *Drosophila* wing development. *Curr Opin Cell Bio*, 24(2): 158-165.
RAPOSO, G. & STOORVOGEL, W. 2013. Extracellular vesicles: exosomes, microvesicles, and friends. *J Cell Biol,* 200**,** 373-83.
REITER, L. T., POTOCKI, L., CHIEN, S., GRIBSKOV, M. & BIER, E. 2001. A systematic analysis of human disease-associated gene sequences in Drosophila melanogaster. *Genome Res,* 11**,** 1114-25.
RAHMAN, M. S., AKHTAR, N., MOHAMMAD, H., BANIK, R & ASADUZZAMAN, S. TGF-B BMP signaling and other molecular events: regulation of osteoblastogensis and bone formation. *Bone Research,* 14;3:15005.
RIDEOUT, E. J., DORNAN, A. J., NEVILLE, M. C., EADIE, S. & GOODWIN, S. F. 2010. Control of sexual differentiation and behavior by the doublesex gene in Drosophila melanogaster. *Nat Neurosci,* 13**,** 458-66.
RINK, J., GHIGO, E., KALAIDZIDIS, Y. & ZERIAL, M. 2005. Rab conversion as a mechanism of progression from early to late endosomes. *Cell,* 122**,** 735-49.
ROBERTS, R. L., BARBIERI, M. A., PRYSE, K. M., CHUA, M., MORISAKI, J. H. & STAHL, P. D. 1999. Endosome fusion in living cells overexpressing GFP-rab5. *J Cell Sci,* 112 (Pt 21)**,** 3667-75.
ROHRER, J. & KORNFELD, R. 2001. Lysosomal hydrolase mannose 6-phosphate uncovering enzyme resides in the trans-Golgi network. *Mol Biol Cell,* 12**,** 1623-31.
RUBIN, G. M. & LEWIS, E. B. 2000. A brief history of Drosophila's contributions to genome research. *Science,* 287**,** 2216-8.
RUNYAN, C. E., HAYASHIDA, T., HUBCHAK, S., CURLEY, J. F. & SCHNAPER, H. W. 2009. Role of SARA (SMAD anchor for receptor activation) in maintenance of epithelial cell phenotype. *J Biol Chem,* 284**,** 25181-9.
RUSTEN, T. E., RODAHL, L. M., PATTNI, K., ENGLUND, C., SAMAKOVLIS, C., DOVE, S., BRECH, A. & STENMARK, H. 2006. Fab1 phosphatidylinositol 3-phosphate 5-kinase controls trafficking but not silencing of endocytosed receptors. *Mol Biol Cell,* 17**,** 3989-4001.
RYLETT, C. M., WALKER, M. J., HOWELL, G. J., SHIRRAS, A. D. & ISAAC, R. E. 2007. Male accessory glands of Drosophila melanogaster make a secreted angiotensin I-converting enzyme (ANCE), suggesting a role for the peptide-processing enzyme in seminal fluid. *J Exp Biol,* 210**,** 3601-6.
SAFTIG, P. & KLUMPERMAN, J. 2009. Lysosome biogenesis and lysosomal membrane proteins: trafficking meets function. *Nat Rev Mol Cell Biol,* 10**,** 623-35.
SAUNDERS, A. & ASHE, H. L. 2013. Taking a pause to reflect on morphogenesis. *Cell,* 153**,** 941-3.
SAVINA, A., FADER, C. M., DAMIANI, M. T. & COLOMBO, M. I. 2005. Rab11 promotes docking and fusion of multivesicular bodies in a calcium-dependent manner. *Traffic,* 6**,** 131-43.
SAVINA, A., FURLAN, M., VIDAL, M. & COLOMBO, M. I. 2003. Exosome release is regulated by a calcium-dependent mechanism in K562 cells. *J Biol Chem,* 278**,** 20083-90.
SAVINA, A., VIDAL, M. & COLOMBO, M. I. 2002. The exosome pathway in K562 cells is regulated by Rab11. *J Cell Sci,* 115**,** 2505-15.
SAWALA, A., SCARCIA, M., SUTCLIFFE, C., WILCOCKSON, S. G. & ASHE, H. L. 2015. Peak BMP Responses in the Drosophila Embryo Are Dependent on the Activation of Integrin Signaling. *Cell Rep,* 12**,** 1584-93.
SCOTT, C. C., BISSIG, C. & GRUENBERG, J. 2011. Duelling functions of the V-ATPase. *EMBO J,* 30**,** 4113-5.
SCHANK, G., DALESSI, SASCHA., YANG, S-F., YAGI, R., LACHAPELLE, A., AFOLTER, M., BERGANN, S AND BASLER, K. 2011. ORMATION OF LONG RANGE PP MORPHOGEN GRADIENT. *PLOS BIOLOGY*, 9(7):e1001111.
SETTEMBRE, C., FRALDI, A., MEDINA, D. L. & BALLABIO, A. 2013. Signals from the lysosome: a control centre for cellular clearance and energy metabolism. *Nat Rev Mol Cell Biol,* 14**,** 283-96.
SHAKYA, R., WATANABE, T. & COSTANTINI, F. 2005. The role of GDNF/Ret signaling in ureteric bud cell fate and branching morphogenesis. *Dev Cell,* 8**,** 65-74.
SHEFF, D., PELLETIER, L., O'CONNELL, C. B., WARREN, G. & MELLMAN, I. 2002. Transferrin receptor recycling in the absence of perinuclear recycling endosomes. *J Cell Biol,* 156**,** 797-804.

SHIELDS, S. B., OESTREICH, A. J., WINISTORFER, S., NGUYEN, D., PAYNE, J. A., KATZMANN, D. J. & PIPER, R. 2009. ESCRT ubiquitin-binding domains function cooperatively during MVB cargo sorting. *J Cell Biol,* 185**,** 213-24.
SHINDE, S. R. & MADDIKA, S. 2016. PTEN modulates EGFR late endocytic trafficking and degradation by dephosphorylating Rab7. *Nat Commun,* 7**,** 10689.
SIMONSEN, A., GAULLIER, J. M., D'ARRIGO, A. & STENMARK, H. 1999. The Rab5 effector EEA1 interacts directly with syntaxin-6. *J Biol Chem,* 274**,** 28857-60.
SINKA, R., GILLINGHAM, A. K., KONDYLIS, V. & MUNRO, S. 2008. Golgi coiled-coil proteins contain multiple binding sites for Rab family G proteins. *J Cell Biol,* 183**,** 607-15.
SITNIK, J. L., GLIGOROV, D., MAEDA, R. K., KARCH, F. & WOLFNER, M. F. 2016. The Female Post-Mating Response Requires Genes Expressed in the Secondary Cells of the Male Accessory Gland in Drosophila melanogaster. *Genetics,* 202**,** 1029-41.
SONNICHSEN, B., DE RENZIS, S., NIELSEN, E., RIETDORF, J. & ZERIAL, M. 2000. Distinct membrane domains on endosomes in the recycling pathway visualized by multicolor imaging of Rab4, Rab5, and Rab11. *J Cell Biol,* 149**,** 901-14.
SORKIN, A. & VON ZASTROW, M. 2002. Signal transduction and endocytosis: close encounters of many kinds. *Nat Rev Mol Cell Biol,* 3**,** 600-14.
SORKIN, A. & VON ZASTROW, M. 2009. Endocytosis and signalling: intertwining molecular networks. *Nat Rev Mol Cell Biol,* 10**,** 609-22.
SPANG, A. 2013. Retrograde traffic from the Golgi to the endoplasmic reticulum. *Cold Spring Harb Perspect Biol,* 5.
SREELATHA, A., BENNETT, T. L., CARPINONE, E. M., O'BRIEN, K. M., JORDAN, K. D., BURDETTE, D. L., ORTH, K. & STARAI, V. J. 2015. Vibrio effector protein VopQ inhibits fusion of V-ATPase-containing membranes. *Proc Natl Acad Sci U S A,* 112**,** 100-5.
STAEHLING-HAMPTON, K., JACKSON, P. D., CLARK, M. J., BRAND, A. H. & HOFFMANN, F. M. 1994. Specificity of bone morphogenetic protein-related factors: cell fate and gene expression changes in Drosophila embryos induced by decapentaplegic but not 60A. *Cell Growth Differ,* 5**,** 585-93.
STENMARK, H. 2009. Rab GTPases as coordinators of vesicle traffic. *Nat Rev Mol Cell Biol,* 10**,** 513-25.
STEPHENS, D. J. 2003. De novo formation, fusion and fission of mammalian COPII-coated endoplasmic reticulum exit sites. *EMBO Rep,* 4**,** 210-7.
STORRIE, B. & DESJARDINS, M. 1996. The biogenesis of lysosomes: is it a kiss and run, continuous fusion and fission process? *Bioessays,* 18**,** 895-903.
SUGAWARA, K., SHIBASAKI, T., MIZOGUCHI, A., SAITO, T. & SEINO, S. 2009. Rab11 and its effector Rip11 participate in regulation of insulin granule exocytosis. *Genes Cells,* 14**,** 445-56.
SUSTER, M. L., SEUGNET, L., BATE, M. & SOKOLOWSKI, M. B. 2004. Refining GAL4-driven transgene expression in Drosophila with a GAL80 enhancer-trap. *Genesis,* 39**,** 240-5.
SUTTON, R. B., FASSHAUER, D., JAHN, R. & BRUNGER, A. T. 1998. Crystal structure of a SNARE complex involved in synaptic exocytosis at 2.4 A resolution. *Nature,* 395**,** 347-53.
SZULWACH, K. E., LI, X., SMRT, R. D., LI, Y., LUO, Y., LIN, L., SANTISTEVAN, N. J., LI, W., ZHAO, X. & JIN, P. 2010. Cross talk between microRNA and epigenetic regulation in adult neurogenesis. *J Cell Biol,* 189**,** 127-41.
TANAKA, S., YORA, T., NAKAYAMA, K., INOUE, K. & KUROSUMI, K. 1997. Proteolytic processing of pro-opiomelanocortin occurs in acidifying secretory granules of AtT-20 cells. *J Histochem Cytochem,* 45**,** 425-36.
TANAKA, T. & NAKAMURA, A. 2008. The endocytic pathway acts downstream of Oskar in Drosophila germ plasm assembly. *Development,* 135**,** 1107-17.
TANG, K., WU, H., MAHATA, S. K., MAHATA, M., GILL, B. M., PARMER, R. J. & O'CONNOR, D. T. 1997. Stimulus coupling to transcription versus secretion in pheochromocytoma cells. Convergent and divergent signal transduction pathways and the crucial roles for route of cytosolic calcium entry and protein kinase C. *J Clin Invest,* 100**,** 1180-92.
TAUPENOT, L., HARPER, K. L. & O'CONNOR, D. T. 2005. Role of H+-ATPase-mediated acidification in sorting and release of the regulated secretory protein chromogranin A: evidence for a vesiculogenic function. *J Biol Chem,* 280**,** 3885-97.
TAYLER, T. D., PACHECO, D. A., HERGARDEN, A. C., MURTHY, M. & ANDERSON, D. J. 2012. A neuropeptide circuit that coordinates sperm transfer and copulation duration in Drosophila. *Proc Natl Acad Sci U S A,* 109**,** 20697-702.
TELEMAN, A. A. & COHEN, S. M. 2000. Dpp gradient formation in the Drosophila wing imaginal disc. *Cell,* 103**,** 971-80.
THERY, C., ZITVOGEL, L. & AMIGORENA, S. 2002. Exosomes: composition, biogenesis and function. *Nat Rev Immunol,* 2**,** 569-79.

THOMAS, J. D., ZHANG, Y. J., WEI, Y. H., CHO, J. H., MORRIS, L. E., WANG, H. Y. & ZHENG, X. F. 2014. Rab1A is an mTORC1 activator and a colorectal oncogene. *Cancer Cell,* 26**,** 754-69.
TIAN, C., GONG, Y., YANG, Y., SHEN, W., WANG, K., LIU, J., XU, B., ZHAO, J. & ZHAO, C. 2012. Foxg1 has an essential role in postnatal development of the dentate gyrus. *J Neurosci,* 32**,** 2931-49.
TKACH, M. & THERY, C. 2016. Communication by Extracellular Vesicles: Where We Are and Where We Need to Go. *Cell,* 164**,** 1226-32.
TRAJKOVIC, K., HSU, C., CHIANTIA, S., RAJENDRAN, L., WENZEL, D., WIELAND, F., SCHWILLE, P., BRUGGER, B. & SIMONS, M. 2008. Ceramide triggers budding of exosome vesicles into multivesicular endosomes. *Science,* 319**,** 1244-7.
TSUNEIZUMI, K., NAKAYAMA, T., KAMOSHIDA, Y., KORNBERG, T. B., CHRISTIAN, J. L. & TABATA, T. 1997. Daughters against dpp modulates dpp organizing activity in Drosophila wing development. *Nature,* 389**,** 627-31.
UKKONEN, P., LEWIS, V., MARSH, M., HELENIUS, A. & MELLMAN, I. 1986. Transport of macrophage Fc receptors and Fc receptor-bound ligands to lysosomes. *J Exp Med,* 163**,** 952-71.
ULLRICH, O., HORIUCHI, H., BUCCI, C. & ZERIAL, M. 1994. Membrane association of Rab5 mediated by GDP-dissociation inhibitor and accompanied by GDP/GTP exchange. *Nature,* 368**,** 157-60.
URBE, S., PAGE, L. J. & TOOZE, S. A. 1998. Homotypic fusion of immature secretory granules during maturation in a cell-free assay. *J Cell Biol,* 143**,** 1831-44.
VALENTE, C., POLISHCHUK, R. & DE MATTEIS, M. A. 2010. Rab6 and myosin II at the cutting edge of membrane fission. *Nat Cell Biol,* 12**,** 635-8.
VANLANDINGHAM, P. A. & CERESA, B. P. 2009. Rab7 regulates late endocytic trafficking downstream of multivesicular body biogenesis and cargo sequestration. *J Biol Chem,* 284**,** 12110-24.
VARGA, A. C. & WRANA, J. L. 2005. The disparate role of BMP in stem cell biology. *Oncogene,* 24**,** 5713-21.
VILLASENOR, R., KALAIDZIDIS, Y. & ZERIAL, M. 2016. Signal processing by the endosomal system. *Curr Opin Cell Biol,* 39**,** 53-60.
VINCENT, S., RUBERTE, E., GRIEDER, N. C., CHEN, C. K., HAERRY, T., SCHUH, R. & AFFOLTER, M. 1997. DPP controls tracheal cell migration along the dorsoventral body axis of the Drosophila embryo. *Development,* 124**,** 2741-50.
WANG, R. N., GREEN, J., WANG, Z., DENG, Y., QIAO, M., PEABODY, M., ZHANG, Q., YE, J., YAN, Z., DENDULURI, S., IDOWU, O., LI, M., SHEN, C., HU, A., HAYDON, R. C., KANG, R., MOK, J., LEE, M. J., LUU, H. L. & SHI, L. L. 2014. Bone Morphogenetic Protein (BMP) signaling in development and human diseases. *Genes Dis,* 1**,** 87-105.
WANG, Y., THIELE, C. & HUTTNER, W. B. 2000. Cholesterol is required for the formation of regulated and constitutive secretory vesicles from the trans-Golgi network. *Traffic,* 1**,** 952-62.
WATSON, F. L., HEERSSEN, H. M., BHATTACHARYYA, A., KLESSE, L., LIN, M. Z. & SEGAL, R. A. 2001. Neurotrophins use the Erk5 pathway to mediate a retrograde survival response. *Nat Neurosci,* 4**,** 981-8.
WHEELER, D. B., ZONCU, R., ROOT, D. E., SABATINI, D. M. & SAWYERS, C. L. 2015. Identification of an oncogenic RAB protein. *Science,* 350**,** 211-7.
WHITE, J., JOHANNES, L., MALLARD, F., GIROD, A., GRILL, S., REINSCH, S., KELLER, P., TZSCHASCHEL, B., ECHARD, A., GOUD, B. & STELZER, E. H. 1999. Rab6 coordinates a novel Golgi to ER retrograde transport pathway in live cells. *J Cell Biol,* 147**,** 743-60.
WILCKE, M., JOHANNES, L., GALLI, T., MAYAU, V., GOUD, B. & SALAMERO, J. 2000. Rab11 regulates the compartmentalization of early endosomes required for efficient transport from early endosomes to the trans-golgi network. *J Cell Biol,* 151**,** 1207-20.
WILDE, A., BEATTIE, E. C., LEM, L., RIETHOF, D. A., LIU, S. H., MOBLEY, W. C., SORIANO, P. & BRODSKY, F. M. 1999. EGF receptor signaling stimulates SRC kinase phosphorylation of clathrin, influencing clathrin redistribution and EGF uptake. *Cell,* 96**,** 677-87.
WILSON, C., LEIBLICH,A., GOBERDHAN, D., HAMDY, F. 2016. The Drosophila accessory gland as a model for prostate cancer and other pathologies. *Current Topics in Developmental Biology,* In Press.
WOLFNER, M. F. 2007. "S.P.E.R.M." (seminal proteins (are) essential reproductive modulators): the view from Drosophila. *Soc Reprod Fertil Suppl,* 65**,** 183-99.
WOLLERT, T., WUNDER, C., LIPPINCOTT-SCHWARTZ, J. & HURLEY, J. H. 2009. Membrane scission by the ESCRT-III complex. *Nature,* 458**,** 172-7.
WOODMAN, P. G. 1997. The roles of NSF, SNAPs and SNAREs during membrane fusion. *Biochim Biophys Acta,* 1357**,** 155-72.

WRIGHTON, K. H., LIN, X. & FENG, X. H. 2009. Phospho-control of TGF-beta superfamily signaling. *Cell Res,* 19**,** 8-20.
WU, C., RAMIREZ, A., CUI, B., DING, J., DELCROIX, J. D., VALLETTA, J. S., LIU, J. J., YANG, Y., CHU, S. & MOBLEY, W. C. 2007. A functional dynein-microtubule network is required for NGF signaling through the Rap1/MAPK pathway. *Traffic,* 8**,** 1503-20.
WU, M. M., GRABE, M., ADAMS, S., TSIEN, R. Y., MOORE, H. P. & MACHEN, T. E. 2001. Mechanisms of pH regulation in the regulated secretory pathway. *J Biol Chem,* 276**,** 33027-35.
XUE, L. & NOLL, M. 2000. Drosophila female sexual behavior induced by sterile males showing copulation complementation. *Proc Natl Acad Sci U S A,* 97**,** 3272-5.
YAPICI, N. B., BI, Y., LI, P., CHEN, X., YAN, X., MANDALAPU, S. R., FAUCETT, M., JOCKUSCH, S., JU, J., GIBSON, K. M., PAVAN, W. J. & BI, L. 2015. Highly stable and sensitive fluorescent probes (LysoProbes) for lysosomal labeling and tracking. *Sci Rep,* 5**,** 8576.
YOSHIHISA, T., BARLOWE, C. & SCHEKMAN, R. 1993. Requirement for a GTPase-activating protein in vesicle budding from the endoplasmic reticulum. *Science,* 259**,** 1466-8.
ZHANG, Y., MOHEBAN, D. B., CONWAY, B. R., BHATTACHARYYA, A. & SEGAL, R. A. 2000. Cell surface Trk receptors mediate NGF-induced survival while internalized receptors regulate NGF-induced differentiation. *J Neurosci,* 20**,** 5671-8.
ZHAO, L., HUA, T., CROWLEY, C., RU, H., NI, X., SHAW, N., JIAO, L., DING, W., QU, L., HUNG, L. W., HUANG, W., LIU, L., YE, K., OUYANG, S., CHENG, G. & LIU, Z. J. 2014. Structural analysis of asparaginyl endopeptidase reveals the activation mechanism and a reversible intermediate maturation stage. *Cell Res,* 24**,** 344-58.